The Department of Engineering

The University of Liverpool

Vibration Suppression by Using Magnetic Damping

Thesis submitted in accordance with the requirements of the University of Liverpool for the degree of Doctor in Philosophy

by

Jianfeng Zhu

May 2007

Summary

The dynamic effects of rare earth permanent magnets on the vibration of structures made from paramagnetic (or diamagnetic) conducting light materials show both resonance amplitude suppression and natural frequency changes. A complex-valued viscous damping model has been developed to predict this particular phenomenon. The real part of this damping model represents a viscous type damping effect while the imaginary part represents the dynamic stiffness effect. This thesis provides a comprehensive evaluation about the complex valued viscous damping model and its application to dynamic system. The analyses of damped natural frequencies, complex mode shapes and frequency response functions are given.

The dynamic behaviour of the complex-valued viscous damping system shows that this damping depends on the amplitude and frequency of cyclical oscillations. Another damping model, a frequency-rate stiffness model, provides a physical understanding for the complex viscous damping but has certain application restrictions. Both models result in the same steady state forced harmonic response.

In order to obtain the time domain response of the dynamic structure with complex-valued viscous damping, an iterative technique is proposed for response computation. The iterative technique uses the Hilbert transform and yields an integral-differential equation for the motion equation when real-valued signals are introduced in the formulation. The time domain response results show the non-causal effect of complex valued viscous damping model. This appears in the form of a small precursor response before the excitation.

Another aspect on the complex valued viscous damping model is its application to structural modifications. This thesis presents the changes of eigenvalues and eigenvectors caused by local complex viscous damping modification. The sensitivities of eigenvalues and eigenvectors with respect to damping variables are investigated. Analysis of the inverse problem with the complex viscous damping illustrates the assignment of desired natural frequencies, antiresonances and receptances. One

important application of the complex viscous damping is its application to the suppression of unwanted vibration. An absorber with complex viscous damping may be determined through an optimization procedure to suppress receptances at chosen frequencies.

To my family

Acknowledgements

I would first like to thank The Universities UK (ORS) and The University of Liverpool Graduates Association (HongKong) for their kind financial supports to my research programme.

I wish to take this opportunity to express my sincere gratitude and appreciation to my supervisor, Prof. J.E. Mottershead, for his expertise, guidance and kindness throughout my past four year's program. His invaluable knowledge and support were indispensable for my work.

Special thanks are due to my advisor, Dr. H. Ouyang, for his kind help in my research programme. His instructions are important for both my present and future research work. I would also like to thank Dr. Simon James for his technical supports during my work.

Thanks are also given to Dr. A. Kyprianou in University of Cyprus who helped with the Groebner Basis algorithm and Dr. E. Bonisoli in Politecnico di Torino whose original research on magnetic damping and complex viscous damping provided the basis for the work presented in this thesis.

Contents

Nomenclature

m, c, k	mass, viscous damping, stiffness of a single degree of freedom system
$\ddot{x}, \dot{x}, x$	acceleration, velocity, displacement
$f, f(t), w(t)$	external force
t	time
ω	radial frequency
X	amplitude of displacement
W	energy lost per cycle
V	peak potential energy stored in the system
η	loss factor
η_i	the modal loss factor for *i*th modal
U_i	total strain energy at maximum displacement during one cycle of vibration in the *i*th mode
ΔU_i	strain energy dissipated in one cycle in the *i*th mode
$\mathbf{I}$	unity matrix
$\mathbf{M,C,K}$	mass, damping and stiffness matrix of a dynamic system
$\mathbf{x}$	displacement vector of a dynamic system
$\mathbf{X}$	original displacement amplitude vector
$\overline{\mathbf{X}}$	modified displacement amplitude vector
$\Delta\mathbf{M}$, $\delta\mathbf{M}$, $\Delta\mathbf{K}$, $\delta\mathbf{K}$	modification of mass and stiffness matrices
$\mathbf{K}_C$	complex stiffness matrix of the structure
$\mathbf{K}_R$	real part matrix of the complex stiffness matrix $\mathbf{K}_C$

$\mathbf{K}_{\mathrm{I}}$	the imaginary part matrix of the complex stiffness matrix $\mathbf{K}_{\mathrm{C}}$
$\mathbf{W}(j\omega)$	force vector in the frequency domain
$\mathbf{F}$	the force magnitude vector in frequency domain
$\mathbf{w}(t)$, $\mathbf{f}$	force vector in the time domain
$\mathbf{\Lambda} = diag(\omega_1^2, \omega_2^2, ..., \omega_N^2)$	eigenvalue matrix for undamped system
λ_j, u_j	jth eigenvalue
ω_{nj}	jth natural frequency
$\omega_n = \sqrt{\frac{k}{m}}$	natural frequency
u, $\mathbf{\Phi}$	eigenvalue and eignvector
$\mathbf{\Phi}_i$, $\mathbf{\Phi}_j$, $\mathbf{\Phi}_k$	ith, jth, kth eigenvector column of original system
$\overline{\mathbf{\Phi}}_j$	jth eigenvector column of the modified system
$[\mathbf{\Phi}]$	eigenvector matrix, mode shape matrix
φ_{pj}	the p, jth element of eigenvector matrix $[\mathbf{\Phi}]$
$[\overline{\mathbf{\Phi}}]$	the eigenvector matrix of the modified system.
$\frac{\partial}{\partial\theta}$	sensitivity to a variable θ
r	resistivity of magnetic material
$2a \times 2b \times 2c$	size of the permanent magnets
Δ	air gap between a couple of permanent magnets
$\mu_0 = 4\pi \times 10^{-7} H/m$	the magnetic permeability of the vacuum
μ_r	the relative permeability
M	the residual magnetization
$B_r = \mu_0 M$	the residual magnetic induction

dB	magnetic induction in a point $P(x, y, z)$
dB_x	magnetic induction along the x-axis
$\frac{dB_x}{dx}$	the gradient of the x-component of the magnetic induction
$\frac{dB_{x,m}}{dx}$	the gradient of the mean magnetic induction
d	a distance from the infinitesimal portion of the side of a rectangular coil
$d\mathbf{s}$	a rectangular coil
$\mathbf{u}_d$	versor from the infinitesimal portion $d\mathbf{s}$ set in ($u=0$, v, w) of the side of a rectangular oil
P_d	the dissipated power
i	the induced current
R	the electrical resistance of the conducting mass
fem	the electromotive force
c_v	the viscous damping of the original system without magnetic damping
$c^* = c_m - jc_e$	complex damping coefficient
c_m	the real part of a complex viscous damping
$-c_e$	the imaginary part of a complex viscous damping
$c_t = c_v + c_m$	real part of the whole system damping
$\chi = \frac{c_e}{c_m}$	choking volume coefficient
$\gamma = \frac{-c_e}{c_m}$	the imaginary part factor of a complex viscous damping
$\psi = \frac{-c_e}{c_v + c_m}$	the imaginary part factor of the whole system damping

$\zeta_m = \frac{\sqrt{(c_v + c_m)^2 + c_e^{\,2}}}{2\sqrt{km}}$	the complex damping ratio
$\mathrm{sgn}(\omega)$	sign function, 1 for $\omega > 0$, 0 for $\omega = 0$, -1 for $\omega < 0$
x(s), W(s)	the Laplace transform for displacement and force
s	eigenvalue
$H(\omega)$, $\alpha(\omega)$	frequency response function (receptance)
$\alpha^*(\omega)$	non-dimensional receptance
X_0, X, A	amplitudes of displacement for harmonic vibration
F_0, F	amplitude of force for harmonic excitation
$\delta(t)$	the unit impulse function
h(t)	impulse response function
f_r	restoring force
S_0	mean square spectral density of the force
$S_x(\omega)$	mean square spectral density of the response
$E[x^2]$	means square of the response
σ^2	variance
σ	standard deviation
$F(j\omega)$, $W(j\omega)$	Fourier transform for the force
$\ddot{X}(j\omega), \dot{X}(j\omega), X(j\omega)$	Fourier transform for acceleration, velocity and displacement
H[ ]	Hilbert transform
FT[ ]	Fourier transform
$HY(j\omega)$	the hysteretic force in frequency domain
$hy(t)$	the hysteretic force in time domain
Re[ ]	real part

Im[ ]	imaginary part
α	nonlinear stiffness factor
$\mathbf{A}=\begin{bmatrix}\mathbf{C} & \mathbf{M}\\ \mathbf{M} & \mathbf{0}\end{bmatrix}$	state space matrix
$\mathbf{D}=\begin{bmatrix}\mathbf{K} & \mathbf{0}\\ \mathbf{0} & -\mathbf{M}\end{bmatrix}$	state space matrix
$\mathbf{A}^*$, $\mathbf{D}^*$	uncoupled diagonal state space matrix
a_r, d_r	the r, rth diagonal element of of matrices $\mathbf{A}^*$ and $\mathbf{D}^*$
$\mathbf{q}$	a $1\times n$ row vector indicating the location of the modification
$\mathbf{Q}=[\mathbf{q},\ \mathbf{0}_{1\times n}]$	the modification position vector
$\mathbf{Y}$	modified eigenvector
$\mathbf{Z}$	the column of original eigenvector participation factors
ε_j	small changes to the *j*th eigenvalue
$\frac{\partial\lambda}{\partial c^*}$	sensitivity of eigenvalue to added damping
$\frac{\partial\mathbf{Y}_j}{\partial c^*}$	sensitivity of *j*th eigenvector to added damping
$\mathbf{B}=-\omega^2\mathbf{M}+j\omega\mathbf{C}+\mathbf{K}$	matrix
m_a, c_a, k_a	mass, damping, spring stiffness of the added absorber
$b_n(\omega)$	dynamic stiffness
$\Delta\mathbf{B}$	dynamic stiffness matrix
$\mathbf{H}$	the receptance matrix of the original system
$\overline{\mathbf{H}}$	the receptance matrix of the modified system
$\mathbf{e}_i$	a column vector, whose *i*th element is unity one and the other elements are zeros
h_{ij}	the *i, j*th element of the original receptance

$\bar{h}_{ij}$	the *i, j*th element of the modified receptance
$\mathbf{M}^*$	modal mass matrix
$\mathbf{K}^*$	model stiffness matrix
m_i	*i*th modal mass
k_i	*i*th modal stiffness
$\mathbf{u}$	the modal displacement vector
μ_j	the *j*th modal displacement
f_j	the *j*th modal force
$\mathbf{R}$	the modal receptance matrix of the original system
R_{jj}	*j*th modal receptance
$\overline{\mathbf{R}}$	the modal receptance matrix of the modified system
$\widetilde{\mathbf{R}}$	the new modal receptance matrix of the modified system
$\widetilde{R}_{ij}$	the *i, j*th element of the new modal receptance matrix of the modified system
$u = \frac{m_a}{m_n}$,	the absorber mass ratio
m_n	the mass of component at the degree of freedom where the absorber is attached.
$\beta = \frac{\omega_a}{\omega_p}$	the absorber natural frequency ratio
$\omega_a = \sqrt{\frac{k_a}{m_a}}$	the natural frequency of the absorber without complex damping,
ω_p	the *p*th natural frequency of original system
$\zeta_r = \frac{c_a}{2\omega_p m_a}$	the related absorber viscous damping ratio

Chapter 1

General Introduction

1.1 Rare-earth permanent magnets

In the early 1970s, a new class of magnet, the rare earth magnet, was discovered, the properties of which showed a significant improvement on the then available technology. By the early 1990s, the new magnet technologies had matured. At present, the commonly used rare earth permanent magnets are Sintered samarium-cobalt (SmCo) and Sintered neodymium-iron- boron (NdFeB) rare earth magnets.

Sintered samarium cobalt rare earth (SmCo) magnets are manufactured by using powder metallurgy techniques, which include stringent process controls and complicated heat treatment cycles. The composition of this alloy is approximately 35% samarium, 60% cobalt with the balance being Fe & Cu. Being extremely brittle, great care must be taken when handling magnetised samarium cobalt to prevent personal injury or damage to the magnets.

Sintered neodymium-iron-boron rare earth (NdFeB) magnets are again manufactured using a powder metallurgy route. After sintering the material is ground or sliced to size before coating and magnetisation. Sintered NdFeB magnets offer the highest

energy per unit volume of any permanent magnetic material. It can lift up to 1000 times its own weight [1].

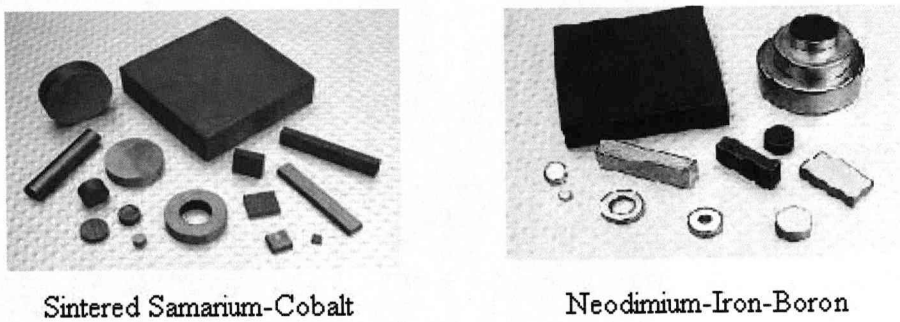

Figure 1.1 Rare earth permanent magnets

Rare earth permanent magnets show some advantages. They can provide both high coercive force and high magnetic field strength related to their small volume and low weight. The magnetization of the rare earth magnets can be reasonably considered unidirectional, of constant magnitude throughout the volume of the magnet [1]. For rare-earth permanent magnets, the hysteresis loops (magnetization M vs. magnetic field strength H) as shown in Figure 1.2 is nearly square in shape so that the magnetization M is likely to be constant for values of the demagnetising field less than the coercive force intensity. A consequence of the rigidity of the magnetization is that the superposition of flux produced by rare-earth permanent magnets is linear, and the magnetic material is effectively transparent, behaving like a vacuum. Therefore, for a pair of similar magnets in attraction or repulsion, the magnetization M of each magnet is not influenced by the magnetic field generated by the other one [1, 3].

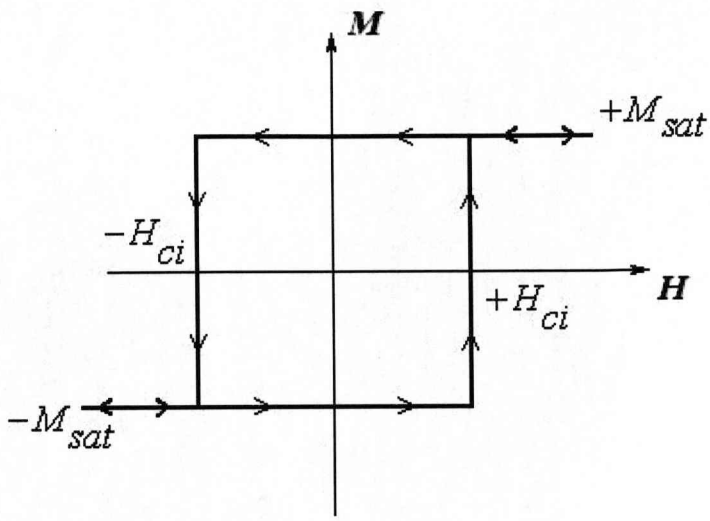

Figure 1.2 Hysteresis loop of rare-earth permanent magnets

1.2 Magnetic damping overview

The suppression of unwanted vibrations in mechanical systems is an issue of critical importance in aircraft, rotorcraft and space applications. Conventional vibration absorbers are widely used but have the disadvantage of a narrow bandwidth even when damping is included. Dampers using viscous fluids or rubber-like materials may degrade or have other problems in extreme environments and dashpot dampers may develop leaks. Coulomb damping results in wear and possible damage to the surfaces in contact. Considerable energy dissipation in structures results from air damping, which is not present in space applications.

There is therefore a widespread need for alternative damping mechanisms. When a magnetic field exists, the attractive or repulsive force may be produced in some ways such as magnets to magnets, magnets to structures in magnetic fields, or in the form of magnetic interaction to currents. The employment of this kind of magneto-elastic force allows obtaining high energy dissipation in the vibration of a structure in the similar way as a damper acts. As an example, Ruzzene *et al.* [2] have developed a

magnetic constrained layer damping to study the interactions between the permanent magnets and their influence on the dynamic behaviour of treated beams.

Rare earth permanent magnets, such as sintered samarium-cobalt or neodymium-iron-boron provide both high coercive forces and energy products. Being a damping mechanism, they have the advantage of being very suitable for applications involving lightweight metallic materials (para- and dia-magnetic materials in particular) as used in space vehicles, space stations, satellites, antennae etc. Compared to other dampers, rare-earth permanent magnetic dampers show some important properties that permit the dissipation of energy without contact or mechanical friction and they can be operated in a vacuum. Since no extra heat is produced, a cooling system is not required. The rare earth permanent magnets are expensive, but this can be justified in the case of many exotic applications (such as space) where the alternatives are very limited or the safety of human life is an issue. Active control of vibration is not fail-safe whereas magnetic damping can be applied passively.

These rare-earth permanent magnets are capable of producing large energy dissipative and stiffness forces by means of eddy currents generated in paramagnetic or diamagnetic materials such as Aluminum, Copper and Brass. Professor Piombo and his colleagues [3] firstly investigated this phenomenon in the frequency domain. It is found that when employing these magnets, the frequency response of the mechanical system shows great amplitude suppression accompanied with the change of the natural frequency. That means besides the viscous-type damping effect a dynamic stiffness effect exists, which is known as the "phantom effect". The same authors proposed a mathematical model to represent observed behaviour in mechanical systems when vibrating inside a magnetic field. The model is used to determine the influence of the magneto-elastic interaction with eddy currents on the dynamic behaviour of structures. It includes a conventional viscous damping force together with a force proportional to velocity but in phase with displacement – a complex valued viscous damping model. A certain complex form similarity exists between

magnetic damping and conventional hysteretic damping, which is used to represent viscoelastic materials. Whereas the hysteretic damping model is characterized by a damping force proportional to displacement but in phase with velocity, magnetic damping gives rise to a stiffness force proportional to velocity and in phase with displacement.

The work of Piombo *et al.* [3] includes a theoretical analysis of the cantilever beam with a magnetic damper placed on its free end. Through these works, the influence of the magnetic damper on the dynamic behaviour of the structure has been studied. It is illustrated that magnetic damping will affect the dynamic behaviour of the structure by both suppressing the resonance peak and increasing the value of the resonance frequency of the system [4]. The complex viscous damping model has also been compared and related to a fractional derivative model, suitable to extend to the analysis to transient dynamics [5].

Furthermore, Bonisoli and Mottershead [6] undertook a thorough analysis of the single degree-of-freedom complex-damped mass-spring system. The analysis covers both time and frequency domains and includes the root locus, the (non-causal) impulse response, the frequency response and the transmissibility. Regions of different behaviour in the frequency response and transmissibility are described in detail. Their results demonstrate that like the hysteretic complex-stiffness model, the complex damping model satisfies the reality conditions but is non-causal.

Recently, Bonisoli and Vigliani investigated the passive effects of rare-earth permanent magnets on flexible conductive structures [110]. They designed an experimental passive elasto-magnetic suspension that is based on rare-earth permanent magnets coupled to traditional linear elastic spring. The experiment presents a negligible dependence on mass of its natural frequency for small amplitude vibration. Moreover it shows relevant nonlinear motion amplitude dependent behaviour [111].

1.3 Original contributions of the work

The benefit of the complex valued viscous damping model is obvious as presented in previous work. It can conveniently predict both viscous damping effect and stiffness force simultaneously in the frequency domain. However, the damping mechanism of this kind of damping model is still not very clearly understood. And how to predict its effect on the general dynamic behaviour of the vibrating system is also a huge task. The main purpose of this thesis it to take a detail account of the theory and technique of the complex value magnetic damping. These analyses include various models discussions, time history response analyses techniques, and sensitivity analysis. The analytical results will provide a good understanding for this particular damping model.

The main original contributions of this work include:

1). An explanation of the energy dissipation mechanism in complex viscous damping.

2). A comparison of the complex viscous damping model and the frequency-rate stiffness model for magnetic damping.

3). A Nyquist diagram obtained for the system with magnetic damping.

4). The calculation of the response of the system with magnetic damping under the random excitation.

5). A proposed an iterative technique using the Hilbert transform. This method can be used to calculate directly the time history response of the system with complex viscous damping.

6). The modified characteristic equation was obtained for the system modified by an added damper. The new characteristic equation can be expressed from the original dynamical properties and can be easily calculated by existed numerical method.

7). The calculation of the sensitivities of new eigenvalues and eigenvectors of the modified system with respect to the damping coefficient.

8). The development of a new method to assign the natural frequency, antiresonance and receptance of the system by using complex viscous damping modification. The method only needs some specified receptance of the original system and the inverse matrix calculation is not required.

9). The proposal of a new concept for modal receptance of the modified system. And the appropriate absorber can be determined to suppress receptance corresponding to the desired natural frequency when using this new modal receptance of the modified system as the optimization objective function.

1.4 Scope of contents

The thesis is briefly outlined as below.

Chapter two provides a brief survey of the literature. Discussion of hysteretic damping is included in some detail because this kind of damping shows a similar complex form to the complex viscous damping. Other discussions are focused on the structural modification, which is the mainly on the application of complex magnetic damping. This also includes the sensitivity studies and absorber optimization.

Chapter three gives a brief introduction of the complex viscous damping model and then makes a thorough analysis for the complex-damped single degree of freedom

system. The analysis includes the root locus, the (non-causal) impulse response and the frequency response function. Viscous type damping effect accompanied with dynamical stiffness effect can by seen from the frequency response function analysis. The complex viscous damping provides a stable and realistic system. But it is non-causal in time domain.

Chapter four discusses the energy dissipation mechanism of complex viscous damping. Then the frequency-rate stiffness model is discussed and the forced harmonic vibration response of the system with magnetic damping is calculated by using the frequency-rate stiffness. The Nyquist diagram of the system with magnetic damping is illustrated and random vibration of the system is considered also.

Chapter five addresses the concept of the complex viscous damping model in both frequency domain and time domain. Consequently, the time history responses for vibration of complex viscous damping systems have been calculated through two techniques, the FFT method and an iterative technique using the Hilbert transform. The advantages and restrictions of these two methods are then compared. The two methods provide excellent coincidence of computation results and demonstrate the non-causal property of the complex viscous damping model.

Chapter six develops a procedure to determine the new eigenvalue and eigenvector of the system modified by an added damper. The modified characteristic equation can be expressed from the original dynamical properties. Numerical examples for the linear viscous damping modification and complex viscous damping modification are then given. The sensitivities of modified eigenvalues and eigenvectors with respect to the damping coefficient is derived and discussed.

Chapter seven studies the application of complex viscous damping on the inverse problem of structural modification and tries to investigate the possibility of structural modification with complex viscous damping and a spring to assign some dynamic

characteristics of the system. The natural frequency, antiresonance and receptance of the system can be assigned by complex viscous damping modification. The calculation procedure should satisfy the realistic requirement that the spring stiffness and viscous damping coefficient should be positive and the imaginary part factor of the complex viscous damping coefficient to be in a reasonable range.

Chapter eight investigates the receptance suppression by using the complex viscous damping absorber. The concept of a new modal receptance of the modified system is proposed. The selection of the absorber parameters is an optimization procedure. If we use the new modal receptance of the modified system as the optimization objective function, an appropriate absorber can be determined to suppress the receptance corresponding to the desired natural frequency.

Chapter nine makes general conclusions based upon the previous analysis and discussion. Further works are also suggested.

Chapter 2

Literature Review

Damping is the energy dissipation property of a material or system under cyclic stress. An effective measurement of damping is damping ratio. Damping ratio is the ratio of the actual resistance in damped harmonic motion to that necessary to produce critical damping. Table 2-1 lists some typical viscous damping ratio values of typical materials [112].

Table 2-1 Typical viscous damping ratio values of typical materials (approx. 20° C)

Material	Longitudinal	Flexural
Aluminum	0.15 to 5 ($\times 10^{-5}$)	$\approx$0.5 ($\times 10^{-4}$)
Lead (Pure)	2.5 to 15 ($\times 10^{-2}$)	$\approx$1.0 ($\times 10^{-2}$)
Iron	0.5 to 2.0 ($\times 10^{-4}$)	1.0 to 3.0 ($\times 10^{-4}$)
Steel	0.1 to 1.5 ($\times 10^{-4}$)	
Copper (Polycrystalline)	$\approx$1.0 ($\times 10^{-3}$)	$\approx$1.0 ($\times 10^{-3}$)
Brass	0.1 to 0.5 ($\times 10^{-3}$)	$<$0.5 ($\times 10^{-3}$)
Gold	$\approx$ 1.5 ($\times 10^{-4}$)	
Silver	$\approx$2.0 ($\times 10^{-4}$)	$<$1.5 ($\times 10^{-3}$)
Zinc		$\approx$ 1.5 ($\times 10^{-4}$)
Tin		$\approx$ 10 ($\times 10^{-4}$)

Notes: Some viscous damping ratios are unavailable.

Being some examples of the vibration structures with magnets, Wang and his colleague [113] designed damping induced by magnetic force for magnetic bearing motor. After damping, the natural damping ratio in the radial direction of the rotor increases to 0.1401 from 0.0655. Sodano *et al.* [114] described an eddy current damping system, which consists of a cantilever beam with a copper conducting plate located in the magnetic field generated by a single cylindrical permanent magnet. When the magnets gap reduced from 10 mm to 1 mm, the damping ratio increased from 0.01 to 0.4. Kim and Lee [115] proposed a high-temperature superconducting magnetic bearing flywheel energy storage system. The damping ratios corresponding to the first three modes are measured as 0.033, 0.0263 and 0.0208.

As being a new type of damping, complex magnetic damping shows a complex-valued viscous damping coefficient. This particular characteristic will cause some new phenomena to appear in the dynamic response of the vibration system and consequently induce some new applications in engineering science. Before the analyses for this special damping, a brief survey is undertaken of the related literature. The review is focused on both mathematical theoretic and modeling investigations on hysteretic damping that shows a similar complex form to the complex viscous damping. Structural modification studies are also considered. The work described in this chapter provides the necessary techniques, information and guidelines for further analyses of magnetic damping and complex viscous damping.

2.1 Hysteretic damping

Since the main phenomenon of vibration is the cyclic oscillation, the energy of the dynamical system cyclically transforms from potential energy into kinetic energy and back again. The "damping" is the mechanism determining the removal of energy from a vibration system. And the major feature of a dynamic system is to understand how energy is dissipated in a cycle of oscillation.

2.1.1 Linear Kelvin damping model

For the well known linear damping model, called a Kelvin model when a linear spring is in parallel with a linear viscous dashpot, if a structure modeled with this damping element oscillates in a sinusoidal motion, the energy lost per cycle generally is proportional to the square of the amplitude of motion and proportional to the frequency. And the loss factor, defined by comparing the energy lost in a cycle to the peak potential energy stored in the system during that cycle, is amplitude independent while frequency dependent [7] as shown below.

Considering the motion equation of a single degree of freedom (SDOF) system with a linear damper.

$$m\ddot{x} + c\dot{x} + kx = f \tag{2.1}$$

Under a steady-state simple harmonic motion $x = X\cos\omega t$.

The energy lost in a cycle is calculated as

$$W = \int_0^{2\pi/\omega} (c\dot{x})\dot{x}dt = c\pi|\omega|X^2 \tag{2.2}$$

While the peak potential energy stored in the system is

$$V = \frac{1}{2}kX^2 \tag{2.3}$$

Thus, the loss factor for the linear damper in the system is

$$\eta = \frac{W}{2\pi V} = \frac{c|\omega|}{k} \tag{2.4}$$

It should be noticed that the absolute value of the frequency ω is shown in the expressions of lost energy and loss factor. Thus, thinking of the function of frequency ω, the energy lost per cycle and the loss factor are real, positive and even since $\eta(-\omega) = \eta(\omega)$.

Then for this Kelvin damping model with constant damping coefficient c for a dashpot, it may be expressed as

$$c(\omega) = \frac{k\eta(\omega)}{|\omega|} \tag{2.5}$$

which is a frequency dependent parameter.

2.1.2 Hysteretic damping model

However, many materials in fact show an energy loss per cycle with a very small frequency dependency, even independent, of frequency. For example, in recent years elastomers have been developed with vastly enhanced damping capability. These materials behave viscoelastically showing very small frequency dependent behaviour [9], usually called "hysteretic". Actually, as early as in 1955, Bishop [10] discussed the linear model for hysteretic damping. Subsequently, many investigations on linear hysteretic, structural damping and complex value stiffness have appeared [8, 11, 19]. In these models, the energy loss per cycle is independent of frequency.

Caughey and Vijayaraghavan [12] described four commonly used mathematical models for hysteretic damping. For each model, the restoring force is represented as,

(1) Complex value stiffness

$$F(x) = (a + ib)x \tag{2.6}$$

where, a and b are constant.

(2) Frequency dependent damping

$$F(x) = kx + \frac{h}{\omega}\dot{x} \tag{2.7}$$

(3) Biot's visco-elastic model

$$F(x) = k\left\{x - g\int_{1} Ei[-\varepsilon(t-\tau)]\frac{dx}{d\tau}d\tau\right\} \tag{2.8}$$

where, Ei is the exponential integral

$$Ei(u) = \int_{\infty}^{-u}\frac{e^{-\xi}}{\xi}d\xi \tag{2.9}$$

(4)Non-linear model

$$F(x) = k[x + g \mid x \mid Sgn\dot{x}] = kx[1 + gSgnx\dot{x}] \tag{2.10}$$

where

$$Sgn(v)=\begin{cases}1 & if \quad v>0\\ 0 & if \quad v=0\\ -1 & if \quad v<0\end{cases} \tag{2.11}$$

It is very clear that the first and second models will cause serious mathematic and physical confusion. For the first model, the complex force is yielded from a real displacement value. While for the second model, the interpretation of the frequency ω is only clear in the case of sinusoidal motion but is ambiguous for transient motion or complicated forced motion. Thus, the hysteretic damping model has to be represented in the frequency domain,

$$F(\omega)=k[1+j\eta\,\mathrm{sgn}(\omega)]X(\omega) \tag{2.12}$$

where, k is the stiffness parameter and η, the frequency-independent loss factor, is the ratio of the loss and storage module. The term $\mathrm{sgn}(\omega)$ allows the frequency to take any negative value. Otherwise for the corresponding force would not precede the displacement in the complex plane, the model would not be dissipative and no stable solution would be possible. Furthermore the term $\mathrm{sgn}(\omega)$ is present to ensure that the response $x(t)$ to any arbitrary input $f(t)$ is strictly real.

Biot's model leads to a hereditary integral type force-displacement relation. Thus the strict frequency independence is approximately transformed to be weak frequency dependence. Caughey [13] investigated this model and showed that it will yields well-posed mathematical problems for transient and steady-state oscillation of all kinds. Through the study of the free and forced oscillation of a dynamic system using the non-linear hysteretic damping model, Caughey [12] also demonstrated that the non-linear hysteretic damping model shows the hysteretic behaviour with quadratic dependence on deformation amplitude and independence of frequency. And it is proved that this model leads to well-posed mathematical problems for transient and steady-state oscillation of all kinds as well.

A commonly used method to determine the hysteretic damping model is the modal strain energy method. By using the concept of modal strain energy, the modal loss

factor η_i of a structure executing steady state vibration can be defined in terms of energy quantities as

$$\eta_i = \frac{\Delta U_i}{2\pi U_i} \tag{2.13}$$

where U_i is the total strain energy at maximum displacement during one cycle of vibration in the ith mode. ΔU_i is the strain energy dissipated in one cycle in the same mode of vibration.

Let the complex stiffness matrix of the structure analyzed be expressed as

$$\mathbf{K}_C = \mathbf{K}_R + j\mathbf{K}_I \tag{2.14}$$

in which, $\mathbf{K}_R$ and $\mathbf{K}_I$ are the real part matrix and the imaginary part matrix of the complex stiffness matrix respectively. The modal strain energy method makes the assumption that the undamped mode shapes are equal to the damped mode shapes [116]. This assumption holds only for lightly damped systems. Hence, the following expressions can be written

$$U_i = \frac{1}{2}\boldsymbol{\Phi}_i^T \mathbf{K}_R \boldsymbol{\Phi}_i \tag{2.15}$$

$$\Delta U_i = \pi\, \boldsymbol{\Phi}_i^T \mathbf{K}_I \boldsymbol{\Phi}_i \tag{2.16}$$

where $\boldsymbol{\Phi}_i$ is the undamped mode shape corresponding to the ith natural mode of vibration. Then from equations (2.13) to (2.16), the modal loss factor for the ith mode is given by

$$\eta_i = \frac{\boldsymbol{\Phi}_i^T \mathbf{K}_I \boldsymbol{\Phi}_i}{\boldsymbol{\Phi}_i^T \mathbf{K}_R \boldsymbol{\Phi}_i} \tag{2.17}$$

Nashif *et al.* [25] presented a modal strain energy method that has seen increased use in the finite element community to estimate modal loss factors in elastic–viscoelastic structures. The method enables one to predict dynamic response without explicitly accounting for hysteretic damping in the free vibration analysis. Saravanan, Ganesan and Ramamurti [117] developed a semianalytical finite element for multilayered doubly curved shells of revolution using the modal strain energy method. This element has been used to study the vibration and damping characteristics of multilayered, cylindrical, fluid-filled shells with alternating layers of elastic and

viscoelastic material. Davis and Lesieutre [118] used a modified modal strain energy approach to predict the structural damping added by the use of resistively shunted piezoceramic damping. Scarpa and Landi *et al.* [119] developed a dyadic matrix based perturbation method to evaluate the natural frequencies and modal loss factors of viscoelastically damped structures. This approach improves the accuracy of the prediction given by the modal strain energy method by making use of the modal basis of the undamped system.

More recently, fractional derivative terms have been introduced in order to improve the models of complex viscoelastic materials, such as teflon and nylon, in which the frequency-independent loss factor is an unsatisfactory representation [14-18].

Gaul [120] points out that replacing integer time derivatives in the conventional equations by fractional time derivatives in the generalized equations leads to improved curve fitting properties of measured data with less parameters and assures causality [121] which is violated by the constant hysteretic damping model [19].

A fractional derivative time model without space variables is typically expressed as [122]

$$D^2x + \gamma D^{(1+\eta)}x + F(x) = 0 \tag{2.18}$$

where $D^{(1+\eta)}$ with $0 < \eta < 1$ represents the $(1+\eta)$-order fractional derivative with respect to time in the sense of Caputo [123] and models the anomalous damping, and γ is the thermoviscous coefficient.

The Riemann-Liouville fractional integral [124, 125] and the Caputo fractional derivative [123, 126] are essential concepts to understand the fractional derivative. If it is given that

$$J^q\{\psi(t)\} = \frac{1}{\Gamma(q)}\int_a^t \frac{\psi(\tau)}{(t-\tau)^{1-q}}d\tau \qquad (0 < q) \tag{2.19}$$

where q and a are real valued. The corresponding Riemann-Liouville fractional derivative is interpreted as

$$D_*^{\lambda}\{\psi(t)\} = \frac{d}{dt}\left[J^{(1-\lambda)}\{\psi(t)\}\right] \qquad (0 < \lambda < 1) \tag{2.20}$$

The Caputo fractional derivative is defined below.

$$D^{\lambda}\{\psi(t)\} = J^{(1-\lambda)}\left[\frac{d}{dt}\psi(t)\right] \tag{2.21}$$

The Riemann-Liouville fractional derivative has some disadvantages. For the hyper-singular improper integral, where the order of singularity is higher than the dimension, and nonzero of the fractional derivative of constants, e.g. $D^{\lambda}(1) \neq 0$, which would entail that dissipation does not vanish for a system in equilibrium and invalidates the causality. But the Caputo fractional derivative is to overcome this drawback.

Bonisoli [6] also briefly investigated the root loci using fractional derivative model for the magnetic damping. By applying the Riemann-Liouville fractional derivative theory in order to build a linear damping model which is real and causal, the complex damping term may be replaced with a fractional derivative one, thus the resulting equilibrium equation is written as

$$m\frac{d^2x(t)}{dt^2} + c_f\frac{d^{\alpha}x(t)}{dt^{\alpha}} + kx(t) = F_0e^{j\omega t} \tag{2.22}$$

where c_f is a generalized damping coefficient and $\alpha \in (0,\ 2)$ is the order of the fractional derivative. Analogously to the complex damped model, the generalized damping force vector represents a stiffness increase ($0 < \alpha < 1$) or an inertial increase ($1 < \alpha < 2$). Equation (2.22) can be expressed in canonic form as

$$\ddot{x}(t) + 2\zeta_f\omega_n^{(2-\alpha)}\frac{d^{\alpha}x(t)}{dt^{\alpha}} + \omega_n^2x(t) = \frac{F_0}{k}\omega_n^2e^{j\omega t} \tag{2.23}$$

in which $\zeta_f = \dfrac{c_f\omega_n^{\alpha}}{2k}$. Hence the characteristic equation becomes

$$s^2 + 2\zeta_f\omega_n^{(2-\alpha)}s^{\alpha} + \omega_n^2 = 0 \tag{2.24}$$

The fractional derivative model for the magnetic damping was not the main issue of the thesis and is therefore not considered further in the thesis.

2.1.3 Hysteretic damping analyses and noncausality

Because the hysteretic damping models are usually represented in the frequency domain, accordingly the frequency domain techniques have been used to solve the equations of motion of structures modelled in this way. Crandall [8] investigated the problem of the impulse response of a simple oscillatory system with structural damping by using the Fourier integral. Gaul *et al.* [19] considered the linear model as a constant hysteretic damping or structural damping. The transient free vibration as well as the impulse response of a single degree of freedom oscillator with structural damping is calculated analytically by contour integration. The results for impulse response are in agreement with those obtained by Crandall. Another work can be found in the paper by the same author [20]. Woodhouse [21] mentioned that the complex module should be defined in the frequency domain. Although in some cases the complex moduli are almost independent of frequency in the low audio range, considerations of causality show that it is not possible for the complex modulus to be entirely independent of frequency. Thus, if the inverse Fourier transformation is used to obtain results in the time domain, this inevitable frequency dependence of the complex module must be taken into account. Tsai [22] presented a procedure to ensure that the calculated response of the rate-independent damping model conforms to the prescribed condition at the initial time. First, response functions excited by unit initial displacement and unit initial velocity respectively, are derived in the frequency domain. A free vibration response composed of these unit response functions is then superposed on the steady-state response solved by the discrete Fourier transform, so that the calculated transient response can satisfy the initial condition.

The linear hysteretic damping model is noncausal. This is because a small response occurs prior to the application of the excitation. This important feature has been investigated by Crandall [8] and Gaul [19]. Feriani and Perotti [23] discussed the noncausal phenomenon again. They evaluated the unit-impulse function of SDOF with hysteretic damping by the FFT technique, as the inverse Fourier Transform of the frequency response function. If the hysteretic impulse frequency response function is separated into the real part and imaginary part, they proved that the impulse response at time $t=0$ is only introduced by the integration of the real part of the frequency response function. The integration of the imaginary part of the frequency

response function at time $t=0$ is zero because the imaginary part of the frequency response function is odd and its inverse transform is everywhere continuous [24]. Nashif *et al.* [25] interpreted that for the linear hysteretic damping, if stiffness k and loss factor η are considered as constant, the integration calculation will lead to noncausality. This happens because for all physically real materials or systems, k and η must vary with the frequency over a sufficiently wide range and cannot be constant. If $k(\omega)$ and $\eta(\omega)$ are expressed by functions of the frequency representing actual measured data, no problems of noncausality can arise.

Although the frequency analysis provides a better flexibility to deal with dissipative effects, the time-domain method is sometimes more straightforward and without being restricted to the limitation of linear system problems. Inaudi and Kelly [26] proposed a time-domain representation for linear hysteretic damping and developed a step-by step iterative technique using Hilbert transform to solve the equations of motion of structures with linear hysteretic damping. This method can be extended easily to multiple degree of freedom (MDOF) systems and nonlinear systems. However the convergence condition has to be satisfied when this iterative method is used. The Hilbert transform is used here because of its property that the transform does not change the amplitude of a sine or cosine signal and only produces a phase angle shift of $\pi/2$ in these signals. Meanwhile, the Hilbert transform operator is also noncausal, because in order to calculate the transformed signal, the original signal function is required in the whole time region from $-\infty$ to ∞; meaning that the future of the signal is required to compute the Hilbert transform of the signal at the present time. An important understanding is that Hilbert transform changes the signal between time-domain and time-domain while Fourier transform transfers the signal between time-domain and frequency-domain. Other applications of a time-domain method using Hilbert transform were in Inaudi and Makris *et al.* [27, 28, 29].

Chen and You [30, 31] employed a direct iteration method to solve the time-domain equation for harmonic excitation. The hysteretic loop is constructed by using the time-domain approach. An integral-differential equation in the time domain is used for the free vibration of a SDOF system with hysteretic damping. The integral of the

Hilbert transform is embedded in the integral-differential equation and is calculated numerically using Cauchy's principle.

2.2 Structural modification

The problem of vibration absorption has appeared in practical engineering science and been studied for several years. In many cases, structural modification is a very effective way to avoid unwanted vibration. Another method is to connect some vibration absorbers to the original system.

The earliest classical vibration absorber was found in Frahm's patent in 1909 [32]. In 1928, Ormondroyd and Den Hartog [33] firstly investigated the theory of the vibration absorber in their paper. In the famous book "Mechanical vibrations" by Den Hartog [34], the vibration absorber design is also be thought of as structural modification problem to change the natural frequency of the system and produce antiresonance at the appointed frequency. To the present day, more complicated modifications have been extensively studied for the vibration problems of natural frequencies and antiresonances. These works investigate both mathematical theories of vibration absorption and their application examples.

Inman [35] has introduced the basic design principle of the single degree of freedom system with an absorber attached. More complicated structure modification designs can be used for more general dynamical properties assignments for such as natural frequencies and antiresonances, eigenvalues and eigenvectors, poles and zeros, form of receptances and nodes etc. In their paper, Sun *et al.* [36] gave a review of modern absorber developments. Mottershead and Ram [37] reviewed a great range of literature on structural modification problems for vibration absorption. They proposed to explain the mathematical theories of structural modifications as applied to the problem of vibration absorption in elasto-mechanical systems. Their work included both passive modifications and active controls. In this chapter, we make a brief review of the vibration suppression literature.

2.2.1 Natural frequency and mode shapes

Ewins [38] has presented a very general methodology to predict the changes of dynamical properties resulting from a given structural modification. The modified egienvalues and eigenvectors can be determined through the new mass matrix and stiffness matrix. They are defined using mode shapes of the original system, which might be obtained by a modal test.

If we consider the motion equation of the modified system

$$(\mathbf{M}+\Delta\mathbf{M})\ddot{\mathbf{x}}+(\mathbf{K}+\Delta\mathbf{K})\mathbf{x}=\mathbf{0} \tag{2.25}$$

Then, using the original system modal transformation $\mathbf{x}=[\Phi]\mathbf{p}$, we can get.

$$(\mathbf{I}+[\Phi]^T\Delta\mathbf{M}[\Phi])\ddot{\mathbf{p}}+(\Lambda+[\Phi]^T\Delta\mathbf{K}[\Phi])\mathbf{p}=\mathbf{0} \tag{2.26}$$

in which, $\Lambda=diag(\omega_1^{\,2},\omega_2^{\,2},...,\omega_N^{\,2})$

Thus, the new mass matrix and new stiffness matrix are described as

$$\mathbf{M}'=\mathbf{I}+[\Phi]^T\Delta\mathbf{M}[\Phi] \tag{2.27}$$

$$\mathbf{K}'=\Lambda+[\Phi]^T\Delta\mathbf{K}[\Phi] \tag{2.28}$$

Then, the eigenvalues and eigenvectors of these new mass and stiffness matrices can be calculated by the usual method. The natural frequency and mode shapes of the modified structure are obtained.

It can be found that this method doesn't require that all the mode shapes are measured. If we only have the information about m ($m<N$) modes at n ($n<N$) coordinates, the new mass matrix can be calculated by

$$\mathbf{M}'_{m\times m}=\mathbf{I}_{m\times m}+[\Phi]^T{}_{m\times n}\Delta\mathbf{M}_{n\times n}[\Phi]_{n\times m} \tag{2.29}$$

Weissenburger [39, 40] is the author who firstly addressed the inverse structural modification problem. The objective of the inverse problem is to determine the modification needed to assign some predefined dynamic behaviour such as the natural frequencies and antiresonances. Weissenburger concentrated his work on undamped systems. He considered the mass modifications as a symmetric unit rank effect on the eigenvalue problem of the original system as shown in equation

$$(\mathbf{K}-\overline{\omega}_j^2\mathbf{M}-\overline{\omega}_j^2\delta m\mathbf{u}\mathbf{u}^T)\overline{\Phi}_j=\mathbf{0} \tag{2.30}$$

in which, δm is the mass modification, $\mathbf{u}$ is a unit vector column that indicates the position of the structural modification. $\overline{\omega}_j$ and $\overline{\mathbf{\Phi}}_j$ are *j*th natural frequency and *j*th mode of the modified system.

Pomazal and Snyder [41] extended Weissenburgers' work to damped systems and considered the best choice of modification coordinates. They determined the eigenvalues and eigenvectors of a discrete linear vibration system resulting from the addition or removal of a discrete element. In their procedure, the modified characteristic equation is directly generated by using the known characteristics of the original system.

Dowell [42] considered the general placement pattern of natural frequencies after modification through an added mass and spring by using a Rayleigh quotient approach. The simple unit-rank modifications method, such as an addition of a mass, is applied to assign a single natural frequency. Only the measurement of the point receptance at the modification coordinate at the frequency is required. However, the practice of adding a spring is more difficult than an added mass case.

Another inverse problem work was considered by Bucher and Braun [43, 44]. In their paper, structural modifications are required in order to reallocate eigenvalues and specify eigenvectors. They developed an exact method for the assignment of vibration mode shapes by extracting the left eigenvectors from receptances. Their work showed how the necessary mass and stiffness modifications could be computed using modal test results only, even when only a partial set of eigensolutions is available from such tests. They proved that the steady-state response of the structure could be expressed exactly by the truncated modes when this structure is excited by a force vector that lies in the span of the truncated left modal vectors. Based on this, they concluded that the modal vectors of the modified structures could be formalised exactly by the superposition of the modal vectors of the unmodified structure. And they used this modifications method to assign predefined eigenvectors that locate in the subspace of the truncated modes. For those modes that are not in this subspace, they applied the least-squares method to find the mode in the original subspace that lies closest to the desired eigenvector.

Ram and Braun [45] considered the assignment of mode shapes as an optimised inverse eigenvalue problem. The optimisation aimed to find those changes of mass and stiffness that approximate best some desired dynamic response by minimising the Frobenious norm of a residual matrix. The desired behaviour was expressed by natural frequencies and mode shapes. The modified eigenvectors were constrained to the linear span of the measured original truncated experimental mode shapes.

Tsuei and Yee [46] developed a method to change natural frequencies by using measured frequency response data. They treated the modification matrices $\delta\mathbf{M}$ and $\delta\mathbf{K}$ as forcing on the unmodified structure.

$$\mathbf{M}\ddot{\mathbf{x}} + \mathbf{K}\mathbf{x} = -(\delta\mathbf{M}\ddot{\mathbf{x}} + \delta\mathbf{K}\mathbf{x}) \tag{2.31}$$

They discussed the structure of matrices $\delta\mathbf{M}$ and $\delta\mathbf{K}$, and then they derived the $\delta\mathbf{M}$ and $\delta\mathbf{K}$ that provided a predefined natural frequency ω_i. In this paper they also showed the sensitivity of the modification parameters with respect to the desired frequency. In another paper [47], the same authors applied the same method to determine the necessary mass and stiffness modifications that assign the damped natural frequencies of a viscously damped system. It is demonstrated that the natural frequencies of a structure can be assigned by local modifications and by using only the frequency response functions at the modification positions.

Similarly by treating the modification as a forcing term on the unmodified structure, Kyprianou, Mottershead and Ouyang [48] demonstrated the assignment of natural frequencies and antiresonances by the added mass connected by one or more springs. The added mass and stiffnesses are determined using receptances from the original system. And realistic modifications should be bounded within certain frequency ranges. They also discussed the effect of the modification on the natural frequencies not assigned and the antiresonances. They concluded that it is impossible to assign more than two natural frequencies independently by using only a simple spring-mass absorber. In order to assign a third natural frequency independently, they connected an additional spring between the added absorber mass and another coordinate.

Ram and Elhay [49] investigated an inverse eigenvalue problem solved by a multi degree of freedom vibration absorber. They demonstrated that the oscillations of the original system at frequency ω_i may be absorbed when a multi degree of freedom vibration absorber with eigenvalue (natural frequencies) ω_i is attached to the original structure. Cha and Pierre [50] also considered the multi degree of freedom absorber application case. They used oscillators in a chain form to assign nodes to the original system.

The simple modifications such as the addition of masses and grounded springs can be easily implemented and only require the measurement of translational receptances at the connection coordinates. However, realistic modifications of practices are more complicated since both rotation receptance and translation receptance measurement are required. Mottershead, Kyprianou and Ouyang [51] discussed the method called the "T-block" approach to determine a full matrix of receptances for in-plane motion of a beam structure. The T-block is attached to the structure at the modification point, so that a force applied to the T-block generates a moment together with a force at the connection point between the T-block and the original structure. In their subsequent paper [52], the same authors solved the inverse problem of structural modification by an added beam. The dimension of the cross section of the beam was determined in order to assign natural frequencies or antiresonances as predefined.

Singh and Ram [53] investigated the dynamic absorption for conservative systems and a criterion for implementing the control by either passive or active control. They also extended the analyses of the stability of the system and damped systems.

2.2.2 Receptance modelling

In 1941, Duncan [54] firstly addressed the problem of combining two or more dynamical systems. The problem considered was to determine the dynamic behaviour of a compound system formed from two or more subsystems with known receptances and known interconnection properties. This approach is now considered to be a direct structural modification method.

Bishop and Johnson [55] described the properties of receptances and method for the straightforward structural modification problem called "receptance modeling" in detail. The dynamic behaviour of the overall system could be determined through the effect of linking subsystems by using their separate receptances. And the effect of structural modifications on the system receptances may be determined when the receptances of the original system at the modification coordinates are measured.

Ram [56] developed a general formula to determine the receptances of a compound system using measured receptances from the separate components. He calculated the eigenvalues of damped subsystems with known connections using transfer function and modal data from the separate subsystems. It requires the inversion of a matrix of connection-point receptances, which is known to be an ill-posed problem [57, 58].

Vincent [59] took the first application of receptance modelling for the assignment of antiresonances. He developed the method now known as the "Vincent circle", thereby the problem of vibration absorption then transfers to find the point on the circle closest to the origin of the complex response. Furthermore, Done and Hughes [60] described this method in detail. And Nagy [61] extended the Vincent circle analysis to a spring-mass absorber application.

Lallement and his colleagues [62, 63] considered another application of receptance modeling, sometime called as pseudo-testing, which aims to determine of the receptances of a modified system from measured receptances of the original structure. They concentrated on the antiresonance constraints. Similar work has taken by Nalitolela, Penny and Friswell [64]. Mottershead, Mares, and James [65] used a pseudo test on aero-engine casings to separate close natural frequencies that appear because of the close axisymmetry of the test structures.

2.2.3 Nodes and zeros

The effect of structural modifications on the system receptances may be determined when the receptances of the original system at the modification coordinates are measured. Mottershead, Mares and Friswell [66] used an inverse method to assign nodes of vibration by the addition of grounded springs and concentrated masses. The

method is based only upon measured receptances at the coordinates of the nodes and the modifications. The modifications were determined from the null space of a matrix containing the measured vibration data. And a finite element model is not necessary.

Mottershead and Lallement [67] cancelled poles with zeros by a receptance modelling method, and thereby created a vibration node of an undamped structure. They assigned natural frequencies and antiresonances at the same values with the theory of unit rank modification [39, 40]. The anti-resonance frequencies are the eigenvalues of the adjoint system in mathematics. And the system can be obtained by deleting a row and a column from the original dynamic stiffness matrix.

Li *et al.* [68] used a method that required the **K**, **C**, **M** matrices to create a global pole-zero cancellation, that is to cancel a natural frequency with an antiresonance, while another uncancelled pole was left at the same frequency. The cancellation can be achieved either for a single-frequency response function or for all frequency response functions of the system.

Another work can be found in the paper by Li *et al.* [69]. In this paper, the author discussed the problem of antiresonance assignment and used the adjoint system to eliminate a resonance peak by creating a node. They obtained the eigenmodes from the adjoint system. But their analysis was limited by the necessity to find the modes of the "grounded" system having eigenvalues corresponding to the antiresonances.

Inman [35] gave a good description of the dynamic vibration absorber, which can be though as a device for the assignment of point-receptance zeros. When the classical undamped absorber is applied, the zeros locate on the imaginary axis of the complex eigenvalue plane while zeros generally become complex in the case when the absorber includes a damper.

Mottershead [70] investigated the problem of assignment of zeros in point and cross receptances by passive stiffness, damping, and mass modifications. He developed a method of the adjoint system to determine the eigenvalues, eigenvectors and receptances by using measured receptances. In order to derive the frequency response function matrix of the adjoint system from the original frequency response matrix, he

applied force constraints to measured receptances at the modification coordinates. And then he used the adjoint frequency response function matrix to assign zeros at predetermined frequency values. In this paper antiresonances were assigned to a by passive modification for the first time.

According to the paper by Mottershead [71], the zeros of different point and cross receptances generally occur at different frequencies, whereas the poles are unchanged. They can be determined by investigating the subsidiary matrices formed by deleting a single row and column from the stiffness and mass matrices of the system. When the row and column have the same index the resulting matrix system will be symmetric and its eigenvalues will be the zeros of a point receptance. They will interlace the eigenvalues of the poles. However, the same author [72] has also shown that when the deleted row and column have different indices the resulting matrices will not be symmetric, interlacing rules will not apply, and the zeros may become complex and/or defective.

2.3 Sensitivity analyses

Structural sensitivity is often used in system dynamic analysis, such as structural modification, system optimization, and system identification and control. Sensitivity analysis aims to study the effect of changes in system dynamic characteristics with respect to parameter variables. Many different methods have been developed in the last four decades for sensitivity theory and computation efficient of sensitivity.

The most commonly quoted literature about sensitivity theory may be Fox and Kapoor's paper "Rates of Change of eigenvalues and eigenvectors" [73]. They analyzed the sensitivity of the natural frequencies by determining the first order partial derivative of the eigenvalues and eigenvectors with respect to the modification parameters. It is shown that both the sensitivity of eigenvalue and the sensitivity of eigenvector to updating parameters involve only the eigenvalue and eigenvector under consideration and the known quantities. While the sensitivity of eigenvalue is in a simple expression, the calculation of the sensitivity of eigenvector requires an inversion of a full order matrix. Another formula of the sensitivity of eigenvector in

the same paper is expressed as a sum of all the eigenvectors defined by the eigensystems.

If we consider the structural eigenvalue problem

$$(\mathbf{K}-\lambda_j\mathbf{M})\mathbf{\Phi}_j=\mathbf{0} \quad j=1,2,\ldots,n \tag{2.32}$$

The sensitivity of eigenvalues can be claculated as

$$\frac{\partial\lambda_j}{\partial\theta}=\mathbf{\Phi}_j{}^T\left(\frac{\partial\mathbf{K}}{\partial\theta}-\lambda_j\frac{\partial\mathbf{M}}{\partial\theta}\right)\mathbf{\Phi}_j \tag{2.33}$$

and the sensitivity of eigenvector can be calculated as

$$\frac{\partial\mathbf{\Phi}_j}{\partial\theta}=-\left[(\mathbf{K}-\lambda_j\mathbf{M})^2-2\mathbf{M}\mathbf{\Phi}_j\mathbf{\Phi}_j^T\mathbf{M}\right]^{-1}\left[(\mathbf{K}-\lambda_j\mathbf{M})\left(\frac{\partial\mathbf{K}}{\partial\theta}-\lambda_j\frac{\partial\mathbf{M}}{\partial\theta}\right)+\mathbf{M}\mathbf{\Phi}_j\mathbf{\Phi}_j^T\frac{\partial\mathbf{M}}{\partial\theta}\right]\mathbf{\Phi}_j \tag{2.34}$$

or in another way,

$$\frac{\partial\mathbf{\Phi}_j}{\partial\theta}=\sum_{k=1}^{n}A_{jk}\mathbf{\Phi}_k \tag{2.35}$$

$$\text{in which, } A_{jk}=\frac{\mathbf{\Phi}_k{}^T\left(\frac{\partial\mathbf{K}}{\partial\theta}-\lambda_j\frac{\partial\mathbf{M}}{\partial\theta}\right)\mathbf{\Phi}_j}{(\lambda_j-\lambda_k)} \tag{2.36}$$

However, Fox's work is restricted to conservative systems. It means that only symmetric eigenvalue problems with the changes of physical parameters in mass and stiffness matrices are considered. As significant extension works, Rogers [74] and Garg [75] investigated the unsymmetrical eigenvalue problems. Nelson [76] provided a simplified method to calculation the sensitivity of eigenvector of arbitrary *n*th order symmetric or unsymmetrical systems. This procedure only requires the left and right eigenvectors and associated eigenvalues under consideration. By using this method, the sensitivity of eigenvector may be expressed to a combination of one vector with a factor multiplied by the considered eigenvector. But an *N*-1 dimension matrix inverse is also need to solve the linear algebraic equation.

Yoshimura [77] derived the design sensitivity coefficients of frequency response evaluative functions including the sensitivity of modal flexibility, sensitivity of

damping ratio and sensitivity of receptance. These design sensitivity coefficients can be calculated using partial derivative of fundamental structural elements such as stiffness, mass and damping matrices with respect to a design variable vector. He later used design sensitivity analyses and evaluated parameters to improve machine structural dynamics [78]. Later, Lin and Ewins [79] improved his derivation of the receptance sensitivity in their work on the structural finite element model improvement.

Brandon has a series of papers on system sensitivity including high order sensitivity analysis [80, 81] and receptance sensitivity analysis [82] in particular. And he [83] undertook a review of sensitivity analyses of eigenvalue and eigenvector in the book "Strategies for structural dynamic modification". Here, he described two primary applications of sensitivity analysis. The first is aim to indicate the location and approximate scale of design changes cause by structural properties. The second is to directly predict the effects of proposed structural changes. Besides, he also mentioned the benefit of higher order sensitivity as a measure of confidence in the application. Also in his book, Brandon presented the sensitivity of frequency responses that can be obtained in two ways, binomial form and Kron's equation. Neither of them requires the explicit evaluation of modal properties. However, it should be noticed that the convergence criterion has to be satisfied when matrix binomial expansion is considered. As examples of application of response sensitivities, he derived the response sensitivity with respect to simple design modifications, such as response sensitivity with respect to mass, response sensitivity with respect to stiffness and response with respect to damping.

Chen [84] computed the sensitivities of eigenvalues, eigenvectors and frequency responses in a reduced approximate model. He considered the complex frequency response function, and discussed the sensitivities of both real part and imaginary part of the frequency response. Consequently the sensitivities of the amplitude and phase angle of frequency response were obtained. The sensitivities of frequency response for the modified structure were also derived in the approximate model.

Kajiwara and Nagamatsu [85] defined the sensitivity of anti-resonance frequency in a new way. They derived the sensitivity of anti-resonance frequency by using the

reciprocal of eigenvalue instead of eigenvalue itself. Furthermore, Mottershead [71] investigated the sensitivity of the zeros and system antiresonances. It was demonstrated that the sensitivities of the zeros may be expressed as a linear combination of the sensitivities of the eigenvalues and mode shapes, and thus the zeros of the model cannot be converged independently of the eigenvalues and eigenvectors. In addition, the sensitivities of the closest eigenvalues and mode shapes are shown to contribute most to the sensitivities of the zeros in a numerical exercise.

In order to improve computation efficiency, Lim *et al.* [86] proposed an improved modal method, which aims to derive the required eigenvalue derivatives approximately by using the calculation of lower modes and the known flexibility. This method has been successfully applied by Lin *et al.* [87] to the case of analytical modal improvement. Lin and Lim [88] developed an effective method to calculate the sensitivities of receptance, eigenvalue and eigenvector from limited vibration test data. Unlike previous method, this method does not need accurate finite element models. They also demonstrated that design sensitivities calculated directly from measured data are more accurate than those calculated from finite element models because structural modelling errors are inevitable due to the complications of engineering systems.

2.4 Vibration optimisation

The damped vibration absorber is itself a passive vibration system, and has been used for many years [34, 89]. An important problem is to find the absorber system guarantee to minimise the design criteria of the system dynamical behaviour, which also is an optimisation procedure. The optimum design is focused on a set of absorber parameters, i.e., the absorber mass, stiffness, and damping ratio. Den Hartog [34] and Inman [35] have discussed the vibration suppression effect of the simple one SDOF system connected with a tuning damped absorber and computed the absorber optimisation parameters. However, it should be noticed that it will be more complicated for MDOF system with multi absorbers because the optimisation equations became the non-linear considering the more design parameters and even the parameter of the position of the absorbers. In order to solve these nonlinear equations,

many optimisation methods have been applied in the procedures. And the task frequency regions of the optimal absorber may also expand from one or two special resonance frequencies to the whole frequency domain.

2.4.1 Min-Max optimisation

Most optimum works are mainly involved in the minimisation of the maximum values of the transfer function. Kitis *et al.* [90, 91] proposed an efficient optimal design method for steady state vibration under harmonic loading for a range of excitation frequencies has been developed. This reduction is achieved by an effective re-analysis technique for computing both the cost function and its derivatives. Since the design goal is to suppress vibration response of selected system degrees of freedom over a certain range of excitation frequencies, the objective function to be minimised is

$$G(x) = \max_{\substack{\Omega_1 \le \omega \le \Omega_2 \\ j \in J}} \left| u_j \right| \tag{2.37}$$

where, u_j is the displacement response. $[\Omega_1, \Omega_2]$ is the frequencies interval, and J is an integer set specifying response components of interest.

Jorkama and Hertzen [92] investigated the optimal absorber for a rotating Rayleigh beam. The optimisation consists of minimising the maximum of the frequency response function in the vicinity of the original resonance that is to be attenuated. This min-max problem is solved by first finding the maximum of the two peaks (due to the absorber and original beam resonance) using a global maximisation algorithm, and then by determining the tuning and damping values to minimise this maximum value.

In Koo *et al.*'s work [93], the performances of each of the optimised cases were compared along with the equivalent passive model using the peak transmissibility criteria. The transmissibility is defined as the ratio of output displacement of the structure to input displacement excitation. Smaller value of transmissibility indicates more vibration reduction. Another work aiming at the minimisation of the transmissibility by proper selection for the absorber parameters was taken by Vakakis and Paipetis [94].

2.4.2 Objective functions

In another aspect on optimal work, optimisation functions (objective functions) rather than minimising the maximum displacement has been examined widely. Soom and Lee[95] applied nonlinear programming techniques to obtain optimal tuning and damping parameters for dynamic absorbers. They discussed an example where an absorber is attached to the primary single degree of freedom system. In their work, they considered objective functions as optimisation criteria rather than minimising the maximum displacement. The objective functions to be used are based on information at a number of discrete points on the displacement response curves of the primary main mass. Assuming the steady state responses of the primary main mass is $x_1 = |A_1| \cos(\omega t + \phi_1)$, the following objective functions are considered.

1) $F_1 = \text{maximum}(|A_1|)$ (2.38)

This function minimises the maximum value of the displace response in the frequency domain.

2) $F_2 = \sum(|A_1| - 1)^2$ at frequencies where $|A_1| > 1$ (2.39)

This function minimises the part of the frequency response where there is some dynamic amplification of motion.

3) $F_3 = \text{maximum}(\omega|A_1|)$ (2.40)

This function minimises the maximum velocity in the linear case.

4) $F_4 = \sum|A_1|^2$ (2.41)

This function minimises the mean squared displacement response to white noise excitation for linear systems.

5) $F_5 = \sum(\omega|A_1|)^2$ (2.42)

This function minimises the mean squared velocity response to white noise excitation for linear systems.

Their results show that objective functions, other than the traditional one minimizing the maximum amplitude, lead to different optimal design parameters.

Ro and Baz [96] developed the optimal placement strategies of the active constrained layer damping (ACLD) patches, which are devised using the modal strain energy (MSE) method. In this work, the MSE distribution is calculated using a finite element

model of the plate. The patches are applied to the elements with the highest MSE in order to target specific mode of vibration. The optimisation procedure aims at minimizing the total weight of the treatments while satisfying constraints imposed on the modal damping ratios.

Huang and his colleagues [97, 98] studied the optimal design of dynamic absorbers for reducing the vibration and the interior noise of an aircraft's fuselage. Optimum design of absorbers is studied for obtaining the minimum vibration of the fuselage or the minimum noise level. In order to minimise the vibration, the kinetic energy (KE) of the entire shell is chosen as the object function.

In Thompson's work [99], the optimal tuning dynamic vibration absorber was computed together with the objective function, the mean-square tyre dynamic deflection for a random load input. The mean-square motion has also been used as the objective function in Jacquot's work [100], in which he studied the effect of the application of the absorber to suppress stationary random vibration of rectangular simply supported plate. Jacquot's paper [101] considers the addition of damping to a beam system in order to limit the response due to random forcing. The optimisation process for such a method uses an objective function called as the spatial average of the mean square response over the extent of the beam.

Nagaya *et al.* [102] designed a magnetic damping absorber for the higher modes. In order to have the optimal parameters of the absorber, the cost function of an integration of the vibration amplitude of displacement in the considered frequency region was taken into account, and the optimal absorber parameters make the cost function minimum. The frequency response curve near higher peaks is divided into n-pieces for n-higher peaks in the considered region. Each divided curve is integrated with respect to the frequency in the considered frequency region from Ω_{1i} to Ω_{2i} for *i*th piece.

2.4.3 Optimisation Methods

Lai and Liao [103] studied the semi vibration control of a suspension a system via a magnetorheological fluid damper. In order to obtain the optimised parameters for magneto-rheological fluid damper model from the experimental data, a least-squares optimisation method was used. Some parameters were estimated by minimizing the error between the model-predicted force and the force from experimental result.

In Zuo and Nayfeh's paper [104], a descent-subgradient method was used to maximize the minimal damping in a prescribed frequency range for a general structure to which was attached a MDOF tuned-mass damper (TMD) or multiple SDOF TMDs. Taking the location and inertias of the absorbers as well as the locations of the springs and dampers connecting the absorber as an optimisation problem in the framework of decentralized static output control in state space.

H_2 and H_∞ approaches are widely employed in the optimisation control procedure. It is based on the linear quadratic regulator (LQR) design techniques, which was used as the replacement of the frequency domain technique, thus provides a time domain design method for tuning vibration absorber system. However, LQR controllers need a full state, i.e., all displacement and velocities, for the feedback. Stech [105] developed an improved H_2 approach for tuning vibration absorbers design based on output regulator theory. Two methods were considered, designed by subspace assignment, and design by subspace assignment combined with numerical optimisation. Arfiadi and Hadi [106] considered the H_2 norm as the performance measure of the optimality. In this type of performance objective, the norm of transfer functions form external disturbance to the regulated output should be minimal.

Genetic Algorithms are random search techniques, which was be used to solve difficult problems with objective functions that do not posses properties such as continuity, differentiability at all over the domain of interest. A basic characteristic of this method is that an initial population evolves over generations to produce new and hopefully better elements. The elements of the initial population are randomly or heuristically generated. As an example, Steffen, Rade and Inman [107] formulated a

general non-linear optimisation problem and used a genetic algorithm to minimise single or multi-objective functions, which are expressed using frequency response function relations. Based on this optimisation procedure, they proposed a general methodology for the optimal design of passive devices for vibration reduction in mechanical systems when several natural frequencies are present in the frequency band of interest.

Nagaya and Li [108] developed a method for obtaining optimal parameters for noise reduction absorbers. In this method, an integrated value of sound pressure in a frequency domain is taken as a cost function. Because the equation for predicting tuning parameters becomes non-linear with respect to the tuning parameters, and a number of parameters must be obtained from the non-linear equation, a neural network is used to obtain optimal parameters of vibration absorbers by minimizing the cost function in terms of the radiated sound.

2.5 Closure

The theories about hysteretic damping have firstly been presented in this chapter firstly. These theories involve the techniques, computation modelling and application. Since the traditional hysteretic damping is expressed in a similar complex form to the complex viscous damping, these research methods can be used analogously in the further analyses of complex viscous damping.

Also in this chapter, a comprehensive review of the theory of structural modification is given. These works show some study directions for the application of complex viscous damping in engineering science.

Chapter 3

Complex Magnetic Damping Model

A complex-damped model may represent the dynamic behaviour of elasto-mechanical systems when acted upon by a magnetic. The problem is how this complex viscous type damping affects the dynamical characteristics of a vibrating mechanical system. This chapter introduces briefly the concept of a complex magnetic damping model. Then, a thorough analysis of the complex-damped single degree of freedom mass spring system is presented. The analysis includes the root locus, the (non-causal) impulse response and the frequency response function. Dr. Bonisoli has mainly undertaken the work presented in this chapter [3-6].

3.1 Concept of complex viscous damping model

The magnetic model is based on the analogy of the equivalent currents method in a quasi-static open-circuit-type configuration. The model is used to determine the influence of eddy currents on the dynamic behaviour of structures made of paramagnetic or diamagnetic conducting materials inside a magnetic field.

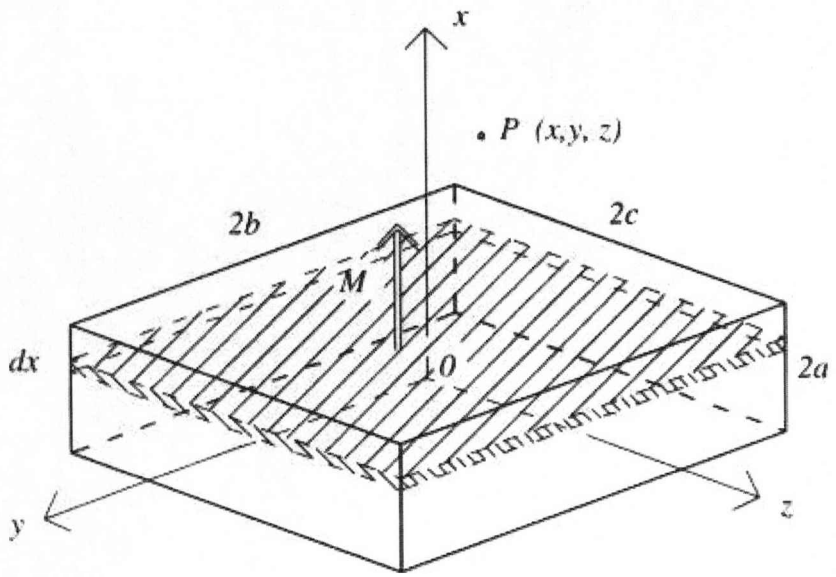

Figure 3.1 Permanent magnets geometry

The parallelepiped - rectangular shaped permanent magnet, shown in Figure 3.1 is considered. Based on the analogy of the equivalent current method, the magnet can be compared to a rectangular-coil solenoid. Thus, referring to the Laplace's inverse square law, the infinitesimal contribution to the magnetic induction dB in a point $P(x, y, z)$ at a distance d from the infinitesimal portion of the side of a rectangular coil $d\mathbf{s}$ is

$$dB = \frac{\mu_0 i}{4\pi} \frac{d\mathbf{s} \times \mathbf{u}_d}{d^2}$$

where d is the distance, identified by vector $\mathbf{u}_d$, from the infinitesimal portion $d\mathbf{s}$ set in $(u=0, v, w)$ of the side of a rectangular coil whose centre is in the reference system (x, y, z), $\mu_0 = 4\pi \times 10^{-7} H/m$, is the magnetic permeability of the vacuum and i is the current flowing through the coil. The vector product $d\mathbf{s} \times \mathbf{u}_d$, in the side of positive z parallel to y-axis, results

$$d\mathbf{s} \times \mathbf{u}_d = \frac{-(z-c)dv}{\sqrt{x^2 + (y-v)^2 + (z-c)^2}} \mathbf{i} + \frac{xdv}{\sqrt{x^2 + (y-v)^2 + (z-c)^2}} \mathbf{k} \qquad \textbf{(3.1)}$$

where, a, b and c are the magnet sides.

For the electro-mechanical analysis, the contribution along the x-axis of magnetisation needs to be considered. Integrating along the four sides of the rectangular coil, the infinitesimal contribute to the magnetic induction dB_x is

$$dB_x = \frac{\mu_0 i}{4\pi}\int_{-b}^{+b}\left(\frac{(z+c)}{[x^2+(y-v)^2+(z+c)^2]^{3/2}}-\frac{(z-c)}{[x^2+(y-v)^2+(z-c)^2]^{3/2}}\right)dv$$
$$+\frac{\mu_0 i}{4\pi}\int_{-c}^{+c}\left(\frac{(y+b)}{[x^2+(y+b)^2+(z-w)^2]^{3/2}}-\frac{(y-b)}{[x^2+(y-b)^2+(z-w)^2]^{3/2}}\right)dw \tag{3.2}$$

If the residual magnetisation M of the permanent magnet is replaced with the linked currents ni per length unit of the equivalent solenoid, then integrating along the length and assuming the relative permeability μ_r to be nearly unity, for the magnet sketched in Fig.1, the value of the magnetic induction B_x can be expressed as

$$B_x = \int_{-a}^{+a} dB_x(u) = \frac{\mu_0 M}{4\pi}\int_{-a}^{+a} f_x(u)du \tag{3.3}$$

where,

$f_x(u) =$

$$\begin{aligned}
&\frac{-(z+c)}{[(x-u)^2+(z+c)^2]}\cdot\frac{(y-b)}{\sqrt{[(x-u)^2+(y-b)^2+(z+c)^2]}}\\
&-\frac{-(z+c)}{[(x-u)^2+(z+c)^2]}\cdot\frac{(y+b)}{\sqrt{[(x-u)^2+(y+b)^2+(z+c)^2]}}\\
&+\frac{(z-c)}{[(x-u)^2+(z-c)^2]}\cdot\frac{(y-b)}{\sqrt{[(x-u)^2+(y-b)^2+(z-c)^2]}}\\
&-\frac{(z-c)}{[(x-u)^2+(z-c)^2]}\cdot\frac{(y+b)}{\sqrt{[(x-u)^2+(y+b)^2+(z-c)^2]}}\\
&+\frac{-(y+b)}{[(x-u)^2+(y+b)^2]}\cdot\frac{(z-c)}{\sqrt{[(x-u)^2+(y+b)^2+(z-c)^2]}}\\
&-\frac{-(y+b)}{[(x-u)^2+(y+b)^2]}\cdot\frac{(z+c)}{\sqrt{[(x-u)^2+(y+b)^2+(z+c)^2]}}\\
&+\frac{(y-b)}{[(x-u)^2+(y-b)^2]}\cdot\frac{(z-c)}{\sqrt{[(x-u)^2+(y-b)^2+(z-c)^2]}}\\
&-\frac{(y-b)}{[(x-u)^2+(y-b)^2]}\cdot\frac{(z+c)}{\sqrt{[(x-u)^2+(y-b)^2+(z+c)^2]}}
\end{aligned} \tag{3.4}$$

The gradient of the x-component of the magnetic induction is

$$\frac{dB_x}{dx} = -\frac{\mu_0 M}{4\pi}[f_x(u=+a) - f_x(u=-a)] \tag{3.5}$$

That is, the value of the variation of B_x over x evaluated in P equals the difference of the gradients of the magnetic induction originated by the two equivalent coils corresponding to the faces of the magnet.

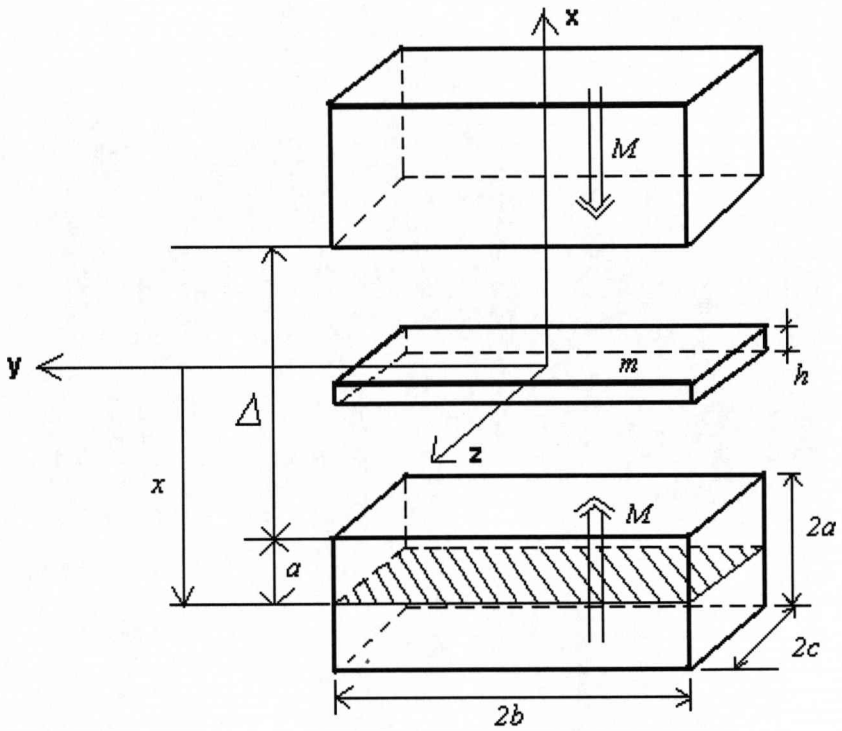

Figure 3.2 Geometric characteristics and pattern of the SDOF system

The magnetic model is then used to evaluate the gradient of the magnetic induction generated on the symmetry plane $x = 0$ by two equal magnets disposed with opposite directions of magnetisation as shown in Figure 3.2. Because of the symmetry of the configuration, the magnetic induction on the considered plane is zero. It is more rigorous to evaluate the mean value of the magnetic induction on the entire surface linked with the magnetic flux, rather than its axial value as an estimated for the whole surface. The reason is that any plane parallel with the terminal faces of the magnet is characterized by a variable distribution of both magnetic induction and its gradient. In regards to the magnitude of the gradient, the top value shows the effect of demagnetization because of the presence of the magnetic poles close to the terminal faces of the magnet. It also clear that variations of the air gap Δ between the two magnets significantly modify the distribution of the gradient of magnetic induction. Therefore the mean value on the whole surface crossed by the magnetic flux is estimated. Once the air gap has been fixed, the gradient of the mean magnetic induction $B_{x,m}$ is given by

$$\frac{dB_{x,m}}{dx} = \frac{2B_r}{4\pi(4bc)} \int_{-c}^{+c} \int_{-b}^{+b} [f_x(u=-a) - f_x(u=+a)] dydz \tag{3.6}$$

where $B_r = \mu_0 M$ is the residual magnetic induction. The spatial variable x is the distance from the middle plane of the vibration element to the middle plane of the magnets, that is, $x = 0.5\Delta + a$, in which, the Δ is the air gap dimension as shown in Figure 3.2.

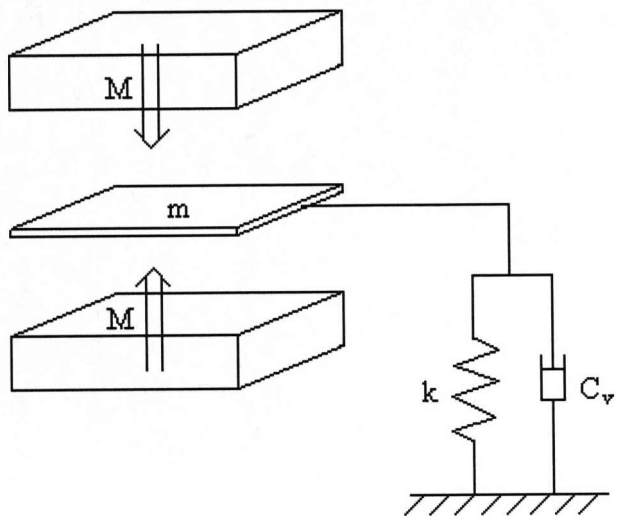

Figure 3.3 A SDOF system in a couple of magnets

Considering a single degree of freedom system of mass m, stiffness k and damping coefficient c_v as shown in Figure 3.3. A pair of equal permanent magnets with opposite magnetisation is located on both sides of the conducting mass characterised by resistively r and having the same dimensions as described in Figure 3.2. The influence of the two magnets as damping elements is analysed. And the equation of motion of the system is

$$m\ddot{x}(t) + (c_v + c_m)\dot{x}(t) + kx(t) = 0 \tag{3.7}$$

where c_m is the coefficient of the magnetic viscous damping produced by the Joule effect due to the flow of an induced current. The coefficient c_m can be obtained by

expressing the dissipated power P_d as

$$P_d = c_m \dot{x}^2 = \frac{fem}{R} = R\, i^2 \tag{3.8}$$

where i is the induced current, R is the electrical resistance of the conducting mass and fem is the electromotive force evaluated through Faraday's electromagnetic induction law

$$fem = -\dot{x} \int_s \frac{dB_x}{dx} ds \tag{3.9}$$

in which, $\frac{dB_x}{dx}$ represents the gradient of magnetic induction estimated as before.

Assuming a constant gradient of the magnetic induction on the whole surface and using permanent magnets with similar base size ($b \cong c$), the electromotive force is

$$fem(y) = -\dot{x} \frac{2b2c}{b^2} y^2 \frac{dB_{x,m}}{dx} \tag{3.10}$$

with $y \in [0, b]$, while the resistance of a ring of infinitesimal section hdy is

$$dR(y) = r \frac{4\frac{b+c}{b} y}{hdy} \tag{3.11}$$

Therefore, the global current i flowing through the vibrating element is

$$i = \int_0^{i_{max}} di(y) = \int_0^b -\dot{x} \frac{ch}{r(b+c)} \frac{dB_{x,m}}{dx} y dy = -\dot{x} \frac{b^2 ch}{2r(b+c)} \frac{dB_{x,m}}{dx} \tag{3.12}$$

Using equation (3.10) and (3.12), the global electrical resistance R is

$$R = r \frac{4(b+c)}{bh} \cong r \frac{8}{h} \tag{3.13}$$

Hence, the power P_d dissipated by Joule effect is proportional to the square of the velocity of vibrating element.

$$P_d = c_m \dot{x}^2 = \dot{x}^2 \frac{b^3 c^2 h}{r(b+c)} \left(\frac{dB_{x,m}}{dx} \right)^2 \cong \dot{x}^2 \frac{b^2 c^2 h}{2r} \left(\frac{dB_{x,m}}{dx} \right)^2 \tag{3.14}$$

Finally, the magnetic viscous damping coefficient c_m can be expressed as

$$c_m = \frac{b^2 c^2 h}{2r}\left(\frac{dB_{x,m}}{dx}\right)^2 \tag{3.15}$$

The flow of relevant induced currents inside the conductor generates a variable magnetic field that produces a magneto-elastic force. The essentially dynamic phenomenon, called "phantom effect", affects the response of the mass. If the mass is excited by a harmonic force $F = F_0 e^{j\omega t}$ with $\omega > 0$, the equation of motion of the system becomes

$$m\ddot{x}(t) + (c_v + c_m - jc_e)\dot{x}(t) + kx(t) = F_0 e^{j\omega t} \tag{3.16}$$

where c_e is the coefficient corresponding to the phantom effect and j is the imaginary operator, introduced because the associated elastic force $F_e = -c_e \dot{x}$ is conservative and there, even though proportional to the velocity. It is in phase with the displacement of the mass. c_e is defined by

$$c_e = \chi \frac{b^2 c^2 h}{2r}\left(\frac{dB_{x,m}}{dx}\right)^2 \tag{3.17}$$

where χ is called choking volume coefficient taking into account the fact that not all the circulating eddy currents produce a concordant resultant elastic force. And it results that c_m and c_e are linearly related.

3.2 Eigenvalue and root locus

If a dynamic system is considered with a complex viscously damped model, it means that we need to describe a dynamic increase of stiffness (or mass) proportional to velocity coupled with a viscous-type damping effect. Thus, the eigenvalue of the system is definitely changed. Now we investigate a single degree of freedom system

moving between a couple of permanent magnets as represented in Figure 3.3.

By using the complex magnetic damping model, the motion equation of the system may be written as.

$$m\ddot{x}(t)+(c_v+c_m-jc_e)\dot{x}(t)+kx(t)=f(t) \tag{3.18}$$

in which, c_v is the original viscous damping, (c_m-jc_e) is the complex damping coefficient. This equation could be written in the canonical form as

$$\ddot{x}(t)+2\zeta_m\frac{1+j\psi}{\sqrt{1+\psi^2}}\omega_n\dot{x}(t)+\omega_n^2x(t)=w(t) \tag{3.19}$$

$$\text{in which, } w(t)=\frac{f(t)}{m} \tag{3.20}$$

If we define that

$$\zeta_m=\frac{\sqrt{(c_v+c_m)^2+c_e^{\,2}}}{2\sqrt{km}} \text{ as the complex damping ratio} \tag{3.21}$$

$$\psi=\frac{-c_e}{c_v+c_m} \text{ as the imaginary part coefficient factor} \tag{3.22}$$

$$\text{and } \omega_n=\sqrt{\frac{k}{m}} \text{ as the natural frequency of the original system} \tag{3.23}$$

Suppose the initial conditions $x(0)=x_0$ and $\dot{x}(0)=\dot{x}_0$. The eigenvalue problem could be solved through the Laplace transform for this equation.

$$x(s)s^2+2\zeta_m\frac{1+j\psi}{\sqrt{1+\psi^2}}\omega_n x(s)s+\omega_n^2x(s)=W(s) \tag{3.24}$$

Thus, we get the characteristic equation as below

$$s^2+2\zeta_m\frac{1+j\psi}{\sqrt{1+\psi^2}}\omega_n s+\omega_n^{\,2}=0 \tag{3.25}$$

For the realistic property requirement, that is, the Fourier transform of the impulse response satisfies the conditions

$$\mathrm{Re}[H(\omega)] = \mathrm{Re}[H(-\omega)] \tag{3.26}$$

$$\mathrm{Im}[H(\omega)] = -\mathrm{Im}[H(-\omega)] \tag{3.27}$$

$$|H(\omega)| = |H(-\omega)| \tag{3.28}$$

$$angle[H(\omega)] = -angle[H(-\omega)] \tag{3.29}$$

Also the eigenvalues should be located symmetrically with respect to the real axis of the complex plane and have negative real part that demonstrates the system is stable. So, a **sgn** operator is introduced.

$$\mathrm{sgn}(v) = \begin{cases} 1 & if \quad v > 0 \\ 0 & if \quad v = 0 \\ -1 & if \quad v < 0 \end{cases} \tag{3.30}$$

Therefore, by using this **sgn** operator, we enforce the complex magnetic damping model to be stable.

Thus, the equation (3.25) is rewritten as

$$s^2 + 2\zeta_m \frac{1 + j\,\mathrm{sgn}(\omega)\psi}{\sqrt{1+\psi^2}} \omega_n s + \omega_n{}^2 = 0 \tag{3.31}$$

That is

$$s^2 + 2\zeta_m \frac{1 + j\,\mathrm{sgn}[\mathrm{Im}(s)]\psi}{\sqrt{1+\psi^2}} \omega_n s + \omega_n{}^2 = 0 \tag{3.32}$$

Then the eigenvalues can be found to be

$$s_1 = -\zeta_m \frac{1+j\psi}{\sqrt{1+\psi^2}} \omega_n + j\omega_n \sqrt{1 - \zeta_m{}^2 \frac{(1+j\psi)^2}{1+\psi^2}} \tag{3.33}$$

$$s_2 = -\zeta_m \frac{1-j\psi}{\sqrt{1+\psi^2}}\omega_n - j\omega_n\sqrt{1-\zeta_m{}^2\frac{(1-j\psi)^2}{1+\psi^2}} \tag{3.34}$$

They can be expressed in the couple form as

$$s_{1,2} = -\frac{\omega_n}{\sqrt{1+\psi^2}}\left[\zeta_m - \mathrm{sgn}(\psi)\sqrt{\frac{u-v}{2}}\right] \pm j\frac{\omega_n}{\sqrt{1+\psi^2}}\left[-\zeta_m\psi + \sqrt{\frac{u+v}{2}}\right] \tag{3.35}$$

where, $u = \sqrt{[(1+\psi^2)-\zeta_m(1-\psi^2)]^2 + (2\zeta_m\psi)^2}$ (3.36)

$$v = (1+\psi^2)-\zeta_m(1-\psi^2) \tag{3.37}$$

For two particular cases,

1) When $\zeta_m = 0$, it is a conservative system

$$s_{1,2} = \pm j\omega_n \tag{3.38}$$

The two eigenvalues are located on the imaginary axis in the complex plane.

2) When $\psi = 0$, it is a general pure viscous damped system

$$s_{1,2} = -\zeta_m\omega_n \pm j\omega_n\sqrt{1-\zeta_m{}^2} \tag{3.39}$$

which is a well-known result. The two eigenvalues are located on the circle with the radius of ω_n in the complex plane.

Figure 3.4 and Figure 3.5 show the root locus in the complex plane, for damping parameters $\zeta_m \geq 0$ and ψ. It is noted that all root loci will set out from the imaginary axis points $\pm j\omega_n$.

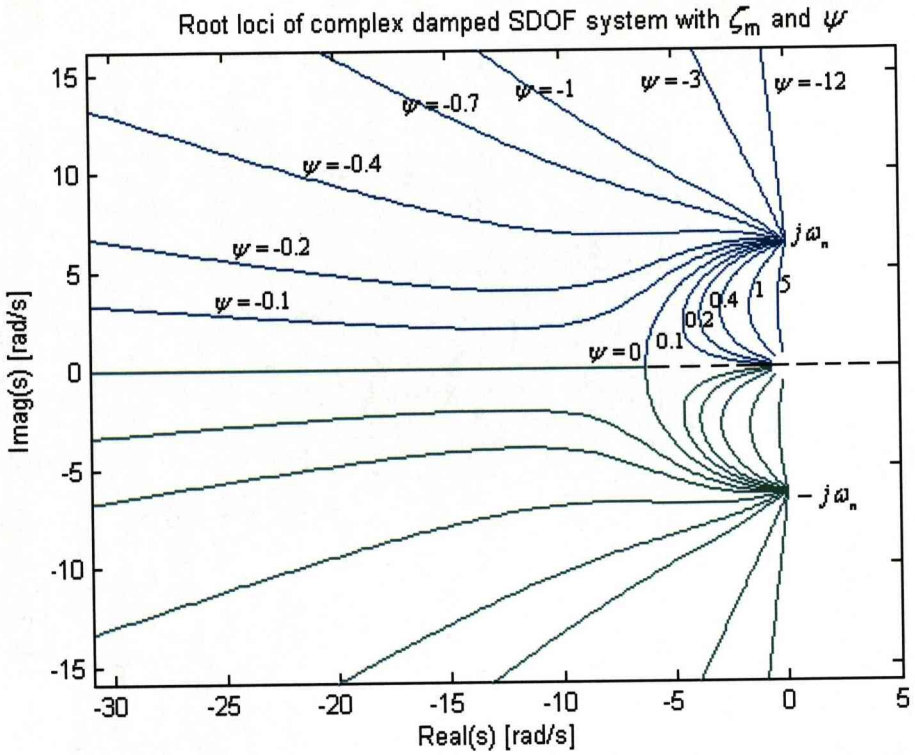

Figure 3.4 Root loci of a complex damped SDOF system with function of ψ

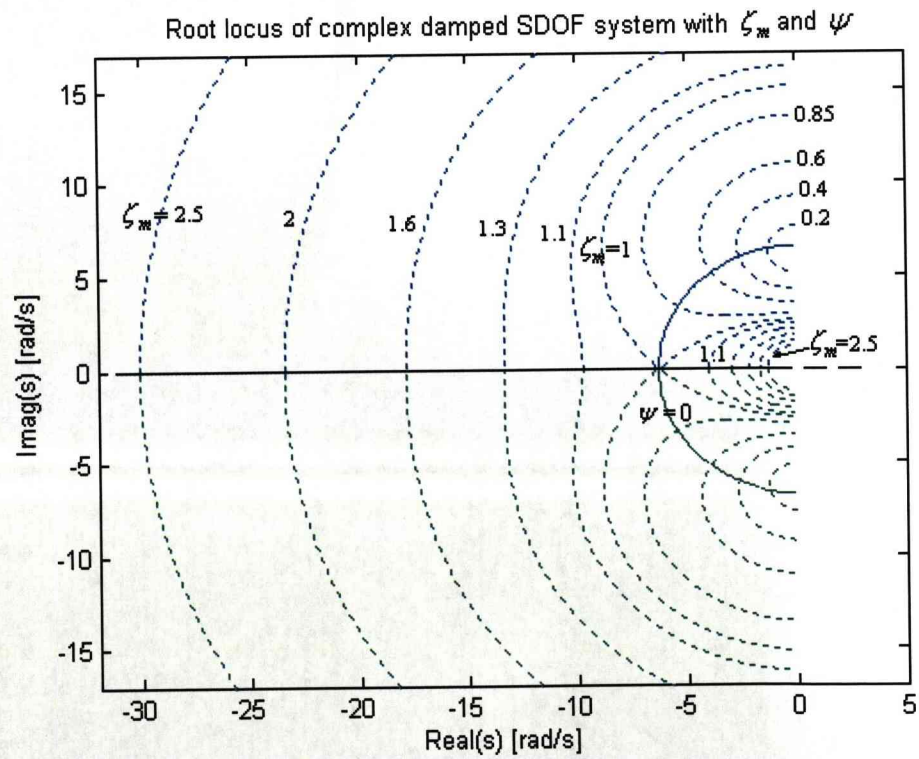

Figure 3.5 Root loci of a complex damped SDOF system with function of ζ_m

But their routes and ends with the increment of damping ratio ζ_m are different according to the values of ψ. When $\psi > 0$, the root locus takes an arc line and end at the zero point. When $\psi = 0$, the system is the pure viscous damping case, the root locus is not closed. It firstly goes along a circle and then goes out along the negative real axis to $-\infty$. When $\psi < 0$, the root locus is also not in closed form and diverges.

An important property is that all eigenvalues have the negative real part, which shows that complex viscous damped system is dynamically stable. The damped system will take an oscillation.

3.3 Frequency response function

Considering the above single degree of freedom system in the magnetic field subjected to harmonic excitation $f(t) = F_0 e^{j\omega t}$, in which ω is the excitation frequency, then the motion equation yields:

$$m\ddot{x}(t) + (c_v + c_m - jc_e)\dot{x}(t) + kx(t) = F_0 e^{j\omega t} \tag{3.40}$$

By setting $x(t) = X_0 e^{j\omega t}$, the equation is written as

$$[-m\omega^2 + j\omega(c_v + c_m - jc_e) + k]X_0 e^{j\omega t} = F_0 e^{j\omega t} \tag{3.41}$$

Hence, the non-dimension frequency response function can be written in form as.

$$H(\omega)=\frac{X_0}{\left(\frac{F_0}{k}\right)}=\frac{1}{1+j\omega\frac{(c_v+c_m-jc_e)}{k}-\frac{m}{k}\omega^2} \tag{3.42}$$

or it can be expressed by using the previous definitions

$$H(\omega)=\frac{1}{1+j2\zeta_m\frac{1+j\,\mathrm{sgn}(\omega)\psi}{\sqrt{1+\psi^2}}\left(\frac{\omega}{\omega_n}\right)-\left(\frac{\omega}{\omega_n}\right)^2} \tag{3.43}$$

The modulus and phase angle of the frequency response function can be calculated as,

$$|H(\omega)|=\frac{1}{\sqrt{\left[1-2\zeta_m\frac{\mathrm{sgn}(\omega)\psi}{\sqrt{1+\psi^2}}\left(\frac{\omega}{\omega_n}\right)-\left(\frac{\omega}{\omega_n}\right)^2\right]^2+\left[2\zeta_m\frac{1}{\sqrt{1+\psi^2}}\left(\frac{\omega}{\omega_n}\right)\right]^2}} \tag{3.44}$$

$$angle[H(\omega)]=arctg\left[\frac{-2\zeta_m\frac{1}{\sqrt{1+\psi^2}}\left(\frac{\omega}{\omega_n}\right)}{1-2\zeta_m\frac{\mathrm{sgn}(\omega)\psi}{\sqrt{1+\psi^2}}\left(\frac{\omega}{\omega_n}\right)-\left(\frac{\omega}{\omega_n}\right)^2}\right] \tag{3.45}$$

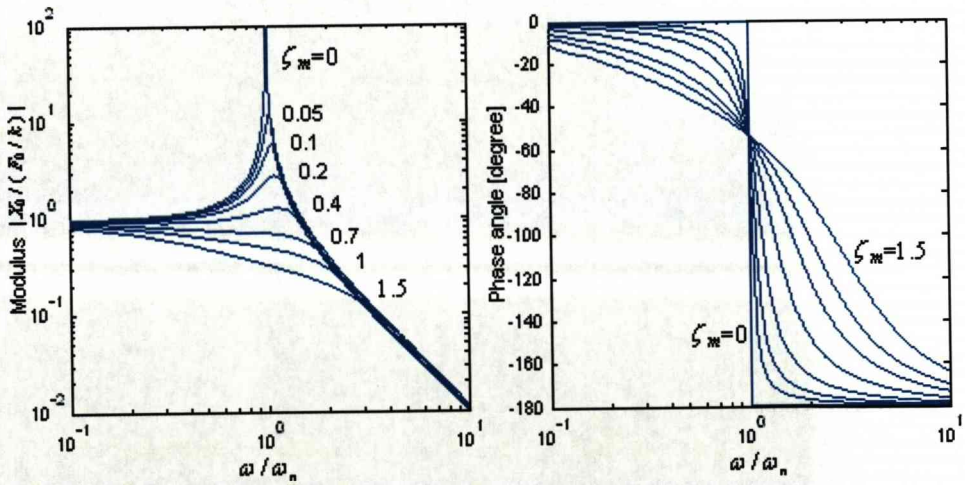

Figure 3.6 FRF of complex damping SDOF system for $\psi = -0.75$

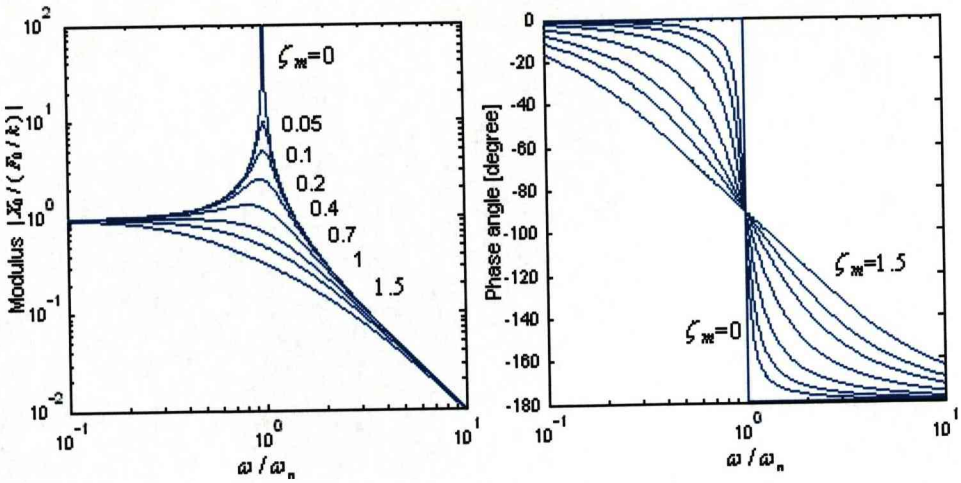

Figure 3.7 FRF of complex damping SDOF system for $\psi = 0$

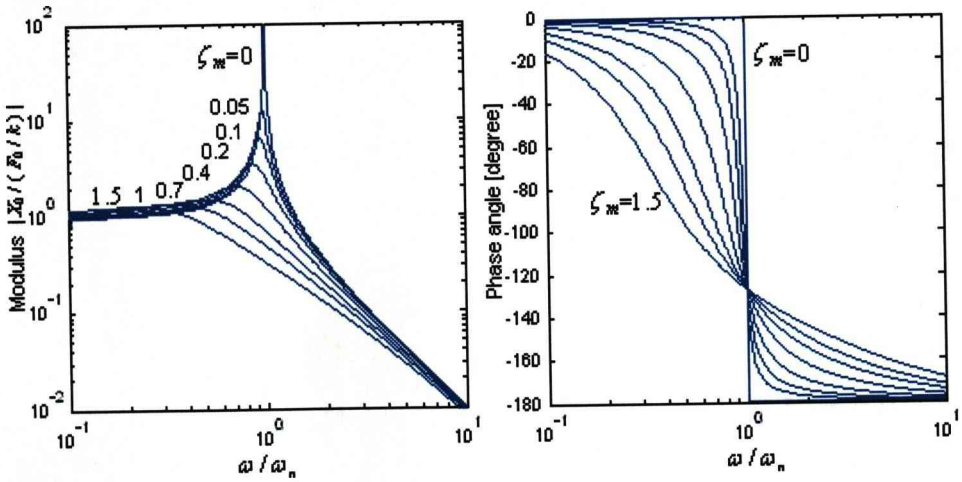

Figure 3.8 FRF of complex damping SDOF system for $\psi = 0.75$

The behaviour of both modulus and phase of the frequency response function depend on the parameters ζ_m and ψ, as shown in Figure 3.6, Figure 3.7 and Figure 3.8. It is found that for increasing values of ζ_m and the positive ψ the resonance peak decreases and the resonance peaks shift to increasing values of resonance frequency for the case of negative ψ and in verse. Additionally, if we compare the phase angles of frequency response functions in these figures, we can find that when we choose negative ψ, the phase angle will shifts at an angle between $\left[0,-\frac{\pi}{2}\right]$, while the phase

angle will shifts at an angle between $\left[-\frac{\pi}{2},-\pi\right]$ for the positive ψ. And when ψ=0, that is there is no stiffness effect, the phase angle shifts at the angle of $-\frac{\pi}{2}$. The exact understanding of this behaviour of the system with complex viscous damping can be obtained by calculating the modulus and phase angle of the frequency response function at the frequency $\omega = \omega_n$.

For the complex viscous damping system, the modulus and phase angle of frequency response function at the frequency $\omega = \omega_n$ are obtained as below.

$$|H(\omega_n)| = \frac{1}{2\zeta_m} \tag{3.46}$$

$$angle[H(\omega_n)] = arctg\left(\frac{1}{\psi}\right) \qquad for\ \ \zeta_m > 0 \tag{3.47}$$

For comparison to the general pure viscous damping system, where the modulus and phase angle at the resonance frequency are

$$|H(\omega_n)|_{viscous} = \frac{1}{2\zeta_{viscous}} \tag{3.48}$$

$$angle[H(\omega_n)]_{viscous} = -\frac{\pi}{2} \tag{3.49}$$

It is clear that the complex viscous damping will cause same suppression effect as the effect induced by the general viscous damping at the frequency $\omega = \omega_n$ in the case of $\zeta_m = \zeta_{viscous}$, but the phase angle will shift in the angle of $arctg\left(\frac{1}{\psi}\right)$ when $\psi \neq 0$ instead of $-\frac{\pi}{2}$. Figure 3.9 and Figure 3.10 demonstrate this difference in detail.

This phenomenon can also be clearly interpreted through the force relation analysis by using force diagram as shown in Figure 3.11. For the case that there is no stiffness effect, the phase angle is 90°. The inertia force is balanced with the spring force. Whereas the impressed force overcomes the damping force, as shown in Figure

3.11_(a). When the stiffness effect applies ($c_{el}\omega x$), the equivalent spring force increases and the inertia force becomes smaller than the equivalent spring force. This results in a small phase angle ϕ, as shown in Figure 3.11_(b).

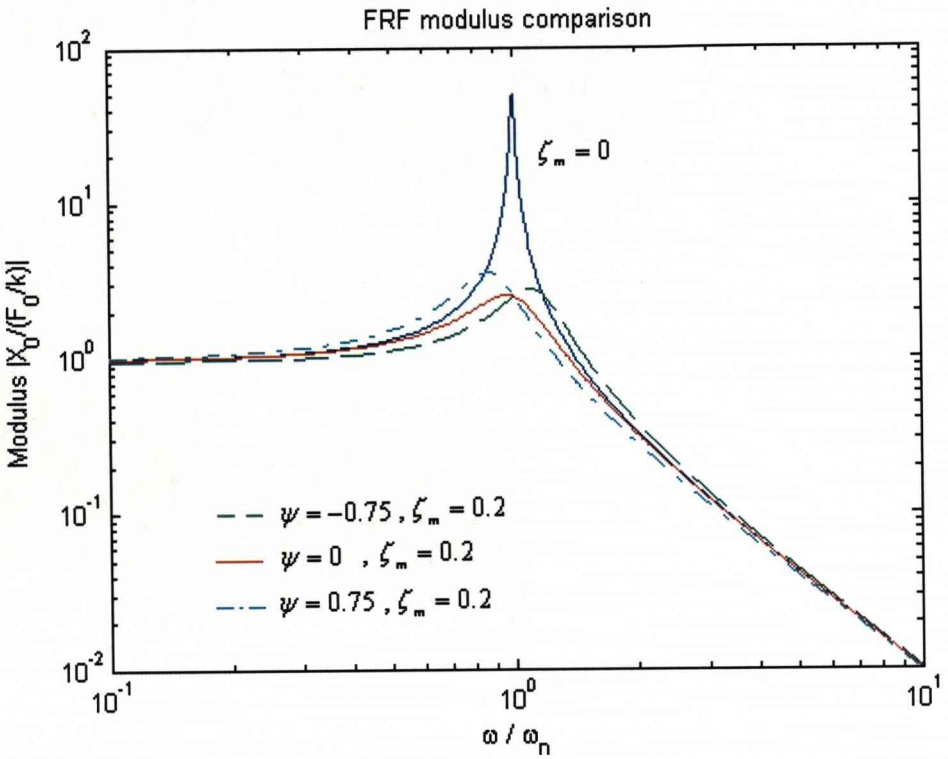

Figure 3.9 Comparison of FRF Modulus for different ψ

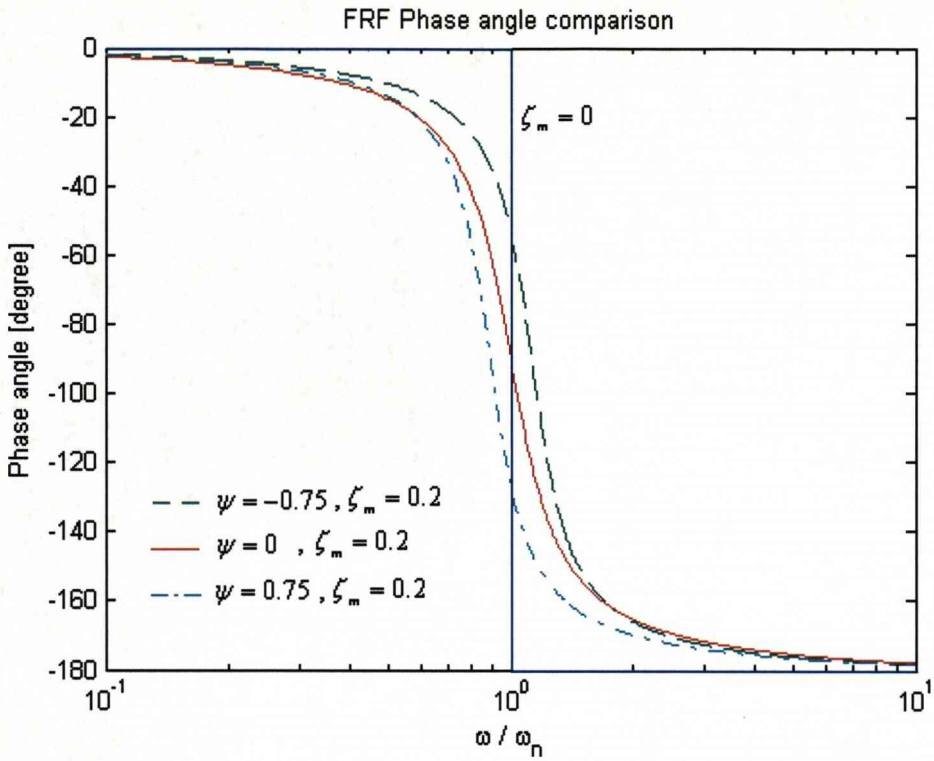

Figure 3.10 Comparison of FRF phase angle for different ψ

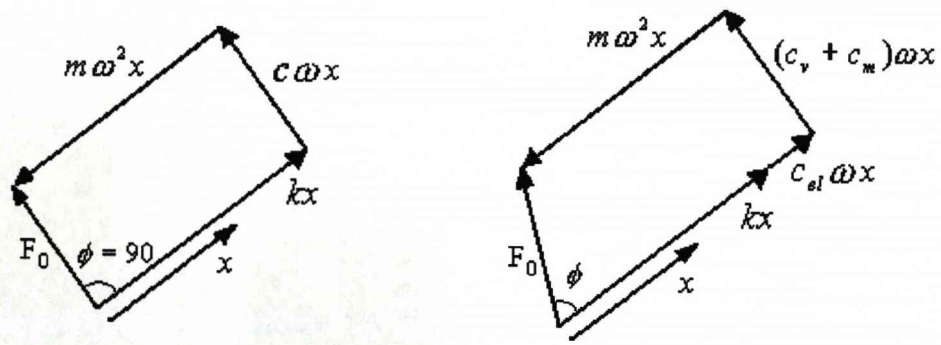

(a) $\omega / \omega_0 = 1$

Non phantom effect

(b) $\omega / \omega_0 = 1$

Phantom effect

Figure 3.11 Force Diagram

3.4 Impulse response

For the motion equation (3.18) of the system, if the excitation *f(t)* is the unit impulse function $\delta(t)$, the response *h(t)* is called impulse response function. This function shows its importance from two ways. Firstly, it describes free vibrations of the system, which is under the zero displacement and velocity initial conditions, for vanishing force thus allow us to identify the energy loss by amplitude decay from measurement. In the second, this function can be used to solve the response to an arbitrary force *f(t)* by the Duhamel convolution integral.

In principle, the impulse response can be calculated through the frequency response function because the Fourier transform of function $\delta(t)$ is equal to one. Thus we have

$$h(t)=\frac{1}{2\pi}\int_{-\infty}^{\infty}H(\omega)e^{j\omega t}d\omega \tag{3.50}$$

Through the equation (3.41), it is easily to get

$$\begin{aligned}H(\omega)=\frac{X_0}{F_0}&=\frac{1}{-m\omega^2+j\omega(c_v+c_m-jc_e)+k}\\&=\frac{1}{m}\frac{1}{\omega_n{}^2+j2\zeta_m\omega_n\omega\dfrac{1+j\,\mathrm{sgn}(\omega)\psi}{\sqrt{1+\psi^2}}-\omega^2}\end{aligned} \tag{3.51}$$

Thus,

$$h(t)=\frac{1}{2m\pi}\int_{-\infty}^{\infty}\frac{e^{j\omega t}}{\omega_n{}^2+j2\zeta_m\omega_n\omega\dfrac{1+j\,\mathrm{sgn}(\omega)\psi}{\sqrt{1+\psi^2}}-\omega^2}d\omega \tag{3.52}$$

This integral can be calculated numerically, which will be discussed later. Here, a special problem oriented by residual integral theory is presented. Contour integration is the process of calculating the values of a contour integral around a given contour in the complex plane. Such integrals can be computed easily simply by using Cauchy's

integral formula, that is, summing the values of the complex residues inside the contour [127]. In complex analysis, contour integration is an effective method of evaluating certain integral of real valued functions along intervals on the real line that are not readily found by using only real variables. This technique is usually used in previous works [19].

The integral contour is selected to provide the closed form solution. As two conjugate complex poles have been determined according to equation (3.35), the integral can be extended from real variable ω to the complex variable $s = \sigma + j\omega$ in the complex plane.

$$h_1(t) = \frac{1}{j2m\pi} \int_C \frac{e^{st}}{\omega_n^{\,2} + 2\zeta_m \omega_n s \frac{1 + j\,\mathrm{sgn}[\mathrm{Im}(s)]\psi}{\sqrt{1+\psi^2}} + s^2} ds \tag{3.53}$$

And we can define the integral

$$I_s = \int_C \frac{e^{st}}{\omega_n^{\,2} + 2\zeta_m \omega_n s \frac{1 + j\,\mathrm{sgn}[\mathrm{Im}(s)]\psi}{\sqrt{1+\psi^2}} + s^2} ds = \int_C f(s) ds \tag{3.54}$$

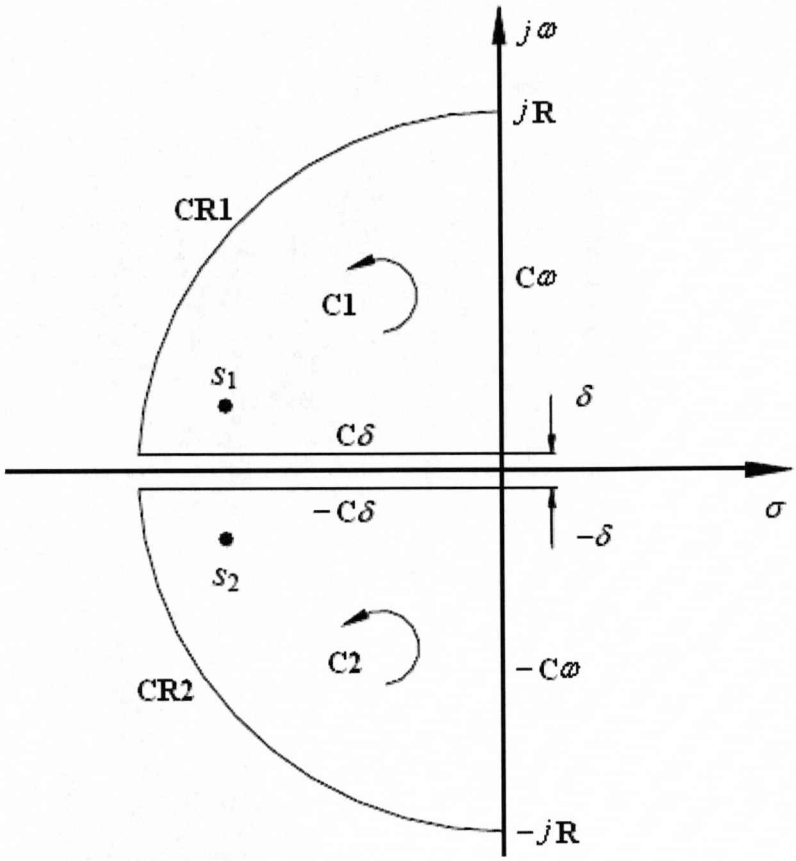

Figure 3.12 Integration contour for $t \geq 0$

In the residues theory the integral is applied along the contour C1 and C2 shown in Figure 3.12, which provide the limits $\delta \to 0$ and $R \to \infty$. The split appears in the contours to avoid the integral passing the singularity point $\omega = 0$, where the integral is not analytical. So, we have

$$I_s = I_{C1} + I_{C2} = (I_{C\omega} + I_{CR1} + I_{C\delta}) + (I_{-C\omega} + I_{-C\delta} + I_{CR2}) \tag{3.55}$$

in which, I_{C1} and I_{C2} are integrals with contour C1 and C2 respectively. And $I_{C\omega}$, I_{CR1}, $I_{C\delta}$, $I_{-C\omega}$, I_{CR2} and $I_{-C\delta}$ are integrals along the corresponding routes.

The integrals along the imaginary axis where $s = j\omega$ because $\sigma = 0$ can be written as

$$I_{C\omega} = j\int_0^{\infty} \frac{e^{j\omega t}}{\omega_n{}^2 + j2\zeta_m\omega_n\omega\dfrac{1+j\,\mathrm{sgn}(\omega)\psi}{\sqrt{1+\psi^2}} - \omega^2}\,d\omega \tag{3.56}$$

$$I_{-C\omega} = j\int_{-\infty}^{0} \frac{e^{j\omega t}}{\omega_n^{\,2} + j2\zeta_m\omega_n\omega\dfrac{1+j\,\mathrm{sgn}(\omega)\psi}{\sqrt{1+\psi^2}} - \omega^2}\,d\omega \tag{3.57}$$

Thus, we obtain that

$$h(t) = \frac{1}{j2m\pi}(I_{-C\omega} + I_{C\omega}) \tag{3.58}$$

in which, $(I_{C\omega} + I_{-C\omega})$ can be calculated by other integrals.

$$(I_{C\omega} + I_{C\omega}) = (I_{C1} + I_{C2}) - (I_{CR1} + I_{CR2} + I_{C\delta} + I_{-C\delta}) \tag{3.59}$$

Applying the residues theorem, a closed integral is equal to the sum of all residues contained inside the contour.

$$\int_c f(z)dz = j2\pi\sum_k Res[f(z_k)] \tag{3.60}$$

And using the residue formula

$$Res[f(z_k)] = \frac{a(z_k)}{b'(z_k)} \quad \text{for} \quad f(z) = \frac{a(z)}{b(z)} \tag{3.61}$$

So we can get

$$I_{C1} = j2\pi Res[f(s_1)] = j\pi \frac{e^{s_1 t}}{\left(s_1 + \zeta_m\omega_n\dfrac{1+j\psi}{\sqrt{1+\psi^2}}\right)} \tag{3.62}$$

$$I_{C2} = j2\pi Res[f(s_2)] = j\pi \frac{e^{s_2 t}}{\left(s_2 + \zeta_m\omega_n\dfrac{1-j\psi}{\sqrt{1+\psi^2}}\right)} \tag{3.63}$$

Now considering the integral along the semicircle route $I_{CR1} + I_{CR2}$, where $s = Re^{j\varphi}$, $(\pi/2 \le \varphi \le 3\pi/2)$, which leads to

$$I_{CR1} + I_{CR2} = \int_{\pi/2}^{\pi} \frac{e^{Rt\cos\varphi}e^{jRt\sin\varphi}}{\omega_n^{\,2} + 2\zeta_m\omega_n Re^{j\varphi}\dfrac{1+j\,\mathrm{sgn}[\mathrm{Im}(s)]\psi}{\sqrt{1+\psi^2}} + R^2e^{j2\varphi}} jRe^{j\varphi}d\varphi$$

$$+\int_{\pi}^{\pi/2}\frac{e^{Rt\cos\varphi}e^{jRt\sin\varphi}}{\omega_n^{\,2}+2\zeta_m\omega_n Re^{j\varphi}\dfrac{1+j\,\mathrm{sgn}[\mathrm{Im}(s)]\psi}{\sqrt{1+\psi^2}}+R^2e^{j2\varphi}}jRe^{j\varphi}d\varphi \tag{3.64}$$

This integral vanishes when $R\to\infty$, because the function

$$F(Re^{j\varphi})=\frac{1}{\omega_n^{\,2}+2\zeta_m\omega_n Re^{j\varphi}\dfrac{1+j\,\mathrm{sgn}[\mathrm{Im}(s)]\psi}{\sqrt{1+\psi^2}}+R^2e^{j2\varphi}} \tag{3.65}$$

shows that $\lim_{R\to\infty}\left|F(Re^{j\varphi})\right|=0$ since the order of magnitude $\vartheta\left(\frac{1}{1+R+R^2}\right)\to 0$ when $R\to\infty$. The proof is similar to the Jordan's lemma and can be found in Appendix A.

The integrals along the contour $C\delta$ and $-C\delta$ as $\delta\to 0$ and $R\to\infty$ are given by

$$I_{C\delta}=\int_{-\infty}^{0}\frac{e^{t\sigma}}{\omega_n^{\,2}+2\zeta_m\omega_n\sigma\dfrac{1+j\psi}{\sqrt{1+\psi^2}}+\sigma^2}d\sigma \tag{3.66}$$

$$I_{-C\delta}=\int_{0}^{\infty}\frac{e^{t\sigma}}{\omega_n^{\,2}+2\zeta_m\omega_n\sigma\dfrac{1-j\psi}{\sqrt{1+\psi^2}}+\sigma^2}d\sigma$$

$$=-\int_{-\infty}^{0}\frac{e^{t\sigma}}{\omega_n^{\,2}+2\zeta_m\omega_n\sigma\dfrac{1-j\psi}{\sqrt{1+\psi^2}}+\sigma^2}d\sigma \tag{3.67}$$

For the reason that the two poles $s_{1,2}$ are conjugate, the integrations show the relations as

$$\begin{cases}\mathrm{Im}(I_{C1})=\mathrm{Im}(I_{C2})\\ \mathrm{Im}(I_{C\delta})=\mathrm{Im}(I_{-C\delta})\end{cases} \tag{3.68}$$

Hence, based on above integral calculation we obtain the impulse response of the system through equation (3.58) and (3.59) by extracting the real part of the integrand.

$$h(t)=\mathrm{Re}\left[\frac{1}{j2m\pi}(I_{-C\omega}+I_{C\omega})\right]=\frac{1}{m}(I_1+I_2) \tag{3.69}$$

in which

$$I_1 = \mathrm{Re}\left[\frac{e^{s_1 t}}{\left(s_1 + \zeta_m \omega_n \frac{1+j\psi}{\sqrt{1+\psi^2}}\right)}\right] \tag{3.70}$$

$$I_2 = -2\,\mathrm{Re}\left[\frac{1}{j2\pi}\int_{-\infty}^{0} \frac{e^{t\sigma}}{\omega_n{}^2 + 2\zeta_m \omega_n \sigma \frac{1+j\psi}{\sqrt{1+\psi^2}} + \sigma^2} d\sigma\right]$$

$$= \frac{1}{\pi}\int_{0}^{\infty} \frac{-2\zeta_m \omega_n \sigma \frac{\psi}{\sqrt{1+\psi^2}} e^{-t\sigma}}{\left(\omega_n{}^2 - 2\zeta_m \omega_n \sigma \frac{1}{\sqrt{1+\psi^2}} + \sigma^2\right)^2 + \left(2\zeta_m \omega_n \sigma \frac{\psi}{\sqrt{1+\psi^2}}\right)^2} d\sigma \tag{3.71}$$

It should be noticed that the above integrals are restricted in the negative σ region because of the restriction condition of time $t \geq 0$. So, the equation (3.69) should be changed to be

$$h(t)_{t\geq 0} = \frac{1}{m}(I_1 + I_2) \tag{3.72}$$

For the case of $t \leq 0$, the integral has to be taken in the positive σ region and the integral contour is chosen as Figure 3.13. Thus, the impulse response in whole time domain should be the combination of two integral parts for $t \geq 0$ and $t \leq 0$.

$$h(t) = h(t)_{t\geq 0} + h(t)_{t\leq 0} \tag{3.73}$$

The integrations for time $t \leq 0$ are very similar to the calculations above for time $t \geq 0$.

$$h(t)_{t\leq 0} = \frac{1}{j2m\pi}(I_{-C\omega'} + I_{C\omega'}) \tag{3.74}$$

and

$$(I_{C\omega'} + I_{C\omega'}) = (I_{C1'} + I_{C2'}) - (I_{CR1'} + I_{CR2'} + I_{C\delta'} + I_{-C\delta'}) \tag{3.75}$$

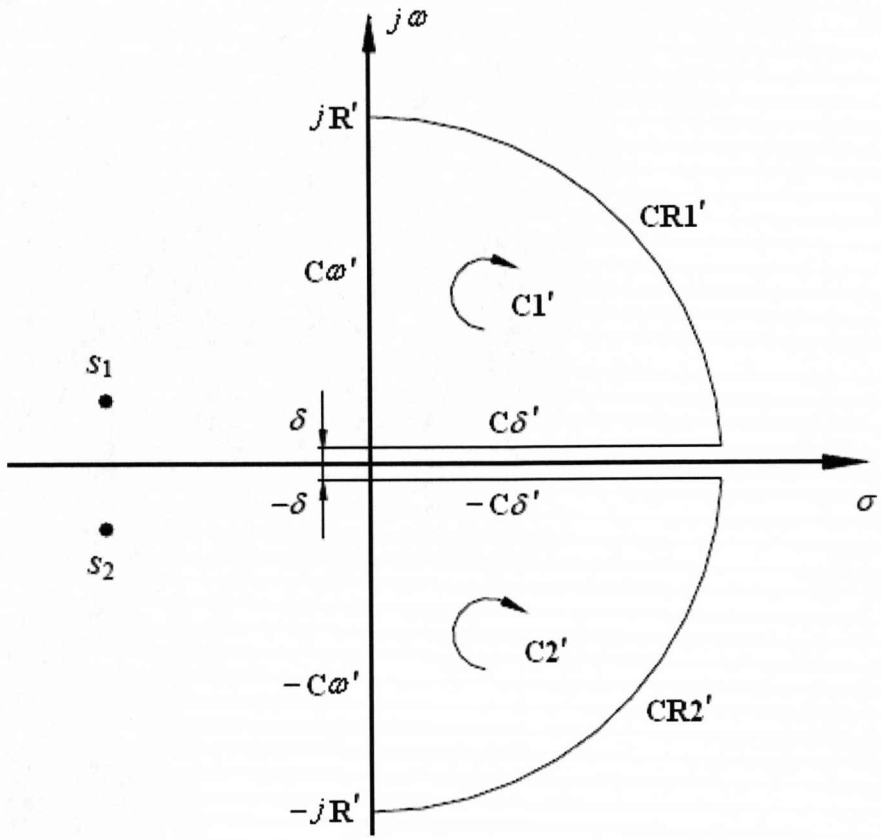

Figure 3.13 Integration contour for $t \le 0$

By using Cauchy's integration theorem, the integration around the closed contour without any residues is zero. Thus,

$$I_{C1'} = I_{C2'} = 0 \tag{3.76}$$

Besides, it also can be proved that

$$(I_{CR1'} + I_{CR2'}) = 0 \quad \text{for the infinite } R \tag{3.77}$$

and the integrations $I_{C\delta'}$ and $I_{-C\delta'}$ can be calculated when $\delta \to 0$ as

$$I_{C\delta'} = \int_{\infty}^{0} \frac{e^{t\sigma}}{\omega_n^{\,2} + 2\zeta_m \omega_n \sigma \dfrac{1+j\psi}{\sqrt{1+\psi^2}} + \sigma^2} d\sigma$$

$$= -\int_{0}^{\infty} \frac{e^{t\sigma}}{\omega_n^{\,2} + 2\zeta_m \omega_n \sigma \dfrac{1+j\psi}{\sqrt{1+\psi^2}} + \sigma^2} d\sigma \tag{3.78}$$

$$I_{-C\delta} = \int_0^\infty \frac{e^{t\sigma}}{\omega_n{}^2 + 2\zeta_m\omega_n\sigma\dfrac{1-j\psi}{\sqrt{1+\psi^2}} + \sigma^2}\,d\sigma \tag{3.79}$$

It can also be seen that

$$\mathrm{Im}(I_{C\delta'}) = \mathrm{Im}(I_{-C\delta'}) \tag{3.80}$$

So, the real impulse response of the system for $t \le 0$ can be obtained

$$h(t)_{t\le 0} = \mathrm{Re}\left[\frac{1}{j2m\pi}(I_{-C\omega'} + I_{C\omega'})\right] = \frac{1}{m}I_3 \tag{3.81}$$

in which

$$I_3 = -2\,\mathrm{Re}\left[\frac{1}{j2\pi}\int_0^\infty \frac{e^{t\sigma}}{\omega_n{}^2 + 2\zeta_m\omega_n\sigma\dfrac{1+j\psi}{\sqrt{1+\psi^2}} + \sigma^2}\,d\sigma\right]$$

$$= \frac{1}{\pi}\int_0^\infty \frac{-2\zeta_m\omega_n\sigma\dfrac{\psi}{\sqrt{1+\psi^2}}e^{t\sigma}}{\left(\omega_n{}^2 + 2\zeta_m\omega_n\sigma\dfrac{1}{\sqrt{1+\psi^2}} + \sigma^2\right)^2 + \left(2\zeta_m\omega_n\sigma\dfrac{\psi}{\sqrt{1+\psi^2}}\right)^2}\,d\sigma \tag{3.82}$$

Thus, we acquire the impulse response of a SDOF system with complex viscous damping.

$$h(t) = \begin{cases} \dfrac{1}{m}(I_1 + I_2) & for \quad t \ge 0 \\ \dfrac{1}{m}I_3 & for \quad t \le 0 \end{cases} \tag{3.83}$$

The integration part I_1, I_2 and I_3 are defined as above. And these integrations can be computed numerically.

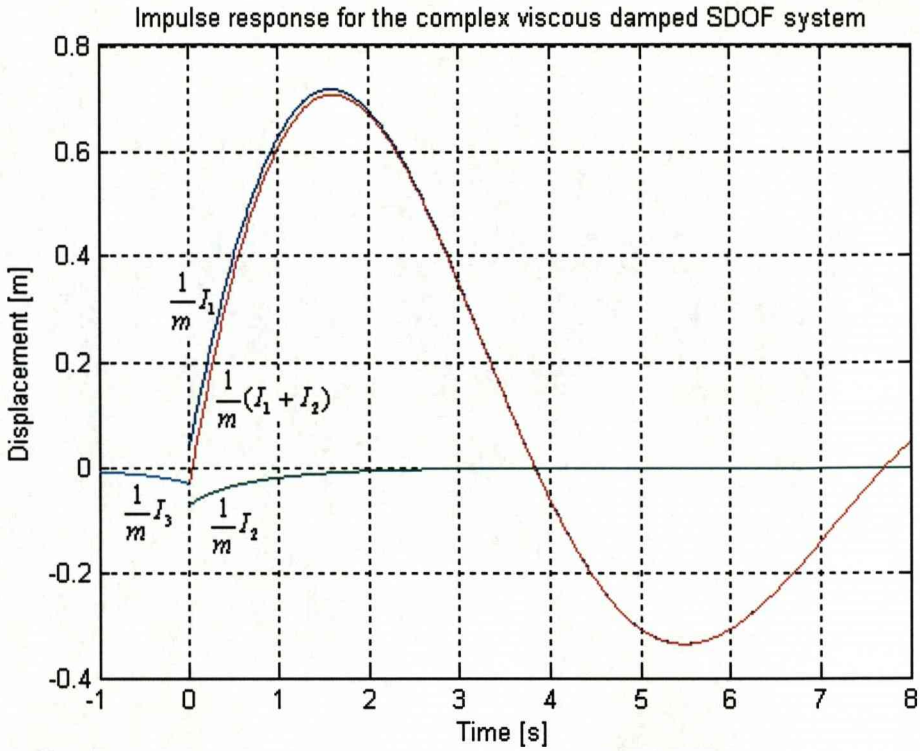

Figure 3.14 Impulse response and integration terms

Figure 3.14 illustrates the effect of each integration and the whole time impulse response as an example of $m=1kg$, $\omega_n=1\,rad/s$, $\zeta_m=0.3$ and $\psi=0.75$. It can be noted that, the impulse response of the model is given by a sum of two parts $h(t)_{t\geq 0}$ and $h(t)_{t\leq 0}$. When in the time $t\geq 0$, two integrations I_1 and I_2 contribute the impulse response together. The first integration I_1 represents a damped oscillation, which is periodic movement with an exponential decrement of amplitude, analogous to that of underdamped linear pure viscous systems. The second term I_2 is a residual integral characterizing the exponential attenuation behaviour. For the time $t\leq 0$ the impulse response is due to only one residual integral I_3, which is similar to the integration I_2 and also shows an exponential movement. This integration also involves the non-causality of the system. Both three integrations provide a non-zeros movement at the time $t=0$. And it shows that

$(I_1 + I_2)_{t=0} = (I_3)_{t=0}$. Thus, the impulse response is continuous at $t = 0$. When we think about the special case of $\psi = 0$, it is found that $I_2 = I_3 = 0$ and the impulse response is contributed only by integration I_1. The result is the well-known impulse response for general pure viscous damping system.

It is worth to note that both continuous and real impulse response of the SDOF system with complex viscous damping is achieved here although the non-causality property produced a movement prior to the excitation thus a time delay or time advanced involved for $\psi > 0$ or $\psi < 0$ respectively as shown in Figure 3.15, which illustrates the impulse response of the example SDOF system with complex viscous damping with respect to the variables ψ for the example of $m = 1\,kg$, $\omega_n = 1\ rad/s$ and $\zeta_m = 0.3$. Figure 3.16 is to show the impulse response with respect to the variables ζ_m for the example of $m = 1\,kg$, $\omega_n = 2\pi\ rad/s$ and $\psi = 0.75$.

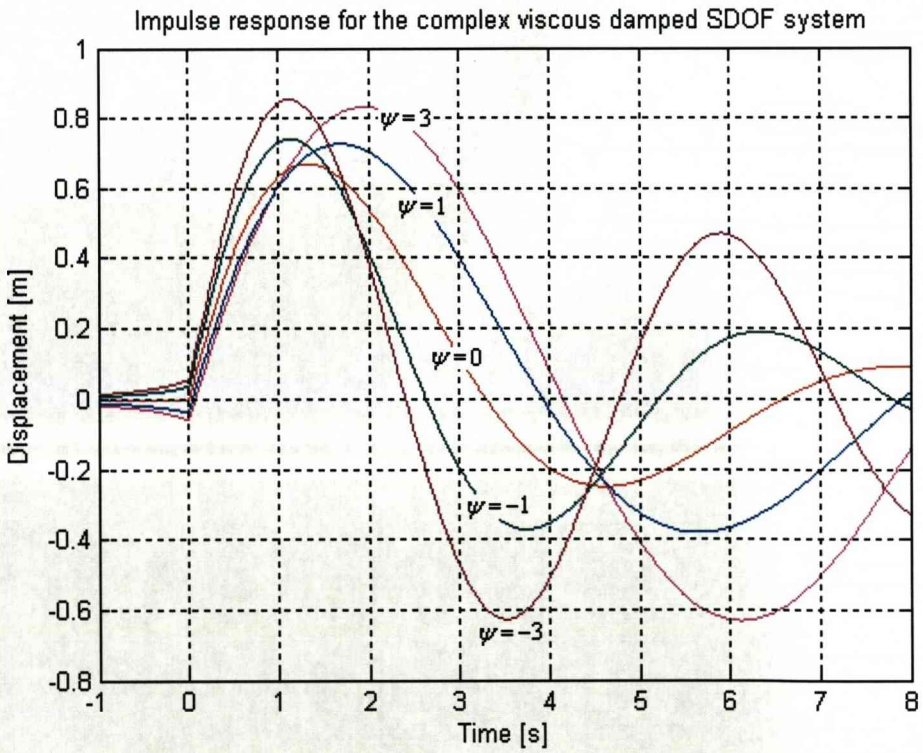

Figure 3.15 Impulse response for different ψ

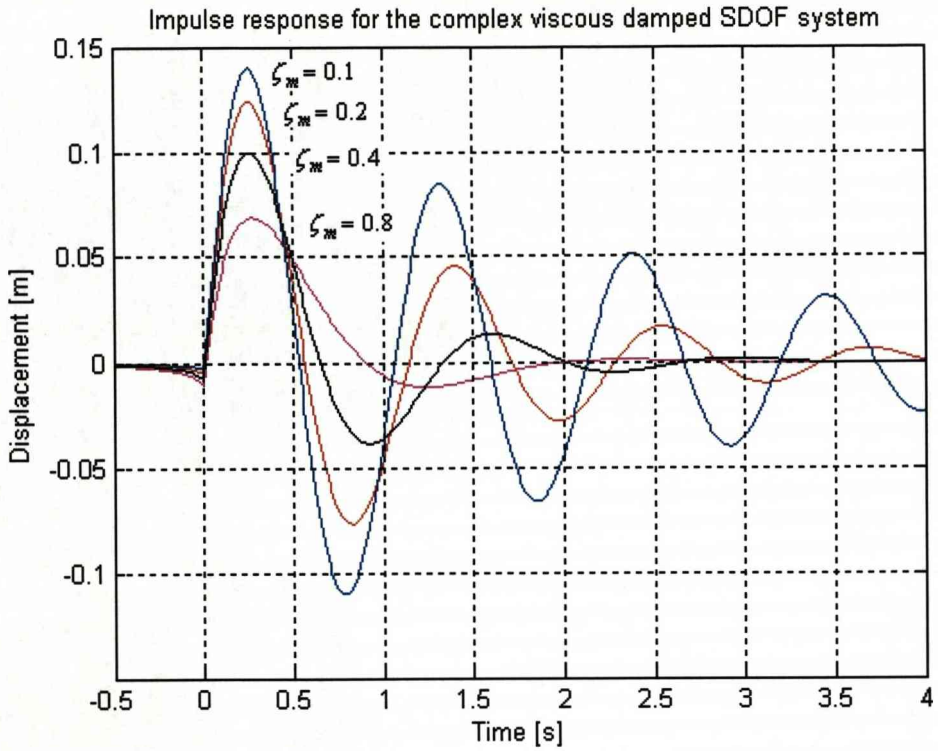

Figure 3.16 Impulse response for different ζ_m

It should be mentioned that the complex magnetic damping model must be defined in the frequency domain or limited to the transient work to periodic harmonic excitation. Although in this section the response of system with complex magnetic damping under the impulse force is calculated, the used contour integral technique is only a mathematical method. This method can obtain reasonable response result except non-causal.

3.5 Closure

In magnetic coupling with elasto-mechanical systems, a complex viscously damped model is needed in order to describe a dynamic increase of stiffness (or mass) proportional to velocity, coupled with a viscous-type damping effect. An analysis of

the single degree-of-freedom complex-damped model is presented. The complex viscous damping shows conjugate eigenvalues with negative real parts. They make sure that the complex viscous damping system is stable. It can be clearly found from the frequency response function of the complex damped SDOF system that complex viscous damping has the strong vibration amplitude suppression with the natural frequency shift.

The impulse response of the complex damped system is continuous and realistic but non-causal in time domain. However, the complex magnetic damping model must be defined in the frequency domain or limited to the transient work to periodic harmonic excitation. Although the impulse response of system with complex magnetic damping is calculated, the used contour integral technique is only a mathematical method. This method can obtain reasonable response result except non-causal.

Chapter 4

Damping Mechanism and Dynamic Responses

The work here is concerned with the subject of complex viscous damping. In a simple single degree of freedom system, this type of damping implies a stiffness force that is in phase with displacement but the magnitude of force is proportional to velocity but not displacement. When the system has multiple degrees of freedom, complex viscous damping implies that the stiffness phantom force is proportional to the relative velocity while it is in phase with the relative displacement.

The magnetic model is based on the analogy of the equivalent currents method in a quasi-static open circuit-type configuration and it is used to determine the influence of eddy currents on the dynamic behaviour of structures made of conducting materials. The effect of the magnetic interactions consists in a viscous-type damping effect as well as in an interesting stiffening effect denoted as "phantom effect", which is modeled by adding an imaginary term in the damping coefficient. The advantage of this mathematic model is that it demonstrates a good agreement for system dynamic response in the frequency domain (frequency response function) with the experimental results [4, 5]. On the other hand, this model will not cause too many mathematical difficulties for the vibration system. For the dynamic system with a complex viscous damping, the motion equation is still written in the well-known second order differential equation form, in which the mass and stiffness item of the original system keep unchanged and then the natural frequencies of original system could be considered easily.

In this chapter, the purpose is to discuss the mathematic theories of complex viscous

damping in vibration system. It includes the damping mechanism and the discussion of frequency-rate dependent stiffness model. The theories are obtained through the analyses of the harmonic forced oscillation and the random response of a system with a single degree of freedom.

4.1 Damping mechanism

The main idea of a damped vibration system is the cyclic movement with the decreasing amplitude. The energy will dissipate during the motion because of the existence of the damping force. However, these damping forces are complicated. Thus a mathematic theory has to be formulated, in which the damping can be represented in some reasonable ways. Generally, if the excitation and response of the system is harmonic, energy dissipation per cycle can be thought as a combination effect of the amplitude and related frequency. A convenient measurement of a damping is called loss factor that is defined by the energy lost in a cycle with the peak potential energy stored in the system during that cycle. The loss factor can depend on both amplitude and frequency of the oscillation. If however the system is completely linear, in which both energy lost per cycle and the peak potential energy are proportional to the square of the amplitude, the loss factor will generally have a dependence only on the frequency while being amplitude independent. In some application cases of hysteretic material, the loss factor may even be considered to be a constant. That means the loss factor is both amplitude and frequency independent in whole frequency range or at least over a wide range of frequencies.

Now, let us consider a system with one single degree of freedom moving in a couple of magnets as shown in Figure 3.3. By using complex viscous damping model, if the stretch of the spring is x, the total restoring force can be calculated as following.

$$f_r = (c_v + c_m - jc_e)\dot{x} + kx \tag{4.1}$$

For harmonic movement, we can assume the displacement x to be given as

$$x = A\sin\omega t \tag{4.2}$$

in which, A is the amplitude, and ω is frequency of oscillation, t is the time. As it is well known that $e^{j\omega t} = \cos\omega t + j\sin\omega t$, if we set

$$u = Ae^{j\omega t} \tag{4.3}$$

Then

$$x = \mathrm{Im}[Ae^{j\omega t}] = \mathrm{Im}[u] \tag{4.4}$$

Thus, the restoring force is obtained as

$$\begin{aligned} f_r &= \mathrm{Im}[(c_v + c_m - jc_e)\dot{u} + ku] \\ &= (c_e\omega + k)A\sin\omega t + (c_v + c_m)\omega A\cos\omega t \end{aligned} \tag{4.5}$$

or,

$$f_r = A_0\sin(\omega t + \phi) \tag{4.6}$$

in which,

$$A_0 = A\sqrt{(c_e\omega + k)^2 + (c_v + c_m)^2\omega^2} \tag{4.7}$$

$$\phi = arctg\left[\frac{(c_v + c_m)\omega}{(c_e\omega + k)}\right] \tag{4.8}$$

From equation (4.6), it can be seen that for a harmonic response x, the restoring force f_r is not in phase with displacement x and this characteristic accounts for the energy dissipation. The relation between restoring force f_r and displacement x can be expressed with respect to the parameter t by combining equation (4.2) and (4.5). Thus, the shape of the curve (f_r, x) may be obtained by eliminating t between these two equations. So, it is found that

$$f_r = (c_e\omega + k)x \pm (c_v + c_m)\omega\sqrt{A^2 - x^2} \tag{4.9}$$

The curve (f_r, x) is presented in Figure 4.1, It is a closed loop, which travels around in a clockwise direction. So, the energy dissipation in a cycle is the area of this loop. It can be found that if the amplitude A is set as a constant, when ω is decreases, the loop becomes thinner and the energy lost per cycle will be smaller.

The energy lost per cycle is calculated as,

$$\begin{aligned} W &= \oint f_r dx \\ &= \int_0^{2\pi/\omega}\left[(c_e\omega + k)A\sin\omega t + (c_v + c_m)\omega A\cos\omega t\right]\omega A\cos\omega t dt \\ &= \omega\pi(c_v + c_m)A^2 \end{aligned} \tag{4.10}$$

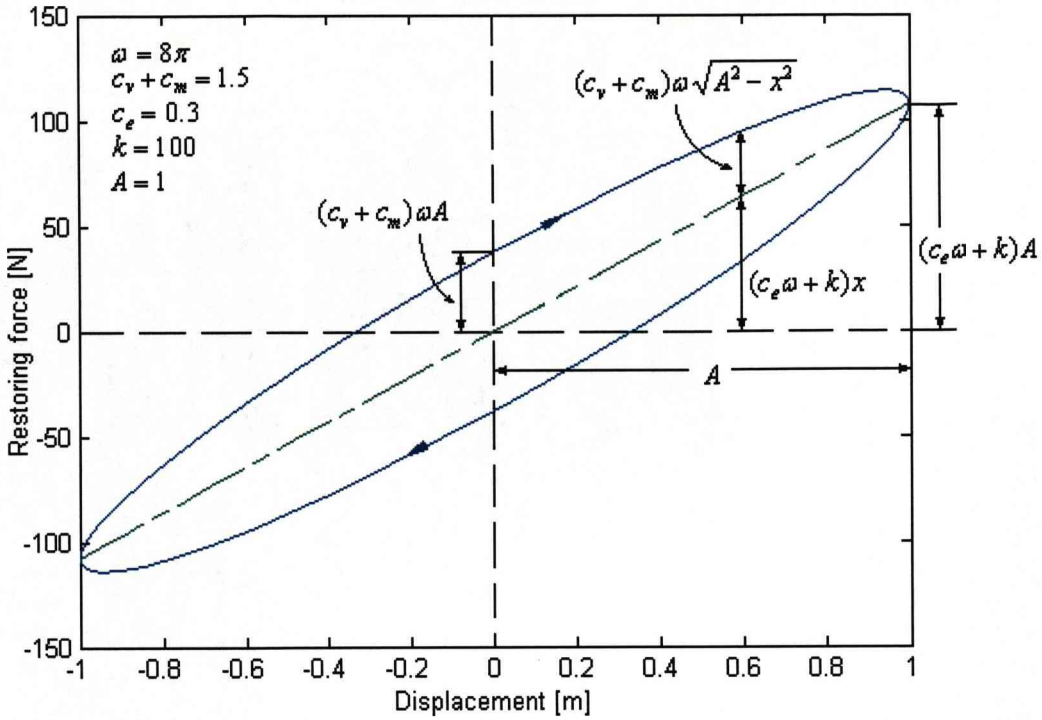

Figure 4.1 Hysteretic loop

This result is in the same form as the pure viscous damping model. The energy lost per cycle is proportional to frequency of oscillation and the square of the amplitude.

We can investigate the model in more detail by separating the restoring force into two parts using equation (4.5) as following

$$f_r = (c_e\omega + k)x + (c_v + c_m)\dot{x} = f_{r1} + f_{r2} \tag{4.11}$$

In which

$$f_{r1} = (c_e\omega + k)x \tag{4.12}$$

$$f_{r2} = (c_v + c_m)\dot{x} \tag{4.13}$$

Accordingly, we also calculate the energy of each force part during a cycle movement into two parts.

$$W = W_1 + W_2 \tag{4.14}$$

in which,

$$W_1 = \oint f_{r1}dx$$

$$= \int_0^{2\pi/\omega} [(c_e\omega + k)A\sin\omega t]\omega A\cos\omega t dt$$

$$= 0 \tag{4.15}$$

and

$$W_2 = \oint f_{r2} dx$$

$$= \int_0^{2\pi/\omega} [(c_v + c_m)\omega A \cos \omega t] \omega A \cos \omega t dt$$

$$= \omega \pi (c_v + c_m) A^2 \tag{4.16}$$

It is obviously that the energy lost per cycle caused by complex viscous damping is wholly contributed by the force item f_{r2} , which is a viscous type damping force. Because the force item f_{r1} does zero work during a cycle of movement, it is a conservative force as pure spring force. And it will not cause any energy lost but contributes to the potential energy. Thus, the dynamical effect of the complex viscous damping $(c_v + c_m - jc_e)$ includes two aspects. The real part of the complex viscous damping brings viscous damping type energy dissipation while the imaginary part does not cause any energy lost but changes the potential energy stored in system during the oscillation. We can calculate the potential energy at any position x as

$$v = \int_0^x f_{r1} dx$$

$$= \int_0^x (c_e \omega + k) x dx = \frac{1}{2}(c_e \omega + k) x^2 \tag{4.17}$$

And the peak potential energy should be

$$V = \frac{1}{2}(c_e \omega + k) A^2 \tag{4.18}$$

Hence, we obtain the loss factor as below

$$\eta = \frac{W}{2\pi V} = \frac{(c_v + c_m)\omega}{(c_e \omega + k)} \tag{4.19}$$

So, for complex viscous damping model, the energy loss factor has an important dependence upon the frequency of oscillation while amplitude independent.

The energy loss factor can be rewritten as

$$\eta = \frac{(c_v + c_m)}{(c_e + \frac{k}{\omega})} \tag{4.20}$$

Thus, we can find that if the system is oscillating at a very high frequency, the energy

loss factor will become a constant

$$\eta \approx \frac{(c_v + c_m)}{c_e} = -\frac{1}{\psi} \tag{4.21}$$

By using the definition in equation (4.20), because $\frac{k}{\omega} \to 0$ when $\omega \to \infty$.

Additionally, it is noticed that only the "light damping" case is considered.

4.2 Frequency-rate stiffness model

When the restoring force caused by magnetic damping is expressed in the form as shown in equation (4.11),

$$f_r = (c_e\omega + k)x + (c_v + c_m)\dot{x} \tag{4.22}$$

it provides a frequency-rate stiffness model understanding of this type of damping. This model is a quasi-viscous damping since it has a constant viscous damping coefficient with a variable stiffness proportional to frequency as shown in Figure 4.2.

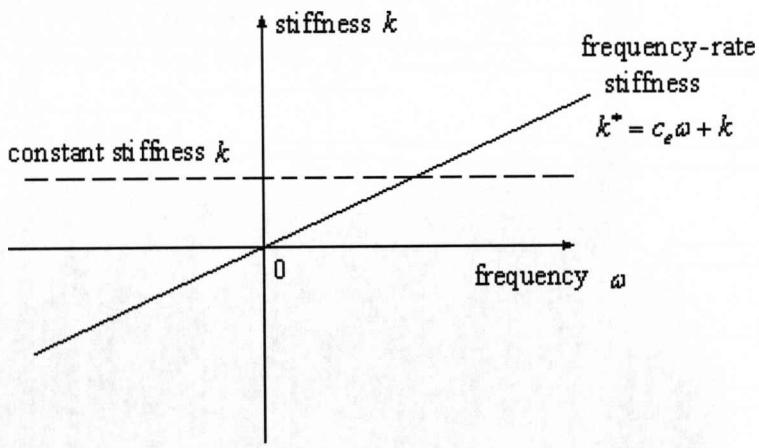

Figure 4.2 Frequency-rate stiffness model

For the same system as shown in Figure 3.3, when applying the frequency-rate stiffness model, the system may be simply simulated as Figure 4.3, and the response of mass to the excitation $f(t)$ is given by the following motion equation.

$$m\ddot{x}(t) + (c_v + c_m)\dot{x}(t) + (k + c_e\omega)x(t) = f(t) \tag{4.23}$$

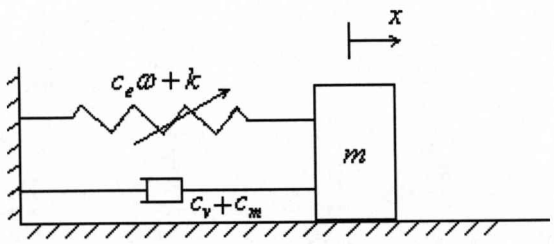

Figure 4.3 A SDOF system with frequency-rate stiffness

The frequency-rate stiffness model is restricted to the harmonic excitation. Otherwise, the frequency parameter ω in the motion equation (4.23) will become non-physical.

4.3 Forced harmonic vibration

The response of the system presented in Figure 4.3 to the harmonic excitation $F\sin\omega t$ is given by the following equation,

$$m\ddot{x}(t)+(c_v+c_m)\dot{x}(t)+(k+c_e\omega)x(t)=F\sin\omega t \tag{4.24}$$

Considering the assumptions (3.21)-(3.23) and the realistic requirements (3.26)-(3.29), the equation can be rewritten as,

$$\ddot{x}(t)+\frac{2\zeta_m\omega_n}{\sqrt{1+\psi^2}}\dot{x}(t)+[\omega_n^2-\frac{2\zeta_m\psi\,\mathrm{sgn}(\omega)\omega\omega_n}{\sqrt{1+\psi^2}}]x(t)=\frac{F}{m}\sin\omega t \tag{4.25}$$

Thus only the steady state response in the frequency ω may be sought through this equation because of the inclusion of ω in the coefficient of $x(t)$. This equation is a second order linear differential equation for a know excitation frequency ω. The steady state response can be obtained by trying a solution in the form of

$$x_p=\mathrm{Im}[Xe^{j\omega t}]=\alpha\,\mathrm{Im}[\frac{F}{m}e^{j\omega t}] \tag{4.26}$$

By substituting the right side of the motion equation (4.25) into $\frac{F}{m}e^{j\omega t}$ for the reason that

$$\frac{F}{m}\sin\omega t = \mathrm{Im}[\frac{F}{m}e^{j\omega t}] \tag{4.27}$$

So, it is found that the receptance α is given as

$$\alpha = \frac{X}{\left(\frac{F}{m}\right)} = \frac{1}{-\omega^2 + j\omega\frac{2\zeta_m\omega_n}{\sqrt{1+\psi^2}} + \left(\omega_n^2 - \frac{2\zeta_m\psi\,\mathrm{sgn}(\omega)\omega\omega_n}{\sqrt{1+\psi^2}}\right)} \tag{4.28}$$

Consequently, we obtain the steady state response

$$x_p = A_1\sin(\omega t + \phi) \tag{4.29}$$

in which,

$$A_1 = |X| = \frac{F}{m\sqrt{\left(\omega_n^2 - \frac{2\zeta_m\psi\,\mathrm{sgn}(\omega)\omega\omega_n}{\sqrt{1+\psi^2}} - \omega^2\right)^2 + \left(\frac{2\zeta_m\omega_n\omega}{\sqrt{1+\psi^2}}\right)^2}} \tag{4.30}$$

$$\phi = arctg\left(\frac{-\frac{2\zeta_m\omega_n\omega}{\sqrt{1+\psi^2}}}{\omega_n^2 - \frac{2\zeta_m\psi\,\mathrm{sgn}(\omega)\omega\omega_n}{\sqrt{1+\psi^2}} - \omega^2}\right) \tag{4.31}$$

The steady state response is a harmonic movement with the amplitude A_1 in the same frequency as the excitation frequency ω however is not in phase with the excitation because of the existence of ϕ.

Obviously, the frequency-rate stiffness model leads some easy understanding for magnetic (complex viscous) damping and is good for harmonic motion. However, we have to be aware that the frequency-rate stiffness model is invalid for the free vibration since the presence of the frequency ω in the motion equation (4.23) is ambiguous when the force term is set to vanish.

Let us consider the steady state response of the system in detail. Particularly in the case that the excitation frequency ω is equal to the undamped system natural frequency ω_n, the amplitude quantity and phase angle of the steady state response is obtained as

$$A_{1(\omega=\omega_n)} = \frac{F}{2\zeta_m m\omega_n^2} = \frac{F}{2\zeta_m k} \tag{4.32}$$

$$\phi_{(\omega=\omega_n)} = arctg\left(\frac{1}{\psi}\right) \tag{4.33}$$

We find that $\frac{F}{k}$ is the displacement of the system under the static force F. Thus, the complex damping ratio coefficient ζ_m can be understood to be the comparison of the static response and the harmonic dynamic response amplitude of the system under the same force. And the imaginary part coefficient factor can be considered as the reciprocal of the slope of the phase angle.

$$\zeta_m = \frac{F/k}{2A_{1(\omega=\omega_n)}} \tag{4.34}$$

$$\psi = \frac{1}{tg[\phi_{(\omega=\omega_n)}]} \tag{4.35}$$

This result provides us a practical method to measure the magnetic (complex viscous) damping parameters. That is, when the system with complex viscous damping is harmonically excited in the undamped system natural frequency ω_n, we can calculate the complex damping ratio coefficient and the imaginary part coefficient factor through the amplitude quantity and phase angle of the steady state response.

4.4 Nyquist diagram

Considering the receptance α in equation (4.28) for frequency-rate stiffness model, it can be rewritten in the following form

$$\alpha = \frac{X}{\left(\frac{F}{m}\right)} = \frac{1}{\omega_n^2} \frac{1}{\left[1 - \frac{2\zeta_m \psi\, \mathrm{sgn}(\omega)}{\sqrt{1+\psi^2}}\left(\frac{\omega}{\omega_n}\right) - \left(\frac{\omega}{\omega_n}\right)^2\right] + j\frac{2\zeta_m}{\sqrt{1+\psi^2}}\left(\frac{\omega}{\omega_n}\right)} \tag{4.36}$$

Thus, we may obtain the non-dimensional receptance

$$\alpha^* = \frac{X}{\left(\frac{F}{k}\right)} = \frac{1}{\left[1 - \frac{2\zeta_m \psi\, \mathrm{sgn}(\omega)}{\sqrt{1+\psi^2}}\left(\frac{\omega}{\omega_n}\right) - \left(\frac{\omega}{\omega_n}\right)^2\right] + j\frac{2\zeta_m}{\sqrt{1+\psi^2}}\left(\frac{\omega}{\omega_n}\right)} \tag{4.37}$$

It is same as the frequency response $H(\omega)$ in equation (2.31) for complex viscous damping model. Thus, both frequency-rate stiffness mode and complex viscous damping model will provide the same understanding for magnetic damping in the frequency domain.

The receptance α^* is a complex valued function with

$$\mathrm{Re}(\alpha^*)=\frac{1-\frac{2\zeta_m\psi\,\mathrm{sgn}(\omega)}{\sqrt{1+\psi^2}}\left(\frac{\omega}{\omega_n}\right)-\left(\frac{\omega}{\omega_n}\right)^2}{\left[1-\frac{2\zeta_m\psi\,\mathrm{sgn}(\omega)}{\sqrt{1+\psi^2}}\left(\frac{\omega}{\omega_n}\right)-\left(\frac{\omega}{\omega_n}\right)^2\right]^2+\left[\frac{2\zeta_m}{\sqrt{1+\psi^2}}\left(\frac{\omega}{\omega_n}\right)\right]^2} \tag{4.38}$$

$$\mathrm{Im}(\alpha^*)=\frac{-\frac{2\zeta_m}{\sqrt{1+\psi^2}}\left(\frac{\omega}{\omega_n}\right)}{\left[1-\frac{2\zeta_m\psi\,\mathrm{sgn}(\omega)}{\sqrt{1+\psi^2}}\left(\frac{\omega}{\omega_n}\right)-\left(\frac{\omega}{\omega_n}\right)^2\right]^2+\left[\frac{2\zeta_m}{\sqrt{1+\psi^2}}\left(\frac{\omega}{\omega_n}\right)\right]^2} \tag{4.39}$$

Therefore, the modulus of the receptance and the phase angle should be

$$|\alpha^*|=\sqrt{[\mathrm{Re}(\alpha^*)]^2+[\mathrm{Im}(\alpha^*)]^2}$$

$$=\frac{1}{\sqrt{\left[1-\frac{2\zeta_m\psi\,\mathrm{sgn}(\omega)}{\sqrt{1+\psi^2}}\left(\frac{\omega}{\omega_n}\right)-\left(\frac{\omega}{\omega_n}\right)^2\right]^2+\left[\frac{2\zeta_m}{\sqrt{1+\psi^2}}\left(\frac{\omega}{\omega_n}\right)\right]^2}} \tag{4.40}$$

$$angle(\alpha^*)=arctg\left[\frac{-\frac{2\zeta_m}{\sqrt{1+\psi^2}}\left(\frac{\omega}{\omega_n}\right)}{1-\frac{2\zeta_m\psi\,\mathrm{sgn}(\omega)}{\sqrt{1+\psi^2}}\left(\frac{\omega}{\omega_n}\right)-\left(\frac{\omega}{\omega_n}\right)^2}\right] \tag{4.41}$$

Taking $\left(\frac{\omega}{\omega_n}\right)=0$, the real part and imaginary part is obtained

$$\mathrm{Re}(\alpha^*)=1 \tag{4.42}$$

$$\mathrm{Im}(\alpha^*)=0 \tag{4.43}$$

And when $\left(\frac{\omega}{\omega_n}\right) \to 0$, we have

$$\mathrm{Re}(\alpha^*) \to 0 \tag{4.44}$$

$$\mathrm{Im}(\alpha^*) \to 0 \tag{4.45}$$

Thus in the complex plane, the Nyquist diagram of the system shows a distorted approximately circular arc. The arc clockwise starts from the point (1, 0) and ends at the point (0, 0).

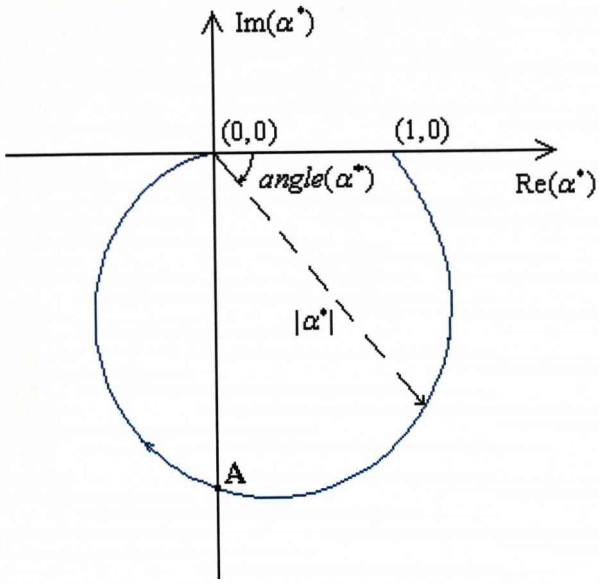

Figure 4.4 Nyquist diagram of system with magnetic damping

Specifically, the real part of the receptance is equal to zero at the A point. This means there is a phase angle shift. Thus, a resonance happens at this frequency. If we set

$$\mathrm{Re}(\alpha^*) = \frac{1 - \frac{2\zeta_m \psi\, \mathrm{sgn}(\omega)}{\sqrt{1+\psi^2}}\left(\frac{\omega}{\omega_n}\right) - \left(\frac{\omega}{\omega_n}\right)^2}{\left[1 - \frac{2\zeta_m \psi\, \mathrm{sgn}(\omega)}{\sqrt{1+\psi^2}}\left(\frac{\omega}{\omega_n}\right) - \left(\frac{\omega}{\omega_n}\right)^2\right]^2 + \left[\frac{2\zeta_m}{\sqrt{1+\psi^2}}\left(\frac{\omega}{\omega_n}\right)\right]^2} = 0 \tag{4.46}$$

The calculation gives the result

$$\left(\frac{\omega}{\omega_n}\right)_{res} = \frac{1}{\sqrt{1+\psi^2}}\left(\sqrt{\zeta_m^2\psi^2 + \psi^2 + 1} - \zeta_m\psi\right) \tag{4.47}$$

The resonant receptance modulus is

$$|\alpha^*|_{res} = \frac{1}{\frac{2\zeta_m}{1+\psi^2}\left(\sqrt{\zeta_m^2\psi^2+\psi^2+1}-\zeta_m\psi\right)} \tag{4.48}$$

This discussion is agreement to the representation of the Figure 3.9

Figure 4.5, Figure 4.6 and Figure 4.7 illustrate Nyquist diagrams calculated for a single degree of freedom system having different magnetic damping parameters ζ_m and ψ. From Figure 4.5, it is found that with the increment of ζ_m, the radius of the arc decreases. On the other hand, Figure 4.6 shows that the radius of the arc will increase with the increment of ψ when $\psi \geq 0$.

For the case of $\psi < 0$, a significant characteristic is that a small distortion occurs near the start point (1,0) of the diagram arc. And with the increment of the absolute value of ψ, the distortion become stronger as shown in the zoom window in Figure 4.7. The radius of the diagram arc will also increase with the increment of the absolute value of ψ when $\psi \leq -1$. And when $0 > \psi > -1$, the radii of the arcs are close.

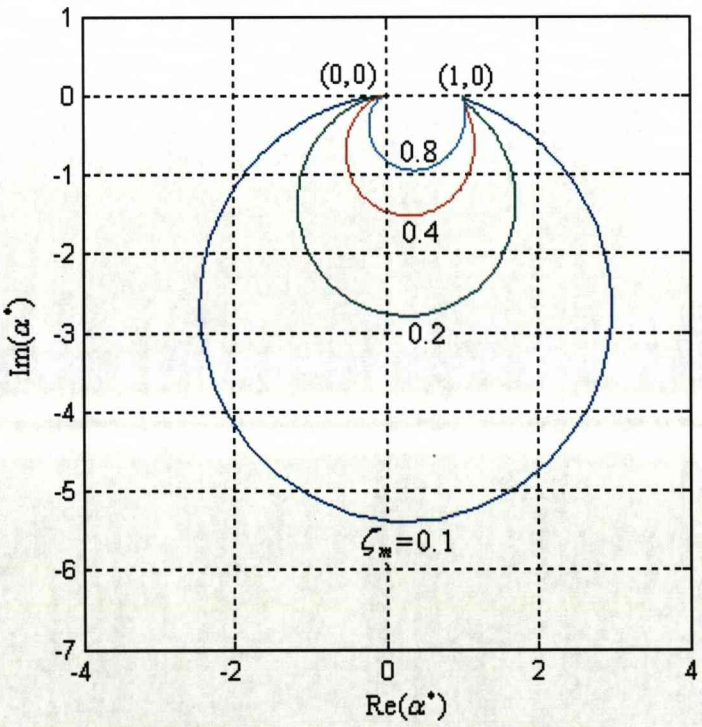

Figure 4.5 Nyquist diagram of system with $\psi = 0.3$

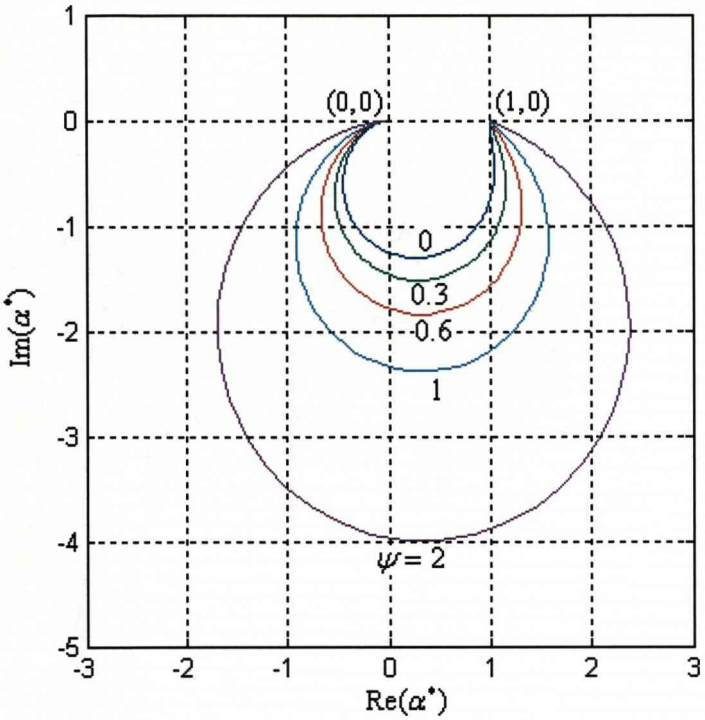

Figure 4.6 Nyquist diagram of system with $\zeta_m = 0.4$ for $\psi > 0$

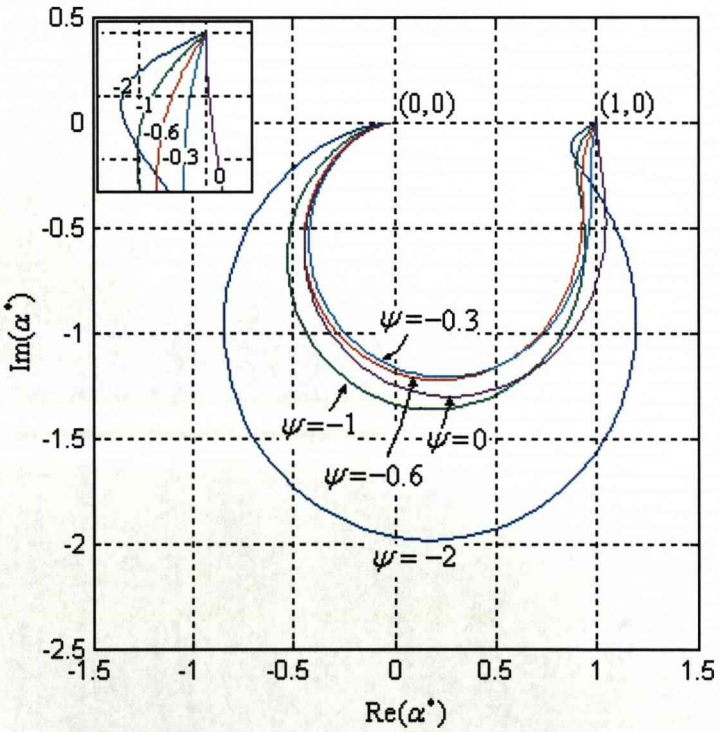

Figure 4.7 Nyquist diagram of system with $\zeta_m = 0.4$ for $\psi < 0$

In order to understand clearer the dynamical property of the magnetic damping, a comparison of Nyquist diagrams for the systems with viscous damping, magnetic damping and hysteretic damping is taken as shown in Figure 4.8. In this example, the equation of motion for the system with hysteretic damping is written as $\ddot{x} + \omega_n^2[1 + j\eta\,\mathrm{sgn}(\omega)]x = f$ with $\eta = 0.3$. For viscous damping system the damping ratio is chosen as $\zeta = 0.2$. For the magnetic damping system, the damping ratio and imaginary factor is set as $\zeta_m = 0.2$ and $\psi = 0.3$ using the model described before.

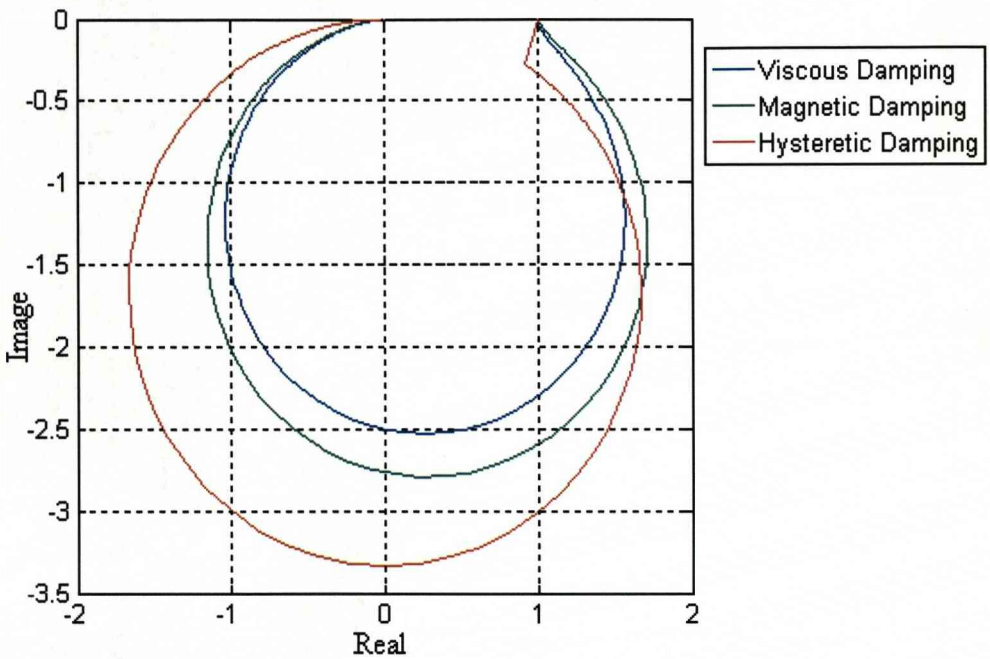

Figure 4.8 Comparison of Nyquist diagrams of three kinds of damping

It can be seen from Figure that for these three kinds of damping all diagrams start from the point (1,0) and end to the point (0,0). But the arc shapes are different.

4.5 Random vibration of the SDOF system with magnetic damping

When a system is excited by a random force, the exciting force is continually changing with the time. In particular, the force is unpredictable and it is very difficult to exactly depict it. In this case, the exact determination of the response of the system becomes impossible and unimportant.

When the excitation is stationary, the spectrums obtained through different time intervals are close and an average spectrum can be obtained. On the other hand, the statistical properties of this excitation do not change with the time. Thus an alternative method is to consider the response in terms of the average spectrum, especially in terms of the mean square average of the spectrum.

White ergodic noise is stationary because it is a random signal with an equal power spectral density in any band and in this ergodic random process time averages approach ensemble averages in the limit.

For the single degree of freedom system with magnetic damping as shown in Figure 3.3, we consider the excitation $f(t)$ to be a white ergodic noise with a constant mean square spectral density S_0 over the all frequency range from $\omega=-\infty$ to $\omega=\infty$. Then the mean square spectral density $S_x(\omega)$ of the response $x(t)$ can be calculated through the receptance α of the system in equation (4.36) [8].

$$
\begin{aligned}
S_x(\omega) &= \frac{1}{m^2}\alpha(\omega)\alpha(-\omega)S_0 \\
&= \frac{S_0}{m^2\omega_n^4}\frac{1}{\left\{\left[1-\frac{2\zeta_m\psi\,\mathrm{sgn}(\omega)}{\sqrt{1+\psi^2}}\left(\frac{\omega}{\omega_n}\right)-\left(\frac{\omega}{\omega_n}\right)^2\right]+j\frac{2\zeta_m}{\sqrt{1+\psi^2}}\left(\frac{\omega}{\omega_n}\right)\right\}} \\
&\qquad \frac{1}{\left\{\left[1-\frac{2\zeta_m\psi\,\mathrm{sgn}(\omega)}{\sqrt{1+\psi^2}}\left(\frac{\omega}{\omega_n}\right)-\left(\frac{\omega}{\omega_n}\right)^2\right]-j\frac{2\zeta_m}{\sqrt{1+\psi^2}}\left(\frac{\omega}{\omega_n}\right)\right\}} \\
&= \frac{S_0}{m^2\omega_n^4}\frac{1}{\left[1-\frac{2\zeta_m\psi\,\mathrm{sgn}(\omega)}{\sqrt{1+\psi^2}}\left(\frac{\omega}{\omega_n}\right)-\left(\frac{\omega}{\omega_n}\right)^2\right]^2+\left[\frac{2\zeta_m}{\sqrt{1+\psi^2}}\left(\frac{\omega}{\omega_n}\right)\right]^2}
\end{aligned}
\tag{4.49}
$$

If we set $\eta=\frac{\omega}{\omega_n}$, equation (4.49) can be simplified as

$$S_x(\omega)=\frac{S_0}{m^2\omega_n^4}\frac{1}{\left(1-\frac{2\zeta_m\psi\eta\,\mathrm{sgn}(\eta)}{\sqrt{1+\psi^2}}-\eta^2\right)^2+\left(\frac{2\zeta_m\eta}{\sqrt{1+\psi^2}}\right)^2} \tag{4.50}$$

since $\omega_n>0$.

Now, the expected means square of the response can be expressed

$$E[x^2]=\int_{-\infty}^{\infty}S_x(\omega)d\omega$$

$$=\frac{S_0}{m^2\omega_n^3}\int_{-\infty}^{\infty}\frac{1}{\left(1-\frac{2\zeta_m\psi\eta\,\mathrm{sgn}(\eta)}{\sqrt{1+\psi^2}}-\eta^2\right)^2+\left(\frac{2\zeta_m\eta}{\sqrt{1+\psi^2}}\right)^2}d\eta \tag{4.51}$$

This integral also shows a singularity at the origin. However because the integral function is real and even it can be reduced to the real integration in the positive-real range as following

$$E[x^2]=\frac{2S_0}{m^2\omega_n^3}\int_{0}^{\infty}\frac{1}{\left(1-\frac{2\zeta_m\psi\eta}{\sqrt{1+\psi^2}}-\eta^2\right)^2+\left(\frac{2\zeta_m\eta}{\sqrt{1+\psi^2}}\right)^2}d\eta \tag{4.52}$$

If four complex poles of the function $f_{\mathrm{int}}=\frac{1}{\left(1-\frac{2\zeta_m\psi\eta}{\sqrt{1+\psi^2}}-\eta^2\right)^2+\left(\frac{2\zeta_m\eta}{\sqrt{1+\psi^2}}\right)^2}$ may be in the following forms

$$s_{1,2}=a_1\pm jb_1 \tag{4.53}$$

$$s_{3,4}=a_2\pm jb_2 \tag{4.54}$$

where,

$$a_1=-\left(\frac{\zeta_m\psi}{\sqrt{1+\psi^2}}-W\right) \tag{4.55}$$

$$b_1=\left(\frac{\zeta_m}{\sqrt{1+\psi^2}}-\mathrm{sgn}(\psi)Z\right) \tag{4.56}$$

$$a_2=-\left(\frac{\zeta_m\psi}{\sqrt{1+\psi^2}}+W\right) \tag{4.57}$$

$$b_2 = \left(\frac{\zeta_m}{\sqrt{1+\psi^2}} + \mathrm{sgn}(\psi) Z \right) \tag{4.58}$$

in which,

$$W = \frac{\sqrt{2}}{2} \sqrt{\sqrt{\left[\zeta_m^2 \left(\frac{\psi^2 - 1}{\psi^2 + 1} \right) + 1 \right]^2 + 4 \left(\frac{\zeta_m^2 \psi}{\psi^2 + 1} \right)^2} + \left[\zeta_m^2 \left(\frac{\psi^2 - 1}{\psi^2 + 1} \right) + 1 \right]} \tag{4.59}$$

$$Z = \frac{\sqrt{2}}{2} \sqrt{\sqrt{\left[\zeta_m^2 \left(\frac{\psi^2 - 1}{\psi^2 + 1} \right) + 1 \right]^2 + 4 \left(\frac{\zeta_m^2 \psi}{\psi^2 + 1} \right)^2} - \left[\zeta_m^2 \left(\frac{\psi^2 - 1}{\psi^2 + 1} \right) + 1 \right]} \tag{4.60}$$

This function can be expressed by a partial fraction function expansion as

$$\begin{aligned} f_{\mathrm{int}} &= \frac{1}{(\eta - s_1)(\eta - s_2)(\eta - s_3)(\eta - s_4)} \\ &= \frac{1}{[(\eta - a_1)^2 + b_1^2][(\eta - a_2)^2 + b_2^2]} \end{aligned} \tag{4.61}$$

Since the poles of this integral function appear in the conjugate complex couple form. Thus, the integration of equation (4.52) can be calculated as below

$$\begin{aligned} E[x^2] &= \frac{2S_0}{m^2 \omega_n^3} \int_0^\infty \frac{1}{[(\eta - a_1)^2 + b_1^2][(\eta - a_2)^2 + b_2^2]} d\eta \\ &= \frac{2S_0}{m^2 \omega_n^3} \int_0^\infty \left(\frac{c_1 \eta + c_2}{[(\eta - a_1)^2 + b_1^2]} - \frac{c_1 \eta + c_4}{[(\eta - a_2)^2 + b_2^2]} \right) d\eta \end{aligned} \tag{4.62}$$

Here, c_1, c_2 and c_4 are real constants. They can be calculated by expanding the function and letting the factors of the items η^3, η^2 and η to be zeros, while setting the constant item to be one. So,

$$c_1 = \frac{2(a_2 - a_1)}{[(a_2^2 + b_2^2) - (a_1^2 + b_1^2)]^2 + 4[a_1^2(a_2^2 + b_2^2) + a_2^2(a_1^2 + b_1^2)] - 4a_1 a_2[(a_2^2 + b_2^2) + (a_1^2 + b_1^2)]}$$

$$c_2 = \frac{[(a_a^2 + b_2^2) - (a_1^2 + b_1^2)] + 4a_1(a_1 - a_2)}{[(a_2^2 + b_2^2) - (a_1^2 + b_1^2)]^2 + 4[a_1^2(a_2^2 + b_2^2) + a_2^2(a_1^2 + b_1^2)] - 4a_1 a_2[(a_2^2 + b_2^2) + (a_1^2 + b_1^2)]}$$

$$c_4 = \frac{[(a_a^2 + b_2^2) - (a_1^2 + b_1^2)] + 4a_2(a_1 - a_2)}{[(a_2^2 + b_2^2) - (a_1^2 + b_1^2)]^2 + 4[a_1^2(a_2^2 + b_2^2) + a_2^2(a_1^2 + b_1^2)] - 4a_1 a_2[(a_2^2 + b_2^2) + (a_1^2 + b_1^2)]}$$

(4.63 a. b. c)

Thus, the final integral results can be obtained

$$E[x^2]=\frac{2S_0}{m^2\omega_n^3}\left\{\frac{c_1}{2}\ln\left(\frac{a_2^2+b_2^2}{a_1^2+b_1^2}\right)+\frac{(c_1a_1+c_2)}{|b_1|}\left[\frac{\pi}{2}+arctg\left(\frac{a_1}{|b_1|}\right)\right]\right.$$
$$\left.-\frac{(c_1a_2+c_4)}{|b_2|}\left[\frac{\pi}{2}+arctg\left(\frac{a_2}{|b_2|}\right)\right]\right\} \tag{4.64}$$

In Figure 4.9 and Figure 4.10 the mean square response following equation (4.64) are plotted with respect to the parameters ζ_m for $\psi>0$ and $\psi<0$. Figure 4.11 illustrates the mean square response to the parameter ψ. It is obvious that the increment of complex damping ratio ζ_m will reduce the response but the increment of the absolute value of ψ will increase the level of the mean square response.

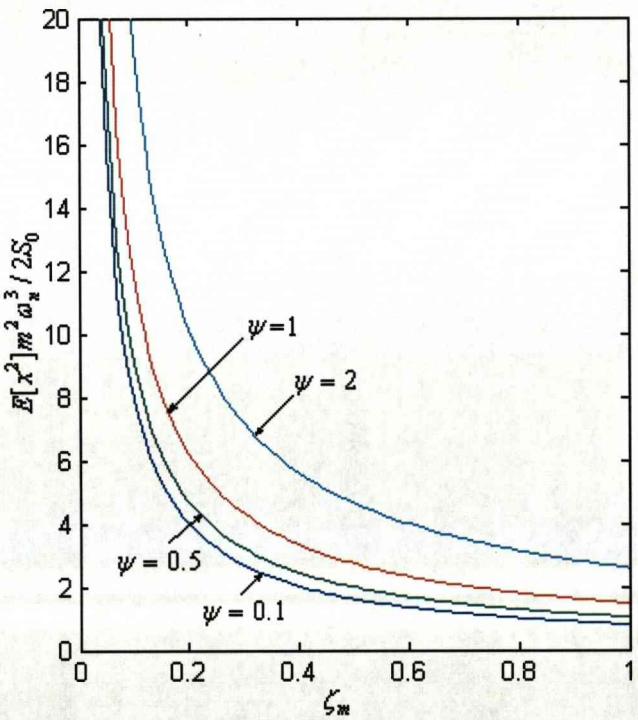

Figure 4.9 Mean square response of the system with ζ_m for $\psi>0$

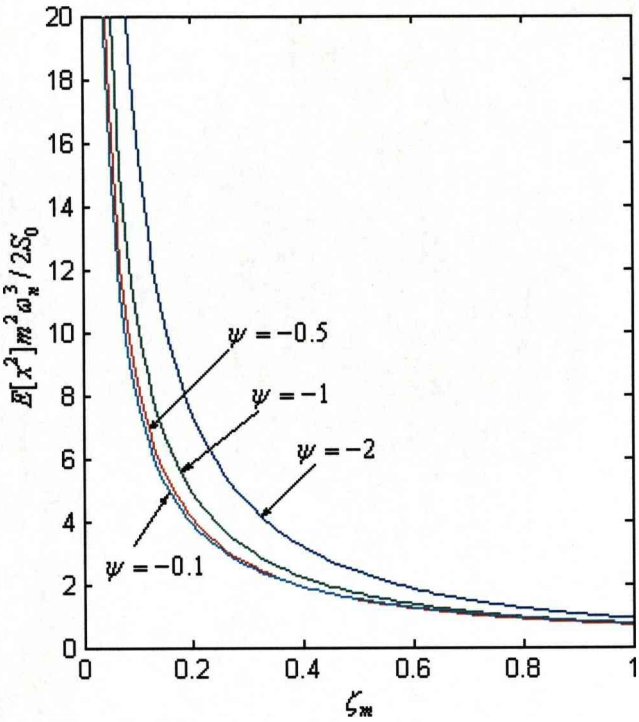

Figure 4.10 Mean square response of the system with ζ_m for $\psi<0$

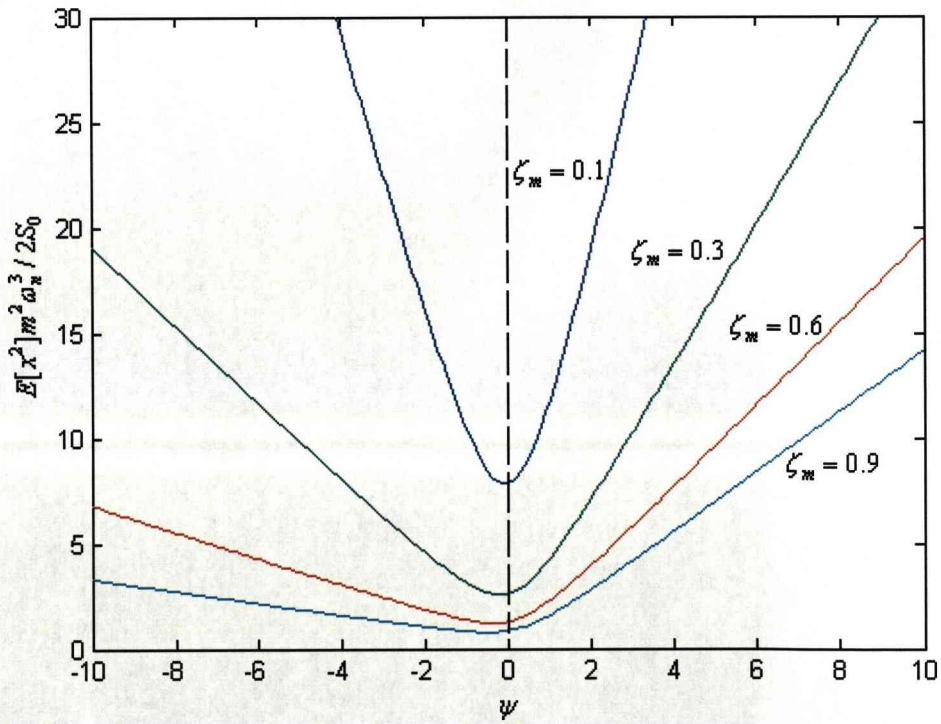

Figure 4.11 Mean square response of the system with ψ

Besides, it can be seen that both mass m and undamped natural frequency ω_n are in the dominator in the equation (4.64). This means that increasing mass and stiffness (increasing undamped natural frequency) will all reduce the level the mean square response of the system with magnetic damping.

It should be noted that the above calculation is not suitable for the special case of $\zeta_m = 1$ and $\psi = 0$. It will cause zero denominators of factors c_1, c_2 and c_4. It can also be found that this is the critical damping case for the system with pure viscous damping.

In this case, the integrals in equation (4.52) can be simplified as

$$E[x^2] = \frac{2S_0}{m^2\omega_n^3}\int_0^\infty \frac{1}{(1-\eta^2)^2 + (2\eta)^2}d\eta$$

$$= \frac{S_0\pi}{2m^2\omega_n^3} \tag{4.65}$$

The reader should be aware that the mean value of the response is not very important in the statistical analysis of a random vibration process since this mean value can be easily withdrawn from the whole signal if it exits. And we pay more attention the difference between the signal and its mean value. The squared value of this difference is call as variance. Thus when we study a random vibration process, we only investigate those signals with zero mean value. Therefore under the zero mean white ergodic noise excitation, the response has a zero mean value and the variance of the response may be simply calculated as,

$$\sigma^2 = E[x^2] \tag{4.66}$$

in which, σ is the standard deviation.

The complex magnetic damping model and the frequency-rate stiffness model all must be defined in the frequency domain or limited in the transient work to periodic harmonic input functions. The technique discussed above just provides a mathematical method that can obtain acceptable response results.

4.6 Closure

Although the magnetic damping will introduce a complex viscous damping model, the energy lost per cycle of the system with magnetic damping is in the similar form of the pure viscous damping system. This means that the imaginary part of the complex viscous damping coefficient will not affect the energy dissipation form of the system. However on the other hand, this imaginary part factor will change the potential energy that is stored in the system. This is the different way that the complex viscous damping model works when compared to the conventional viscous damper. As we know, the potential energies stored in both the conventional viscous damped system and the original undamped system are identical.

Compared to the complex viscous damping model, the frequency-rate stiffness model provides a more clear understanding of the effect of the magnetic damping. But unfortunately this model can only be used in harmonic movement. Otherwise the frequency item in the model becomes meaningless. Both the complex viscous damping model and the frequency-rate stiffness model give us a same understanding of the magnetic damping in the frequency domain. Thus the forced harmonic responses calculated through two models will show same steady state response.

The displacement Nyquist diagram of the system with magnetic damping illustrates an approximate circular arc start from point (1, 0) to the original point (0, 0) in clockwise. It shows a simple way to obtain the resonance frequency and resonance receptance modulus for the system.

The random response analysis results show that increasing mass, stiffness and the complex damping ratio will all reduce the level the mean square response of the system with magnetic damping. However, the increment of the imaginary part will increase the mean square response level.

Chapter 5

Time Domain Response Analyses

The time domain response analyses of the complex viscous damped system are presented in this chapter. And two methods, Fast Fourier Transform analysis and an iterative technique using Hilbert transform, are proposed for the computation of the responses. FFT analysis is based on the mathematical relation of the input signals and the transfer function. On the other hand the iterative technique uses the Hilbert transform and yields integro-differential equations for the equations of motion of structures when real-valued signals are introduced in the formulations. Both methods showed the non-causal effect of complex viscous damping model. Example analyses illustrate the application of the two approaches, and the analysis results demonstrate the validity of these methods.

5.1 Concept of complex viscous damping

As discussed in chapter 3 and chapter 4, the complex viscous damping model is expressed using the following mathematical form, in which the storage and loss moduli is

$$f(t) = c_t(1 + j\psi)\dot{x}(t) + kx(t) \tag{5.1}$$

Alternatively, we have thought of another complex viscous damping model, which is a frequency-rate stiffness model.

$$f(t) = c_t \dot{x}(t) + kx(t) - c_t \psi \omega x(t) \tag{5.2}$$

in which,

$$c_t = c_v + c_m \tag{5.3}$$

However, equation (5.1) is incorrect. For it implies that a complex valued force $f(t)$ results from the real valued deformation $x(t)$ and the real valued velocity $\dot{x}(t)$. Equation (5.2) is also incorrect. The meaning of the term ω in equation (5.2) in only reasonable for the harmonic excitation, and it is far from clear in the case of arbitrary deformation $x(t)$.

In fact, equation (5.1) should be written as

$$F(j\omega) = c_t[1 + j\psi \operatorname{sgn}(\omega)]\dot{X}(j\omega) + kX(j\omega) \tag{5.4}$$

And equation (5.2) should be written as

$$F(j\omega) = c_t \dot{X}(j\omega) - c_t \psi \mid \omega \mid X(j\omega) + kX(j\omega) \tag{5.5}$$

It is noticed that equation (5.3) and equation (5.4) are the same, because

$$\dot{X}(j\omega) = j\omega X(j\omega) \tag{5.6}$$

and

$$\mid \omega \mid = \omega \operatorname{sgn}(\omega) \tag{5.7}$$

5.2 Frequency domain solution of equation of motion

Consider a single-degree-of-freedom (SDOF) system with complex viscous damping as described in equation

$$m\ddot{x}(t) + (c_v + c_m - jc_e)\dot{x}(t) + kx(t) = f(t) \tag{5.8}$$

Or in the canonical form as following equation by using the assumption (3.21)-(3.23),

$$\ddot{x}(t)+2\zeta_m\frac{1+j\psi}{\sqrt{1+\psi^2}}\omega_n\dot{x}(t)+\omega_n^2x(t)=w(t) \tag{5.9}$$

Here, for the sake of simplicity, we consider the unit mass case of $m=1\ kg$, thus we have $w(t)=f(t)$. According to the complex viscous damping model (5.4), equation (5.9) should be rewritten correctly in the frequency domain as

$$\ddot{X}(j\omega)+\frac{2\zeta_m\omega_n}{\sqrt{1+\psi^2}}[1+j\psi\,\mathrm{sgn}(\omega)]\dot{X}(j\omega)+\omega_n^2X(j\omega)=W(j\omega) \tag{5.10}$$

That is,

$$-\omega^2X(j\omega)+\frac{2\zeta_m\omega_n}{\sqrt{1+\psi^2}}[1+j\psi\,\mathrm{sgn}(\omega)]j\omega X(j\omega)+\omega_n^2X(j\omega)=W(j\omega) \tag{5.11}$$

So, we get the relation of response and excitation in frequency domain

$$\{\omega_n^2-\omega^2-\frac{2\zeta_m\omega_n}{\sqrt{1+\psi^2}}\psi\,|\,\omega\,|+j\frac{2\zeta_m\omega_n\omega}{\sqrt{1+\psi^2}}\}X(j\omega)=W(j\omega) \tag{5.12}$$

To compute the impulse response of the system, we let $f(t)=\delta(t)$. Thus, the deformation history $h(t)$ can be computed using inverse Fourier transform

$$h(t)=\frac{1}{2\pi}\int_{-\infty}^{\infty}\frac{e^{j\omega t}}{\omega_n^2-\omega^2-\frac{2\zeta_m\omega_n}{\sqrt{1+\psi^2}}\psi\,|\,\omega\,|+j\frac{2\zeta_m\omega_n\omega}{\sqrt{1+\psi^2}}}d\omega \tag{5.13}$$

As noted by Crandall (1963), the singularity at $\omega=0$ rules out the usual evaluation of equation (5.13) by contour integration. Because the imaginary part of the integration function is odd, the response can be expressed as

$$h(t)=\frac{1}{\pi}\int_0^{\infty}\frac{[\omega_n^2-\omega^2-\frac{2\zeta_m\omega_n}{\sqrt{1+\psi^2}}\psi\,|\,\omega\,|]\cos\omega t+\frac{2\zeta_m\omega_n\omega}{\sqrt{1+\psi^2}}\sin\omega t}{[\omega_n^2-\omega^2-\frac{2\zeta_m\omega_n}{\sqrt{1+\psi^2}}\psi\,|\,\omega\,|]^2+[\frac{2\zeta_m\omega_n\omega}{\sqrt{1+\psi^2}}]^2}d\omega \tag{5.14}$$

Equation (5.14) can be computed using numerical integration. Figure 5.1

demonstrated the system responses with different imaginary damping ratio ψ. An SDOF vibration system with $\omega_n = 1, \zeta_m = 0.30$ was considered. And the imaginary damping ratio ψ=3, 1, 0, -1, and –3. As illustrated in this figure, the non-causal impulse response is yielded for the system, since nonzero response occurs for $t < 0$, prior to the application of the load. Figure 5.2 shows the impulse response of a complex viscous damping SDOF system with $\omega_n = 2\pi \ \ rad/s$, $\psi = 0.75$, and $\zeta_m = 0.10, \ \ 0.20, \ \ 0.40,$ and 0.80. It can be noticed that the above impulse response is same to those results calculated through residues integral method (Figure 3.15 and Figure 3.16) as described in chapter 3.

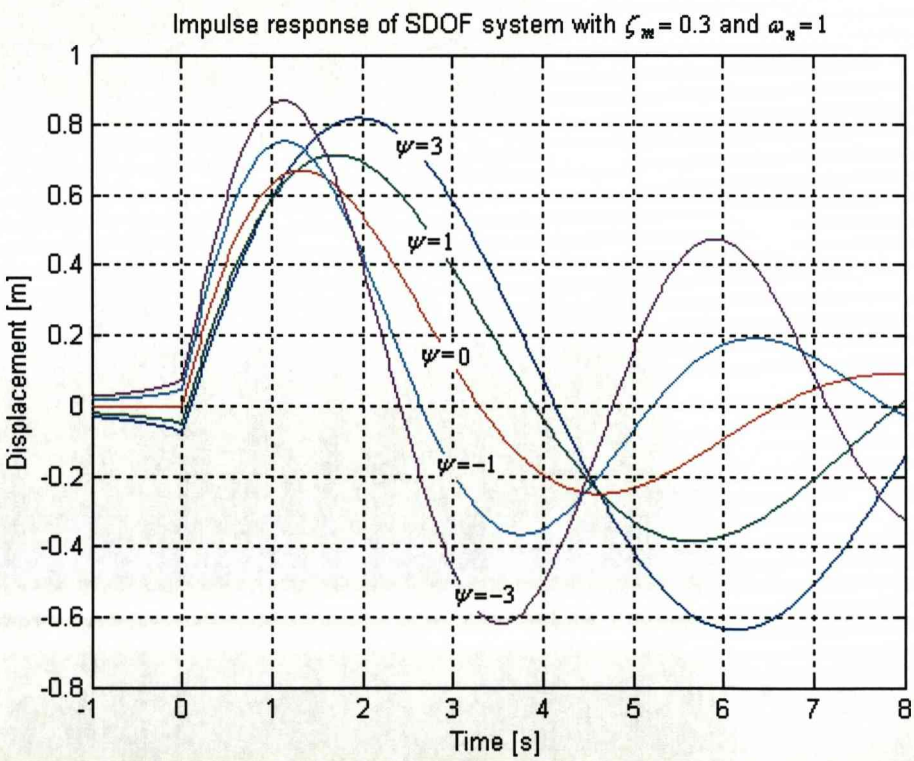

Figure 5.1 Impulse responses of complex damped SDOF system with ψ

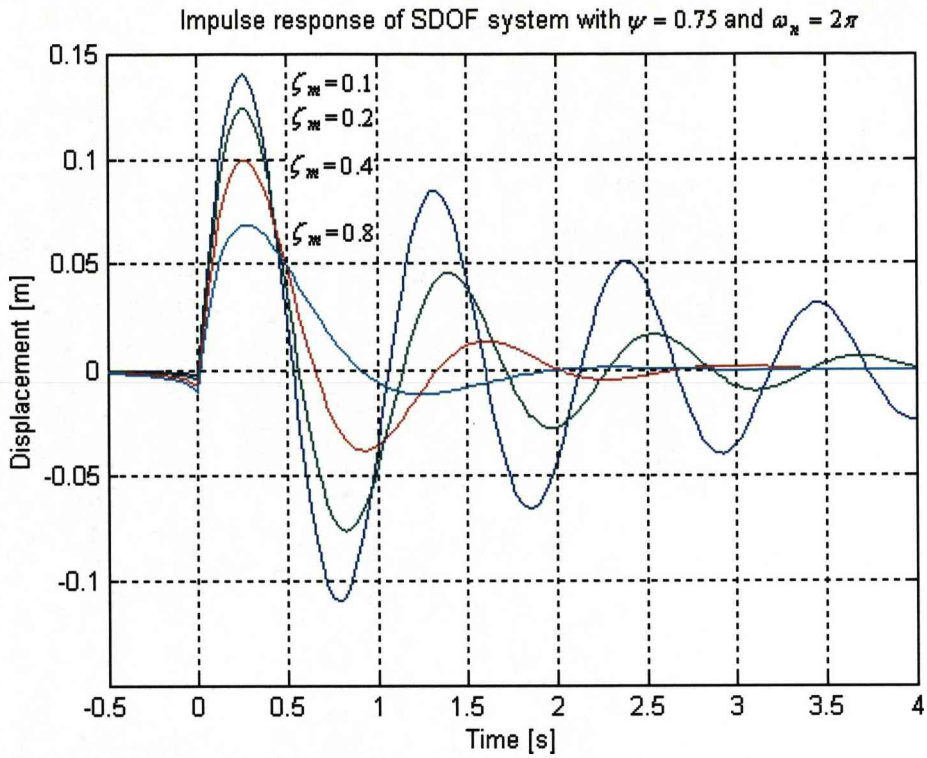

Figure 5.2 Impulse responses of complex damped SDOF system with ζ_m

In the case of arbitrary excitation, the response of the system described in equation (5.10) can be obtained by inverse Fourier transforms. Fast Fourier transform (FFT) techniques can also be used to compute the response. Three steps are involved in this process. The first is to take Fourier transform for the excitation and to get $W(j\omega)$. Then the response in frequency domain $X(j\omega)$ is computed using the equation (5.12). At last, by taking inverse Fourier transform for $X(j\omega)$, the time history response $x(t)$ can be obtained. Because of the non-causality of the model, two zero excitation segments were introduced both before and after the time of the original excitation in order to guarantee the accuracy of the computation.

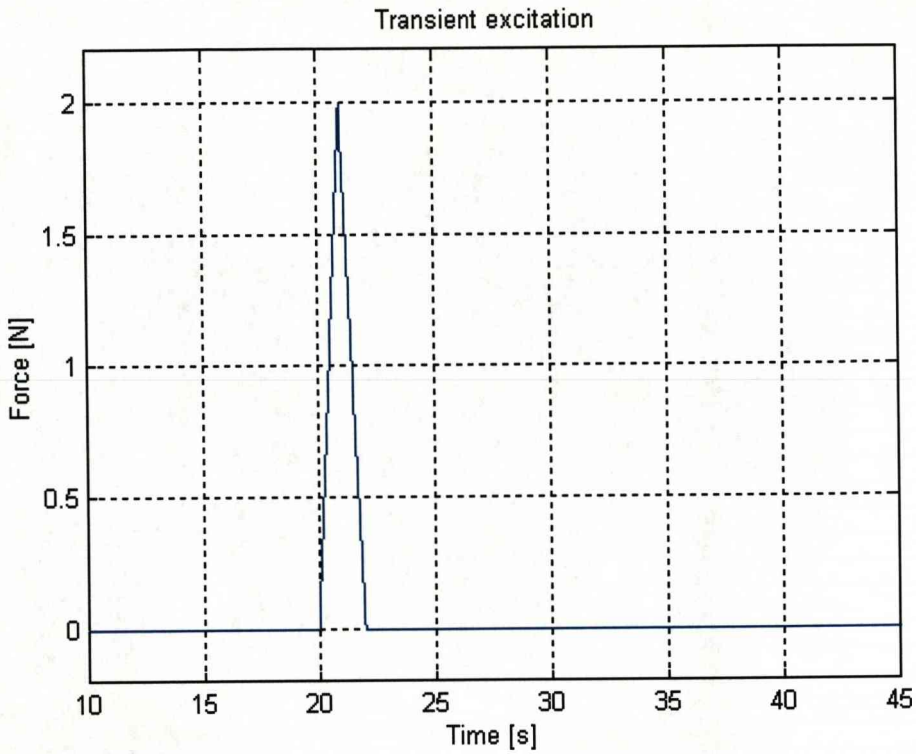

Figure 5.3 Transient triangular excitation

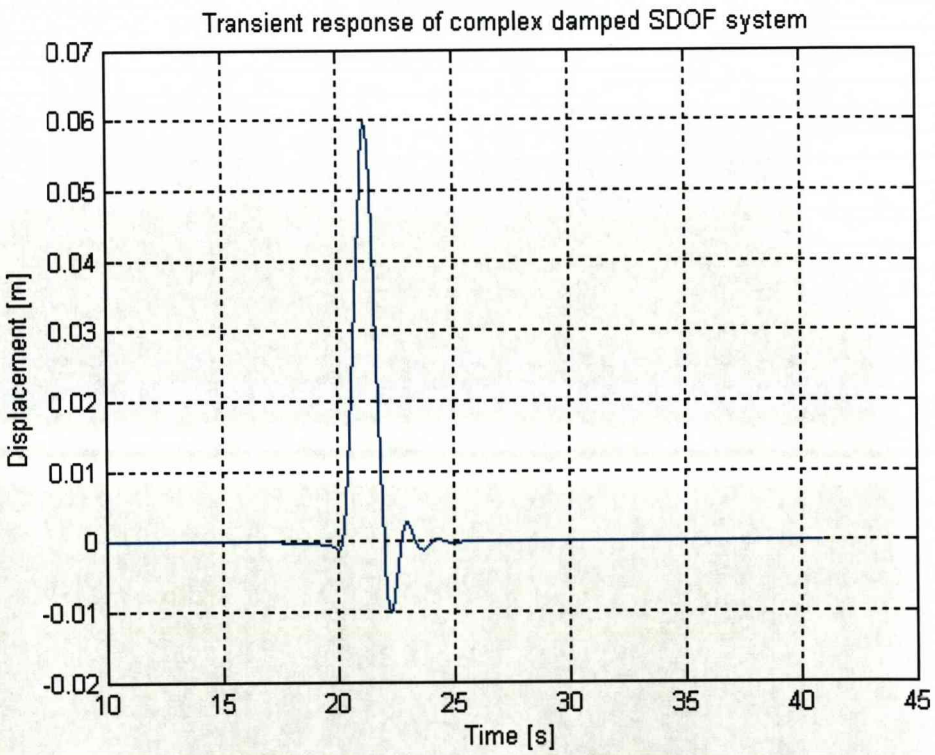

Figure 5.4 Transient response of complex damping SDOF system using FFT

Figure 5.3 presents a transient excitation signal $w(t)$ and Figure 5.4 shows the corresponding transient response $x(t)$ by using FFT computation. In this example, the parameters of the vibration system were selected as $\omega_n = 2\pi \ \ rad/s$, $\psi = 0.75$, and $\zeta_m = 0.40$.

5.3 The Hilbert transform

The functions $y(t)$ and $\hat{y}(t)$ are called a Hilbert transform pair if, for almost all t,

$$\hat{y}(t) = H[y(t)] = \lim_{a\to\infty} P\int_{-a}^{a} \frac{-y(t)}{\pi(t-\tau)}d\tau \tag{5.15}$$

and

$$y(t) = H^{-1}[\hat{y}(t)] = \lim_{a\to\infty} P\int_{-a}^{a} \frac{\hat{y}(t)}{\pi(t-\tau)}d\tau \tag{5.16}$$

where

$$P\int_{-\infty}^{\infty} \frac{f(t)}{\pi(t-\tau)}d\tau = \lim_{\varepsilon\to 0^+}\left[\int_{+\varepsilon}^{\infty} \frac{f(t)}{\pi(t-\tau)}d\tau + \int_{-\infty}^{-\varepsilon} \frac{f(t)}{\pi(t-\tau)}d\tau\right] \tag{5.17}$$

is called the Cauchy principal value around $\tau = t$ of the integral. We say that $\hat{y}(t)$ is the Hilbert transform of $y(t)$, and we write $\hat{y}(t) = H[y(t)]$ [27].

Equation (5.15) shows that the Hilbert transform is a time domain signal operator. And the Hilbert transform is non-causal, because in order to compute $\hat{y}(t)$, the function $y(\tau)$ is required for $-\infty < \tau < \infty$; that is, the future of signal is required to compute the Hilbert transform of the signal at present time.

The Hilbert transform of a constant is zero. The Hilbert transform of a Hilbert

transform is the negative of the original function. Therefore,

$$H[H[y(t)]] = -y(t) \tag{5.18}$$

Consider the $y(t) = \sin \omega t$ with $\omega \neq 0$, its Hilbert transform is

$$H[\sin \omega t] = \cos \omega t \, \mathrm{sgn}(\omega) \tag{5.19}$$

Similarly,

$$H[\cos \omega t] = -\sin |\omega| t \tag{5.20}$$

The Hilbert transform does not change the amplitude of sine or cosine signal and only produces a phase shift of $\frac{\pi}{2}$ or $-\frac{\pi}{2}$ radians in these signals.

And we obtain the Fourier transform (FT) of a Hilbert transform as

$$FT[\hat{y}(t))] = j \, \mathrm{sgn}(\omega) FT[y(t)] \tag{5.21}$$

As indicated in this equation, the Hilbert transform maintains the magnitude of the signal at all frequencies except for $\omega = 0$.

5.4 Iterative technique with Hilbert transform

On many occasions, time domain solutions are more desirable than frequency domain methods. In the case of nonlinear structures, frequency domain techniques will become very difficult and complicated, while the time domain iterative technique can estimate the response of the structure using step-by-step integration schemes. On the other hand, many practical engineering structure analyses are constricted by the analysis method and computation tools such as finite element method. In this case, the time domain technique will be the feasible way to compute the transient response of the structures. In this section, an iterative technique for computation of the response of structures with complex viscous damping is developed.

As discussed above, the correct dynamic equation of a system with complex viscous damping should be described in the frequency domain as Equation (5.10). Thus, the corresponding time domain representation is

$$\ddot{x}(t)+\frac{2\zeta_m\omega_n}{\sqrt{1+\psi^2}}\dot{x}(t)+\frac{2\zeta_m\omega_n\psi}{\sqrt{1+\psi^2}}\hat{\dot{x}}(t)+\omega_n^2x(t)=w(t) \tag{5.22}$$

because of the property of the Hilbert transform (5.21). In this equation, $\hat{\dot{x}}(t)=H[\dot{x}(t)]$ is the Hilbert transform for velocity.

The equation (5.22) can be changed in the following form

$$\ddot{x}(t)+\frac{2\zeta_m\omega_n}{\sqrt{1+\psi^2}}\dot{x}(t)+\omega_n^2x(t)=w(t)-\frac{2\zeta_m\omega_n\psi}{\sqrt{1+\psi^2}}\hat{\dot{x}}(t) \tag{5.23}$$

It should be noticed that since the complex viscous damping model is non-causal, the response velocity $\dot{x}(t)$ anticipates the excitation. That means the initial condition cannot be defined at the time $t=0$, since the response $x(t)$ depends on the past and future values of $\dot{x}(t)$, which is, in turn, determined by $w(t)$ with $-\infty<t<\infty$.

Now, consider the following mathematical effect on equation (5.23). Thus, the $(n+1)^{\text{th}}$ computation result should be obtained from the below equation.

$$\ddot{x}^{(n+1)}(t)+\frac{2\zeta_m\omega_n}{\sqrt{1+\psi^2}}\dot{x}^{(n+1)}(t)+\omega_n^2x^{(n+1)}(t)=w(t)-\frac{2\zeta_m\omega_n\psi}{\sqrt{1+\psi^2}}\hat{\dot{x}}^{(n)}(t) \tag{5.24}$$

In which, n is the iterative step number. And the initial conditions are $x^{(n)}(-\infty)=0$ and $\dot{x}^{(n)}(-\infty)=0$. In equation (5.24), $x^{(n)}(t)$ represents the solution of the nth differential equation.

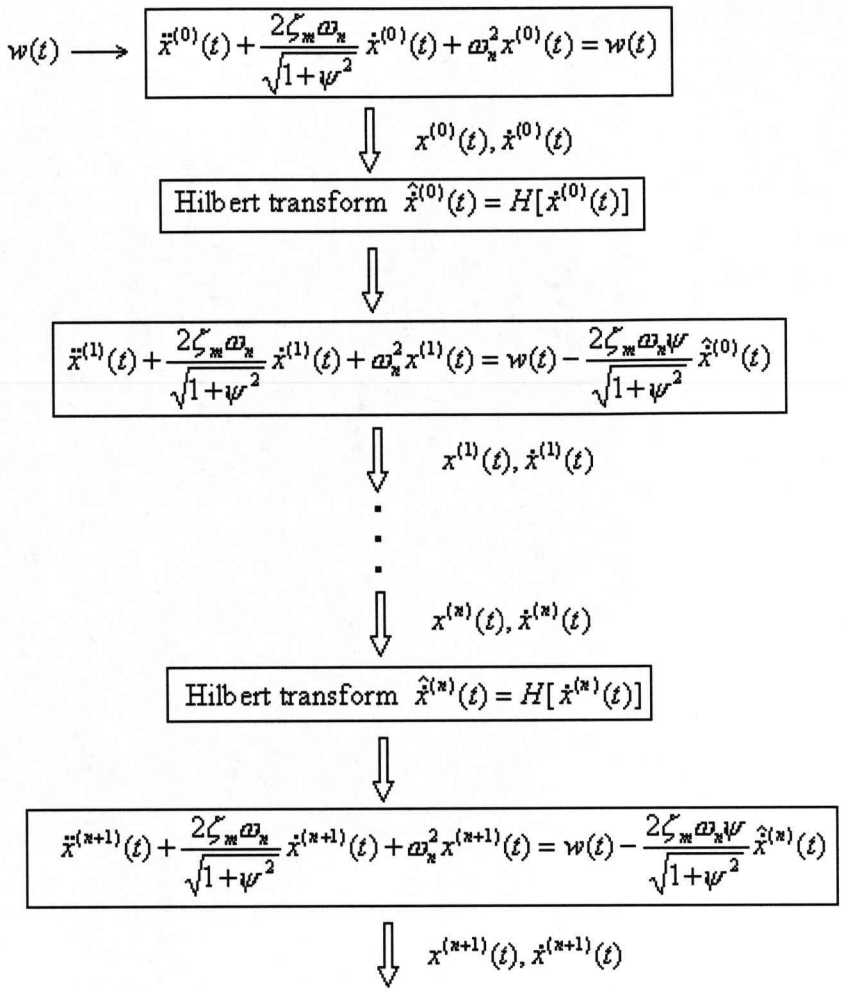

Figure 5.5 Computation procedure of the solution

Figure 5.5 illustrates the computation procedure of differential equations for the solution of equation (5.24).

The convergent solution can be obtained by using the following criteria.

$$\int_{-\infty}^{\infty} | x^{(n+1)} - x^{(n)} |^2 \, dt < \varepsilon \tag{5.25}$$

Next, we will show that this iterative computation technique converges to the solution of the equation (5.24). And the convergence condition will be discussed as well.

For equation (5.24), after Fourier transform

$$-\omega^2 X^{(n+1)}(j\omega) + j\frac{2\zeta_m \omega_n \omega}{\sqrt{1+\psi^2}} X^{(n+1)}(j\omega) + \omega_n^2 X^{(n+1)}(j\omega)$$

$$= W(j\omega) + \frac{2\zeta_m \omega_n \psi |\omega|}{\sqrt{1+\psi^2}} X^{(n)}(j\omega) \tag{5.26}$$

Here, it is noticed that

$$FT[H[\dot{x}(t)]] = -|\omega| X(j\omega) \tag{5.27}$$

Equation (5.26) can be written in the form

$$X^{(n+1)}(j\omega) = X^{(0)}(j\omega) + \Lambda(\omega) X^{(n)}(j\omega) \tag{5.28}$$

In which,

$$X^{(0)}(j\omega) = \frac{W(j\omega)}{\omega_n^2 - \omega^2 + j\frac{2\zeta_m \omega_n \omega}{\sqrt{1+\psi^2}}} \tag{5.29}$$

$$\Lambda(\omega) = \frac{\frac{2\zeta_m \omega_n \psi |\omega|}{\sqrt{1+\psi^2}}}{\omega_n^2 - \omega^2 + j\frac{2\zeta_m \omega_n \omega}{\sqrt{1+\psi^2}}} \tag{5.30}$$

Solving equation (5.28), it is easy to prove that the result of equation (5.28) at the *n*th iteration is

$$X^{(n)}(j\omega) = \Phi_n(\omega) X^{(0)}(j\omega) \tag{5.31}$$

In which,

$$\Phi_n(\omega) = 1 + \Lambda(\omega) + \Lambda^2(\omega) + \cdots + \Lambda^n(\omega) \tag{5.32}$$

From equation (5.31) and (5.32), it is seen that for $X^{(n)}(j\omega)$ to converge as $n \to \infty$, we need $\lim_{n\to\infty} \Phi_n(\omega)$ to converge for all ω, this requires that

$$|\Lambda(\omega)| < 1 \qquad for \ -\infty < \omega < \infty \tag{5.33}$$

We thus obtain

$$|\Lambda(\omega)|^2 = \frac{4\zeta_m^2\omega_n^2\omega^2 \dfrac{\psi^2}{1+\psi^2}}{(\omega_n^2-\omega^2)^2 + 4\zeta_m^2\omega_n^2\omega^2 \dfrac{1}{1+\psi^2}} \tag{5.34}$$

It is found, when $\omega = \omega_n$

$$|\Lambda(\omega)|^2 = \psi^2 \tag{5.35}$$

That is, $|\Lambda(\omega)|_{\omega=\omega_n} = |\psi|$ (5.36)

Therefore, for convergence, it is requires that

$$|\psi| < 1 \tag{5.37}$$

Now, we consider the effect of ζ_m

For equation (5.34), set $\beta = \dfrac{\omega}{\omega_n}$, then we find that,

$$|\Lambda(\omega)|^2 = \frac{4\zeta_m^2\beta^2 \dfrac{\psi^2}{1+\psi^2}}{(1-\beta^2)^2 + 4\zeta_m^2\beta^2 \dfrac{1}{1+\psi^2}} \tag{5.38}$$

That is

$$|\Lambda(\omega)|^2 = \psi^2 \frac{4\zeta_m^2\beta^2}{(1+\psi^2)(1-\beta^2)^2 + 4\zeta_m^2\beta^2} \tag{5.39}$$

It should be noticed that for any ζ_m, we have $\dfrac{4\zeta_m^2\beta^2}{(1+\psi^2)(1-\beta^2)^2 + 4\zeta_m^2\beta^2} \le 1$, which results in $|\Lambda(\overline{\omega})|^2 < 1$ for any ζ_m, because $|\psi| < 1$. Therefore, it is proved that for $|\psi| < 1$, the series $x^{(n)}(t)$ converges for $n \to \infty$, and it converges to the exact solution.

For the system shown in Figure 5.3 and Figure 5.4, the response was obtained by using the iterative technique as following. Figure 5.6 presents the response result of

the SDOF system using iterative technique. Figure 5.7 to Figure 5.10 list the iterative procedures of every step. It is found that for the first step of the calculation, a non-causal effect did not appear. From the second step, a non-causal effect was produced by the introduction of the response velocity. Only after four iterations, the computation result converges to the response with reasonable accuracy. This method provides a high convergence speed as well. Figure 5.11 shows the difference between last two iterations.

It should be noticed that the complex magnetic damping model must be defined in the frequency domain or limited to the transient work to periodic harmonic excitation. Although the impulse response has been determined this is only a mathematical expression representing the system from **sgn** function. This method is applied because it can obtain the reasonable response results although non-causality exists.

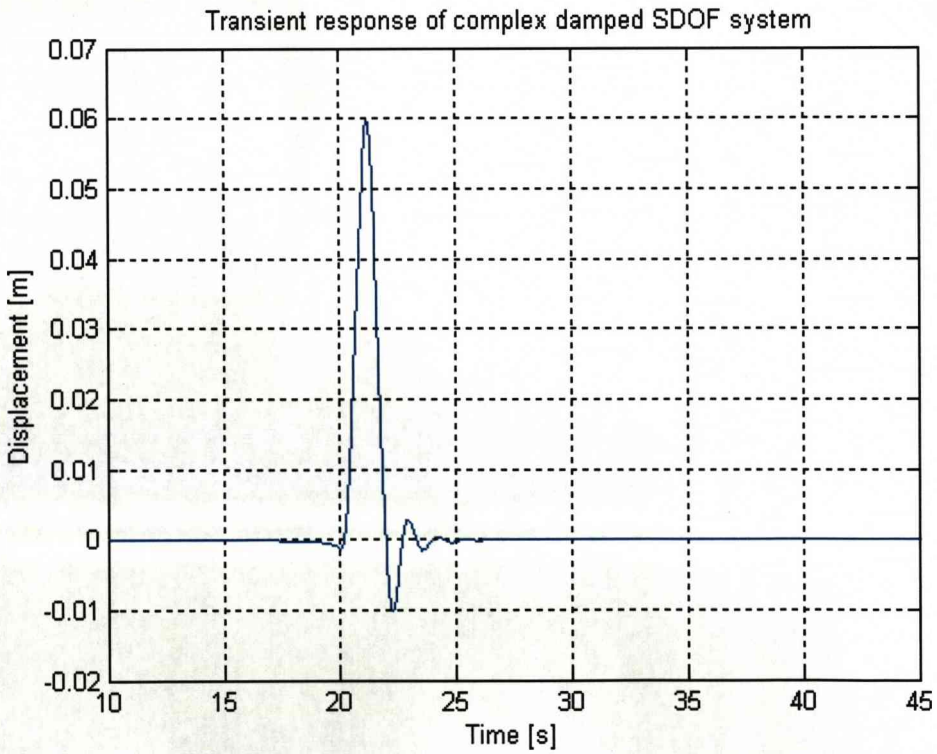

Figure 5.6 Transient response of complex damped system using iterative method

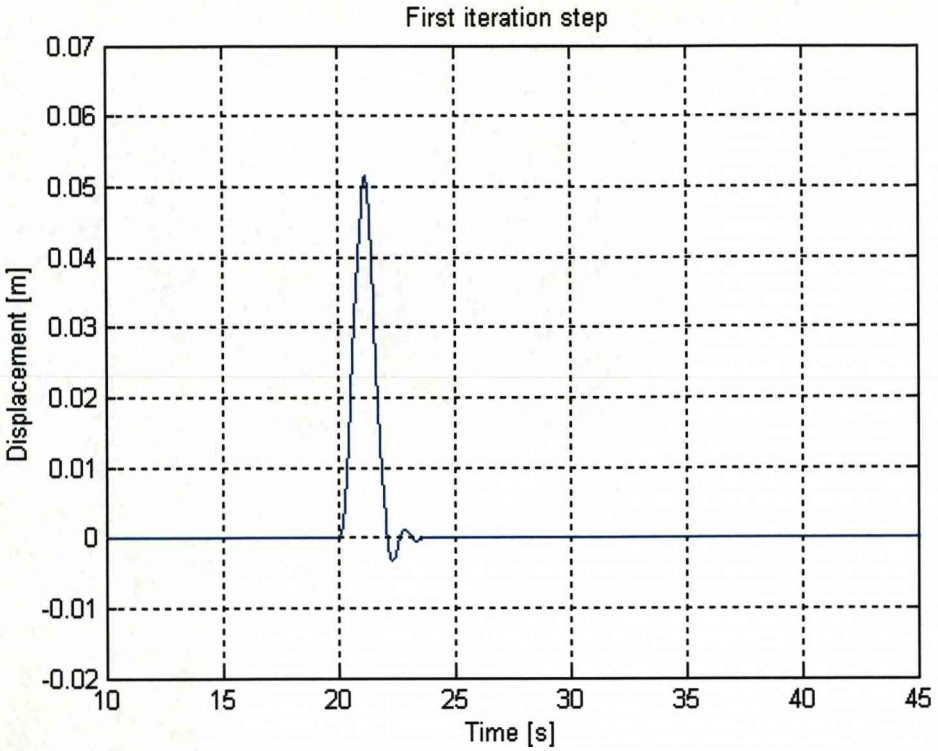

Figure 5.7 Response calculation result after one iteration step

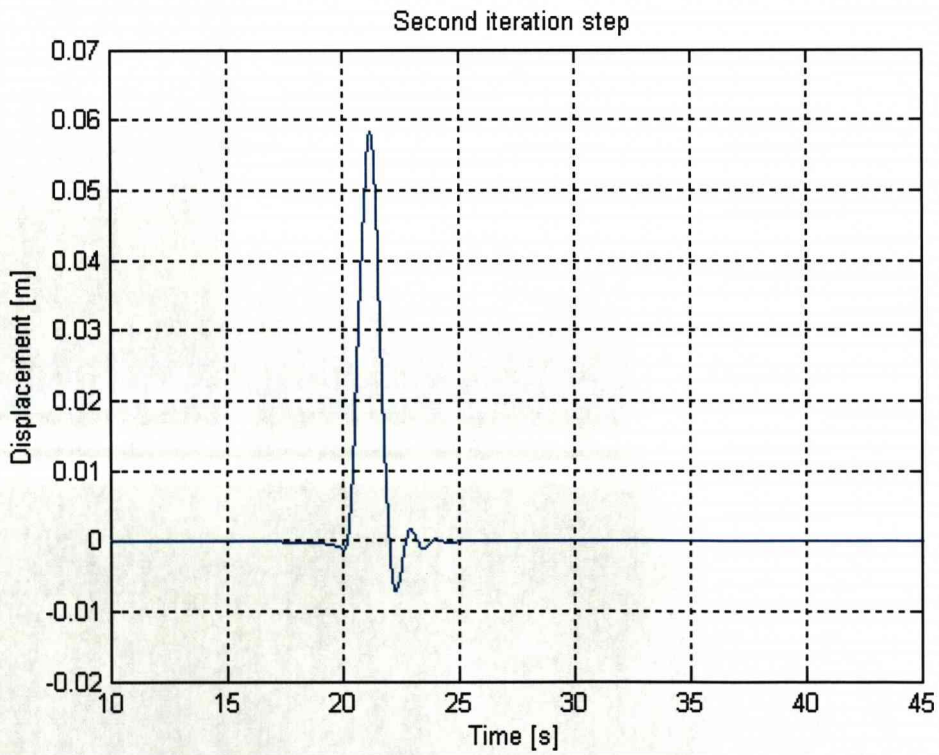

Figure 5.8 Response calculation result after two iteration steps

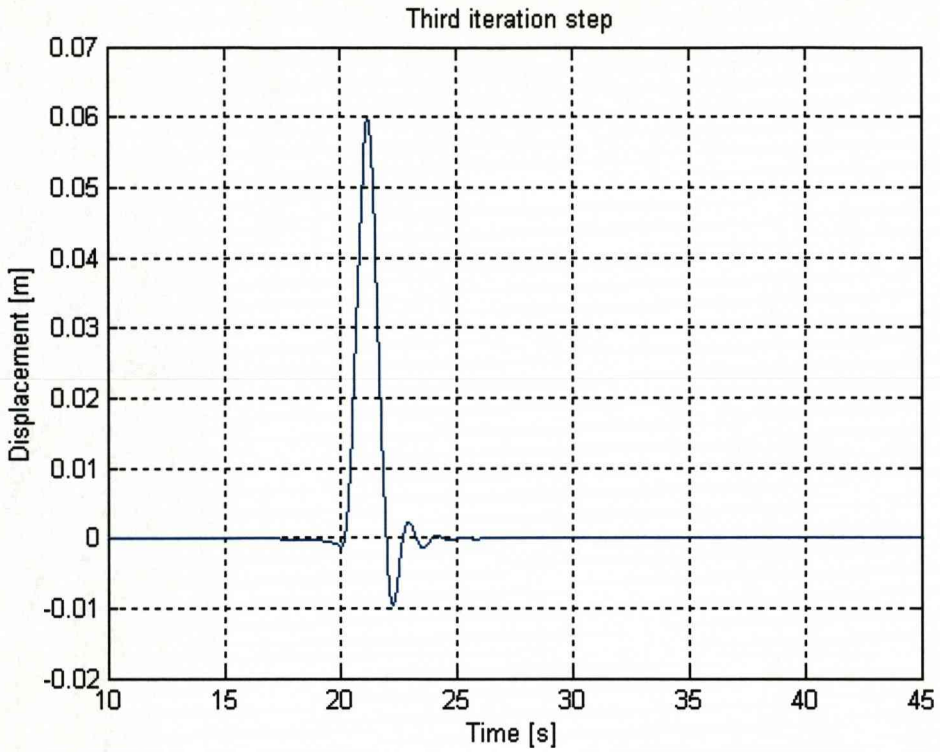

Figure 5.9 Response calculation result after three iteration steps

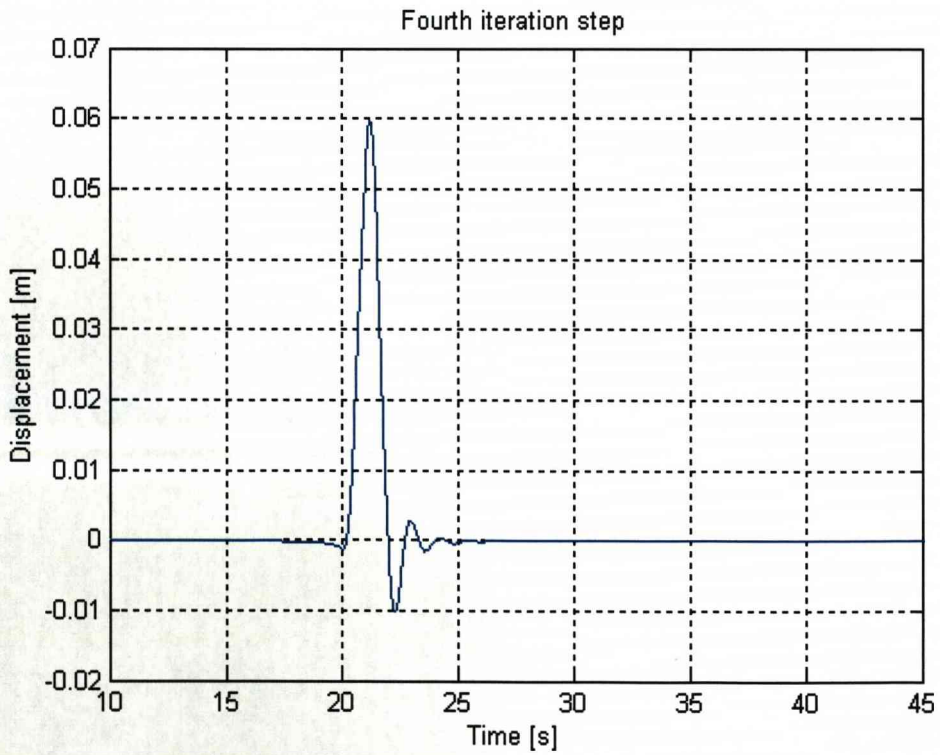

Figure 5.10 Response calculation result after four iteration steps

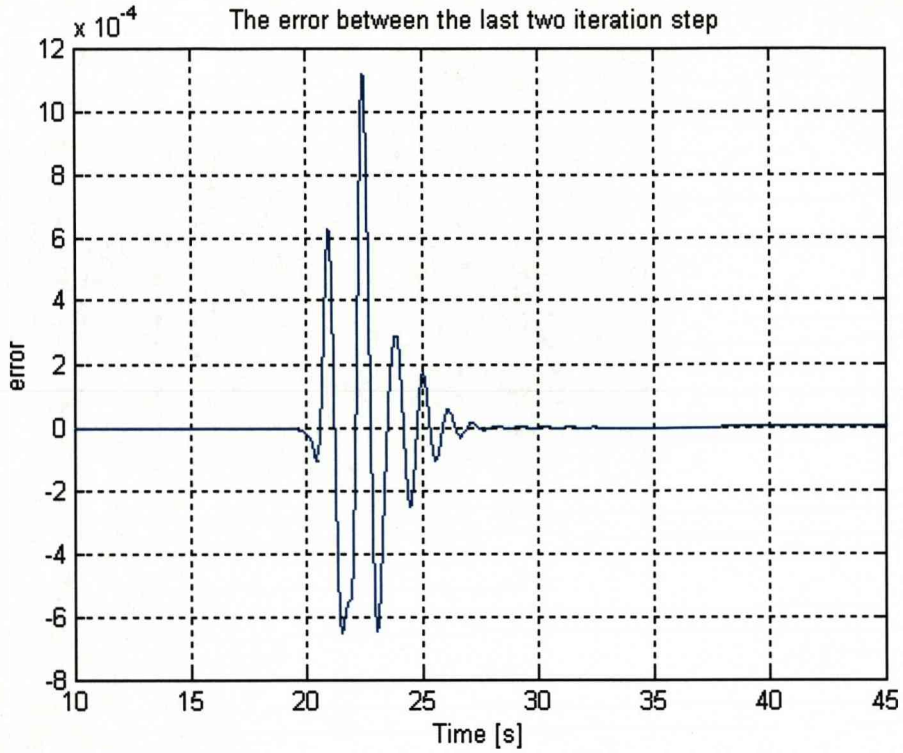

Figure 5.11 The difference between last two iteration steps

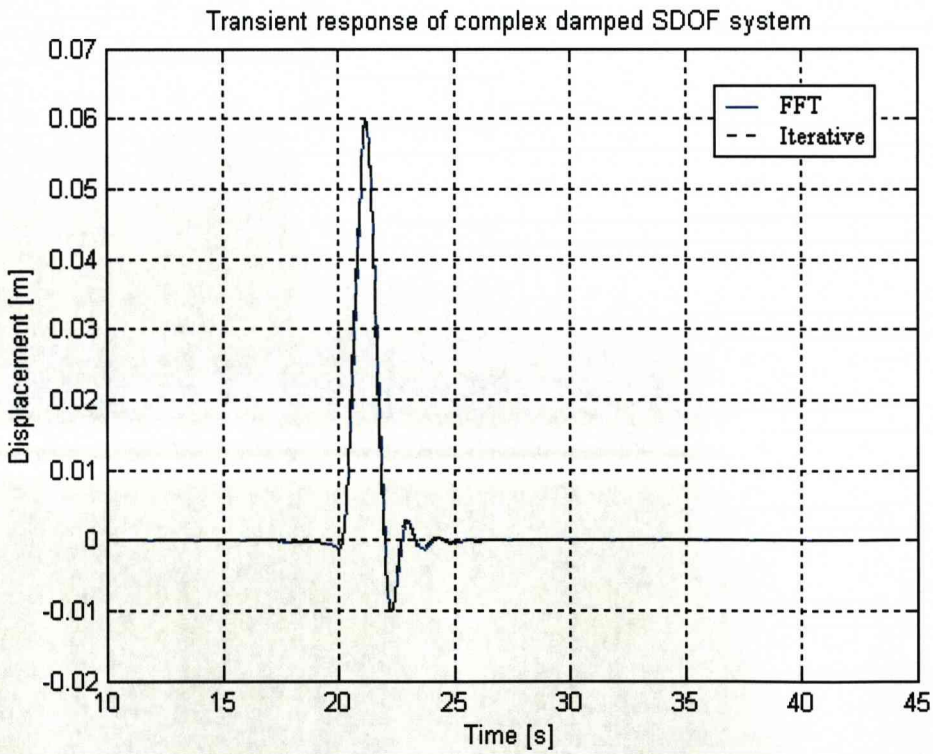

Figure 5.12 Comparison of response results obtained from two methods

Figure 5.12 gives a computation results comparison for FFT method and iterative technique. In this plot, the solid line represents the response using the FFT method and the dash line for the iterative technique. It is shown that the computed responses obtained by two methods are in good agreement, which also gives validity of these two methods

5.5 SDOF system with harmonic excitation

This section presents an example for the application of FFT and iterative techniques. The hysteretic force was solved in both frequency domain and time domain.

Considering the complex viscous damping SDOF system with $\omega_n = 2\pi \ \ rad/s$, $\psi = 0.75$, and $\zeta_m = 0.40$. And the harmonic excitation with $\omega_1 = 2\pi$ as shown in Figure 5.13 was applied to the system. Figure 5.14 shows that response results through two techniques are in good agreement. From Figure 5.14, it will be found that the response history includes two parts, the steady state output occurs in some cycles after the transient state and the non-causal effect exists at the beginning of the transient state. The circle part is zoomed in view.

From equation (5.10), the hysteretic force in the frequency domain can be written as

$$HY(j\omega) = \frac{2\zeta_m \omega_n}{\sqrt{1+\psi^2}}[1 + j\psi \,\mathrm{sgn}(\omega)]\dot{X}(j\omega) + \omega_n^2 X(j\omega) \tag{5.40}$$

That is

$$HY(j\omega) = [\omega_n^2 - \frac{2\zeta_m \omega_n}{\sqrt{1+\psi^2}}\psi\,|\,\omega\,| + j\frac{2\zeta_m \omega_n \omega}{\sqrt{1+\psi^2}}]X(j\omega) \tag{5.41}$$

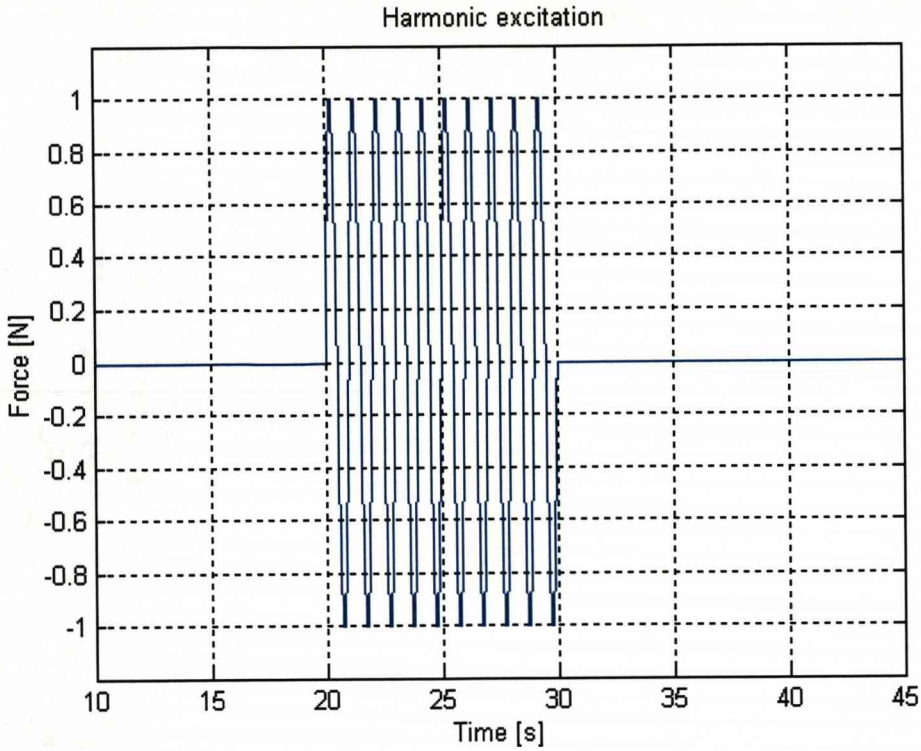

Figure 5.13 Harmonic excitation

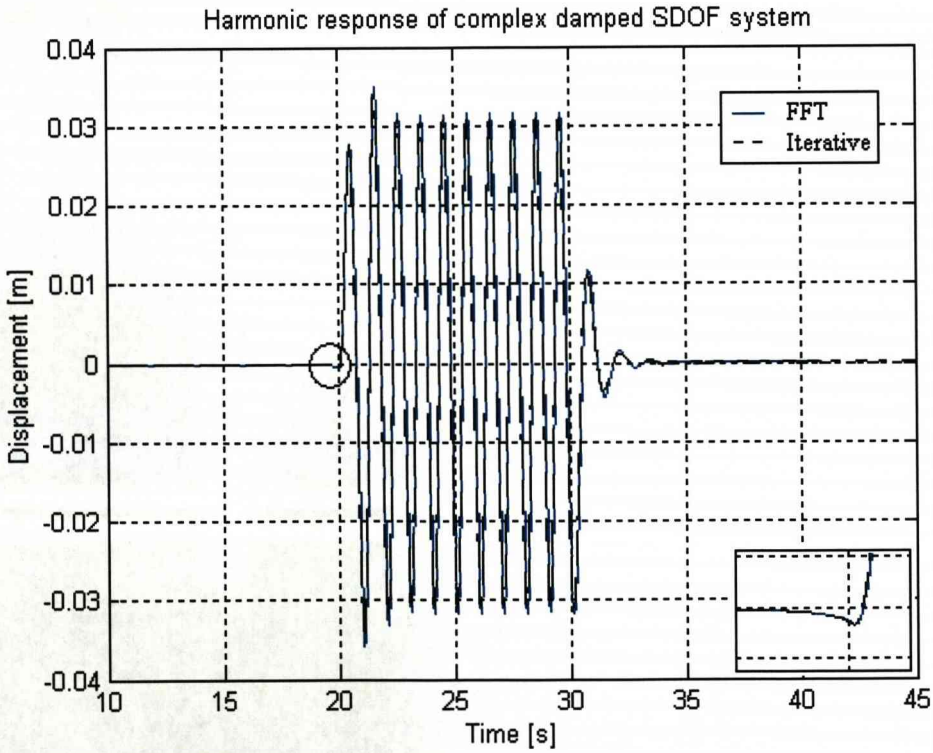

Figure 5.14 Harmonic responses of SDOF system obtained from two methods

Thus, the hysteretic force time history can be computed by using the inverse Fourier transform to $HY(j\omega)$

From equation (5.22), the hysteretic force in the time domain can be written as

$$hy(t) = \frac{2\zeta_m \omega_n}{\sqrt{1+\psi^2}} \dot{x}(t) + \frac{2\zeta_m \omega_n \psi}{\sqrt{1+\psi^2}} \hat{\dot{x}}(t) + \omega_n^2 x(t) \tag{5.42}$$

Figure 5.15 demonstrates the hysteretic loop of the example system for both the frequency domain technique and the time domain technique. It is noticed that the results match very well.

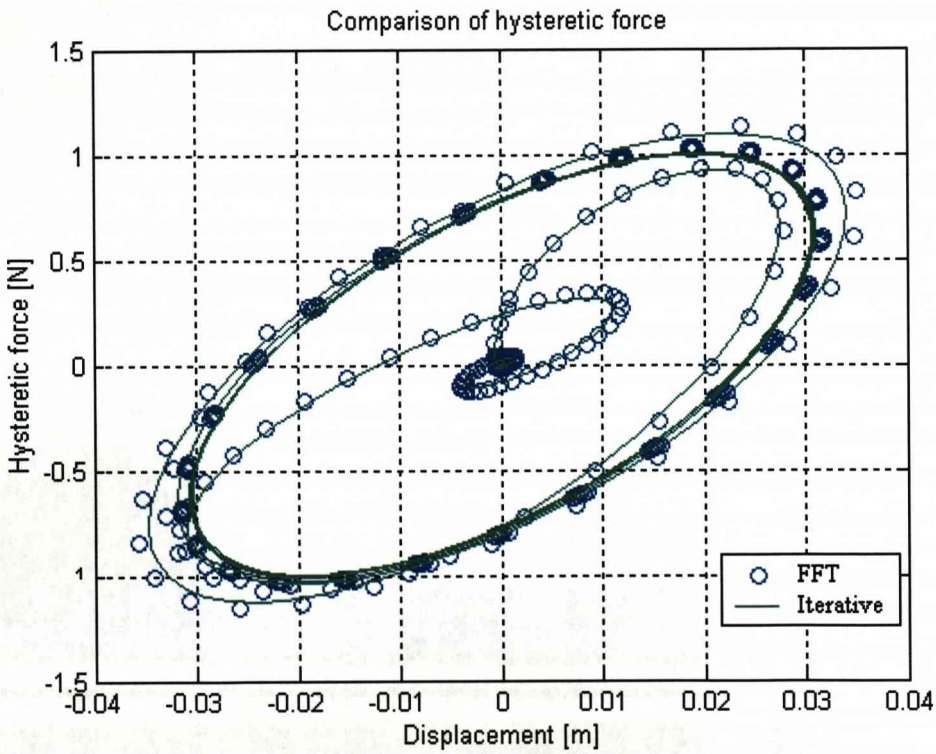

Figure 5.15 Hysteretic loop of SDOF system obtained from two methods

5.6 MDOF system with harmonic excitation

This section extends the SDOF system analyses to MDOF structures modeled with complex viscous damping. The frequency domain method and time domain method are all discussed for MDOF system.

A linear multi-degree-of-freedom dynamic system is considered. The equations of motion of their n generalised coordinates $\mathbf{x}(t)$ should be presented correctly in the frequency domain through the following expression

$$\mathbf{M}\ddot{\mathbf{X}}(j\omega)+\mathbf{C}\dot{\mathbf{X}}(j\omega)+\mathbf{K}\mathbf{X}(j\omega)=\mathbf{W}(j\omega) \tag{5.43}$$

Where **M**, **C** and **K** are the mass, whole complex viscous damping and stiffness matrices, and the system is subject to a generalised forces $\mathbf{W}(j\omega)$. Especially we should pay attention that the damping matrix **C** is expressed in the frequency domain and includes the **sgn** function in its imaginary part for the realistic requirement (3.26)-(3.29).

When the FFT technique is applied, the displacement responses in frequency domain can be obtained in the following form, which is similar to the case of the SDOF system.

$$\mathbf{X}(j\omega)=\boldsymbol{\alpha}(\omega)\mathbf{W}(j\omega) \tag{5.44}$$

in which, $\mathbf{W}(j\omega)$ is the Fourier transform of the excitation. And $\boldsymbol{\alpha}(\omega)$ is the frequency response function.

$$\boldsymbol{\alpha}(\omega)=[-\omega^2\mathbf{M}+j\omega\mathbf{C}+\mathbf{K}]^{-1} \tag{5.45}$$

And the corresponding time domain expression of the equation (5.43) will be written in the form

$$\mathbf{M}\ddot{\mathbf{x}}(t)+\mathrm{Re}[\mathbf{C}]\dot{\mathbf{x}}(t)+\mathrm{Im}[\mathbf{C}]\hat{\dot{\mathbf{x}}}(t)+\mathbf{K}\mathbf{x}(t)=\mathbf{w}(t) \tag{5.46}$$

in which, $\hat{\mathbf{x}}(t)$ is the Hilbert transform of $\dot{\mathbf{x}}(t)$. This equation can be changed in the following form.

$$\mathbf{M}\ddot{\mathbf{x}}(t) + \mathrm{Re}[\mathbf{C}]\dot{\mathbf{x}}(t) + \mathbf{K}\mathbf{x}(t) = \mathbf{w}(t) - \mathrm{Im}[\mathbf{C}]\hat{\mathbf{x}}(t) \tag{5.47}$$

Similarly to the case of the SDOF system, the time-step iterative procedure can be carried out to calculate the response result of the MDOF system.

Here, it is found the equation (5.46) is not expressed in the uncoupled form with respect to the modal coordinates since in many cases the complex viscous dampings are not the proportional dampings and it is difficult to get the uncoupled equations shown as in (5.22) for the system with the complex viscous damping. In addition it is more straightforward to calculate the time domain response through the equation (5.46) because the response is obtained through a numerical method.

As an example, we are considering a MDOF system as shown in Figure 5.16.

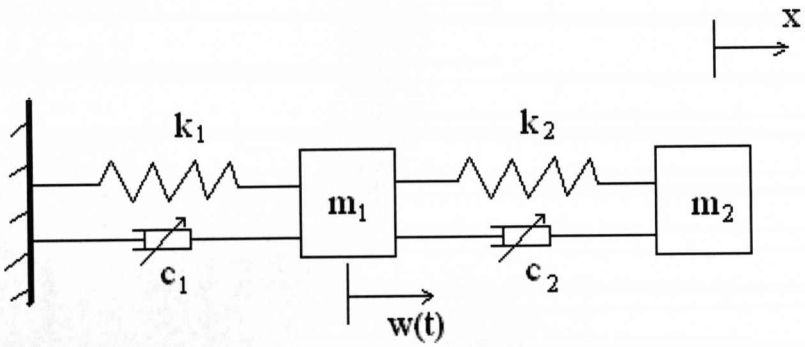

Figure 5.16 Complex viscous damped MDOF system

In this system, two complex-viscous type dampers are considered.

$$c_1(j\omega) = c_{m1}[1 + j\gamma_1 \,\mathrm{sgn}(\omega)] \quad , \quad c_2(j\omega) = c_{m2}[1 + j\gamma_2 \,\mathrm{sgn}(\omega)] \tag{5.48 a,b}$$

in which, c_m and γ are defined through equation (3.1)

$$\gamma = \frac{-c_e}{c_m} \tag{5.49}$$

And we chose

$m_1 = 1$ kg, $m_2 = 2$ kg, $k_1 = 4\pi^2$ N/m, $k_2 = 2\pi^2$ N/m

$c_{m1} = 3$ Ns/m, $c_{m2} = 4$ Ns/m, $\gamma_1 = 0.7$, $\gamma_2 = 0.4$

and the sine load $w(t)$ is applied on the mass m_1 as shown in Figure 5.13.

Thus the dynamic equation in the frequency domain can be written in the form as

$$\begin{bmatrix} m_1 & 0 \\ 0 & m_2 \end{bmatrix}\begin{bmatrix} \ddot{X}_1(j\omega) \\ \ddot{X}_2(j\omega) \end{bmatrix}+\begin{bmatrix} c_1+c_2 & -c_2 \\ -c_2 & c_2 \end{bmatrix}\begin{bmatrix} \dot{X}_1(j\omega) \\ \dot{X}_2(j\omega) \end{bmatrix} + \begin{bmatrix} k_1+k_2 & -k_2 \\ -k_2 & k_2 \end{bmatrix}\begin{bmatrix} X_1(j\omega) \\ X_2(j\omega) \end{bmatrix}=\begin{bmatrix} W(j\omega) \\ 0 \end{bmatrix} \tag{5.50}$$

Here, Figure 5.17 and Figure 5.18 show the time response of this MDOF system by using the Fourier transform method (solid line) and Iterative method (dash line). From these figures, it is noticed that the two results are in exact agreement, and the non-causal behaviour exists in both set of results as shown in circle part that is zoomed in view.

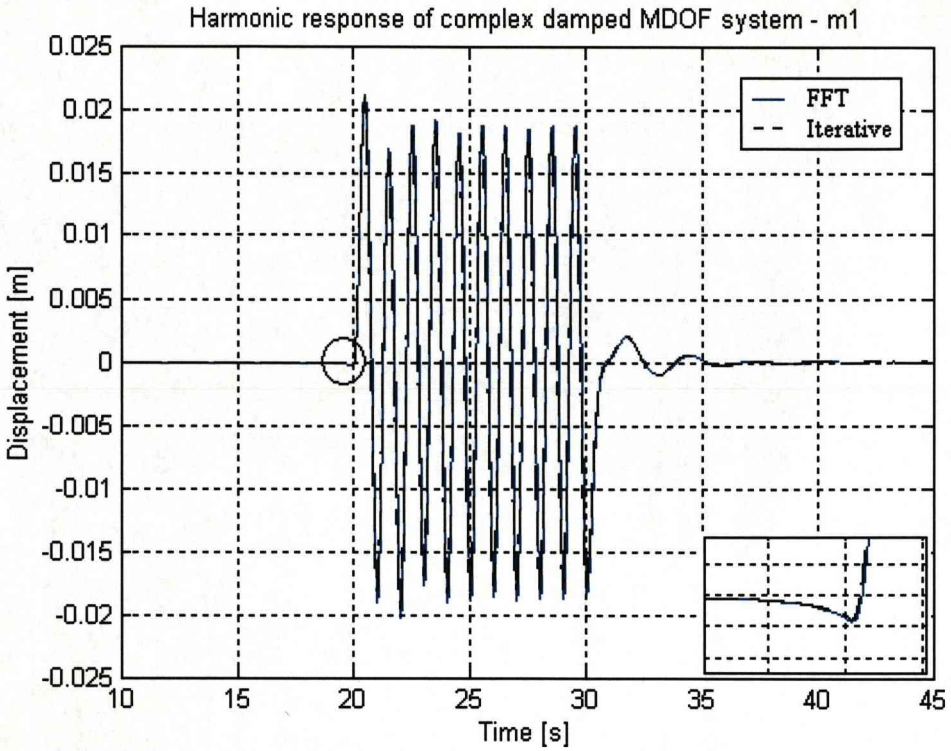

Figure 5.17 Harmonic response of m1

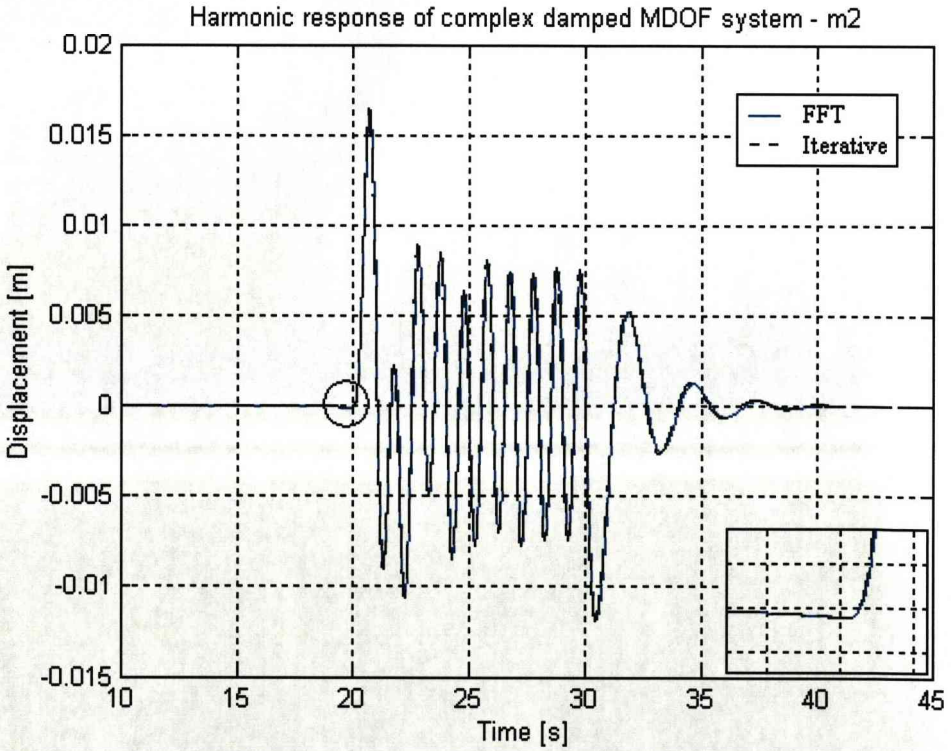

Figure 5.18 Harmonic response of m2

5.7 Extension to nonlinear structures

Based on the discussion above, it is believable that the iterative technique is also suitable for the nonlinear structure with complex viscous damping. In order to illustrate this consider the follow SDOF system with complex viscous damping:

$$\ddot{x}(t)+\frac{2\zeta_m\omega_n}{\sqrt{1+\psi^2}}\dot{x}(t)+\frac{2\zeta_m\omega_n\psi}{\sqrt{1+\psi^2}}\hat{\dot{x}}(t)+\omega_n^2[1+\alpha x^2(t)]x(t)=w(t) \tag{5.51}$$

It is noticed that the elastic resistance of the structure consists of a linear spring and a cubic hardening. Since this model is nonlinear, the solution cannot be obtained by direct frequency domain technique. And the direct integration of the equation of motion cannot be used. However, the results can be computed by the step-by-step time domain iterative method.

As done in above linear SDOF system, the equation (5.51) can be changed to the following form

$$\ddot{x}(t)+\frac{2\zeta_m\omega_n}{\sqrt{1+\psi^2}}\dot{x}(t)+\omega_n^2[1+\alpha x^2(t)]x(t)=w(t)-\frac{2\zeta_m\omega_n\psi}{\sqrt{1+\psi^2}}\hat{\dot{x}}(t) \tag{5.52}$$

Thus, the solution can be obtained by solving the following series of equations:

$$\ddot{x}^{(n+1)}(t)+\frac{2\zeta_m\omega_n}{\sqrt{1+\psi^2}}\dot{x}^{(n+1)}(t)+\omega_n^2\{1+\alpha[x^{(n+1)}(t)]^2\}x^{(n+1)}(t)=w(t)-\frac{2\zeta_m\omega_n\psi}{\sqrt{1+\psi^2}}\hat{\dot{x}}^{(n)}(t) \tag{5.53}$$

Figure 5.19 and Figure 5.20 show the response of this nonlinear structure subjected to the same triangle excitation previously considered in figure 5.3. The parameters of the system was selected as: $\omega_n=2\pi \quad rad/s$, $\psi=0.75$, and

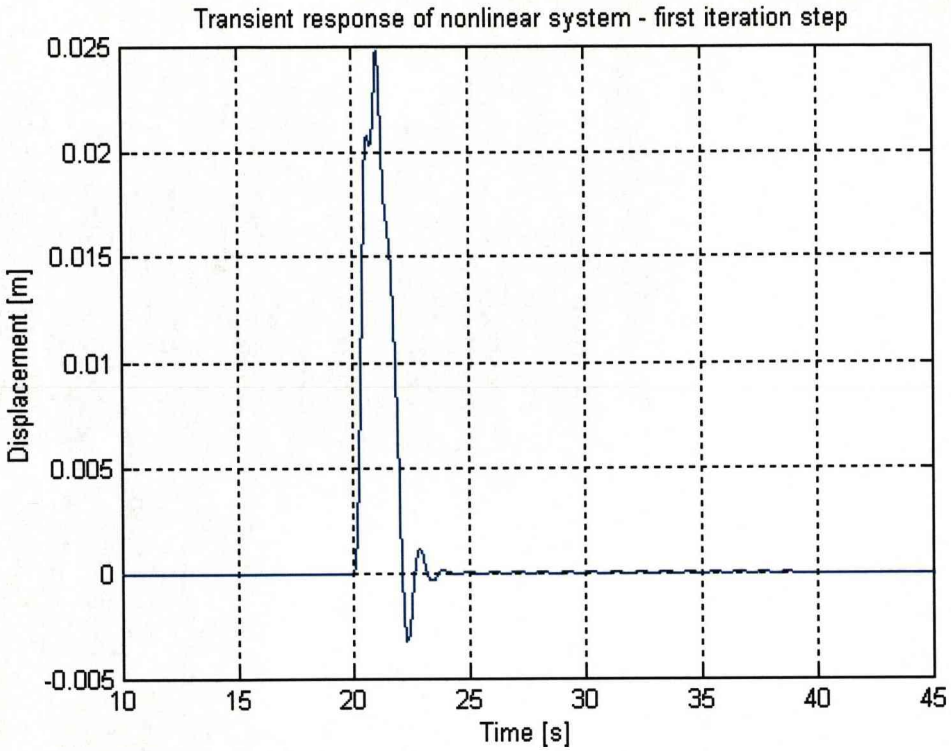

Figure 5.19 Response calculation results of nonlinear system after first iteration step

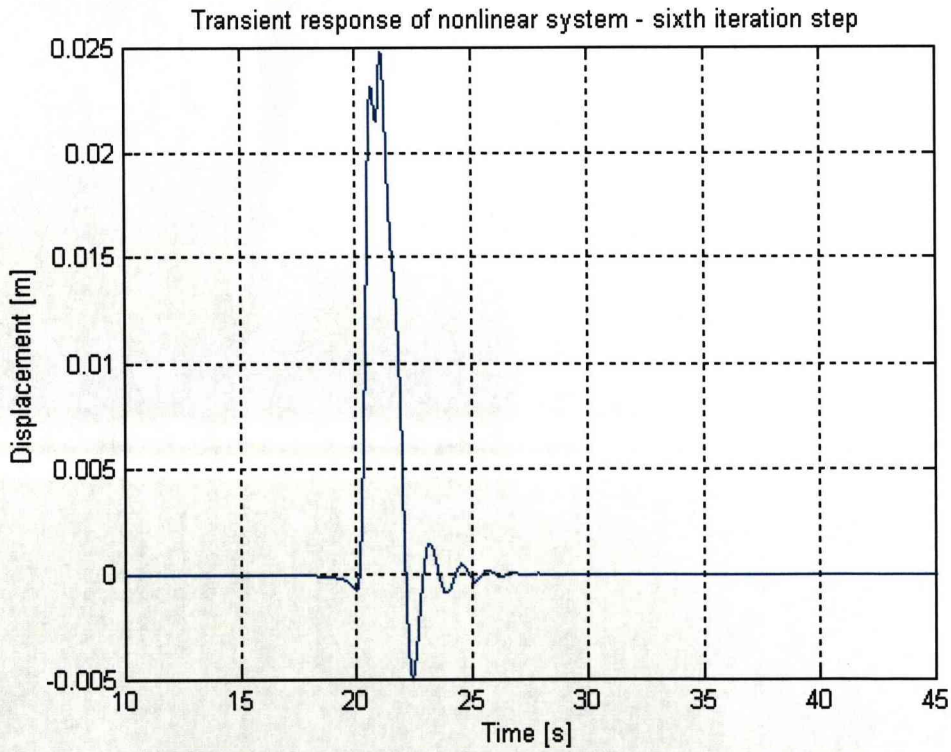

Figure 5.20 Response calculation results of nonlinear system after six iteration steps

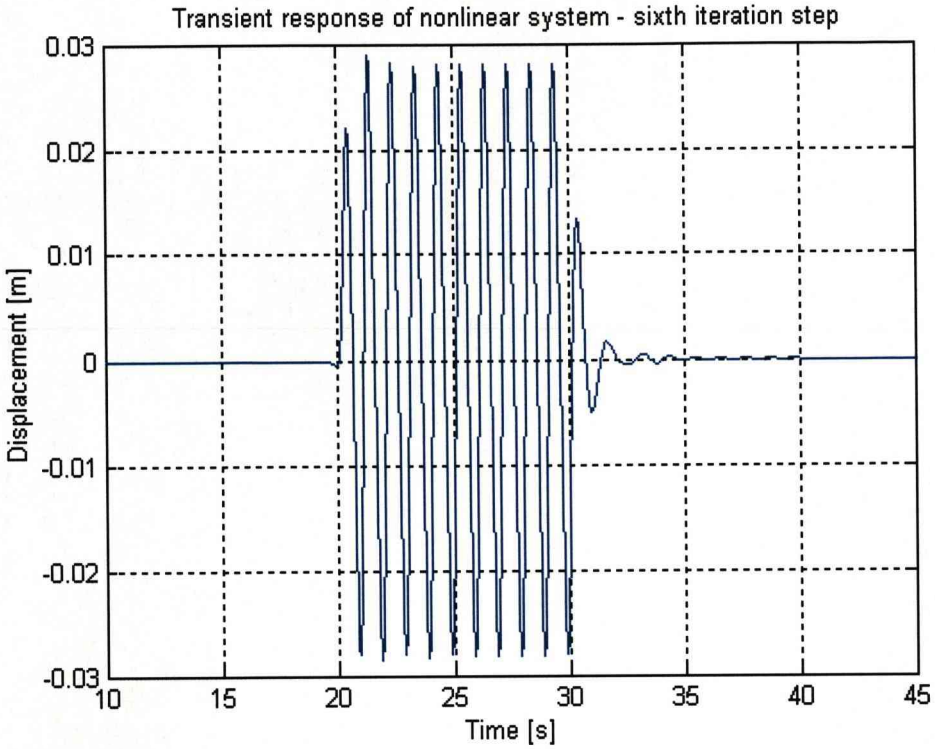

Figure 5.21 Harmonic response of nonlinear system

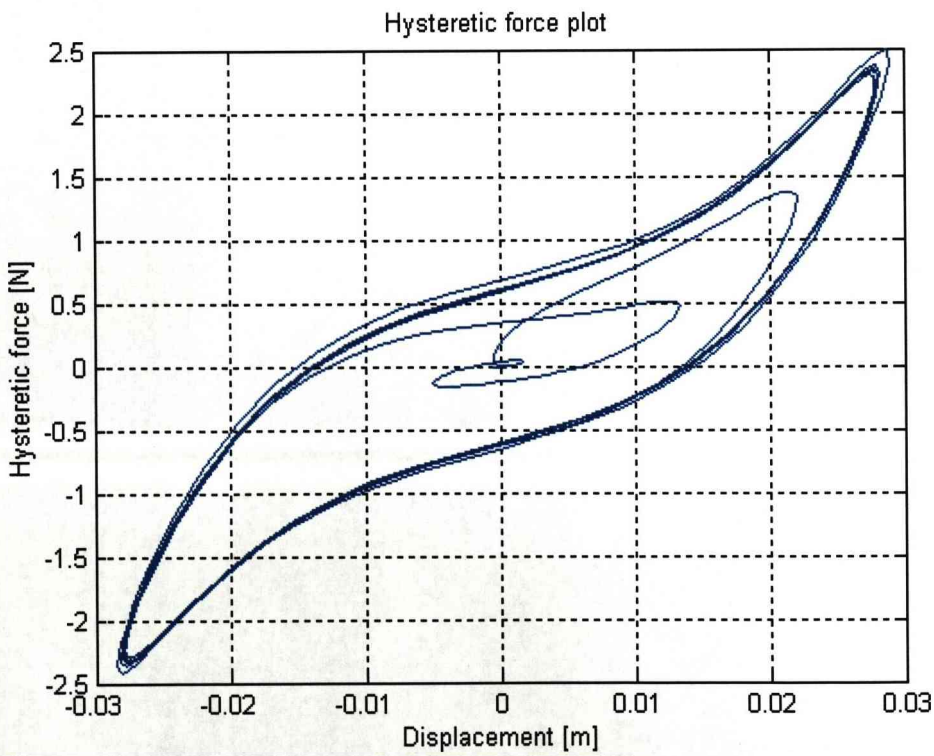

Figure 5.22 Hysteretic loop of nonlinear SDOF system

$\zeta_m = 0.40$, and $\alpha = 2\times10^3$ 1/m^2. The Figure 5.19 presents the response after first iteration without non-causal behaviour. The Figure 5.20 shows the result after six iterations. Since no significant change in the response exists when n > 6, Convergence is achieved. It is found that non-causal behaviour appears as in the case of the linear system.

Figure 5.21 demonstrates the response of this nonlinear system under the harmonic excitation as shown in the Figure 5.13. And Figure 5.22 presents the hysteretic loops of the nonlinear system under this harmonic movement.

It is also worth mentioned that although only the SDOF nonlinear structure with the complex viscous damping was discussed here, the extension of MDOF models is acceptable. Furthermore, the proposed iterative technique can be applied in both linear and nonlinear structures containing complex viscous damping.

5.8 Closure

The concept of complex viscous damping model was addressed both in frequency domain and time domain. Consequently, the time history responses for vibration of complex viscous damping systems have been calculated in this chapter. Two techniques, the FFT method and the iterative technique using Hilbert transform were utilized in the analyses. The excellent coincidence of computation results through FFT technique and iterative technique provides a reasonable validity of these methods as well.

The FFT method makes use of the mathematical relation between input signal and transfer function, while the Hilbert transform replaces the complex valued coefficients

in the differential equation model. The Hilbert transform gives a correct time domain expression for the concept of complex viscous damping. Because of integration from $-\infty < \tau < \infty$, the past and future of the signal are required to compute the Hilbert transform of the signal at the present time.

The FFT technique is faster than the iterative technique and has no convergence restriction. However, it can become very difficult and complicated in the case of nonlinear problems. In contrast, the iterative technique can be used in both linear and nonlinear situations. But it has been demonstrated that for the iterative technique, the convergence condition $|\psi|<1$ is required.

The complex viscous damping model results in the non-causal phenomena, which is demonstrated in the response analyses using both frequency domain method and time domain method. The major source of non-causal behaviour is that the damping properties are approximately mathematical modeled in the case of utilization of complex modulus. When this complex damping model is utilized, not only the past output response but also the future response all affect the response at the present time.

However it is important to remember that the complex magnetic damping model must be defined in the frequency domain or limited to the transient work to periodic harmonic excitation. The technique discussed in this chapter is applied to calculate the arbitrary response of the system because it can obtain reasonable response result although non-causal exists.

Chapter 6

Local Modifications with Complex Viscous Damping

In engineering applications, the analytical investigations are commonly needed to determine the dynamic effect of a change in a particular system component on the natural frequency and modes of vibration. These problems are often associated with the addition of a local damper or the cross connection of a damper between two components. This chapter is intended to find the changes of eigenvalue and eigenvector caused by the local damping modification to the original dynamical system. Pomazal and Snyder [41] developed a procedure for determining the eigenvalues and eigenvectors of a system resulting from the change in the stiffness of a linear spring. Following their work, the original work of this chapter is developing the characteristic equation of the system modified by an added damper and deriving an approximate method to solve the new characteristic equation for the small modification and when the original eigenvalues of the system are sufficiently separated. The work also calculated the sensitivities of new eigenvalues and eigenvectors of the modified system with respect to the damping coefficient. The restriction to symmetric positive system is indicated. In additional the system is not defective.

6.1 Eigenvalue problem of the modified system

Generally, dynamical equation of the original linear viscous damping system with n degree of freedoms can be written as

$$\mathbf{M}\ddot{\mathbf{x}} + \mathbf{C}\dot{\mathbf{x}} + \mathbf{K}\mathbf{x} = \mathbf{f} \tag{6.1}$$

in which, $\mathbf{M}$, $\mathbf{C}$ and $\mathbf{K}$ are mass, damping and stiffness matrices of the original system. $\mathbf{f}$ is the external force. Its eigenvalue problem can be solved by a state space characteristic equation associated with a $2n$ degree of freedoms system.

$$(u\mathbf{A} + \mathbf{D})\mathbf{\Phi} = \mathbf{0} \tag{6.2}$$

in which,

$$\mathbf{A} = \begin{bmatrix} \mathbf{C} & \mathbf{M} \\ \mathbf{M} & \mathbf{0} \end{bmatrix} \tag{6.3}$$

$$\mathbf{D} = \begin{bmatrix} \mathbf{K} & \mathbf{0} \\ \mathbf{0} & -\mathbf{M} \end{bmatrix} \tag{6.4}$$

and u and $\mathbf{\Phi}$ is the eigenvalue and its corresponding eigenvector column vector of the original system. Thus the complete solution of equation (6.2) consists of $2n$ eignevalues (u_1 , u_2 , ..., u_{2n}) and a $2n \times 2n$ eigenvector matrix $[\mathbf{\Phi}] = [\mathbf{\Phi}_1, \ \mathbf{\Phi}_2, \ ..., \ \mathbf{\Phi}_{2n}]$. The eigenvector matrix $[\mathbf{\Phi}]$ satisfies the orthogonal conditions providing that $[\mathbf{\Phi}]$ spans the $2n \times 2n$ space of the system and is not defective.

$$[\mathbf{\Phi}]^T \mathbf{A}[\mathbf{\Phi}] = \mathbf{A}^* = diag[a_1, \ a_2, \ \ldots, \ a_{2n},] \tag{6.5}$$

$$[\mathbf{\Phi}]^T \mathbf{D}[\mathbf{\Phi}] = \mathbf{D}^* = diag[d_1, \ d_2, \ \ldots, \ d_{2n},] \tag{6.6}$$

where,

$$u_r = -\frac{d_r}{a_r}, (r = 1, 2, \ldots, 2n) \tag{6.7}$$

When the vibration system considered to be modified locally by introducing a damping, the equation (6.1) is to be modified by a change in the damping matrix. This

change can be typically expressed in the form of an additional matrix of $c^*\mathbf{q}^T\mathbf{q}$ as following.

$$\mathbf{M}\ddot{\mathbf{x}} + \mathbf{C}\dot{\mathbf{x}} + c^*\mathbf{q}^T\mathbf{q}\dot{\mathbf{x}} + \mathbf{K}\mathbf{x} = \mathbf{f} \tag{6.8}$$

where c^* is the damping coefficient of the added damper. For linear viscous damping, this factor is a real number of the viscous damping coefficient. And for the complex viscous damping case, it is a complex value factor as,

$$c^* = c_m[1 + j\gamma\,\mathrm{sgn}(\omega)] \tag{6.9}$$

from the definition (3.1) considering the realistic requirement (3.26)-(3.29), in which,

$$\gamma = \frac{-c_e}{c_m} \tag{6.10}$$

$\mathbf{q}$ is a $1\times n$ row vector indicating the location of the modification. It shows different forms for the different modification ways as shown in Figure 6.1.

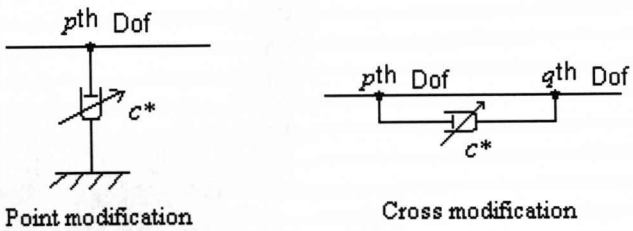

Figure 6.1 System modification plot

For the case of point modification,

$$\mathbf{q} = [0, \ldots, 0, 1, 0, \ldots, 0] \tag{6.11}$$

In which the unit one is at the position where the damper is added.

For the case of cross modification,

$$\mathbf{q} = [0, \ldots, 0, 1, 0, \ldots, 0, -1, 0, \ldots, 0] \tag{6.12}$$

In which, the positive one and negative one are located on the two degree of freedoms, which are connected by the additional damper.

And thus in the $2n$ space, the eigenvalue problem of the modified system has the following form

$$(\lambda \mathbf{A} + \mathbf{D} + \lambda c^* \mathbf{Q}^T \mathbf{Q})\mathbf{Y} = \mathbf{0} \tag{6.13}$$

where, the modified eigenvalue is represented by λ and its corresponding eigenvector column vector is $\mathbf{Y}$. Besides the modification position vector is changed by

$$\mathbf{Q} = [\mathbf{q}, \ \mathbf{0}_{1\times n}] \tag{6.14}$$

If we assume that $\mathbf{B} = \mathbf{A} + c^* \mathbf{Q}^T \mathbf{Q}$, the solution of the modified eigenvalue characteristic equation (6.13) can be obtained by the same procedure that is used to calculate the eigenvalue of the original system. However, considering the orthogonal property of the original eigenvector matrix, the modified eigenvalue equation can be expressed in one simple form.

In order to demonstrate this simplification, let's transform the equation (6.13) by replacing

$$\mathbf{Y} = [\mathbf{\Phi}]\mathbf{Z} \tag{6.15}$$

in which $\mathbf{Z}$ is the column of original eigenvector participation factors. And then premultiplying the result by $[\mathbf{\Phi}]^T$ to obtain

$$(\lambda \overline{\mathbf{A}} + \overline{\mathbf{D}} + \lambda c^* \mathbf{V}^T \mathbf{V})\mathbf{Z} = \mathbf{0} \tag{6.16}$$

where

$$\mathbf{V} = \mathbf{Q}[\mathbf{\Phi}] \tag{6.17}$$

Equation (6.16) can uncoupled and the arbitrary *r*th equation may be written as

$$(\lambda a_r + d_r) z_r + \lambda c^* v_r \sum_{k=1}^{2n} v_k z_k = 0 \tag{6.18}$$

in which, $r=1, 2, \ldots, 2n$. z_r is the *r*th element of the vector $\mathbf{Z}$, v_r and v_k are the

*r*th and *k*th element of the row vector $\mathbf{V}$ respectively. For non zero v_r, we have

$$\frac{(\lambda a_1 + d_1)z_1}{v_1} = \frac{(\lambda a_2 + d_2)z_2}{v_2} = \ldots = \frac{(\lambda a_{2n} + d_{2n})z_{2n}}{v_{2n}} = -\lambda c^* \sum_{k=1}^{2n} v_k z_k \tag{6.19}$$

which may be simplified as,

$$\frac{(\lambda a_k + d_k)z_k}{v_k} = \frac{(\lambda a_r + d_r)z_r}{v_r} \tag{6.20}$$

Substituting equation (6.20) into equation (6.18), the calculation results in the following equation

$$1 + \lambda c^* \sum_{k=1}^{2n} \frac{v_k^2}{(\lambda a_k + d_k)} = 0 \tag{6.21}$$

which may be rewritten as,

$$1 + \lambda c^* \sum_{k=1}^{2n} \frac{v_k^2}{a_k(\lambda - u_k)} = 0 \tag{6.22}$$

as defined in equation (6.7).

Thus, equation (6.21) or (6.22) is the characteristic equation of the modified system because its *2n* roots λ_j (*j=1, 2,..., 2n.*) are the eigenvalues of the modified system. For each eigenvalue λ_j, its corresponding eigenvector column may be obtained through multiplying the original eigenvector matrix with the corresponding vector $\mathbf{Z}_j$, which is generated from equation (6.20). That is

$$\mathbf{Y}_j = [\mathbf{\Phi}]\mathbf{Z}_j \tag{6.23}$$

The each element z_{kj} of this vector can be written as

$$z_{kj} = \frac{v_k(\lambda_j a_r + d_r)}{v_r(\lambda_j a_k + d_k)} z_{rj} \tag{6.24}$$

or

$$z_{kj} = \frac{v_k a_r}{v_r a_k} \frac{(\lambda_j - u_r)}{(\lambda_j - u_k)} z_{rj} \tag{6.25}$$

From equation (6.24) and (6.25), it is found that the vector $\mathbf{Z}_j$ is also made up of scaled numbers. For the sake of simplicity, it is assumed that $r = j$ and $z_{rj} = z_{jj} = 1$. Thus equation (6.24) and (6.25) can be simplified to be

$$z_{kj} = \frac{v_k(\lambda_j a_j + d_j)}{v_j(\lambda_j a_k + d_k)} \tag{6.26}$$

or

$$z_{kj} = \frac{v_k a_j}{v_j a_k} \frac{(\lambda_j - u_j)}{(\lambda_j - u_k)} \tag{6.27}$$

The most significant feature of this modification method is that the modified system characteristic equation may be expressed from the known eigenvalues and eigenvectors of the original system. And then the modified eigenvalues, that is the roots of the new characteristic equation, can be easily obtained by numerical methods. However, the reader should be aware that both the original system matrix and the modification matrix are required to be real symmetric and positive and the original system characterized by distinct eigenvalues.

6.2 Numerical example for point modification

In order to demonstrate the use of the modification procedure numerical examples are considered here. The original system is selected as a mass-spring-damper in-line system with three degree of freedom as shown in Figure 6.2. The physical parameters and dynamical characteristics are listed in Table 6-1 and Table 6-2 respectively.

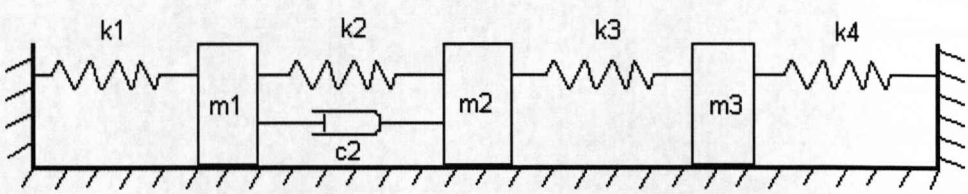

Figure 6.2 Unmodified example in-line system

Table 6-1 Original example system parameters

Mass (kg)	Spring stiffness (N/m)	Damping coefficient (Ns/m)
m1=0.1	*k1=300*	
m2=0.2	*k2=700*	*c2=0.3*
m3=0.1	*k3=1000*	
	k4=600	

Table 6-2 Original example system dynamical characteristics

	Natural frequencies (rad/s)	Eigenvalues
1	4.3795e+001	-8.2590e-003 -4.3795e+001 i -8.2590e-003 +4.3795e+001 i
2	1.0803e+002	-1.6261e+000 -1.0802e+002 i -1.6261e+000 +1.0802e+002 i
3	1.4459e+002	-6.1568e-001 -1.4459e+002 i -6.1568e-001 +1.4459e+002 i

Considering the point modification of an additional damping attached to *m3* as shown in Figure 6.3, the modification location vector should be set as $\mathbf{q} = [0, 0, 1]$. And then we calculate the modified eigenvalues and eigenvectors for two damping cases.

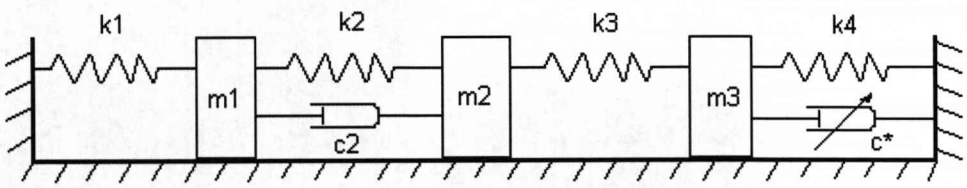

Figure 6.3 Point modified system

For linear viscous damping $c^* = 0.2Ns/m$, substituting the damping coefficient into the modified characteristic equation (6.22) and solving this equation gave the modified eigenvalues directly.

For the complex viscous damping defined in equation (6.9) with $c_m = 0.2Ns/m$ and $\gamma = -3.0$. It should be noticed that this factor in examples is chosen as an exaggerated case in order to show clearly the eigenvalue and eigenvector difference caused by complex viscous damping. However for reasons of reality the factor γ has to be in some limitated range. We have to firstly solve the new characteristic equation (6.22) for $+\omega$ and $-\omega$ respectively and then select the corresponding eigenvalues, the sign of whose imaginary part are same as the sign of the ω since

$$c^* = c_m[1 + j\gamma \operatorname{sgn}(\omega)] = c_m[1 + j\gamma \operatorname{sgn}[\operatorname{Im}(\lambda)]] \tag{6.28}$$

This calculation procedure will obtain the exact conjugate complex eigenvalue couples, which satisfy the realistic requirements (3.26)-(3.29). The new eigenvalues results are listed in Table 6-3.

Table 6-3 Point modified eigenvalues

	Eigenvalues
Linear viscous damping	-1.6321e-001 -4.3795e+001i -1.6321e-001 +4.3795e+001i -1.8384e+000 -1.0800e+002i -1.8384e+000 +1.0800e+002i -1.2484e+000 -1.4460e+002i -1.2484e+000 +1.4460e+002i
Complex viscous damping	-1.5987e-001 -4.4256e+001i -1.5987e-001 +4.4256e+001i -1.8870e+000 -1.0862e+002i -1.8870e+000 +1.0862e+002i -1.2301e+000 -1.4657e+002i -1.2301e+000 +1.4657e+002i

It is found that for both cases of linear viscous damping modification and the complex viscous damping modification, the modified eigenvalues still appear in the conjugated couple form, which leads to the symmetric negative and positive resonance frequencies. In Table 6-4, the modified eigenvectors corresponding to the first two eigenvalues are listed for both linear viscous damping and complex viscous damping

modifications respectively. They are also in the conjugate complex form.

Table 6-4 Point modified eigenvectors corresponding to first two eigenvalues

	1st column eigenvector	2nd column eigenvector
Linear viscous damping	-3.4576e-004 -1.9443e-002i -3.0309e-004 -2.2448e-002i -1.3226e-004 -1.5942e-002i -8.5143e-001 +1.8316e-002i -9.8306e-001 +1.6938e-002i -6.9816e-001 +8.3942e-003i	-3.4576e-004 +1.9443e-002i -3.0309e-004 +2.2448e-002i -1.3226e-004 +1.5942e-002i -8.5143e-001 -1.8316e-002i -9.8306e-001 -1.6938e-002i -6.9816e-001 -8.3942e-003i
Complex viscous damping	-1.3418e-002 +6.2568e-003i -1.5444e-002 +7.1222e-003i -1.0821e-002 +4.9213e-003i 2.7905e-001 +5.9283e-001i 3.1767e-001 +6.8233e-001i 2.1953e-001 +4.7809e-001i	-1.3418e-002 -6.2568e-003i -1.5444e-002 -7.1222e-003i -1.0821e-002 -4.9213e-003i 2.7905e-001 -5.9283e-001i 3.1767e-001 -6.8233e-001i 2.1953e-001 -4.7809e-001i

6.3 Numerical examples for cross modification

For the case of cross modification with an additional damping between *m2* and *m3* as shown in Figure 6.4, the modification location vector should be changed to $\mathbf{q} = [0, 1, -1]$.

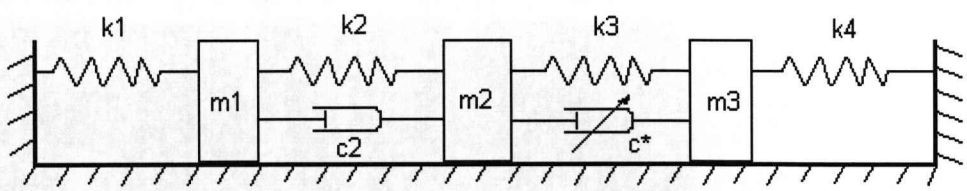

Figure 6.4 Cross modified system

And then we also consider the above two damping cases for linear viscous damping $c^* = 0.2Ns/m$ and complex viscous damping in equation (6.9) with $c_m = 0.2Ns/m$ and $\gamma = -3.0$ respectively. The modified eigenvalues and eigenvector corresponding to the first two eigenvalues can be obtained and shown in Table 6-5 and Table 6-6.

Table 6-5 Cross modified eigenvalues

	Eigenvalues
Linear viscous damping	-3.4077e-002 -4.3795e+001i -3.4077e-002 +4.3795e+001i -1.6935e+000 -1.0801e+002i -1.6935e+000 +1.0801e+002i -2.0224e+000 -1.4459e+002i -2.0224e+000 +1.4459e+002i
Complex viscous damping	-3.2954e-002 -4.3871e+001i -3.2954e-002 +4.3871e+001i -1.7235e+000 -1.0819e+002i -1.7235e+000 +1.0819e+002i -2.0486e+000 -1.4890e+002i -2.0486e+000 +1.4890e+002i

Table 6-6 Cross modified eigenvectors corresponding to first two eigenvalues

	1st column eigenvector	2nd column eigenvector
Linear viscous damping	3.0323e-004+1.9515e-002i 2.8516e-004+2.2531e-002i 2.4652e-004+1.6000e-002i 8.5464e-001-1.3945e-002i 9.8674e-001-1.3256e-002i 7.0070e-001-1.1341e-002i	3.0323e-004-1.9515e-002i 2.8516e-004-2.2531e-002i 2.4652e-004-1.6000e-002i 8.5464e-001+1.3945e-002i 9.8674e-001+1.3256e-002i 7.0070e-001+1.1341e-002i
Complex viscous damping	-3.7236e-003+1.6010e-002i -4.3483e-003+1.8457e-002i -3.0776e-003+1.3219e-002i 7.0251e-001+1.6283e-001i 8.0985e-001+1.9015e-001i 5.8004e-001+1.3458e-001i	-3.7236e-003-1.6010e-002i -4.3483e-003-1.8457e-002i -3.0776e-003-1.3219e-002i 7.0251e-001-1.6283e-001i 8.0985e-001-1.9015e-001i 5.8004e-001-1.3458e-001i

6.4 Approximate results of the modified characteristic equation

The value of the modified characteristic equation is that the root, that is, the modified eigenvalue, may be obtained by a numerical method. However under some particular conditions, an approximate result of this new characteristic equation can be calculated directly. When the original eigenvalues of the system are sufficiently separated and the modification is small, the *j*th modified eigenvalue λ_j can be straightforwardly written by the sum of the *j*th original eigenvalue u_j and a small change ε_j as the following.

$$\lambda_j = u_j + \varepsilon_j \tag{6.29}$$

A substitution of it into the modified characteristic equation (6.22) yields

$$\frac{1}{c^*} + \sum_{k=1}^{2n} \frac{v_k^2}{a_k} \frac{(u_j + \varepsilon_j)}{(u_j + \varepsilon_j - u_k)} = 0 \tag{6.30}$$

That is

$$\frac{1}{c^*}+\frac{v_j^2(u_j+\varepsilon_j)}{a_j\varepsilon_j}+\sum_{\substack{k=1\\k\neq j}}^{2n}\frac{v_k^2}{a_k}\frac{(u_j+\varepsilon_j)}{(u_j+\varepsilon_j-u_k)}=0 \tag{6.31}$$

Thus, for the some change ε_j, it can be simplified as

$$\frac{1}{c^*}+\frac{v_j^2u_j}{a_j\varepsilon_j}+\sum_{\substack{k=1\\k\neq j}}^{2n}\frac{v_k^2u_j}{a_k(u_j-u_k)}=0 \tag{6.32}$$

And then, a reasonable value of change ε_j may be obtained

$$\varepsilon_j=-\frac{v_j^2u_j}{a_j}\frac{1}{\left[\frac{1}{c^*}+\sum_{\substack{k=1\\k\neq j}}^{2n}\frac{v_k^2u_j}{a_k(u_j-u_k)}\right]} \tag{6.33}$$

It should be noticed that when complex viscous damping modification is considered, the calculation have to be carried out for for $+\omega$ and $-\omega$ respectively and then the corresponding eigenvalues are chosen to make sure that the imaginary parts of the eigenalues and ω has the same sign in order to satisfy the realistic requirement (3.26)-(3.29).

Considering the examples in section 6.2 and section 6.3, Table 6-7 lists the approximate modified eigenvalues results. It can be seen that the approximate results of the modified eigenvalues listed in Table 6-7 is very close to the exact numerical results listed in Table 6-3 and Table 6-5.

Table 6-7 Approximate results of modified eigenvalues

	Point modification	Cross modification
Linear viscous damping	-1.6320e-001 -4.3796e+001i -1.6320e-001 +4.3796e+001i -1.8385e+000 -1.0800e+002i -1.8385e+000 +1.0800e+002i -1.2482e+000 -1.4461e+002i -1.2482e+000 +1.4461e+002i	-3.4076e-002 -4.3795e+001i -3.4076e-002 +4.3795e+001i -1.6935e+000 -1.0801e+002i -1.6935e+000 +1.0801e+002i -2.0220e+000 -1.4461e+002i -2.0220e+000 +1.4461e+002i
Complex viscous damping	-1.5682e-001 -4.4252e+001i -1.5682e-001 +4.4252e+001i -1.8848e+000 -1.0862e+002i -1.8848e+000 +1.0862e+002i -1.2159e+000 -1.4654e+002i -1.2159e+000 +1.4654e+002i	-3.2872e-002 -4.3871e+001i -3.2872e-002 +4.3871e+001i -1.7233e+000 -1.0819e+002i -1.7233e+000 +1.0819e+002i -1.9708e+000 -1.4879e+002i -1.9708e+000 +1.4879e+002i

6.5 Sensitivities of the eigenvalue and eigenvector

According to the modified characteristic equation (6.21), let's consider its derivative with respect to the damping parameter c^*. Thus, it is obtained as

$$\frac{\partial \lambda}{\partial c^*} c^* \sum_{k=1}^{2n} \frac{v_k^2}{(\lambda a_k + d_k)} + \lambda \sum_{k=1}^{2n} \frac{v_k^2}{(\lambda a_k + d_k)} + \lambda c^* \frac{\partial \lambda}{\partial c^*} \sum_{k=1}^{2n} \frac{-v_k^2 a_k}{(\lambda a_k + d_k)^2} = 0 \tag{6.34}$$

After some mathematical operations, the derivative of the modified eigenvalue with respect to the added damping coefficient may be written as,

$$\frac{\partial \lambda}{\partial c^*} = -\frac{1}{c^*} \frac{\lambda \sum_{k=1}^{2n} \frac{v_k^2}{(\lambda a_k + d_k)}}{\sum_{k=1}^{2n} \frac{v_k^2 d_k}{(\lambda a_k + d_k)^2}} \tag{6.35}$$

Substituting equation (6.21) into equation (6.35) one then obtains the sensitivity of modified eigenvalue to the added damping.

$$\frac{\partial \lambda}{\partial c^*} = \frac{1}{(c^*)^2 \sum_{k=1}^{2n} \frac{v_k^2 d_k}{(\lambda a_k + d_k)^2}} \tag{6.36}$$

or

$$\frac{\partial \lambda}{\partial c^*} = -\frac{1}{(c^*)^2 \sum_{k=1}^{2n} \frac{v_k^2 u_k}{a_k (\lambda - u_k)^2}} \tag{6.37}$$

Consequently, the derivative of the jth vector $\mathbf{Z}_j$ to the added damping coefficient may be calculated through equation (6.26) or (6.27).

$$\frac{\partial z_{kj}}{\partial c^*} = \frac{v_k}{v_j} \frac{(d_k a_j - d_j a_k)}{(\lambda_j a_k + d_k)^2} \frac{\partial \lambda_j}{\partial c^*} \tag{6.38}$$

or

$$\frac{\partial z_{kj}}{\partial c^*} = \frac{v_k a_j}{v_j a_k} \frac{(u_j - u_k)}{(\lambda_j - u_k)^2} \frac{\partial \lambda_j}{\partial c^*} \tag{6.39}$$

and thus, the sensitivity of the jth modified eigenvector to the added damping can be obtained through the following equation

$$\frac{\partial \mathbf{Y}_j}{\partial c^*} = [\mathbf{\Phi}] \frac{\partial \mathbf{Z}_j}{\partial c^*} \tag{6.40}$$

It also should be noticed that the sensitivities of both the modified eigenvalue and modified eigenvector with respect to the added damping coefficient can be obtained through the known original eigenvalue and eigenvectors. As an example, the above modified system in section 6.2 and 6.3 is considered to investigate its sensitivity effects.

Table 6-8 Sensitivities moduli of modified eigenvalue to additional damping

	Point modification	Cross modification
Linear viscous damping	7.7480e-001 7.7480e-001 1.0662e+000 1.0662e+000 3.1625e+000 3.1625e+000	1.2909e-001 1.2909e-001 3.4377e-001 3.4377e-001 7.0316e+000 7.0316e+000
Complex viscous damping	7.6026e-001 7.6026e-001 9.9999e-001 9.9999e-001 3.3750e+000 3.3750e+000	1.2396e-001 1.2396e-001 2.8573e-001 2.8573e-001 7.3350e+000 7.3350e+000

Table 6-8 lists the sensitivity moduli of modified eigenvalue to the added damping coefficient. The sensitivity absolute values of the eigenvalues in one conjugated couple are same. It is clear that a large sensitivity modulus implies a large eigenvalue change caused by added damping. For example, in the case of linear viscous damping point modification, the sensitivities of the 5^{th} and 6^{th} eigenvalues has the largest moduli, which means the added damping will change these two eigenvalues more than the other eigenvalues.

Table 6-9 and Table 6-10 list the sensitivity moduli of the modified eigenvector with respect to the added damping for point modification and cross modification respectively. As discussed above, the larger sensitivity modulus means the large eigenvctor changes caused by the added damping. For example, as illustrated in the Table 6-9, the added linear viscous damping will induce the largest change for the eigenvectors at the third degree of freedom corresponding to the first two eigenvalues.

Table 6-9 Sensitivity moduli of eigenvector to added damping for point modification

Linear viscous damping	3.2887e-005	3.2887e-005	3.7376e-005	3.7376e-005	3.4062e-004	3.4062e-004
	1.5084e-004	1.5084e-004	2.8750e-004	2.8750e-004	2.4920e-004	2.4920e-004
	5.2670e-004	5.2670e-004	3.0438e-004	3.0438e-004	2.3369e-004	2.3369e-004
	1.6527e-002	1.6527e-002	6.3016e-003	6.3016e-003	4.2438e-002	4.2438e-002
	1.0812e-002	1.0812e-002	3.3337e-002	3.3337e-002	2.5421e-002	2.5421e-002
	1.0700e-002	1.0700e-002	2.7625e-002	2.7625e-002	5.5312e-002	5.5312e-002
Complex viscous damping	3.6016e-005	3.6016e-005	3.0301e-005	3.0301e-005	3.1898e-004	3.1898e-004
	1.4603e-004	1.4603e-004	2.7162e-004	2.7162e-004	2.4645e-004	2.4645e-004
	5.1761e-004	5.1761e-004	2.9761e-004	2.9761e-004	2.1797e-004	2.1797e-004
	1.6414e-002	1.6414e-002	6.5238e-003	6.5238e-003	4.0144e-002	4.0144e-002
	1.0561e-002	1.0561e-002	3.1815e-002	3.1815e-002	2.5295e-002	2.5295e-002
	1.1010e-002	1.1010e-002	2.7583e-002	2.7583e-002	5.5371e-002	5.5371e-002

Table 6-10 Sensitivity moduli of eigenvector to added damping for cross modification

Linear viscous damping	4.8464e-005	4.8464e-005	1.0689e-004	1.0689e-004	4.6383e-004	4.6383e-004
	8.7402e-005	8.7402e-005	1.2071e-004	1.2071e-004	9.6734e-005	9.6734e-005
	1.5341e-004	1.5341e-004	3.3633e-004	3.3633e-004	3.5544e-005	3.5544e-005
	3.9159e-004	3.9159e-004	1.4634e-002	1.4634e-002	5.1903e-002	5.1903e-002
	9.2569e-004	9.2569e-004	1.3775e-002	1.3775e-002	9.6923e-003	9.6923e-003
	8.7796e-003	8.7796e-003	3.4646e-002	3.4646e-002	4.4739e-002	4.4739e-002
Complex viscous damping	4.6545e-005	4.6545e-005	8.9403e-005	8.9403e-005	3.9104e-004	3.9104e-004
	8.3901e-005	8.3901e-005	1.0162e-004	1.0162e-004	8.7213e-005	8.7213e-005
	1.4750e-004	1.4750e-004	2.8163e-004	2.8163e-004	6.2887e-005	6.2887e-005
	3.6867e-004	3.6867e-004	1.2257e-002	1.2257e-002	4.4283e-002	4.4283e-002
	9.0041e-004	9.0041e-004	1.1627e-002	1.1627e-002	1.1298e-002	1.1298e-002
	8.4611e-003	8.4611e-003	2.9127e-002	2.9127e-002	4.1244e-002	4.1244e-002

6.6 Closure

When a damping local modification is considered to the original system, the new eigenvalue and eigenvector may be expressed the known original eigenvalue and eigenvectors. Once the new characteristic equation is obtained, the new eigenvalue, that is the roots of the characteristic equation, would be calculated easily by a numerical method. The approximate results of the modified eigenvalues may be obtained when the modification is small and the original eigenvalues are separated enough.

Two modification cases including point modification and cross modification are discussed here. These two modifications will not change the derivation procedure of the new characteristic equation for the modified system by considering the different modification location indicator vector.

For the complex viscous damping modification, we have to firstly solve the new characteristic equation for $+\omega$ and $-\omega$ respectively since the function sgn in the complex viscous damping coefficient. And then the corresponding eigenvalues can be selected so that the imaginary part of the correct eigenvalue and the ω in the sgn function have the same sign. Thus the calculation results satisfy the realistic requirement, which means that the eigenvalues appears in the conjugated complex couple form.

Consequently, the sensitivities of the modified eigenvalue and eigenvector with respect to the added damping coefficient are investigated. These sensitivities can help us to determine the level of the eigenvalue and eigenvector changes caused by the added damping.

Finally, it should be noticed that the derivation procedure in this chapter has to satisfy

the restriction to symmetric positive system and the system is non defective.

Chapter 7

Inverse Problem Applications with Complex Viscous Damping

It is well known that the physical properties of a system, that is the mass, stiffness and damping determine its dynamical characteristics such as natural frequency, mode shape and frequency response function. Thus structural modification is commonly used to obtain some desired dynamic behaviours of the system through the changing of mass, stiffness and damping. There are two main structural modification procedures. The forward modification procedure evaluates the modified dynamical behaviours by using the known physical parameter changes. Meanwhile, the inverse problem of the structural modification is aimed to determined the modified mass, stiffness and damping through the pre-described dynamic behaviours. Most structural modifications need the addition or removal of mass and stiffness [48, 109]. But complex viscous damping modification may be applied in some particular engineering case that the system mass is not required to be changed since its imaginary part will cause a stiffness phantom effect besides its viscous type effect.

7.1 Dynamic stiffness of the modified system

The dynamic motion equation of original system may be written as,

$$\mathbf{M}\ddot{\mathbf{x}} + \mathbf{C}\dot{\mathbf{x}} + \mathbf{K}\mathbf{x} = \mathbf{f} \tag{7.1}$$

where $\mathbf{x}$ is the displacement vector, $\mathbf{M}$, $\mathbf{C}$, $\mathbf{K}$ and $\mathbf{f}$ are the mass matrix, damping matrix, stiffness matrix and external force vector respectively. Equation (7.1) may be expressed in full in the frequency domain, $\mathbf{x} = \mathbf{X}e^{i\omega t}$, as,

$$\mathbf{BX} = \mathbf{F} \tag{7.2}$$

in which, $\mathbf{B} = -\omega^2\mathbf{M} + j\omega\mathbf{C} + \mathbf{K}$. $\mathbf{F}$ is the force magnitude in frequency domain.

When a mass, a grounded spring or an undamped mass-spring absorber is attached to the nth coordinate, as illustrated in Figure 1, then a modified equation of motion may be written without the need for an additional coordinate in the form,

$$\mathbf{B}\overline{\mathbf{X}} = \mathbf{F} - \Delta\mathbf{B}\overline{\mathbf{X}} \tag{7.3}$$

where $\overline{\mathbf{X}}$ is the modified system displacement vector.

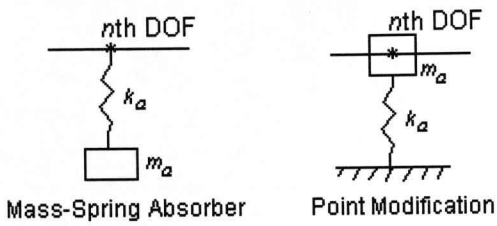

Figure 7.1 System modification

$$\Delta\mathbf{B} = \begin{bmatrix} b_1(\omega) & & & & \\ & 0 & & & \\ & & \ddots & & \\ & & & b_r(\omega) & \\ & & & & \ddots \end{bmatrix} \tag{7.4}$$

is in general a diagonal matrix with non-zero terms at the absorber attachment coordinates. Those non-zeros elements $b_r(\omega)$ are frequency factors related to the absorber and are called as absorber dynamic stiffness.

In the case of an absorber connection, this term may be written as [48],

$$b_n(\omega) = \frac{-\omega^2 m_a k_a}{-\omega^2 m_a + k_a} \tag{7.5}$$

in which, m_a and k_a are absorber mass and spring stiffness coefficients.

And in the mass-spring point modification, $b_n(\omega)$ should be written as,

$$b_n(\omega) = -\omega^2 m_a + k_a \tag{7.6}$$

7.2 Modified system receptance

By using equation (7.3), the modified receptance can be expressed as

$$\overline{\mathbf{H}} = (\mathbf{I} + \mathbf{H}\Delta\mathbf{B})^{-1}\mathbf{H} \tag{7.7}$$

where, $\mathbf{H} = \mathbf{B}^{-1}$ is the receptance matrix of the original system, and $\overline{\mathbf{H}}$ denotes the modified receptance.

If $r \le n$ absorbers are considered, let A be the integer set denoting the attachment coordinates.

$$A = \{a_i : i = 1,2,...,r\} \tag{7.8}$$

Thus, since only selected diagonal elements of the modified matrix are non-zero, $\Delta\mathbf{B}$ may be rewritten as

$$\Delta\mathbf{B} = \mathbf{U}\mathbf{V}^T \tag{7.9}$$

in which,

$$\mathbf{U} = [b_1\mathbf{e}_{a_1}, b_2\mathbf{e}_{a_2} \cdots, b_r\mathbf{e}_{a_r}] \tag{7.10}$$

$$\mathbf{V} = [\mathbf{e}_{a_1}, \mathbf{e}_{a_2} \cdots, \mathbf{e}_{a_r}] \tag{7.11}$$

and $\mathbf{e}_{a_i}$ is the a_i^{th} vector column of the $n \times n$ identity matrix.

By using the Sherman-Morrison-Woodbury formula [37] the receptance matrix of the modified system is found to be given by,

$$\overline{\mathbf{H}} = [\mathbf{I} - \mathbf{H}\mathbf{U}(\mathbf{I} + \mathbf{V}^T\mathbf{H}\mathbf{U})^{-1}\mathbf{V}^T]\mathbf{H} \tag{7.12}$$

Rearranging equation (7.12) leads to,

$$\overline{\mathbf{H}} = \mathbf{H} - \mathbf{H}\mathbf{U}(\mathbf{I} + \mathbf{V}^T\mathbf{H}\mathbf{U})^{-1}\mathbf{V}^T\mathbf{H} \tag{7.13}$$

and hence, for arbitrary pq^{th} element,

$$\overline{h}_{pq} = \mathbf{e}_p^T\overline{\mathbf{H}}\mathbf{e}_q \tag{7.14}$$

Then,

$$\overline{h}_{pq} = \mathbf{e}_p^T\mathbf{H}\mathbf{e}_q - \mathbf{e}_p^T\mathbf{H}\mathbf{U}(\mathbf{I} + \mathbf{V}^T\mathbf{H}\mathbf{U})^{-1}\mathbf{V}^T\mathbf{H}\mathbf{e}_q \tag{7.15}$$

We now define the following matrices,

$$\mathbf{D} = \begin{bmatrix} b_1 & & & \\ & b_2 & & \\ & & \ddots & \\ & & & b_r \end{bmatrix} \tag{7.16}$$

$$\mathbf{p} = [h_{p,a_1}, h_{p,a_2}, \cdots, h_{p,a_r}]^T \tag{7.17}$$

$$\mathbf{q} = [h_{a_1,q}, h_{a_2,q}, \cdots, h_{a_r,q}]^T \tag{7.18}$$

$$\mathbf{G} = \begin{bmatrix} h_{a_1,a_1} & h_{a_1,a_2} & \cdots & h_{a_1,a_r} \\ h_{a_2,a_1} & h_{a_2,a_2} & \cdots & h_{a_2,a_r} \\ \vdots & \vdots & \ddots & \vdots \\ h_{a_r,a_1} & h_{a_r,a_2} & \cdots & h_{a_r,a_r} \end{bmatrix} \tag{7.19}$$

so that the following expressions are obtained,

$$\mathbf{e}_p{}^T \mathbf{H}\mathbf{U} = \mathbf{p}^T \mathbf{D} \tag{7.20}$$

$$\mathbf{V}^T \mathbf{H}\mathbf{U} = \mathbf{G}\mathbf{D} \tag{7.21}$$

$$\mathbf{V}^T \mathbf{H}\mathbf{e}_q = \mathbf{q} \tag{7.22}$$

Consequently, the receptance for modified system with r absorbers is rewritten as,

$$\bar{h}_{pq} = h_{pq} - \mathbf{p}^T \mathbf{D}(\mathbf{I} + \mathbf{G}\mathbf{D})^{-1}\mathbf{q} \tag{7.23}$$

or,

$$\bar{h}_{pq} = h_{pq} - \mathbf{p}^T (\mathbf{D}^{-1} + \mathbf{G})^{-1}\mathbf{q} \tag{7.24}$$

where the inverse of $\mathbf{D}$ is,

$$\mathbf{D}^{-1} = \begin{bmatrix} 1/b_1 & & & \\ & 1/b_2 & & \\ & & \ddots & \\ & & & 1/b_r \end{bmatrix} \tag{7.25}$$

It is found that the original $n \times n$ matrix computation is condensed to the $r \times r$ matrix computation expressed in equation (25). In general, since only a small number of absorbers are considered the computation is considerably reduced. Furthermore, equation (25) shows only the original receptances at the coordinates of absorber attachments $(a_1, a_2, ..., a_r)$ and the receptance coordinates $(p,\ q)$ are needed to determine the modified-system receptances. This is very significant result for the practical application of the method to large-scale systems.

7.3 Complex viscous damping point modification

When the system is connected to the complex viscous damping absorber or point modifications, the dynamic stiffness in equation (7.5) and (7.6) can be easily expanded to be

$$b_n(\omega) = \frac{-\omega^2 m_a[k_a + j\omega(c_m - jc_e)]}{-\omega^2 m_a + [k_a + j\omega(c_m - jc_e)]} \quad \text{for absorber modification} \tag{7.26}$$

$$b_n(\omega) = -\omega^2 m_a + j\omega(c_m - jc_e) + k_a \quad \text{for point modification} \tag{7.27}$$

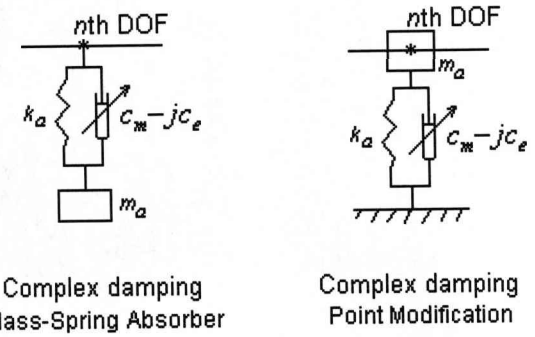

Figure 7.2 System modification with complex viscous damping

If we don't want to introduce the mass change to the original system, the only point modification with complex viscous damping $c_m(1 + j\gamma)$ and spring stiffness k_a are considered. In this case the dynamic stiffness is written as

$$b_n(\omega) = j\omega c_m(1 + j\gamma) + k_a \tag{7.28}$$

in which, γ is defined as previous,

$$\gamma = \frac{-c_e}{c_m} \tag{7.29}$$

It should be noticed that the sign function sgn is not included in the equation (7.28) since the problem is studied in the positive frequency range and then only positive values of $\mathrm{Im}(\lambda)$ are considered. In this case, $\mathrm{sgn}(\omega) = 1$.

Also for the sake of simplicity, one complex viscous damping modification is considered in the work. Thus the modified receptance equation can be simplified as

the following through the equation (7.23).

$$\bar{h}_{pq} = h_{pq} - \frac{bh_{p,a}h_{a,q}}{1+bh_{a,a}} \tag{7.30}$$

where, the absorber is connected to the ath degree of freedom of the original system.

In order to illustrate clearly assignment work, a simple cantilever beam was considered as an example.

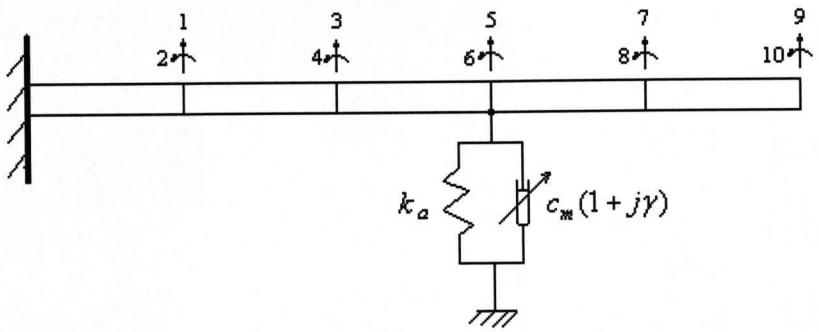

Figure 7.3 Cantilever beam with a complex viscous damping modification

The beam's material properties including length, section area, density, second inertia moment and elastic modulus are selected as $L = 0.5m$, $A = 9\times10^{-5}m^2$, $\rho = 2700kg/m^3$, $I = 6.75\times10^{-11}m^4$, $E = 5.186\times10^{10}Pa$ respectively. The first three natural frequencies are 8.496 Hz, 53.27 Hz and 149.61 Hz respectively.

7.4 Assignment of natural frequencies

Considering modified receptance equation (7.30), the poles of the modified system can be given by the characteristic equation, which is formed by setting the denominator of the equation (7.30) equal to zero. Then substituting the complex viscous damping dynamic stiffness equation (7.28) into this characteristic equation may obtain the modification equation as

$$1+[j\omega c_m(1+j\gamma)+k_a]h_{a,a} = 0 \tag{7.31}$$

It should be noticed that the function of the left side of equation (7.31) also produces a complex number. Thus in order to satisfy this modification equation, both real part

and imaginary part of this function have to be equal to zero. However, it is shown that its imaginary part $\omega c_m h_{a,a}$ cannot be zero unless $c_m = 0$. And it is not acceptable. Thus, the pole will happen when the modulus of the left side of equation (7.31) is minimal, which means the real part of the left side of equation (7.31) is equal to zero. So, we got the new modification equation as below

$$1 + (-\omega\gamma c_m + k_a) h_{a,a} = 0 \tag{7.32}$$

In order to assign a single natural frequency ω_i, just putting $\omega = \omega_i$ transforms the equation (7.32) into an equation with $c_m\gamma$ and k_a as,

$$k_a = \omega_i c_m \gamma - \frac{1}{h_{a,a}(\omega_i)} \tag{7.33}$$

Now fixing c_m, γ and solving this equation may obtain the spring stiffness k_a. It should be paid attention that c_m and k_a have to be positive. Thus the realistic condition should be satisfied as,

$$c_m \gamma > \frac{1}{\omega_i h_{a,a}(\omega_i)} \tag{7.34}$$

Example 1: Now we consider the cantilever beam as shown in Figure 7.3 with a complex damping connected to the 5th DOF. It is assumed that a natural frequency is required to be assigned at 15 Hz. Considering complex viscous damping with $c_m = 0.5$ Ns/m and $\gamma = -0.3$, and then inserting the original receptance $h_{5,5}$ at 15 Hz $h_{5,5}(f = 15Hz) = -1.0375 \times 10^{-3}$ m/N into the equation (7.33) obtain the spring stiffness $k_a = 9.4975 \times 10^2$ N/m. Figure 7.4 demonstrates the frequency response function $h_{3,5}$, $h_{3,7}$ and $h_{3,9}$ of the modified system in which the peak at frequency 15 Hz indicates the presence of the desired natural frequency. In this figure, the dash line presents the original receptance while the solid line presents the modified receptance. Table 7-1 lists the new first three natural frequencies and first six eigenvalues of the modified system. And it can be seen that the first natural frequency is changed to be 15.001 Hz.

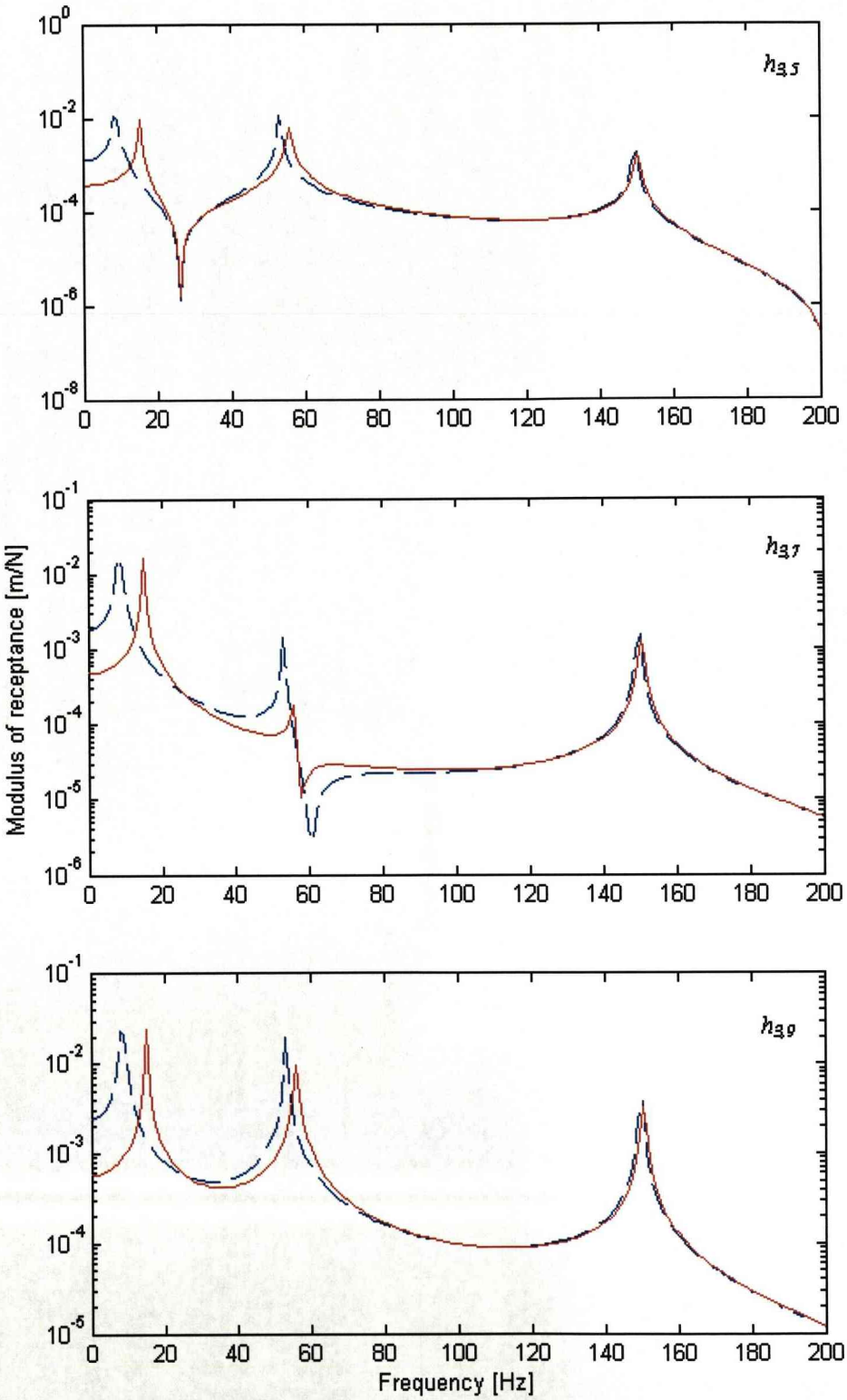

Figure 7.4 The modified FRF for single natural frequency assignment

Table 7-1 Modified first three natural frequencies and first six eigenvalues

Natural frequencies (Hz)	Eigenvalues
15.001	-1.3975e+000 -9.4245e+001i -1.3975e+000 +9.4245e+001i
56.052	-3.1294e+000 -3.5217e+002i -3.1294e+000 +3.5217e+002i
150.31	-1.9503e+000 -9.4445e+002i -1.9503e+000 +9.4445e+002i

If we want to assign two natural frequencies at same time, putting $\omega = \omega_1$ and $\omega = \omega_2$ into equation (7.33) separately, and then solving the two equation together obtain two parameters k_a and $c_m\gamma$ as the following,

$$\begin{cases} k_a = \dfrac{\dfrac{\omega_1}{h_{a,a}(\omega_2)} - \dfrac{\omega_2}{h_{a,a}(\omega_1)}}{\omega_2 - \omega_1} \\ c_m\gamma = \dfrac{\dfrac{1}{h_{a,a}(\omega_2)} - \dfrac{1}{h_{a,a}(\omega_1)}}{\omega_2 - \omega_1} \end{cases} \tag{7.35}$$

Once the parameter $c_m\gamma$ is gotten, c_m may be calculated by selecting an appropriate value of γ. Likewise, the realistic-solutions requirement for $k_a > 0$ has to be satisfied,

$$\frac{\omega_1}{h_{a,a}(\omega_2)} < \frac{\omega_2}{h_{a,a}(\omega_1)} \; for(\omega_2 < \omega_1) \tag{7.36}$$

and

$$\frac{\omega_1}{h_{a,a}(\omega_2)} > \frac{\omega_2}{h_{a,a}(\omega_1)} \; for(\omega_2 > \omega_1) \tag{7.37}$$

Example 2: Considering the same system in Example 1, it is now assumed to assign two natural frequencies at 20 Hz and 60 Hz simultaneously. By using equation (7.35), we obtained

$k_a = 2.4618 \times 10^3$ N/m and $c_m\gamma = 0.1789$ Ns/m,

And then fixing $\gamma = 0.3$ will get $c_m = 0.5964$ Ns/m

Figure 7.5 demonstrates the frequency response function $h_{3,7}$ and $h_{3,9}$ of the modified system in which two natural frequencies 20 Hz and 60 Hz are presented. In this figure, the dash line presents the original receptance while the solid line presents the modified receptance. It if found that two natural frequency appears at 20 Hz and 60 Hz.

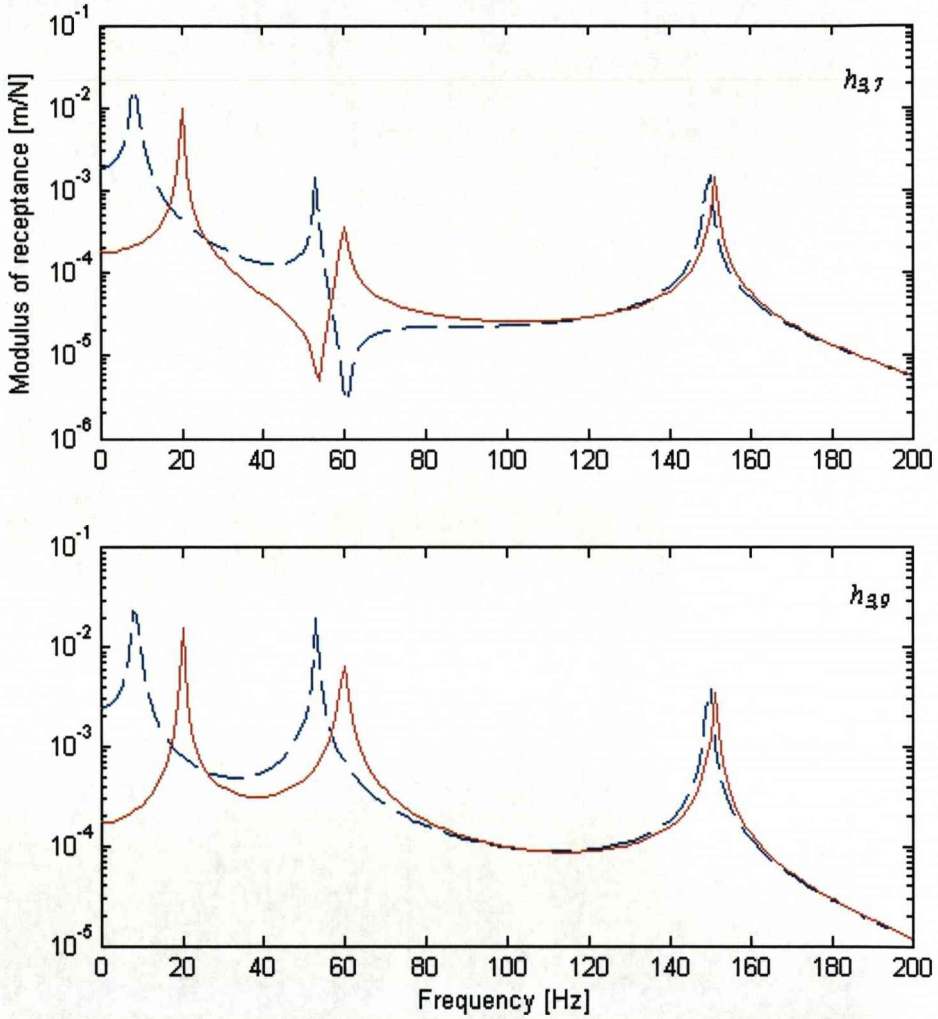

Figure 7.5 The modified FRF for two natural frequencies assignment

7.5 Assignment of an antiresonance

An antiresonance or zero will exist when the numerator of the equation (7.30) is equal to zeros. So, substituting the complex viscous damping dynamic stiffness equation

(7.28) into the numerator of the equation (7.30) gives the following modification equation as

$$h_{pq} + [j\omega c_m(1+j\gamma) + k_a](h_{pq}h_{a,a} - h_{p,a}h_{a,q}) = 0 \tag{7.38}$$

Similarly, the left side of this equation presents a complex value number. However its imaginary part is equal to $\omega c_m(h_{pq}h_{a,a} - h_{p,a}h_{a,q})$ that is non-zero. Thus the zero exists at the frequency where the real part of the left side of the equation (7.38) is equal to zero shown as the below.

$$h_{pq} + [-\omega c_m\gamma + k_a](h_{pq}h_{a,a} - h_{p,a}h_{a,q}) = 0 \tag{7.39}$$

Thus, in order to assign a zero at frequency ω_i, just putting $\omega = \omega_i$ transforms the equation (7.39) into an equation with k_a and $c_m\gamma$ as,

$$k_a = \omega_i c_m\gamma - \frac{h_{pq}(\omega_i)}{[h_{p,a}(\omega_i)h_{a,q}(\omega_i) - h_{pq}(\omega_i)h_{a,a}(\omega_i)]} \tag{7.40}$$

Now fixing c_m, γ and solving this equation may obtain the spring stiffness k_a. It should be paid attention that c_m and k_a have to be positive. Thus the realistic condition should be satisfied as,

$$c_m\gamma > \frac{h_{pq}(\omega_i)}{\omega_i[h_{p,a}(\omega_i)h_{a,q}(\omega_i) - h_{pq}(\omega_i)h_{a,a}(\omega_i)]} \tag{7.41}$$

Another interesting phenomena is that when $p = a$ or $q = a$, the item $(h_{pq}h_{a,a} - h_{p,a}h_{a,q}) = 0$. In these cases, the numerator of the modified receptance equation (7.30) becomes h_{pq}, which is no a zero unless $h_{pq} = 0$. This means that in these cases, the damping modification will not bring a new zero since its effect is eliminated by multiplied with a zero. On the other words, if we want to assign a zero for the receptance h_{pq} through complex viscous damping modification, this damping have to be connected to neither *p*th DOF nor *q*th DOF.

Example 3: Here we also consider the cantilever beam as shown in Figure 7.3 with a complex damping connected to the 5th DOF. And we want to assign an antiresonance at 40 Hz for the receptance $h_{3,9}$. Inserting the original receptances at 40 Hz $h_{3,9} = -5.6450\times10^{-4}$ m/N, $h_{3,5} = 2.0311\times10^{-4}$ m/N, $h_{5,9} = -6.6350\times10^{-4}$

m/N, $h_{5,5} = 1.3099 \times 10^{-4}$ m/N and $c_m = 0.5$ Ns/m and $\gamma = -0.3$ into equation (7.40) gives a value for the spring stiffness $k_a = 9.2437 \times 10^3$ N/m. Figure 7.6 illustrates the frequency response function $h_{3,9}$ of the modified system in which a zero happens at frequency 40 Hz . In this figure, the dash line presents the original receptance while the solid line presents the modified receptance.

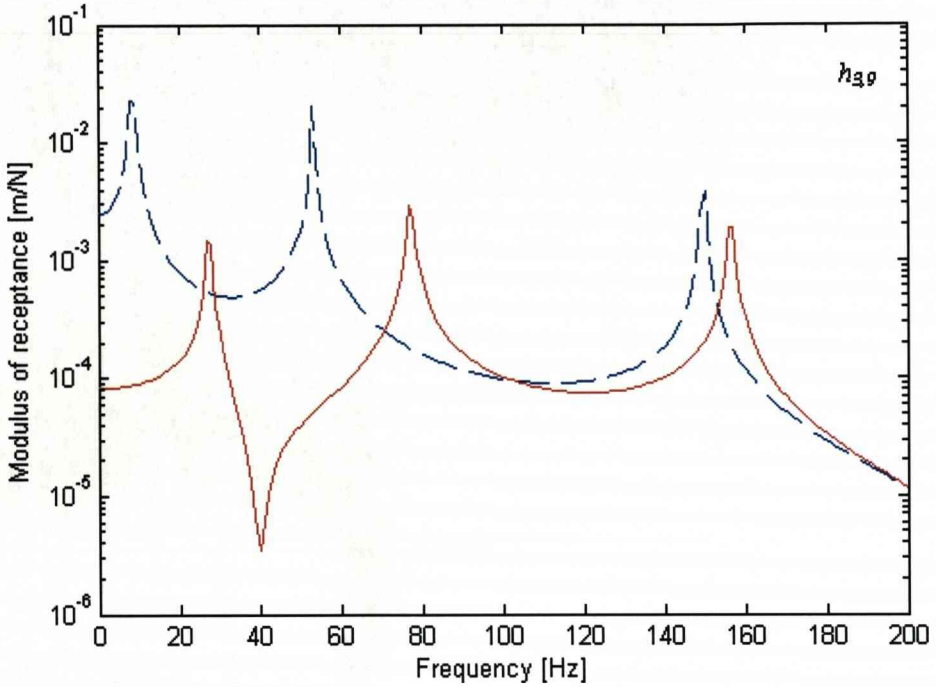

Figure 7.6 The modified FRF for a single antiresonance assignment

7.6 Assignment of a receptance at a single frequency

Based on the modified receptance equation (7.30), the dynamic stiffness can be easily obtained. And then the substituting equation (7.28) for complex viscous damping modification will give the modification equation as below.

$$j\omega c_m(1+j\gamma)+k_a = \frac{(h_{pq}-\bar{h}_{pq})}{h_{p,a}h_{a,q}-h_{a,a}(h_{pq}-\bar{h}_{pq})} \tag{7.42}$$

For the sake of the assignment of the receptance at one frequency, putting $\omega = \omega_i$

can transform the problem into an equation of unknown variables $c_m\gamma$ and k_a. However it also should be found that the left side of the equation (7.42) is a complex value while the right side of this equation is just a real value. So, in order to find appropriate value of parameters c_m, γ and k_a, the real part of the both sides of the equation (7.42) should be equal as shown in the following equation,

$$-\omega_i c_m \gamma + k_a = \frac{[h_{pq}(\omega_i) - \bar{h}_{pq}(\omega_i)]}{h_{p,a}(\omega_i)h_{a,q}(\omega_i) - h_{a,a}(\omega_i)[h_{pq}(\omega_i) - \bar{h}_{pq}(\omega_i)]} \tag{7.43}$$

Actually this calculation procedure is an optimization to found the suitable parameters c_m and γ that make function

$$f = j\omega c_m(1 + j\gamma) + k_a - \frac{(h_{pq} - \bar{h}_{pq})}{h_{p,a}h_{a,q} - h_{a,a}(h_{pq} - \bar{h}_{pq})} \tag{7.44}$$

to be minimal. The above discussions about assignment of natural frequency and antiresonance can be understood similarly. Another reason is that we can select a small viscous damping coefficient that makes the imaginary part of the function (7.44) very small.

Therefore through the equation (7.43), we can fix a $c_m\gamma$ and calculate k_a as,

$$k_a = \omega_i c_m \gamma + \frac{[h_{pq}(\omega_i) - \bar{h}_{pq}(\omega_i)]}{\{h_{p,a}(\omega_i)h_{a,q}(\omega_i) - h_{a,a}(\omega_i)[h_{pq}(\omega_i) - \bar{h}_{pq}(\omega_i)]\}} \tag{7.45}$$

And the realistic requirement should be satisfied,

$$c_m\gamma > -\frac{1}{\omega_i}\frac{[h_{pq}(\omega_i) - \bar{h}_{pq}(\omega_i)]}{\{h_{p,a}(\omega_i)h_{a,q}(\omega_i) - h_{a,a}(\omega_i)[h_{pq}(\omega_i) - \bar{h}_{pq}(\omega_i)]\}} \tag{7.46}$$

Example 4: Again we consider the same cantilever beam as shown in Figure 7.3 with a complex damping connected to the 5th DOF. And it is assumed to assign a new receptance $\bar{h}_{3,9}$ at 80 Hz, which is 0.2 times of the original receptance $h_{3,9}$ Inserting the original receptances at 80 Hz $h_{3,9} = 1.5907\times10^{-4}$ m/N, $\bar{h}_{3,9} = 0.2h_{3,9} = 3.1813\times10^{-5}$ m/N, $h_{3,5} = -1.2258\times10^{-4}$ m/N, $h_{5,9} = 5.8209\times10^{-5}$ m/N, $h_{5,5} = -9.4280\times10^{-5}$ m/N and complex viscous damping parameters $c_m = 0.5$ Ns/m

and $\gamma = -0.3$ into equation (7.45) gives the spring stiffness $k_a = 2.6098 \times 10^4$ N/m.

Figure 7.7 illustrates the frequency response function $h_{3,9}$ of the modified system. In this figure, the dash line presents the original receptance while the solid line presents the modified receptance. And the star "*" presents the original receptance value at frequency 80 Hz. The cross "+" presents the aimed receptance value. The circle "o" presents the actual modified receptance value.

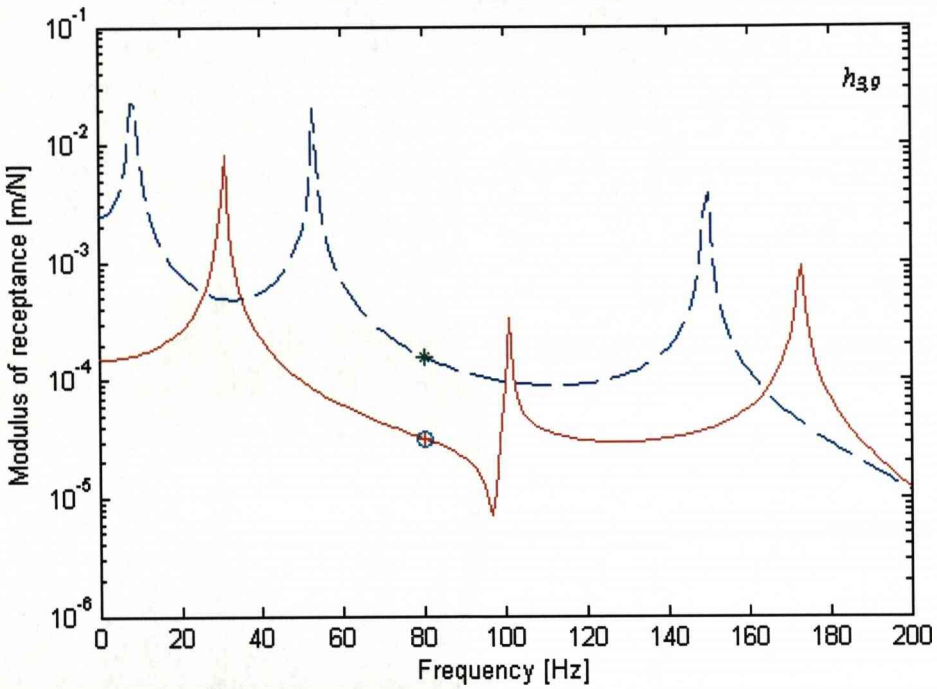

Figure7.7 Example 4 - assignment of one receptance at one frequency

Table 7-2 describes the details of the receptance modification. It can be seen that since the introducing of a damping, the modified receptance becomes a complex values. However, the real part of the new receptance is very close to the desired receptance value and the imaginary part of the new receptance is very small. Particularly, the modulus of modified receptance is same to the modulus of the aimed receptance. Thus it is reasonable to believe that the assignment of the receptance is successful.

Table 7-2. Receptance values of $h_{3,9}$ at frequency 80Hz

	Receptance value	Modulus of receptance
Original Receptance	1.5907×10^{-4}	1.5907×10^{-4}
Desired Receptance	3.1813×10^{-5}	3.1813×10^{-5}
Modified Receptance	$3.1827\times10^{-5}+8.3240\times10^{-7}$ i	3.1837×10^{-5}
Ratio $\bar{h}_{3,7}/h_{3,7}$	0.2001 +0.0052i	0.2002

Example 5: For the same system, it is required to assign a new receptance $\bar{h}_{3,9}$ at 80 Hz to be 1.3 of the original value $h_{3,9}$, that is $\bar{h}_{3,9}=1.3h_{3,9}=2.0678\times10^{-4}$ m/N. The calculation result gives a result of the spring stiffness $k_a=4.0262\times10^{3}$ N/m with the complex viscous damping of $c_m=0.5$ Ns/m and $\gamma=-0.3$. Figure 7.8 demonstrates the original and modified receptance of $h_{3,9}$. It is also found that the pre-described receptance value is assigned appropriately.

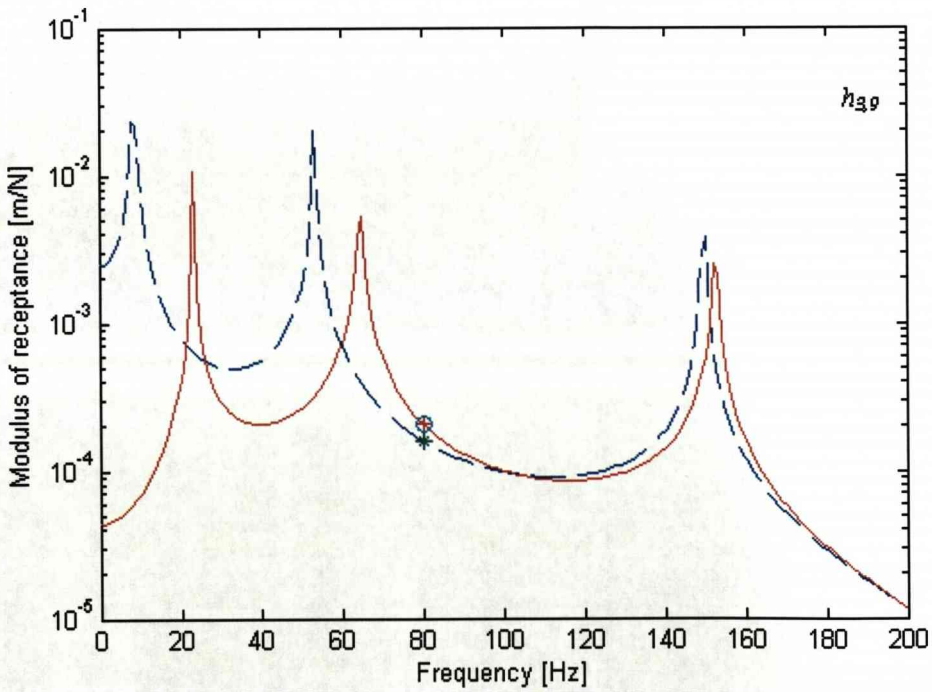

Figure7.8 Example 5 - assignment of one receptance at one frequency

7.7 Closure

The chapter tries to investigate the possibility of structural modification with a complex viscous damping and a spring to assign some dynamic characteristics of the system such as natural frequency, antiresonance and receptance. The most important advantage of this modification is that it can achieve some assignments without leading to any mass change for original system. This special characteristic is totally different to the effect of general mass-spring point modification and mass-spring absorber. The connections of both them will cause the mass change to the original system.

The complex viscous damping can be used to assign some dynamic properties of the system since it introduces a phantom stiffness effect through it imaginary part besides its linear viscous type effect through its real part. The analyses results show that the natural frequency, antiresonance and receptance of the system can be appropriately assigned through the complex viscous damping modification. However, the assignment procedure has to satisfy the realistic requirement. That mans the spring stiffness k_a and viscous damping coefficient c_m should be positive. And the imaginary part factor γ of the complex viscous damping coefficient should be in the reasonable range.

Chapter 8

Vibration Suppression by Using Complex Viscous Damping Absorber

This chapter is aimed to investigate the vibration suppression effect of the complex viscous damping absorber to the original dynamic system. A method is proposed to suppress the receptance at the desired natural frequency. This method requires to using the new modal receptance of the modified system to be the optimization objective function. The modal receptance will clearly present the receptance component corresponding to one natural frequency. The solution of the absorber parameters involves an optimization procedure. And a least square optimum method is used to select the absorber parameters.

8.1 Concepts of modal receptance

It is well know that the dynamic equation of a vibration system can be written as

$$\mathbf{M}\ddot{\mathbf{x}} + \mathbf{K}\mathbf{x} = \mathbf{f} \tag{8.1}$$

in which, $\mathbf{x}$ is the displacement vector, $\mathbf{M}, \mathbf{K}$ and $\mathbf{f}$ are mass matrix, stiffness matrix and external force vector respectively.

And its eigenvalue problem can be solved through the characteristic equation as

$$(-\lambda_j \mathbf{M} + \mathbf{K})\mathbf{\Phi}_j = \mathbf{0} \tag{8.2}$$

in which, λ_j is the jth eigenvalue and $\mathbf{\Phi}_j$ is the jth eigenvector column corresponding to the λ_j. Thus the eigenvector matrix may be obtained as

$$[\Phi]=[\Phi_1 \quad \Phi_2 \quad \cdots \quad \Phi_n] \tag{8.3}$$

For the positive-definite system, the eigenvector matrix shows the following orthogonaltiy,

$$[\Phi]^T \mathbf{M}[\Phi]=\mathbf{M}^* = diag(\mathrm{m}_1,\mathrm{m}_2,\cdots \mathrm{m}_n) \tag{8.4}$$

$$[\Phi]^T \mathbf{K}[\Phi]=\mathbf{K}^* = diag(\mathrm{k}_1,\mathrm{k}_2,\cdots \mathrm{k}_n) \tag{8.5}$$

Thus, the *j*th natural frequency of the system can be obtained as

$$\omega_{nj}=\sqrt{\frac{\mathrm{k}_j}{\mathrm{m}_j}} \tag{8.6}$$

Here $\mathbf{M}^*$ and $\mathbf{K}^*$ are called as modal mass matrix and the modal stiffness matrix respectively. Thus,

So, if we substitute

$$\mathbf{x}=[\Phi]\mathbf{u} \tag{(8.7)}$$

where, $\mathbf{u}$ is the modal displacement vector of the system, into the motion equation (8.1) and then multiply $[\Phi]^T$ at both sides of the equation, the motion equation (8.1) can be rewritten in a uncoupled form with respect to the modal displacement,

$$\mathrm{m}_j\ddot{\mu}_j+\mathrm{k}_j\mu_j=\mathrm{f}_j \tag{8.8}$$

in which, m_j and k_j are the *j*th modal mass and *j*th modal stiffness, μ_j is the *j*th modal displacement, and f_j is the *j*th modal force. And the modal force vector can be obtained through $[\Phi]^T\mathbf{f}$

Supposing harmonic $\mu_j=U_j e^{j\omega t}$ for $\mathrm{f}_j=\mathrm{F}_j e^{j\omega t}$, the *j*th modal receptance may be expressed as

$$R_{jj}=\frac{U_j}{\mathrm{F}_j}=\frac{1}{-\omega^2\mathrm{m}_j+\mathrm{k}_j} \tag{8.9}$$

This modal receptance presents the relation between the *j*th modal displacement μ_j and the *j*th modal force f_j. And, it can be found that the modal receptance is a function with two coupled poles at $s_{1,2}=\pm\sqrt{\frac{\mathrm{k}_j}{\mathrm{m}_j}}$. The positive pole happens at the

corresponding natural frequency ω_{nj} . Figure 8.1 demonstrates typical model receptance with a natural frequency at 62.052 rad/s.

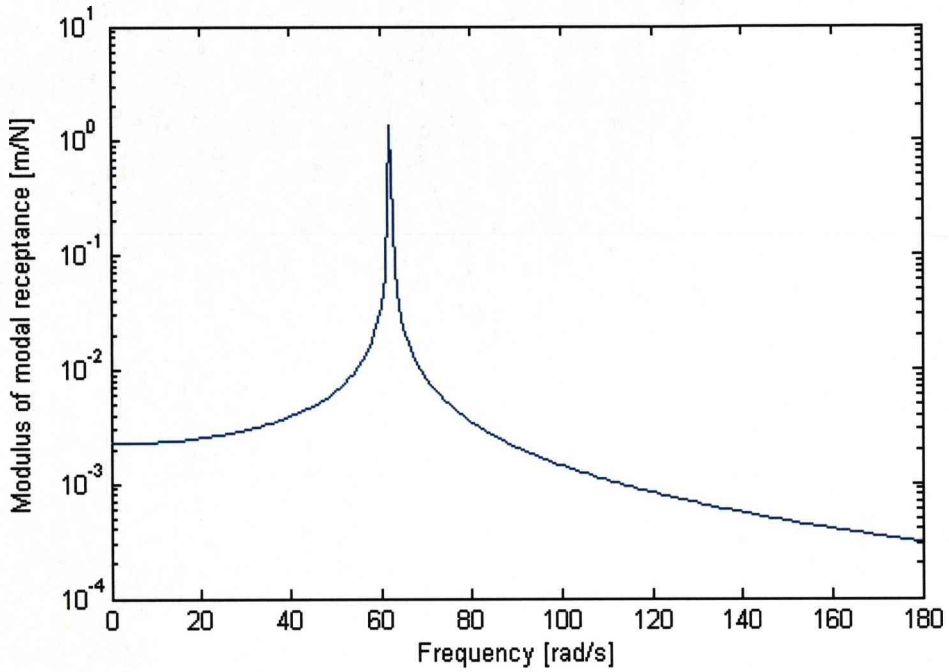

Figure8.1 the modal receptance of the original system

The modal receptance matrix may be easily calculated as following,

$$\mathbf{R} = ([\mathbf{\Phi}]^T \mathbf{B}[\mathbf{\Phi}])^{-1}$$

$$= diag(\frac{1}{-\omega^2 \mathrm{m}_1 + \mathrm{k}_1}, \frac{1}{-\omega^2 \mathrm{m}_2 + \mathrm{k}_2}, \cdots, \frac{1}{-\omega^2 \mathrm{m}_n + \mathrm{k}_n}) \tag{8.10}$$

in which

$$\mathbf{B} = -\omega^2 \mathbf{M} + \mathbf{K} \tag{8.11}$$

It is noticed that the modal receptance matrix is a diagonal matrix, which means each modal receptance is independent to others.

On the other hand, the receptance of this system can be obtained as

$$\mathbf{H} = \mathbf{B}^{-1} \tag{8.12}$$

The receptance presents the relation between the displacement in physical coordinate and the force in physical coordinate. Thus by using equation (8.10) and (8.12), we can obtained the relation between the receptance and the modal receptance as following,

$$\mathbf{R} = [\mathbf{\Phi}]^{-1}\mathbf{H}([\mathbf{\Phi}]^{T})^{-1} \tag{8.13}$$

or

$$\mathbf{H} = [\mathbf{\Phi}]\mathbf{R}[\mathbf{\Phi}]^{T} \tag{8.14}$$

So, for any *p, q*th receptance,

$$h_{pq} = \sum_{j=1}^{n} R_{jj}\varphi_{pj}\varphi_{qj} = \sum_{j=1}^{n} \frac{\varphi_{pj}\varphi_{qj}}{-\omega^2 \mathrm{m}_j + \mathrm{k}_j} \tag{8.15}$$

in which, φ_{pj} and φ_{qj} are the *p, j*th and *q, j*th element of eigenvector matrix $[\mathbf{\Phi}]$.

The equation (8.15) is well-known [38]. It is found that modal receptance presents clearly the characteristics of each modal component in the receptance and allows us to understand the principle of the receptance in a detailed way. This property also provides us an idea to suppress the response at the desired natural frequency since if the *j*th modal receptance is suppressed successfully the *j*th peak in the receptance will be suppressed.

Similar to equation (8.10), the modal receptance matrix of the modified system may be obtained as,

$$\overline{\mathbf{R}} = [\overline{\mathbf{\Phi}}]^{-1}\overline{\mathbf{H}}([\overline{\mathbf{\Phi}}]^{T})^{-1} \tag{8.16}$$

in which, $\overline{\mathbf{R}}$ is the modal receptance matrix of the modified system, $\overline{\mathbf{H}}$ is the receptance matrix of the modified system and $[\overline{\mathbf{\Phi}}]$ is the eigenvector matrix of the modified system.

However, it is not straightforward to measure the changes of the modal receptance between the original system and modified system from equations (8.10) and (8.16) since a modified eigenvector matrix is involved in the equation (8.16). In order to avoid this shortcoming, we propose a new modal receptance concept of the modified system as following,

$$\widetilde{\mathbf{R}} = [\mathbf{\Phi}]^{-1}\overline{\mathbf{H}}([\mathbf{\Phi}]^{T})^{-1} \tag{8.17}$$

in which, $\widetilde{\mathbf{R}}$ is the new modal receptance matrix of the modified system, $\overline{\mathbf{H}}$ is the receptance matrix of the modified system and $[\mathbf{\Phi}]$ is the eigenvector matrix of the original system.

Thus it becomes convenient to evaluate the difference between the modal receptance of the original system and the modal receptance of the modified system by comparing equation (8.10) and (8.17). Another advantage of the equation (8.17) is that the calculation of the new eigenvectors of the modified system is not necessary any more.

When an absorber is attached to the original system, the modified receptance can be calculated through equation (7.13).

$$\overline{\mathbf{H}} = \mathbf{H} - \frac{b_r}{1 + b_r h_{rr}} \mathbf{H} \mathbf{e}_r \mathbf{e}_r^T \mathbf{H} \tag{8.18}$$

By setting

$$\begin{aligned} \mathbf{U} &= b_r \mathbf{e}_r \\ \mathbf{V} &= \mathbf{e}_r \end{aligned} \tag{8.19}$$

for the one absorber attached to the *r*th degree of freedom of the original system. In which b_r is the dynamic stiffness as defined in the Chapter 7. $\mathbf{e}_r$ is the location column vector that has an unit one on the *r*th DOF where the absorber is connected while other elements are all zeros. h_{rr} is the *r, r*th receptance of the original system.

By substituting equations (8.14) and (8.18) into the equation (8.17), the new modal receptance of the modified system may be obtained as,

$$\widetilde{\mathbf{R}} = \mathbf{R} - \frac{b_r}{1 + b_r h_{rr}} \mathbf{R}[\mathbf{\Phi}]^T \mathbf{e}_r \mathbf{e}_r^T [\mathbf{\Phi}] \mathbf{R} \tag{8.20}$$

Hence, for arbitrary *i, j*th element,

$$\begin{aligned} \widetilde{R}_{ij} &= \mathbf{e}_i^T \widetilde{\mathbf{R}} \mathbf{e}_j \\ &= \mathbf{e}_i^T \mathbf{R} \mathbf{e}_j - \frac{b_r}{1 + b_r h_{rr}} \mathbf{e}_i^T \mathbf{R}[\mathbf{\Phi}]^T \mathbf{e}_r \mathbf{e}_r^T [\mathbf{\Phi}] \mathbf{R} \mathbf{e}_j \end{aligned} \tag{8.21}$$

in which, $\mathbf{e}_i$ is the column vector that has an unit one on the *i*th element while other elements are all zeros. $\mathbf{e}_j$ is the column vector that has an unit one on the *j*th element while other elements are all zeros. It is noticed that $\mathbf{R}$ is a diagonal matrix. Thus, we have

$$\widetilde{R}_{ij} = \begin{cases} R_{ii} - \dfrac{b_r}{1 + b_r h_{rr}} (R_{ii} \varphi_{ri})^2 & (i = j) \\ -\dfrac{b_r}{1 + b_r h_{rr}} R_{ii} R_{jj} \varphi_{ri} \varphi_{rj} & (i \neq j) \end{cases} \tag{8.22}$$

As we have known that R_{ii} has only one pole at its corresponding natural frequency. And at the other frequencies far from the natural frequency R_{ii} has very small values. So, if the eigenvalues of the original system are distinct and separated enough, $\widetilde{R}_{ij}\,(i \neq j) \approx 0$ since $R_{ii}R_{jj}$ is close to zero as shown in Figure 8.2.

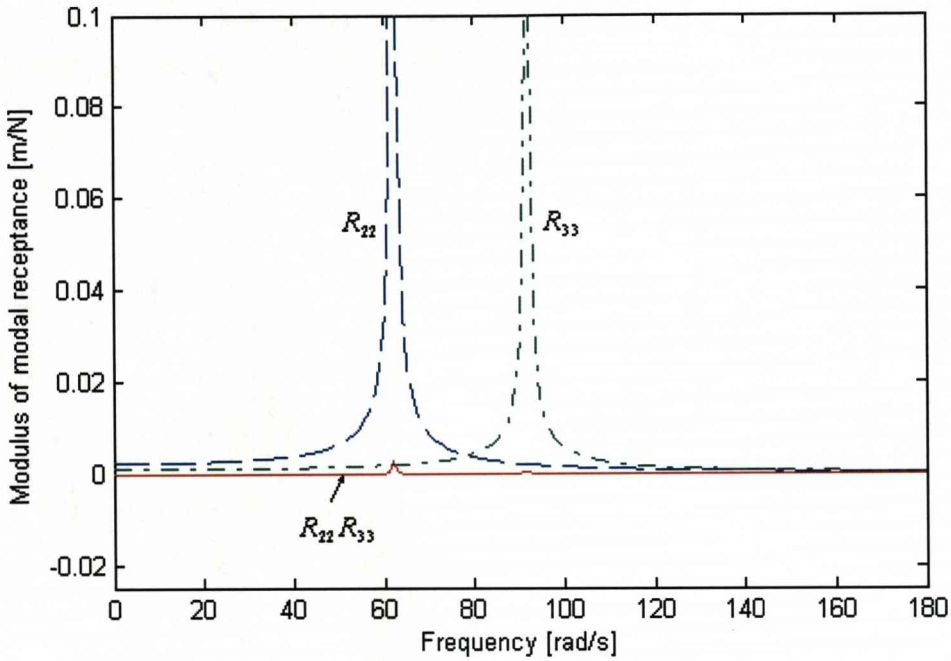

Figure 8.2 Modulus of modal receptance

So the new modal receptance of the modified system can also be thought as an approximate diagonal matrix.

$$\widetilde{\mathbf{R}} = diag(\widetilde{R}_{11},\ \widetilde{R}_{22},\ \ldots,\ \widetilde{R}_{nn}) \tag{8.23}$$

in which,

$$\widetilde{R}_{ii} = R_{ii} - \frac{(R_{ii}\varphi_{ri})^2 b_r}{1 + b_r h_{rr}} \quad (i=1, 2, \ldots, n) \tag{8.24}$$

Thus, the new modal receptance of the modified system can also be thought as independent to each other because the new modal receptance matrix is diagonal.

The equation (8.24) presents clearly the change of the modal receptance caused by the system modification. In particular the new modal receptance can be obtained through the dynamical parameters of the original system and the absorber parameter directly.

And the new eigenvectors of the modified system need not to be calculated.

8.2 Receptance suppression optimization

When the new modal receptance matrix of the modified system $\widetilde{\mathbf{R}}$ is determined the receptance matrix of the modified system $\overline{\mathbf{H}}$ can be easily obtained from the equation (8.17),

$$\overline{\mathbf{H}} = [\mathbf{\Phi}]\widetilde{\mathbf{R}}[\mathbf{\Phi}]^T \tag{8.25}$$

And then the any arbitrary *k, j*th modified receptance may be expressed from the form of a sum of scaled pole functions since its approximate diagonal property.

$$\overline{h}_{kj} = \sum_{i=1}^{n} \widetilde{R}_{ii} \varphi_{ki} \varphi_{ji} \tag{8.26}$$

So, each item $\widetilde{R}_{ii}$ of the new modal receptance matrix $\widetilde{\mathbf{R}}$ will lead the major effect to the modified receptance at the corresponding natural frequency. This discussion provides a simple method to suppress the receptance at a desired natural frequency. If one new modal receptance corresponding to the *j*th natural frequency is suppressed, the receptance at this natural frequency will be suppressed.

However it is well known that the simple increment of damping ratio will not make sure the receptance to be suppressed in a maximal extent. Thus the recptance suppression work will involve an absorber parameter optimization procedure, through which the appropriate absorber could be chosen.

Considering the complex viscous damping absorber shown in Figure 7.2, its dynamic stiffness can be found in equation (7.26)

$$b_n(\omega) = \frac{-\omega^2 m_a [k_a + j\omega c_a (1 + j\gamma)]}{-\omega^2 m_a + [k_a + j\omega c_a (1 + j\gamma)]} \tag{8.27}$$

in which, m_a, k_a and c_a are absorber's mass, spring stiffness and viscous damping coefficient respectively. γ is the factor of complex damping. Similar to the work in Chapter 7, the sign function sgn is not included in the equation (8.27) since this problem is studied in the positive frequency range and then only positive values of

$\mathrm{Im}(\lambda)$ are considered. In this case, $\mathrm{sgn}(\omega) = 1$.

In order to present the optimized parameters clearly, three factors were introduced listed as below:

$$u = \frac{m_a}{m_n}, \quad (0 < u \le 0.25) \tag{8.28}$$

$$\beta = \frac{\omega_a}{\omega_p}, \quad (0 < \beta \le 2) \tag{8.29}$$

$$\zeta_r = \frac{c_a}{2\omega_p m_a}, \quad (0 \le \zeta < 1) \tag{8.30}$$

where, $\omega_a = \sqrt{\frac{k_a}{m_a}}$ is the natural frequency of the absorber without complex damping, ω_p is the pth natural frequency of original system. m_n is the mass of component at the degree of freedom where the absorber is attached. ζ_r is the related absorber viscous damping ratio. These three factors will provide us a more straightforward understanding about the absorber's parameters. It should be noticed that these factors also generally have their engineering application ranges shown in the equations (8.28), (8.29) and (8.30). Thus, the selection of the absorber parameters will be a constraint optimization procedure. For the sake of simplicity, in this work we set the complex viscous damping factor γ to be a constant.

From the equation (8.24), we can calculate the new modal receptance of the modified system. And at last we can chose one set of absorber parameters, which will make the desired new modal receptance of the modified system to have the minimal value or satisfy some requests. Here for example, we considered the least square criterion.

$$F = \min \sum_{\omega} \frac{1}{2} |\widetilde{R}_{ii}(\omega)|^2 \tag{8.31}$$

It's obvious that the other method such as min-max can be applied in the different cases as well.

Since the optimization calculation is nonlinear the different initial parameters will cause a different optimization results. Thus an iterative procedure is used to obtain the final convergent optimal parameters. In this procedure, the calculated results in the

before step will be used as the initial parameters for the next iteration step. The optimization procedure can be demonstrated in Figure 8.3.

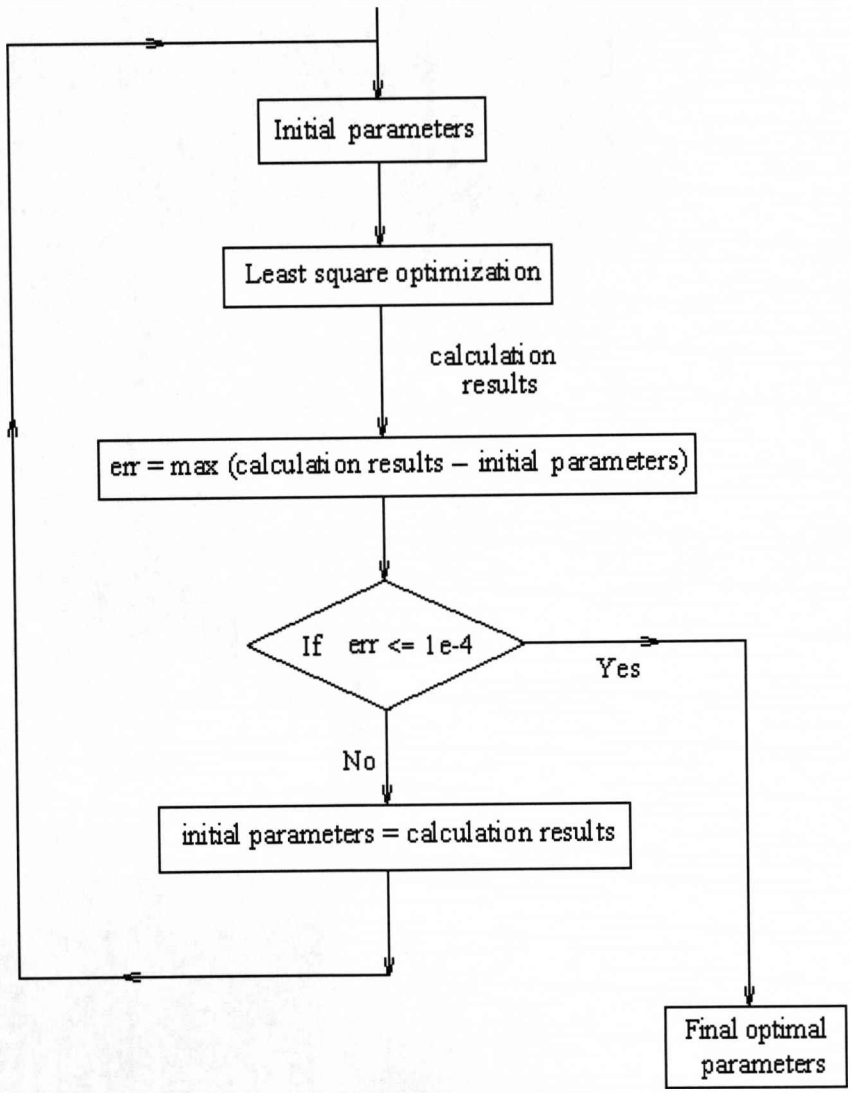

Figure 8.3 The iteration computation flow diagram

8.3 Numerical example

In order to demonstrate the theory discussed on above, we consider a five degree of freedom in-line mass-spring system shown in Figure 8.4. Its characteristics are listed

in Table 8-1.

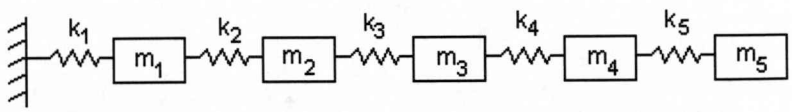

Figure 8.4 Original five DOF in-line system

Table 8-1 Original five degree of freedom system

Mass (kg)	Spring Stiffness (N/m)	Natural Frequency (rad/s)
$m1 = 0.1$	$k1 = 500$	$\omega 1 = 15.037$
$m2 = 0.1$	$k2 = 300$	$\omega 2 = 62.052$
$m3 = 0.1$	$k3 = 600$	$\omega 3 = 91.667$
$m4 = 0.2$	$k4 = 800$	$\omega 4 = 109.433$
$m5 = 0.2$	$k5 = 1000$	$\omega 5 = 143.336$

In this example, we think about the problem for the suppression of the receptance at the second natural frequency by using a complex viscous damping absorber attached to the mass m_5. In addition, we set the imaginary factor of the complex viscous damping is $\gamma = -0.25$.

After computation, we obtained the optimal factors as $u = 0.25$, $\beta = 0.9075$, and $\zeta_r = 0.1102$. Because the absorber would be attached on the mass *m4* and the second model suppression was considered, we can get that $m_n = m_5 = 0.2kg$, $\omega_p = \omega_2 = 62.052 rad/s$. So, the optimum absorber was selected as $m_a = 0.05\text{kg}$, $k_a = 158.5511$ N/m, and $c_a = 0.6838$ Ns/m. Figure 8.5 shows the modal receptance of the original system corresponding to the second natural frequency (dash line) and the new modal receptance of the modified system for the second natural frequency (solid line). It is found that when this optimised absorber was considered, the new modal receptance with respect to the second natural frequency is strongly suppressed.

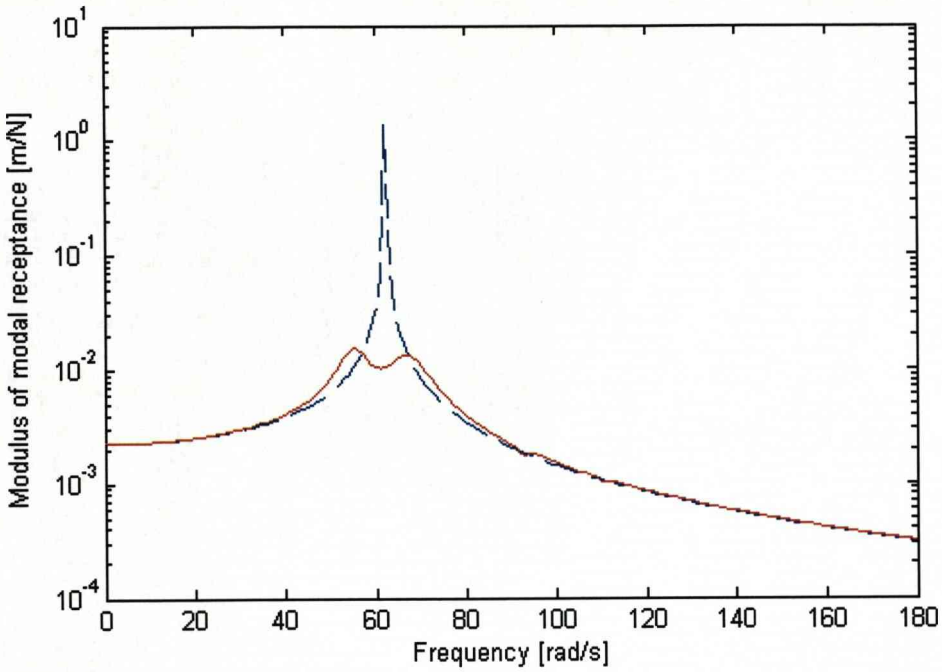

Figure 8.5 modal receptances for original and new modal receptance of the modified system

And then, Figure 8.6 illustrates receptances $h_{1,2}$, $h_{1,3}$, $h_{2,5}$ and $h_{5,5}$ for both original system and modified system. In these figures, the dash line presents the receptance of the original system and the solid line presents the receptance of the modified system.

It can be seen that all receptances corresponding to the second natural frequency are suppressed. So, the selected absorber provides the desired vibration suppression for original system.

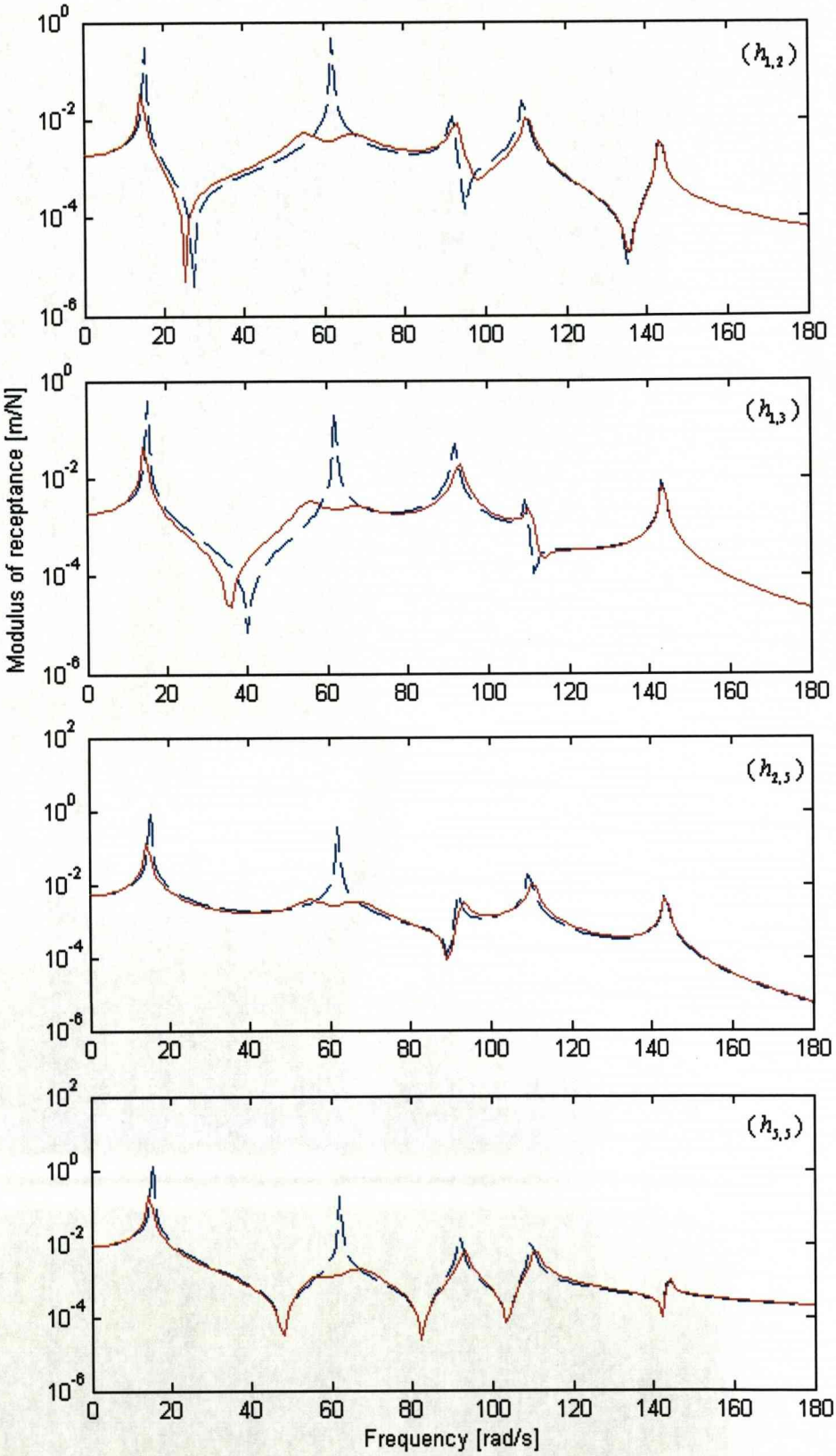

Figure 8.6 Receptances of original and modified system

8.4 Closure

Unlike the receptance, which shows the relation between the displacement in physical coordinate and the force in physical coordinate, the modal receptance presents the relation between the modal displacement and the modal force. The modal receptance is a two poles function and the positive pole happens at the corresponding natural frequency. The modal receptance is independent to each other since the modal receptance matrix is a diagonal matrix. If the *j*th modal receptance is suppressed successfully the the receptance at the *j*th natural frequency will be suppressed.

However, it is not straightforward to measure the changes of the modal receptance between the original system and modified system because the modified eigenvector calculation is involved. Thus, a new modal receptance concept of the modified system is proposed in order to avoid this shortcoming.

The work in this chapter obtains the new modal receptance of the modified system for the one absorber modification. In this case the new modal receptance of the modified system can be gotten through the dynamical parameters of the original system and the absorber parameters directly. In addition, it can also be thought as independent to each other because the new modal receptance matrix is approximately diagonal.

If we want to suppress the receptance of a dynamic system by using an appropriate complex viscous damping absorber, the selection of absorber parameters will involve an optimization procedure. In order to suppress the receptance for one desired natural frequency, the new modal receptance of the modified system can be used as the optimization objective function since the receptance for the corresponding natural frequency is suppressed when the new modal receptance for one natural frequency is suppressed. The numerical example clearly demonstrates its feasibility.

Chapter 9

Concluding Remarks

9.1 Conclusions

The dynamic effects of the rare earth permanent magnets on the vibration of structures made of paramagnetic (or diamagnetic) conducting light materials shows both the resonance amplitude suppression and natural frequency changes. Professor Bruno A. D. Piombo and his colleagues firstly investigated this interesting phenomenon in the frequency domain. And then they proposed a complex valued viscous damping model to predict this particular phenomenon.

The real part of this damping model represents a viscous type damping effect while the imaginary part represents the dynamic stiffness effect. On the view point of energy, the complex viscous damping model demonstrates the damping mechanism that the energy lost per cycle of the system is proportional to frequency and the square of the amplitude that in the similar form of the pure viscous damping system. This means that the imaginary part of the complex viscous damping coefficient will not affect the energy dissipation form of the system. However on the other hand, this imaginary part factor will change the potential energy that is stored in the system. The advantage of this model is that it shows a good agreement for analytical system frequency response function with the experiment results.

However, the complex viscous damping model induces some mathematic confusion since a real valued velocity will cause a complex valued force through this model.

Another model, frequency-rate stiffness model can overcome this shortcoming but also has a restriction that this model can be only used in harmonic movement otherwise the frequency parameter in this model will become physically meaningless. In fact, these two models all should be expressed and understood in frequency domain.

In addition both the complex viscous damping model and the frequency-rate stiffness model give us a same understanding of the magnetic damping in the frequency domain. For the frequency response function, it can be clearly found that magnetic damping has the strong vibration amplitude suppression with the natural frequency shift. And the displacement Nyquist diagram of the system with magnetic damping illustrates an approximate circular arc starting from point (1, 0) to the original point (0, 0) in the clockwise direction.

The eigenvalues of the system with complex viscous damping are complex and in a conjugated couple form by introducing a sign function sgn with respect to the frequency into the imaginary part of the complex viscous damping coefficient. Thus the root locus of the system will become real axis symmetric in the complex plane and all roots are located in the negative real part area. In this case, the system will have conjugated complex eigenvalues couples and show dynamical stability.

The dynamic responses of the system with complex viscous damping, including impulse response, forced harmonic response, random vibration response are obtained in this work. In particular the complex viscous damping presents a noncausal characteristic, which means the response prior to the excitation.

In order to calculate the time history response of the system with the complex viscous damped, an iterative computation method by using Hilbert transform is considered. This method can be applied in both linear and nonlinear problems but the convergent condition is required. For linear system, the responses obtained through this iterative technique are identical to those results calculated by using traditional FFT method.

It should be noted that the complex magnetic damping model must be defined in the frequency domain or limited to the transient work to periodic harmonic input forcing

functions. The technique discussed in this work provides a mathematical method that is used to calculate the arbitrary response of the system. This method can obtain reasonable response result although non-causal exists.

The complex viscous damping also demonstrates its extensive application capabilities in structural modification. We have analyzed the changes of eigenvalues and eigenvectors caused by local complex viscous damping modification. The new characteristic equation may be rewritten from the original eigenvalue and eigenvector. And this equation can be easily solved through some numerical methods. Additionally the sensitivities of eigenvalues and eigenvectors with respect to damping variables are also investigated.

The analyses on the inverse problem of structural modification with a complex viscous damping and a spring illustrate their effect to assign the desired natural frequency, antiresonance and receptance. By selecting appropriate damping and spring parameters, those pre-described dynamic properties may be assigned exactly. In particular this modification will not induce any mass change to the original system.

Besides, as illustrated in work an absorber with complex viscous damping can suppress the frequency response function of a vibration system effectively.

9.2 Suggestions for future work

Most works in the thesis are limited to positive-definite and non-defective system, which means the eigenvalues of the system are assumed to be distinct. Thus the analyses about the dynamic characteristics of a defective system with complex viscous damping are expected in the further works.

Besides only one absorber modification case is considered in this thesis for the application of magnetic damping in the structural modification and vibration suppression. More works are needed to study the structural modification effect of two or more absorbers with complex viscous damping. Additionally the work can be expanded to the nonlinear systems.

The vibration suppression by using magnetic damping will involve an optimisation procedure. And more studies need to be carried out to optimise the number, size and location of the magnets on the structures.

The works presented in this thesis are mainly focused on the theoretical analyses on the dynamic characteristics of complex viscous damping and its applications. Thus more experimental works are needed to be conducted to verify the analytical results of the magnetic damping such as the modal test, structural modification effect test and vibration suppression effect verification. Additionally, the developed numerical method needs to be tested to predict the time history response of the system with the magnetic damping.

More analytical work can be carried out for the application of magnetic damping to the real-life structures such as satellite, antenna, airplane equipment, automotive application, manufacture tool, motion control equipments and measurement systems and so on. These works will involve some complicated finite element analyses and model updating work of the magnetic damping.

In the previous and current work, the magnetic damping is simulated by using complex viscous damping model since magnetic damping provides both viscous type damping effect and stiffness changes to the vibrating system. However it is well known that hysteretic damping also induces these two kinds of effects together because of its complex stiffness form. Thus an interesting question is that we can also try to develop a hysteretic damping model for the magnetic damping and compare the difference between these two damping models. Additionally the nonlinear model and the fractional derivative model of the magnetic damping are hoped to be developed.

Up to present, the research work mainly focuses on the passive control application of the magnetic damping. Although the passive control will not cause the instability of the original system, it will also limit the application range of the magnetic damping. On the other hand, one important characteristic of the magnetic damping is that it can be adjusted easily. So the magnetic damping presents an advantage in the active control as well. Thus, an extension work about the complex viscous damping model

can be concerned on its application on the active vibration control.

In the present program, two rare earth magnets are made in the form of bricks. And its effect to the translation movement is studied. But considering the dynamical effect to a rotation system caused by a couple of rare earth magnets tiles, a new mathematical model has to be re-investigated since the relation between the force and magnetic field is changed. And then further research on this new damping effect has to be undertaken in the future.

The change of physical properties of magnets will affect their damping capabilities to the vibrating system. Some researches on the dynamical characteristics of magnetic damping in different environments such as in high temperature or in different working medium may be carried out.

Bibliography

[1] P. Campbell, "Permanent magnet materials and their application", Cambridge University Press, (1994).

[2] M. Ruzzene, J. Oh and A. Baz, "Finite element modelling of magnetic constrained layer damping", *Journal of Sound and Vibration,* v.236, n.4, (2000), pp.657-682.

[3] B.A.D. Piombo, E. Bonisoli and M. Ruzzene, "A theoretical model of oscillations of paramagnetic or diamagnetic structures subject to passive magnetic elements", *Proceedings of ASME 2001 Design Engineering Technical Conference*, Pittsburgh, Pennsylvania, September 9-12, (2001).

[4] B.A.D. Piombo, E. Bonisoli and M. Ruzzene, "A comparison between the theoretical model and experimental outcomes of oscillations of para- and dia-magnetic structures subject to passive magnetic elements", *SPIE's 9th Annual International Symposium on Smart Structures and Materials*, San Diego, California, v.4697, March 17-21, (2002), pp.274-283.

[5] B.A.D. Piombo, S. Sorrentino and E. Bonisoli, "An experimental validation of complex damping and fractional derivative models on vibrating structures under magnetic effects", *International Conference on Structural Dynamics Modelling: Test, Analysis, Correlation and Validation*, Madeira, Portugal, June 3-5, (2002), pp.307-315.

[6] E. Bonisoli and J.E. Mottershead, "Complex-damped dynamic systems in the time and frequency domains", *Shock and Vibration*, Special Issue: Dedicated to Professor Bruno Piombo, v.11, n.3-4, (2004), pp.209-225.

[7] S.H. Crandall, "The role of damping in vibration theory", *Journal of Sound and Vibration*, v.11, n.1, (1970), pp.3-18.

[8] S.H. Crandall, "Dynamic response of systems with structural damping", *Air, Space and Instruments, Draper Anniversary Volume*, ed. by S.Lees, McGraw-Hill Book Co., New York, (1962), pp.183-193.

[9] D.I. Jones, "Handbook of viscoelastic vibration damping", John Wiley & Sons, Chichester, (2001).

[10] R.E.D. Bishop, "The treatment of damping forces in vibration theory", *Journal of the Royal Aeronautical Society*, v.59, (1955), pp.738-742.

[11] P. Lancaster, "Free vibration and hysteretic damping", *Journal of the Royal Aeronautical Society*, v.64, (1960), pp.229.

[12] T.K. Caughey and A. Vijayaraghavan, "Free and forced oscillations of a dynamic system with linear hysteretic damping (non-linear theory)", *International Journal of Non-Linear Mechanics*, v.5, n.3, (1970), pp.533-555.

[13] T.K. Caughey, "Vibration of dynamic systems with linear hysteretic damping (linear theory)", *Proceeding of the 4th U.S. National Congress of Applied Mechanics, ASME*, New York, (1962), pp.87-97.

[14] R.L. Bagley and P.J. Torvik, "Fractional calculus - a different approach to the analysis of viscoelastically damped structures", *AIAA Journal*, v.21, n.5, (1983), pp.741-748.

[15] M. Soula, T. Vinh and Y. Chevalier, "Transient responses of polymers and elastomers deduced from harmonic responses", *Journal of Sound and Vibrations*, v.205, n.2, (1997), pp.185-203.

[16] Y.A. Rossikhin and M.V. Shitikova, "Applications of fractional calculus to dynamic problems of linear and nonlinear hereditary mechanics of solids", *Applied Mechanical Review*, v.50, n.1, (1997), pp.15-67.

[17] H. Beyer and S. Kempfle, "Definition of physically consistent damping laws with fractional derivatives", *ZAMM-Zeitschrift fur Angewandte Mathematic and Mechanik*, v.75, n.8, (1995), pp.623-635.

[18] S. Kempfle, I. Schafer and H. Beyer, "Fractional calculus via functional calculus: theory and applications", *Nonlinear Dynamics*, v.29, (2002), pp.99-127.

[19] L. Gaul, S. Bohlen and S. Kempfle, "Transient and forced oscillations of systems with constant hysteretic damping", *Mechanics Research Communications*, v.12, n.4, (1985), pp.187-201.

[20] L. Gaul, "Structural damping in frequency and time domain", *Proceeding of the 7th International Modal Analysis Conference*, Las Vegas, (1989), pp.177-184.

[21] J. Woodhouse, "Linear damping models for structural vibration", *Journal of Sound and Vibration*, v.215, n.3, (1998), pp.547-569.

[22] H.C. Tsai and T.C. Lee, "Dynamic analysis of linear and bilinear oscillators with rate-independent damping", *Computers & Structures*, v.80, n.2, (2002), pp.155-164.

[23] A. Feriani and F. Perotti, "The formation of viscous damping matrices for the dynamic analysis of MDOF systems", *Earthquake Engineering and Structural Dynamics*, v.25, (1996), pp.689-709.

[24] D.C. Champeney, "A handbook of Fourier theorems", Cambridge University Press, Cambridge, (1989).

[25] A.D. Nashif, D.I.G. Jones and J.P. Henderson, "Vibration damping", John Wiley & Sons, New York, (1985).

[26] J.A. Inaudi and J.M. Kelly, "Linear hysteretic damping and the hilbert

transform", *Journal of Engineering Mechanics*, v.121, n.5, (1995), pp.626-632.

[27] J.A. Inaudi and N. Makris, "Time-domain analysis of linear hysteretic damping", *Earthquake Engineering and Structural Dynamics*, v.25, n.6, (1996), pp.529-545.

[28] N. Makris, "Time domain analysis of generalized viscoelastic models", *Soil Dynamics and Earthquake Engineering*, v.14, n.5, (1995), pp.375-386.

[29] N. Makris and J. Zhang, "Time-domain viscoelastic analysis of earth structures", *Earthquake Engineering and Structural Dynamics*, v.29, (2000), pp.745-768.

[30] J.T. Chen and D.W. You, "An integral-differential equation approach for the free vibration of a SDOF system with hysteretic damping", *Advances in Engineering Software*, v.30, n.1, (1999), pp.43-48.

[31] J.T. Chen and D.W. You, "Hysteretic damping revisited", *Advances in Engineering Software*, v.28, n.3, (1997), pp.165-171.

[32] H. Frahm, "Devices for Damping Vibration of Bodies", US Patent No. 989958, (1909).

[33] J. Ormondroyd and J.P. Den Hartog, "The theory of the dynamic vibration absorber", *Trans. ASME*, v.50, (1928), pp.9-15.

[34] J.P. Den Hartog, "Mechanical vibrations", 4th edition, McGraw-Hill, New York, (1956).

[35] D.J. Inman, "Engineering vibration", 2nd edition, Upper Saddle River, N.J. Prentice Hall, (2001).

[36] J.Q. Sun, M.R. Jolly and M.A. Norris, "Passive, adaptive, and active tuned

vibration absorbers: a survey", *Trans. ASME, Journal of Vibration and Acoustics*, v.117, (1995), pp.234-342.

[37] J.E. Mottershead and Y.M. Ram, "Inverse eigenvalue problems in vibration absorption: Passive modification and active control", *Mechanical Systems and Signal Processing*, v.20, (2006), pp.5-44.

[38] D.J. Ewins, "Modal Testing: Theory, Practice and Application", Research Studies Press, Letchworth, Hertfordshire, England, (1985).

[39] J.T. Weissenburger, "The effect of local modifications on the eigenvalues and eigenvectors of linear systems", PhD Thesis, Washington University, (1966).

[40] J. T. Weissenburger, "Effect of local modifications on the vibration characteristics of linear systems", *Trans. ASME, Journal of Applied Mechanics*, v.90, (1968), pp.327-332.

[41] R.J. Pomazal and V.W. Snyder, "Local modifications of damped linear systems", *AIAA Journal*, v.9, (1971), pp.2216-2222.

[42] E.H. Dowell, "On some general properties of combined dynamical systems", *Trans. ASME, Journal of Applied Mechanics*, v.46, (1979), pp.206-209.

[43] I. Bucher and S.G. Braun, "The structural modification inverse problem", *Mechanical Systems and Signal Processing*, v.7, (1993), pp.217-238.

[44] I. Bucher and S.G. Braun, "Left eigenvector extraction from measurements and physical interpretation", *Trans. ASME, Journal of Applied Mechanics*, v.64, (1996), pp.97-105.

[45] Y.M. Ram, S.G. Braun, "An inverse problem associated with modification of incomplete dynamic systems", *Trans. ASME, Journal of Applied Mechanics*, v.58, (1991), pp.233–237.

[46] Y.G. Tsuei and E.K.L. Yee, "A method for modifying dynamic properties of undamped mechanical systems", *Trans. ASME, Journal of Dynamics, System, Measurement, Control*, v.111, (1989), pp.403–408.

[47] E.K.L. Yee and Y.G. Tsuei, "Method for shifting natural frequencies of damped mechanical systems", *AIAA Journal*, v.29, (1991), pp.1973–1977.

[48] A. Kyprianou, J.E. Mottershead and H. Ouyang, "Assignment of natural frequencies by an added mass and one or more springs", *Mechanical Systems and Signal Processing*, v.18, n.2, (2004), pp.263-289.

[49] Y.M. Ram and S. Elhay, "The theory of a multi degree of freedom dynamic absorber", *Journal of Sound and Vibration*, v.195, (1996), pp.607-615.

[50] P.D. Cha and C. Pierre, "Imposing nodes to the normal modes of a linear elastic structure", *Journal of Sound and Vibration*, v.219, n.4, (1999), pp.669-687.

[51] J.E. Mottershead, A. Kyprianou and H. Ouyang, "Structural modification, part 1: rotational receptances", *Journal of Sound and Vibration*, v.284, n.1-2, (2005), pp.249-265.

[52] A. Kyprianou, J.E. Mottershead and H. Ouyang, "Structural modification, part 2: assignment of natural frequencies and antiresonances by an added beam", *Journal of Sound and Vibration*, v.284, n.1-2, (2005), pp.267-281.

[53] K.V. Singh and Y.M. Ram, "Dynamic absorption by passive and active control", *Trans. ASME, Journal of Vibration and Acoustics*, v.122, (2000), pp.429-433.

[54] W.J. Duncan, "The admittance method for obtaining natural frequencies of systems", *Philosophical Magazine*, v.32, (1941), pp.401-409.

[55] R.E.D. Bishop and D.C. Johnson, "The Mechanics of Vibration", Cambridge

University Press, (1960).

[56] Y.M. Ram, "Dynamic Structural Modification", *Sound Vibration Digest*, v.32, n.1, (2000), pp.11-18.

[57] A. Berman, "System identification of structural dynamic models – theoretical and practical bounds", *AIAA conference paper 84-0929*, (1984).

[58] A. Berman, "Limitations on the identification of discrete structural dynamic models", *2nd International Conference on Recent Advances in Structural Dynamics*, Southampton, (1984), pp.427-435.

[59] A.H. Vincent, "A note on the properties of the variation of structural response with respect to a single structural parameter when plotted in the complex plane", *Westland Helicopters Ltd, Report GEN/DYN/RES/010R*, (1973).

[60] G.T.S. Done and A.D. Hughes, "The response of a vibrating structure as a function of structural parameters", *Journal of Sound and Vibration*, v.38, n.2, (1975), pp.255-266.

[61] E.J. Nagy, "Vincent's circle as a tool for machine vibration optimisation techniques", *ASME paper 81-DET-78*.

[62] D.A. Rade and G. Lallement, "A strategy for the enrichment of experimental data as applied to an inverse eigensensitivity-based FE model updating method", *Mechanical Systems and Signal Processing*, v.12, (1998), pp.293-307.

[63] G. Lallement and S. Cogan, "Parametric identification based on pseudo tests", *NATO Advanced Study Institute*, Sesimbra, Portugal, (1998).

[64] N. Nalitolela, J.E.T. Penny and M.I. Friswell, "Updating model parameters by adding an imagined stiffness to the structure", *Mechanical Systems and Signal Processing*, v.7, n.2, (1993), pp.161-172.

[65] J.E. Mottershead, C. Mares and S. James, "Fictitious modifications for the separation of close modes", *Mechanical Systems and Signal Processing*, v.16, n.5, (2002), pp.741-755.

[66] J.E. Mottershead, C. Mares and M.I. Friswell, "An inverse method for the assignment of vibration nodes", *Mechanical Systems and Signal Processing*, v.15, n.1, (2001), pp.87-100.

[67] J.E. Mottershead and G. Lallement, "Vibration nodes, and the cancellation of poles and zeros by unit rank modifications to structures", *Journal of Sound and Vibration*, v.222, n.5, (1999), pp.833-851.

[68] T. Li, J. He and M. Sek, "Local and global pole-zero cancellation of mass-spring systems", *Mechanical Systems and Signal Processing*, v.15, n.1, (2001), pp.121-127.

[69] Y.Q. Li, J. He and G. Lleonart, "Relocation of resonances and antiresonances via local structural modifications", *Proceeding of Asia-Pacific Conference*, Kitakyushu, (1993), pp.1300-1306.

[70] J.E. Mottershead, "Structural modification for the assignment of zeros using measured receptances", *Trans. ASME, Journal of Applied Mechanics*, v.68, n.5, (2001), pp.791-798.

[71] J.E. Mottershead, "On the zeros of structural frequency response functions and their sensitivities", *Mechanical Systems and Signal Processing*, v.12, n.5, (1998), pp.591-597.

[72] J.E. Mottershead, "Complex and defective zeros in cross receptances", *Journal of Sound and Vibration*, v.246, n.1, (2001), pp.190-197.

[73] R.L. Fox and M.P. Kapoor, "Rates of change of eigenvalues and eigenvectors", *AIAA Journal*, v.6, (1968), pp.2426-2429.

[74] L.C. Rogers, " Derivatives of eigenvalues and eigenvectors", *AIAA Journal*, v.8, n.5, (1970), pp.943-944.

[75] S. Garg, "Derivatives of eigensolution for general matrix", *AIAA Journal*, v.11, n.8, (1973), pp.1191-1194,

[76] R.B. Nelson, "Simplified calculation of eigenvector derivatives", *AIAA Journal*, v.14, n.9, (1976), pp.1201-1205.

[77] M. Yoshimura, "Design sensitivity analysis of frequency response in machine structures", *Journal of Mechanisms, Transmissions, and automation in Design*, v.106, (1984), pp.119-125.

[78] M. Yoshimura, "Application of design sensitivity analysis for greater improvement on machine structural dynamics ", *NASA. Langley Research Center Sensitivity Analysis in Engineering*, (N87-18855 11-39), (1987), pp.285-298.

[79] R.M. Lin and D.J. Ewins, "analytical model improvement using frequency response functions", *Mechanical Systems and Signal Processing*, v.8, (1994), pp.437-458.

[80] J.A. Brandon, "Derivation and significance of second order modal design sensitivities", *AIAA Journal*, v.22, (1984), pp.723-724.

[81] J.A. Brandon, "Second-order design sensitivities to assess the applicability of sensitivity analysis", *AIAA Journal*, v.29, n.1, (1991), pp.135-139.

[82] J.A. Brandon, "Eliminating indirect analysis - the potential for recepance sensitivities", *International Journal of Analytical and Experimental Modal Analysis*, v.2, (1987), pp.73-75.

[83] J.A. Brandon, "Strategies for structural dynamic modification", Research

Studies Press Ltd., England, (1990).

[84] T.Y. Chen, "Optimum design of structures with both natural frequency and frequency response constraints", *International Journal For Numerical Methods in Engineering*, v.33, (1992), pp.1927-1940.

[85] I. kajiwara and A.Nagamatsu, "Optimum design of optical pick-up by elimination of resonance peaks", *Trans. ASME, Journal of Vibration and Acoustics*, v.115, (1993), pp.377-383.

[86] K.B. Lim, J.L. Junkins and B.P. Wang, "Re-examination of eigenvector derivatives", *AIAA Journal*, v.25, (1987), pp.581-587.

[87] R.M. Lin, M.K. Lim and H. Du, "Improved inverse eigensensitivity method for structural analytical model updating", *Journal of Vibration and Acoustics*, v.17, (1995), pp.192-198.

[88] R.M. Lin and M.K. Lim, "Derivation of structural design sensitivities from vibration test data", *Journal of Sound and Vibration*, v.201, n.5, (1997), pp.613-631.

[89] B.G. Korenev, "Dynamic vibration absorbers: theory and technical applications", Chichester [England], New York, Wiley, (1993).

[90] L. Kitis, B.P. Wang and W.D. Pilkey, "Vibration reduction over a frequency range", *Journal of Sound and Vibration*, v.89, n.4, (1983), pp.559-569.

[91] L. Kitis, W.D. Pilkey and B.P. Wang, "Optimal frequency response shaping by appendant structures", *Journal of Sound and Vibration*, v.95, n.2, (1984), pp.161-175.

[92] M. Jorkama and R.V. Hertzen, "Optimal dynamic absorber for a rotating rayleigh beam", *Journal of Sound and Vibration*, v.217, n.4, (1998), pp.653-664.

[93] J.H. Koo, M. Setareh and T.M. Murrray, "In search of suitable control methods for semi-active tuned vibration absorber", *Journal of Vibration and Control*, v.10, (2004), pp.163-174.

[94] A.F. Vakakis and S.A. Paipetis, "The effect of a viscously damped dynamic absorber on a linear multi-degree-of-freedom system", *Journal of Sound and Vibration*, v.105, n.1, (1986), pp.49-60.

[95] A. Soom and M.S. Lee, "Optimal design of linear and nonlinear vibration absorbers for damped systems", *Trans. ASME, Journal of Vibration, Acoustics, Stress and Reliability*, v.105, (1983), pp.112-119.

[96] J. Ro and A. Baz, "Optimal placement and control of active constrained layer damping using modal strain energy approach", *Journal of Vibration and Control*, v.8, (2002), pp.861-876.

[97] Y.M. Huang and C.R. Fuller, "Vibration and noise control of the fuselage via dynamic absorbers", *Trans. ASME, Journal of vibration and acoustics*, v.120, (1998), pp.496-502.

[98] Y.M. Huang and C.C. Chen, "Optimal design of dynamic absorbers on vibration and noise control of the fuselage", *Computers and Structures*, v.76, (2000), pp.691-702.

[99] A.G. Thompson, "The effect of tyre damping on the performance of vibration absorbers in an active suspension", *Journal of Sound and Vibration*, v.133, n.3, (1989), pp.457-465.

[100] R.G. Jacquot, "Suppression of random vibration in plates using vibration absorbers", *Journal of Sound and Vibration*, v.248, n.4, (2001), pp.585-596.

[101] R.G. Jacquot, "The spatial average mean square motion as an objective function for optimising damping in damped modified system", *Journal of*

Sound and Vibration, v.259, n.4, (2003), pp.955-965.

[102] K. Nagaya, A. Kurusu, S. Ikai and Y. Shitani, "Vibration control of a structure by using a tunable absorber and an optimal vibration absorber under auto-tuning control", *Journal of Sound and Vibration*, v.228, n.4, (1999), pp.773-792.

[103] C.Y. Lai and W.H. Liao, "Vibration control of a suspension system via a magnetorheological fluid damper", *Journal of Vibration and Control*, v.8, (2002), pp.527-547.

[104] L. Zuo and S.A. Nayfeh, "Minimax optimisation of multi-degree-of-freedom tuned mass damper", *Journal of Sound and Vibration*, v.272, (2004), pp.893-908.

[105] D.J. Stech, "An H2 approach for optimally tuning passive vibration absorbers to flexible structures", *Journal of Guidance, Control and Dynamics*, v.17, (1994), pp.636-638.

[106] Y. Arfiadi and M. Hadi, "Passive and active control of the three-dimensional buildings", *Earthquake Engineering and Structural Dynamics*, v.29, (2000), pp.377-396.

[107] V. Steffen Jr, D.A. Rade and D.J. Inman, "Using passive techniques for vibration damping in mechanical systems", *Journal of the Brazilian Society of Mechanical Sciences*, v.22, n.3, Rio de Janeiro, (2000).

[108] K. Nagaya and L. Li, "Control of sound noise radiated from a plate using dynamic absorbers under the optimisation by neural network", *Journal of Sound and Vibration*, v.208, n.2, (1997), pp.289-298.

[109] J. Zhu, A. Kyprianou and J.E. Mottershead, "An inverse method to assign receptances by using classical vibration absorbers", *Journal of Vibration and Control*, Submitted.

[110] E. Bonisoli and A. Vigliani, "Passive effects of rare-earth permanent magnets on flexible conductive structures", *Mechanics Research Communications*, v.33, (2006), pp.302-319.

[111] E. Bonisoli and A. Vigliani, "Identification techniques applied to a passive elasto-magnetic suspension", *Mechanical Systems and Signal Processing*, v.21, (2007), pp.1479-1488.

[112] L. Cremer and M. Heckl, "Structure-Borne Sound", Springer-Verlag, New York, (1988).

[113] C. Wang, Y. Yao, Y. Chang, P. Tung and R. Xiao, "Magnetic force-induced damping effect for magnetic bearing motor", *Journal of Applied Physics*, v.97, (2005), (10Q502), pp.1-3.

[114] H. Sodano, J. Bae, D. Inman and W. Belvin, "Improved concept and model of eddy current damper", *Transactions of the ASME*, v.128, (2006), pp.294-302.

[115] J. Kim and S. Lee, "Dynamic characteristics of a flywheel energy storage system using superconducting magnetic bearings", *Superconductor Science and Technology*, v.16, (2003), pp.473-478.

[116] C. Johnson, D. Keinholz, "Finite element prediction of damping in structures with constrained viscoelastic layers", *AIAA Journal*, v.20, n.9, (1982), pp.1284-1290.

[117] C. Saravanan, N. Ganesan, V. Ramamurti, "Vibration and damping analysis of multilayered fluid filled cylindrical shells with constrained viscoelastic damping using modal strain energy method", *Computers and Structures*, v.75, (2000), pp.395-417.

[118] C.L. Davis and G. A. Lesieutre, "A modal strain energy approach to the prediction of resistively shunted piezoceramic damping", *Journal of Sound*

and Vibration, v.184, n.1, (1995), pp.129-139.

[119] F.P. Landi, F. Scarpa, J. Rongong and G. Tomlinson, "Improving the MSE method using a dyadic matrix perturbation approach", *IMechE Journal of Mechanical Engineering Science*, v.216, n.12, (2002), pp.1207-1216.

[120] L. Gaul, "The influence of damping on waves and vibrations", *Mechanical Systems and Signal Processing*, v.13, n.1, (1999), pp.1-30.

[121] R.L. Bagley and P.J. Torvik, "Fractional derivatives in the description of damping materials and phenomena", *ASME DE-5: The role of damping in Vibration and Noise Control*, (1987), pp.125-135.

[122] M. Seredynska and A. Hanyga, "Nonlinear Hamiltonian equations with fractional damping", *Journal of Mathematical Physics*, v.41, n.4, (2000), pp.2135-2156.

[123] M. Caputo, "Linear models of dissipation whose Q is almost frequency independent-II", *Goephys. J. R. atr. Soc.*, v.13, (1967), pp.529-539.

[124] S.G. Samko, A.A. Kilbas and O.I. Marichev, "Fractional integrals and derivatives: theory and applications", Gordon and Breach Science Publishers, (1987).

[125] K. Diethelm, "An algorithm for the numerical solution of differential equations of fractional order", *Electronic Transactions on Numerical Analysis*, v.5, (1997), pp.1-6.

[126] M. Caputo and F. Mainardi, "A new dissipation model based on memory mechanism", *Pure and Applied Geophysics*, v.91, n.1, (1971), pp.134-147.

[127] G. Arfken, "Cauchy's Integral Formula" §6.4 in *Mathematical Methods for Physicists, 3rd ed.* Orlando, FL: Academic Press, (1985), pp. 371-376.

Appendix A - The proof of equation $(I_{CR1}+I_{CR2})=0$ for the infinite R

Considering the integral along the semicircle route $I_{CR1}+I_{CR2}$, where $s=Re^{j\varphi}$, $(\pi/2\le\varphi\le 3\pi/2)$, it leads to

$$I_{CR1}+I_{CR2}=\int_{\pi/2}^{\pi}\frac{e^{Rt\cos\varphi}e^{jRt\sin\varphi}}{\omega_n{}^2+2\zeta_m\omega_n Re^{j\varphi}\dfrac{1+j\,\mathrm{sgn}[\mathrm{Im}(s)]\psi}{\sqrt{1+\psi^2}}+R^2e^{j2\varphi}}jRe^{j\varphi}d\varphi$$

$$+\int_{\pi}^{3\pi/2}\frac{e^{Rt\cos\varphi}e^{jRt\sin\varphi}}{\omega_n{}^2+2\zeta_m\omega_n Re^{j\varphi}\dfrac{1+j\,\mathrm{sgn}[\mathrm{Im}(s)]\psi}{\sqrt{1+\psi^2}}+R^2e^{j2\varphi}}jRe^{j\varphi}d\varphi \qquad (A.1)$$

If we set the function

$$F(Re^{j\varphi})=\frac{1}{\omega_n{}^2+2\zeta_m\omega_n Re^{j\varphi}\dfrac{1+j\,\mathrm{sgn}[\mathrm{Im}(s)]\psi}{\sqrt{1+\psi^2}}+R^2e^{j2\varphi}} \qquad (A.2)$$

It is clear that $\lim_{R\to\infty}\left|F(Re^{j\varphi})\right|=0$ because the order of magnitude $\vartheta\left(\frac{1}{1+R+R^2}\right)\to 0$ when $R\to\infty$.

Thus, we rewrite the integration (A.1) into

$$I_R=I_{CR1}+I_{CR2}=\int_{\pi/2}^{3\pi/2}F(Re^{j\varphi})e^{Rt\cos\varphi}e^{jRt\sin\varphi}jRe^{j\varphi}d\varphi \qquad (A.3)$$

Then

$$|I_R|\le R\int_{\pi/2}^{3\pi/2}|F(Re^{j\varphi})||e^{Rt\cos\varphi}||e^{jRt\sin\varphi}||j||e^{j\varphi}|d\varphi$$

$$\le R\int_{\pi/2}^{3\pi/2}|F(Re^{j\varphi})|e^{Rt\cos\varphi}d\varphi \qquad (A.4)$$

Because

$$|e^{jRt\sin\varphi}|\le 1 \quad \text{for} \quad e^{jRt\sin\varphi}=\sin[Rt\sin(\varphi)] \qquad (A.5)$$

$$|e^{j\varphi}| \le 1 \quad \text{for} \quad e^{j\varphi} = \sin\varphi \tag{A.6}$$

$$\text{And} \quad |j| = 1 \tag{A.7}$$

Now we choose a small ε so that $\lim_{R\to\infty}\left|F(Re^{j\varphi})\right| \le \varepsilon \to 0$ for the reason of $\lim_{R\to\infty}\left|F(Re^{j\varphi})\right| = 0$. So,

$$|I_R| \le R\varepsilon \int_{\pi/2}^{3\pi/2} e^{Rt\cos\varphi} d\varphi = 2R\varepsilon \int_{\pi/2}^{\pi} e^{Rt\cos\varphi} d\varphi \tag{A.8}$$

If we analyze the function $\cos\varphi$, it can be found that

$$\cos\varphi \le -\frac{2}{\pi}\varphi + 1 \quad \text{for} \quad \pi/2 \le \varphi \le \pi \tag{A.9}$$

Then

$$|I_R| \le 2R\varepsilon \int_{\pi/2}^{\pi} e^{Rt(-2\varphi/\pi+1)} d\varphi$$

$$= 2R\varepsilon \frac{\pi}{2Rt}(1 - e^{-Rt}) = \frac{\pi}{t}\varepsilon(1 - e^{-Rt}) \tag{A.10}$$

Hence, it can be obtained

$$\lim_{R\to\infty} |I_R| \le \frac{\pi}{t} \lim_{R\to\infty} \varepsilon = 0 \tag{A.11}$$

Noticed here, $e^{-Rt}|_{R\to\infty} = 0$

Thus, we have proved that integration $(I_{CR1} + I_{CR2}) = 0$ for the infinite R.

Appendix B - Paper submitted to the *Journal of Vibration and Control*

An Inverse Method to Assign Receptances by Using Classical Vibration Absorbers

Jianfeng Zhu[1], Andreas Kyprianou[2] and John E Mottershead[1]

[1]Department of Engineering, University of Liverpool,
Liverpool L69 3GH, UK
[2] Mechanical and Manufacturing Engineering Dept. University of Cyprus
75 Kallipoleos, PO 20537, 1678 Nicosia, Cyprus

E_mail: j.e.mottershead@liverpool.ac.uk

Abstract

The classical mass-spring absorber can be thought as a very simple structural modification. In this paper the inverse problem of assigning receptances to a dynamic system by using one or more simple mass-spring absorbers is considered. The absorber parameters can be determined using selected receptances from the original system. When more than one absorber is applied, the equations that determine the modified-system receptances may be rearranged to form a set of nonlinear algebraic equations, multivatiate polynomials in the absorber parameters. The desired absorber parameters are determined by the roots of these equations, which may be found by Newton's method or by using Groebner bases. Realistic solutions require that positive values be found for the mass and stiffness of each of the added absorbers. Consequently there may be no acceptable solution, a unique solution or there may be finitely many acceptable solutions. Whenever two receptances are to be assigned at a single frequency by a single absorber, then the available absorber mass and stiffness values are severely restricted. However, arbitrary assignment is possible for many other problems, except for the condition of positiveness on the masses and stiffnesses.

1. Introduction.

The earliest application of structural modification is possibly Frahm's [1] classical vibration absorber, first described in the open literature by Ormondroyd and Den Hartog [2]. Sun *et al.* [3] give a thorough survey of modern absorber developments.

Duncan [4] was the first to develop and use the *forward* structural-modification problem by finding the dynamics of a compound system using vibration measurements from the separate components. Bishop and Johnson [5] described the receptance approach to dynamic-system modeling. Modern applications include the use of fictitious masses for the separation of close modes in aero-engine casings [6] and predicting the dynamics of a helicopter tail cone when modified by a large overhanging mass [7].

The *inverse* problem is to determine the structural modification that will assign some desired dynamical properties. For example, the mass-spring absorber may be used for the assignment of an antiresonance, but as explained in this paper has further possibilities, especially when a number of absorbers are used together. The general inverse structural modification problem was first considered by Weissenburger [8] and Pomazal and Snyder [9].

Bucher and Braun [10] assigned vibration mode shapes by extracting the left eigenvectors from the measured receptance data. They developed a theory to show how the necessary mass and stiffness modifications can be computed using modal test results only, even when only a partial set of eigensolutions is available from such tests. Mottershead, Mares and Friswell [11] used an inverse method to assign natural frequencies and nodes of vibration by the addition of grounded springs and concentrated masses. The method is based only upon measured receptances at the nodal and modification coordinates. Mottershead [12] investigated zero assignments in point and cross receptances by passive stiffness, damping, and mass modifications. The adjoint system was used in determining the modifications.

Mottershead and Lallement [13] showed how to cancel poles with zeros and create a vibration node of an undamped structure, which could be shifted by a unit-rank modification. T.Li, J.He and M. Sek [14] also presented the cancellation of poles and zeros of an undamped dynamic system by using the linear modification method. The cancellation can be achieved either for a single-frequency response function or for all frequency response functions of the system. Ram and his colleagues considered the pole/zero assignment problem in classical rods and beams [15-16] and extended their work to the multi degree of freedom vibration absorber [17]. Mottershead [18] considered the sensitivity of the zeros to parametric changes.

Kyprianou, Mottershead and Ouyang [19] demonstrated the assignment of natural frequencies and antiresonances by the added mass connected by one or more springs. The added mass and stiffnesses are determined using receptances from the original system. And realistic modifications should be bounded within certain frequency ranges. They also discussed the effect of the modification on the natural frequencies not assigned and on the antiresonances. Lawther [20] evacuated the natural frequencies from a chosen frequency range by means of a brace modification - a linear spring connected between two coordinates. Recent practical research includes the indirect measurement of rotational receptances to couple a physical structure to the rotational degrees of freedom of a finite element beam model used to assign natural frequencies and antiresonances [21-22]. Further and more detailed discussion on measuring rotational receptances may be found in [7]. Mottershead and Y.M.Ram [23] reviewed the inverse eigenvalue problem as it relates to vibration absorption in elasto-mechanical systems. Their study included both passive modification and active

control.

In the present paper the inverse problem of assigning receptance terms to particular values at chosen frequencies by using multiple classical undamped vibration absorbers is considered. The modified receptance equation involves to an inversion of the receptance matrix [24-25]. The method proposed in this paper avoids this inversion and results in a nonlinear algebraic modification equation in the absorber parameters. Such equations may be solved numerically using Newton's method, or by using symbolic code based for example upon Grobner bases [19]. In general, realistic solutions, having positive absorber mass and stiffness parameters, are selected from the roots of a system of multivariate polynomials.

2. Dynamic stiffness of the modified system

The undamped dynamic equation of motion may be written as,

$$\mathbf{M}\ddot{\mathbf{x}} + \mathbf{K}\mathbf{x} = \mathbf{f} \tag{1}$$

Where $\mathbf{x}$ is the displacement vector, $\mathbf{M}$, $\mathbf{K}$ and $\mathbf{f}$ are the mass matrix, stiffness matrix and external force vector respectively.

Equation (1) may be expressed in full in the frequency domain, $\mathbf{x} = \mathbf{X}e^{i\omega t}$, as,

$$\begin{bmatrix} k_{11}-\omega^2 m_{11} & k_{12}-\omega^2 m_{12} & \cdots & k_{1n}-\omega^2 m_{1n} \\ k_{21}-\omega^2 m_{21} & k_{22}-\omega^2 m_{22} & \cdots & k_{2n}-\omega^2 m_{2n} \\ & & \ddots & \\ k_{n1}-\omega^2 m_{n1} & k_{n2}-\omega^2 m_{n2} & \cdots & k_{nn}-\omega^2 m_{nn} \end{bmatrix} \begin{bmatrix} X_1(\omega) \\ X_2(\omega) \\ \vdots \\ X_n(\omega) \end{bmatrix} = \begin{bmatrix} f_1(\omega) \\ f_2(\omega) \\ \vdots \\ f_n(\omega) \end{bmatrix} \tag{2}$$

When a mass, a grounded spring or an undamped mass-spring absorber is attached to the nth coordinate, as illustrated in Figure 1, then a modified equation of motion may be written without the need for an additional coordinate in the form,

$$\begin{bmatrix} k_{11}-\omega^2 m_{11} & k_{12}-\omega^2 m_{12} & \cdots & k_{1n}-\omega^2 m_{1n} \\ k_{21}-\omega^2 m_{21} & k_{22}-\omega^2 m_{22} & \cdots & k_{2n}-\omega^2 m_{2n} \\ & & \ddots & \\ k_{n1}-\omega^2 m_{n1} & k_{n2}-\omega^2 m_{n2} & \cdots & k_{nn}-\omega^2 m_{nn} \end{bmatrix} \begin{bmatrix} \overline{X}_1(\omega) \\ \overline{X}_2(\omega) \\ \vdots \\ \overline{X}_n(\omega) \end{bmatrix}$$

$$= \begin{bmatrix} f_1(\omega) \\ f_2(\omega) \\ \vdots \\ f_n(\omega) \end{bmatrix} - \begin{bmatrix} 0 & 0 & \cdots & 0 \\ 0 & 0 & \cdots & 0 \\ & & \ddots & \\ 0 & 0 & \cdots & b_n(\omega) \end{bmatrix} \begin{bmatrix} \overline{X}_1(\omega) \\ \overline{X}_2(\omega) \\ \vdots \\ \overline{X}_n(\omega) \end{bmatrix} \tag{3}$$

Where $b_n(\omega)$ is the dynamic stiffness of the added term. In the case of an absorber this term may be written as [22],

$$b_n(\omega) = \frac{-\omega^2 m_a k_a}{-\omega^2 m_a + k_a} \tag{4}$$

In which, m_a and k_a are absorber mass and spring stiffness coefficients.

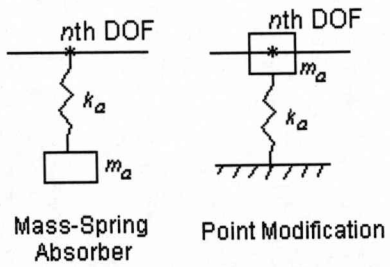

Figure 1. Modified system with absorber

The above analysis is applicable also to the mass-spring point modification. In this case, the dynamic stiffness $b_n(\omega)$ should be written as,

$$b_n(\omega) = -\omega^2 m_a + k_a \tag{5}$$

It can be noticed that the matrix of absorber dynamic stiffness may be written, for the case of a single absorber at coordinate n as,

$$\mathbf{\Delta B} = \begin{bmatrix} 0 & 0 & \cdots & 0 \\ 0 & 0 & \cdots & 0 \\ \vdots & \vdots & \ddots & \vdots \\ 0 & 0 & \cdots & b_n \end{bmatrix} \tag{6}$$

and in general as a diagonal matrix with non-zero terms at the absorber attachment coordinates,

$$\mathbf{\Delta B} = \begin{bmatrix} b_1 & & & & \\ & 0 & & & \\ & & \ddots & & \\ & & & b_r & \\ & & & & \ddots \end{bmatrix} \tag{7}$$

3. Modified-system receptance

The dynamic equation for the modified system, given by equation (3), may be re-written in compact form,

$$\mathbf{B}\overline{\mathbf{X}} = \mathbf{f} - \mathbf{\Delta B}\overline{\mathbf{X}} \tag{8}$$

In which, $\mathbf{B} = -\omega^2\mathbf{M} + \mathbf{K}$ for original system, and $\overline{\mathbf{X}}$ is the modified system displacement vector. Thus, the modified receptance can be expressed as

$$\overline{\mathbf{H}} = \left(\mathbf{I} + \mathbf{H}\Delta\mathbf{B}\right)^{-1}\mathbf{H} \tag{9}$$

Where, $\mathbf{H} = \mathbf{B}^{-1}$ is the receptance matrix of the original system.

If $r \le n$ absorbers are considered, let A be the integer set denoting the attachment coordinates.

$A = \{a_i : i = 1,2,...,r\}$

Thus, since only selected diagonal elements of the modified matrix are non-zero, $\mathbf{\Delta B}$ may be rewritten as

$$\mathbf{\Delta B} = \mathbf{U}\mathbf{V}^T \tag{10}$$

In which,

$$\mathbf{U} = [b_1\mathbf{e}_{a_1}, b_2\mathbf{e}_{a_2} \cdots, b_r\mathbf{e}_{a_r}] \tag{11}$$

$$\mathbf{V} = [\mathbf{e}_{a_1}, \mathbf{e}_{a_2} \cdots, \mathbf{e}_{a_r}] \tag{12}$$

And $\mathbf{e}_{a_i}$ is the a_i^{th} vector column of the $n \times n$ identity matrix.

By using the Sherman-Morrison-Woodbury formula [26] the receptance matrix of the modified system is found to be given by,

$$\overline{\mathbf{H}} = [\mathbf{I} - \mathbf{H}\mathbf{U}(\mathbf{I} + \mathbf{V}^T\mathbf{H}\mathbf{U})^{-1}\mathbf{V}^T]\mathbf{H} \tag{13}$$

Rearranging equation (13) leads to,

$$\overline{\mathbf{H}} = \mathbf{H} - \mathbf{H}\mathbf{U}(\mathbf{I} + \mathbf{V}^T\mathbf{H}\mathbf{U})^{-1}\mathbf{V}^T\mathbf{H} \tag{14}$$

and hence, for arbitrary pq^{th} column element,

$$\overline{h}_{pq} = \mathbf{e}_p^T\overline{\mathbf{H}}\mathbf{e}_q \tag{15}$$

Then,

$$\overline{h}_{pq} = \mathbf{e}_p^T\mathbf{H}\mathbf{e}_q - \mathbf{e}_p^T\mathbf{H}\mathbf{U}(\mathbf{I} + \mathbf{V}^T\mathbf{H}\mathbf{U})^{-1}\mathbf{V}^T\mathbf{H}\mathbf{e}_q \tag{16}$$

We now define the following matrices,

$$\mathbf{D} = \begin{bmatrix} b_1 & & & \\ & b_2 & & \\ & & \ddots & \\ & & & b_r \end{bmatrix} \tag{17}$$

$$\mathbf{p} = [h_{p,a_1}, h_{p,a_2}, \cdots, h_{p,a_r}]^T \tag{18}$$

$$\mathbf{q} = [h_{a_1,q}, h_{a_2,q}, \cdots, h_{a_r,q}]^T \tag{19}$$

$$\mathbf{G} = \begin{bmatrix} h_{a_1,a_1} & h_{a_1,a_2} & \cdots & h_{a_1,a_r} \\ h_{a_2,a_1} & h_{a_2,a_2} & \cdots & h_{a_2,a_r} \\ \vdots & \vdots & \ddots & \vdots \\ h_{a_r,a_1} & h_{a_r,a_2} & \cdots & h_{a_r,a_r} \end{bmatrix} \tag{20}$$

so that the following expressions are obtained,

$$\mathbf{e}_p{}^T\mathbf{H}\mathbf{U} = \mathbf{p}^T\mathbf{D} \tag{21}$$

$$\mathbf{V}^T\mathbf{H}\mathbf{U} = \mathbf{G}\mathbf{D} \tag{22}$$

$$\mathbf{V}^T\mathbf{H}\mathbf{e}_q = \mathbf{q} \tag{23}$$

Consequently, the receptance for modified system with r absorbers is rewritten as,

$$\overline{h}_{pq} = h_{pq} - \mathbf{p}^T\mathbf{D}(\mathbf{I} + \mathbf{G}\mathbf{D})^{-1}\mathbf{q} \tag{24}$$

or,

$$\overline{h}_{pq} = h_{pq} - \mathbf{p}^T(\mathbf{D}^{-1} + \mathbf{G})^{-1}\mathbf{q} \tag{25}$$

Where the inverse of $\mathbf{D}$ is,

$$\mathbf{D}^{-1} = \begin{bmatrix} 1/b_1 & & & \\ & 1/b_2 & & \\ & & \ddots & \\ & & & 1/b_r \end{bmatrix} \tag{26}$$

It is found that the original $n \times n$ matrix computation is condensed to the $r \times r$ matrix computation expressed in equation (25). In general, since only a small number of absorbers are considered the computation is considerably reduced. Furthermore, equation (25) shows only the original receptances at the coordinates of absorber attachments $(a_1, a_2, ..., a_r)$ and the receptance coordinates (p, q) are needed to determine the modified-system receptances. This is very significant result for the practical application of the method to large-scale systems.

4. Modification by a single classical mass-spring absorber

The cases of assigning a value to a receptance at a single frequency and at two frequencies are considered.

4.1 Assigning one receptance at a single frequency

For the single mass-spring absorber modification, the modified receptance may be obtained as,

$$\bar{h}_{pq} = h_{pq} - \frac{b h_{p,a_1} h_{a_1,q}}{1 + b h_{a_1,a_1}} \tag{27}$$

so that the coefficient b is given by,

$$b(\omega) = \frac{(h_{pq} - \bar{h}_{pq})}{h_{p,a_1} h_{a_1,q} - h_{a_1,a_1}(h_{pq} - \bar{h}_{pq})} \tag{28}$$

For the sake of the assignment of the receptance at one frequency, putting $\omega = \omega_1$ can transform the problem into an equation of two unknown variables m_a and k_a through equation (4). Therefore, we can fix a positive m_a and calculate k_a as,

$$k_a = \frac{m_a \omega_1^2 b}{m_a \omega_1^2 + b} \tag{29}$$

Considering the realistic problem, i.e., a positive value of k_a, it is seen that m_a and b should satisfy the following condition

$$\begin{cases} m_a > 0 & when \quad b > 0 \\ -b/\omega_1^2 > m_a > 0 & when \quad b < 0 \end{cases} \tag{30}$$

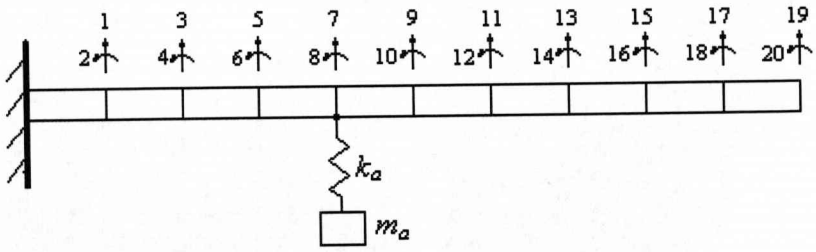

Figure 2. A cantilever beam modified with one single absorber

Example 1: The assignment of a receptance to a cantilever beam modified with a single absorber is considered. The beam is divided into ten elements with DOFs as shown in Figure 2. The beam's material properties including length, section area, density, second inertia moment and elastic modulus are selected as $L = 0.5m$, $A = 9\times10^{-5}m^2$, $\rho = 2700kg/m^3$, $I = 6.75\times10^{-11}m^4$, $E = 5.186\times10^{10}Pa$ respectively. It is required to assign the modified value of the receptance $h_{(5,13)}$ at frequency $f_1 = 60Hz$ to be 0.34 of the original receptance by using an absorber attached at DOF 7. Inserting the values of $h_{(5,7)}$, $h_{(7,13)}$, $h_{(7,7)}$, $h_{(5,13)}$ and $\bar{h}_{(5,13)} = 0.34\times h_{(5,13)}$ at frequency $\omega_1 = 2\pi f_1$ into equation (28) gives an absorber coefficient $b(\omega_1) = -4.1266\times10^3 N/m$. Thus, fixing $m_a = 2.43\times10^{-3}kg$ for absorber mass, the spring stiffness of absorber is calculated to be $k_a = 3.7690\times10^2 N/m$ using equation (29). Table 1 describes the details of the receptance modification and Figure 3 shows that modified receptance $h_{(5,13)}$ at $f_1 = 60Hz$ has been assigned exactly.

Table 1. *Receptance values of $h_{(5,13)}$ at one frequency*

Frequency	Original Receptance	Modified Receptance	Ratio $\bar{h}_{(5,13)} / h_{(5,13)}$
60Hz	-2.2113×10^{-4}	-7.5183×10^{-5}	0.3400

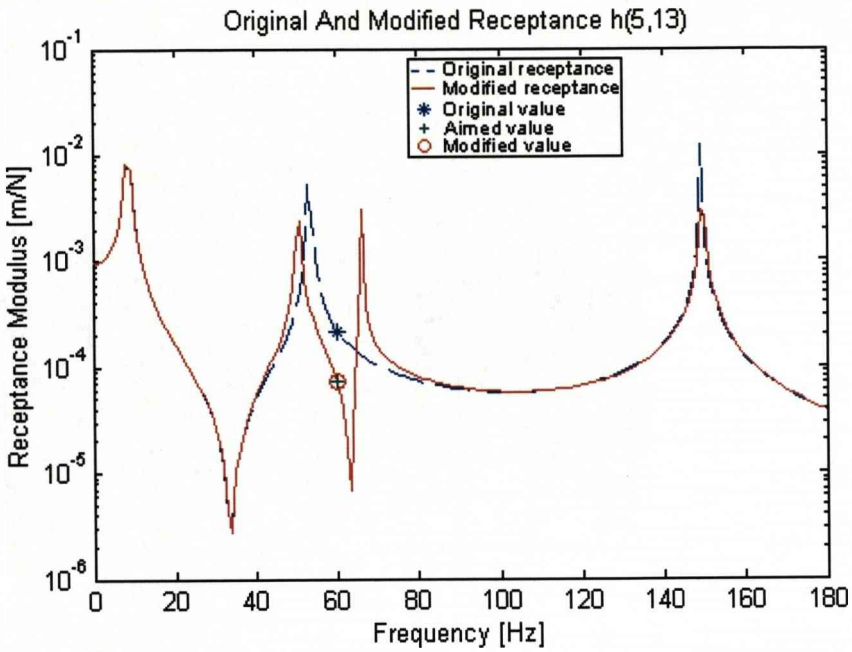

Figure 3. Assignment of one receptance at one frequency

4.2 Assigning one receptance at two frequencies

Putting $\omega = \omega_1$ and $\omega = \omega_2$ into equation (28) separately, and then solving for the absorber dynamic stiffnesses $b(\omega_1)$ and $b(\omega_2)$ at the two frequencies leads to,

$$\begin{cases} b(\omega_1) = \dfrac{-\omega_1^2 m_a k_a}{-\omega_1^2 m_a + k_a} \\ b(\omega_2) = \dfrac{-\omega_2^2 m_a k_a}{-\omega_2^2 m_a + k_a} \end{cases} \tag{31}$$

Now, the absorber parameters variables m_a and k_a may be solved as,

$$m_a = \frac{\dfrac{1}{\omega_2^2} - \dfrac{1}{\omega_1^2}}{\dfrac{1}{b(\omega_1)} - \dfrac{1}{b(\omega_2)}} \quad , \quad k_a = \frac{\omega_1^2 - \omega_2^2}{\dfrac{\omega_1^2}{b(\omega_1)} - \dfrac{\omega_2^2}{b(\omega_2)}} \tag{32}$$

Likewise, the realistic-solutions requirement has to be satisfied,

$$\frac{1}{b(\omega_1)} < \frac{1}{b(\omega_2)} \quad \text{and} \quad \frac{\omega_1^2}{b(\omega_1)} < \frac{\omega_2^2}{b(\omega_2)} \qquad \text{for} \quad \omega_1 < \omega_2 \tag{33}$$

Example 2: Taking the same modification example as before, but now we propose to assign modified values to be 0.34 and 0.27 of the original values for receptance $h_{(5,13)}$ at the frequencies $f_1 = 60Hz$ and $f_2 = 140Hz$ at same time. The absorber stiffnesses at two frequencies were calculated as $b(\omega_1) = -4.1266 \times 10^3 N/m$ and $b(\omega_2) = 2.2414 \times 10^4 N/m$. Then, Combining $b(\omega_1)$ and $b(\omega_2)$, the calculation result in an absorber with mass $m_a = 2.0017 \times 10^{-2} kg$ and spring stiffness

$k_a = 9.1595 \times 10^3 N/m$. Table 2 shows the receptance modification details and Figure 4 presents the original and modified receptances $h_{(5,13)}$.

Table 2. *Receptance values of $h_{(5,13)}$ at two frequencies*

Frequency	Original Receptance	Modified Receptance	Ratio $\bar{h}_{(5,13)} / h_{(5,13)}$
60Hz	-2.2113×10^{-4}	-7.5183×10^{-5}	0.3400
140Hz	-1.6677×10^{-4}	-4.5027×10^{-5}	0.2700

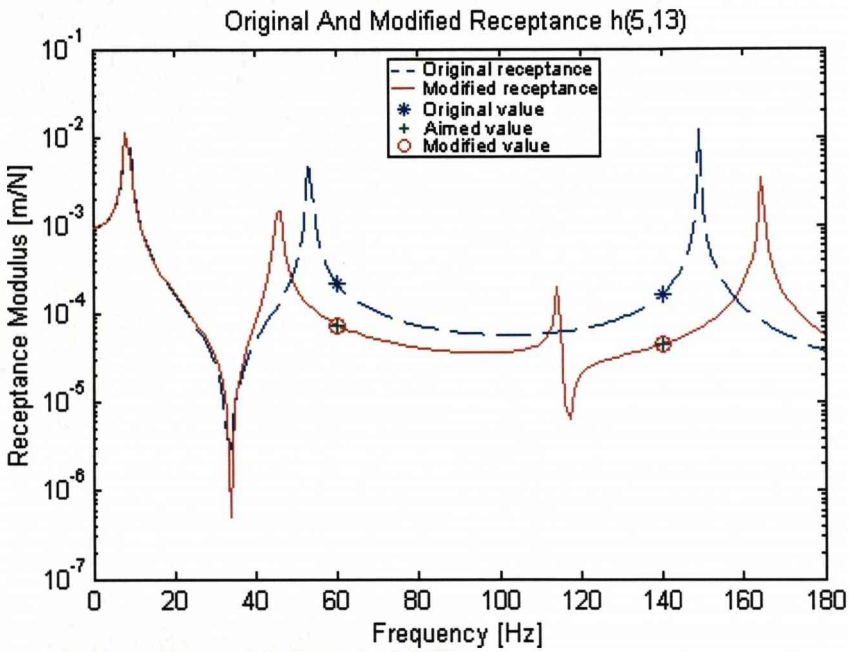

Figure 4. Assignment of one receptance at two frequencies

4.3 Assigning two receptances at one single frequency

If two receptances h_{pq} and h_{kj} were to be assigned at one single frequency with one absorber modification, we would write two equations of absorber stiffness for each receptance from equation (27).

$$\bar{h}_{pq} = h_{pq} - \frac{b(\omega) h_{p,a_1} h_{a_1,q}}{1 + b(\omega) h_{a_1,a_1}}, \quad and \quad \bar{h}_{kj} = h_{kj} - \frac{b(\omega) h_{k,a_1} h_{a_1,j}}{1 + b(\omega) h_{a_1,a_1}} \tag{34}$$

That requires one number $b(\omega)$ to have satisfied these two equations simultaneously. Hence, we can get

$$\frac{h_{pq} - \bar{h}_{pq}}{h_{p,a_1} h_{a_1,q}} = \frac{h_{kj} - \bar{h}_{kj}}{h_{k,a_1} h_{a_1,j}} \tag{35}$$

So, it is impossible to assign arbitrarily two different receptances at a single frequency simultaneously by only one absorber modification except the condition (35) is satisfied. However this case is very rare in practices. Thus, it is found that we cannot

arbitrarily assign two receptances at one single frequency when only one absorber is connected to the original system.

This conclusion can be easily extended to the multiple absorbers case because a unique dynamic stiffness value $b(\omega)$ exists at one frequency for each absorber. Looking back to equation (25), when a number of receptances greater than the number of absorbers, $n > r$, are to be assigned at one single frequency, such as assigning three receptances at one frequency by using two absorbers, the number of equations will be larger than the number of variables. Hence, the solution can only be obtained under particular conditions. In other words the receptance changes cannot assigned arbitrarily.

In the general case of assigning a number of receptances at several frequencies by using many absorbers the result will be a system of multivariate polynomial equations that must be solved to determine the parameters of the absorbers.

5.0 Multivariate polynomials system and its solution

5.1 General theory and Groebner Basis

The natural mathematical setting of a system of multivariate polynomials is the algebraic geometry. In algebraic geometry, geometrical curves are identified with algebraic equations and the set of solutions of such systems of algebraic equations represents the intersection of the curves. The benefit of this framework is twofold; results in algebra may be visualized in geometry, and geometrical problems may be cast and solved algebraically. The geometrical object that relates to finding the roots of a polynomial system is the 'variety'. Given a system of multivariate polynomials $F \equiv \{f_1,...,f_r\}$ in n-variables $(x_1,...x_n)$, its variety $V(F)$ is defined as the set of n-tuples $(a_1,...,a_n)$ for which $f_i(a_1,...a_n) = 0$ for all polynomials f_i of F. In some instances the variety can be visualized as a geometrical shape in the Euclidean space. The intersection, for example, of two planes in a three dimensional Euclidean space is a line, a well defined geometrical object.

The set all polynomials in $(x_1,...x_n)$ may be shown to have the algebraic structure of a 'ring', denoted by $\Re[x_1,..,x_n]$. A ring in general is a set closed in two algebraic operations, addition and multiplication, performed on its elements. It is well known that these two operations are precisely defined for any two polynomials in $\Re[x_1,..,x_n]$. The link between algebra and geometry comes from the fact that varieties are determined by the 'ideals' of the polynomial ring $\Re[x_1,..,x_n]$. An ideal, *I*, is a sub-collection of the polynomials of the ring $\Re[x_1,..,x_n]$ that (a) it contains the polynomial of which all the coefficients are zero , (b) is closed under addition, i.e the summand of two polynomials is another polynomial also contained in *I* and (c)for two arbitrarily chosen polynomials *f* and *h* that one of the two, say *f* belongs in I, their

product *fh* is another polynomial that also belongs to *I*.

The important result in finding the roots of a system of multivariate polynomials is that the variety, *V*, the geometrical object of the common roots, is created by the ideal that contains the polynomials themselves. This changes the problem of finding the common roots of a system of polynomials to the problem of computing the ideal in which the polynomials of the system belong. A brief explanation follows on how this is achieved.

Given a set of polynomials $F \equiv \{f_1,...,f_r\}$, the set $< f_1,...,f_r >$ defined by $\left\{\sum_{i=1}^{r} h_i f_i : h_1,...,h_r \text{ in } \Re[x_1,...,x_n]\right\}$ is the ideal generated by the polynomial set *F*. A very important theorem stated and proved by Hilbert dictates that every polynomial ideal is generated by finitely many polynomials.

B. Buchberger [27] in 1965 in his PhD thesis, motivated by the method of computing orthonormal basis of a general vector space, introduced a simpler basis for a polynomial ideal and named it Groebner after his advisor. One of the many applications that Groebner bases have found is their use in solving a system of multivariate polynomials as explained below.

The polynomials of a multivariate polynomial system generate an ideal. Then the Buchberger algorithm can be implemented on the original system in order to obtain the Grobner basis of this ideal. This basis is composed of polynomials of lesser complexity so that the other solution methodologies can be used to obtain the roots.

According to Bezout's theorem [28] for a system of n polynomials each of degree d_i there are at most, counting the multiplicities and the complex roots, $\prod_{i}^{n} d_i$ roots. The advantage of Groebner basis is that it gives all the solutions of a system of multivariate polynomials as opposed to Newton's method that converges to a single solution, the one nearest to the starting point.

5.1.2 Newton's method

This is an extension to the widely used Newton's method for finding the roots of a function. Viewing the system of multivariate polynomials in $(x_1,...x_n)$ as a non-linear vector function *F*, then Newton's method tries to find its zero, in a neighborhood of point $\vec{x}_0 \equiv (a_1,...,a_n)$, by linearly approximating *F* locally around $\vec{x}_0$ using the truncated Taylor expansion,,

$$F(\vec{x}) = F(\vec{x}_0) + J(\vec{x}_0) \times (\vec{x} - \vec{x}_0) \tag{36}$$

where $J(\vec{x}_0)$ is the Jacobian matrix of *F* at $\vec{x}_0$. Then the root of this linear function is given by,

$$\vec{x}_1 = \vec{x}_0 - \left[J(\vec{x}_0)\right]^{-1} F(\vec{x}_0) \tag{37}$$

This new root $\vec{x}_1$ becomes a new approximation to the root, and the above procedure repeats itself to establish an iterative root-finding scheme [29].

This methodology has two major drawbacks. One is that it is highly local since always the solution computed is near the starting point and the presence of the inverse of the Jacobian makes the system prone to conditioning problems.

6. Modification by two mass-spring absorbers

In what follows two mass-spring absorbers are used to assign (a) two receptances at a single frequency, (b) two receptances at two frequencies simultaneously and (c) one receptance at four frequencies. The analysis is supported by illustrative examples.

6.1 Assigning two receptances simultaneously at a single frequency

When more than one absorber is considered, then equation (25) may be rewritten as the form

$$\bar{h}_{pq} = h_{pq} - \mathbf{p}^T \frac{adj(\mathbf{D}^{-1} + \mathbf{G})}{det(\mathbf{D}^{-1} + \mathbf{G})}\mathbf{q} \tag{38}$$

In which,

$adj(\mathbf{D}^{-1} + \mathbf{G})$ is the adjoint matrix of the matrix $(\mathbf{D}^{-1} + \mathbf{G})$

$det(\mathbf{D}^{-1} + \mathbf{G})$ is the determinant of the matrix $(\mathbf{D}^{-1} + \mathbf{G})$

Then, the equation (38) may be cast as the nonlinear equation,

$$(h_{pq} - \bar{h}_{pq})\, det(\mathbf{D}^{-1} + \mathbf{G}) = \mathbf{p}^T adj(\mathbf{D}^{-1} + \mathbf{G})\mathbf{q} \tag{39}$$

Particularly, in the two-absorbers case,

$$\mathbf{D}^{-1} = \begin{bmatrix} 1/b_1 & 0 \\ 0 & 1/b_2 \end{bmatrix} \tag{40}$$

$$\mathbf{p}^T = [h_{p,a_1}, \quad h_{p,a_2}] \tag{41}$$

$$\mathbf{q} = \begin{bmatrix} h_{a_1,q} \\ h_{a_2,q} \end{bmatrix} \tag{42}$$

$$\mathbf{G} = \begin{bmatrix} h_{a_1,a_1} & h_{a_1,a_2} \\ h_{a_2,a_1} & h_{a_2,a_2} \end{bmatrix} \tag{43}$$

Hence,

$$(\mathbf{D}^{-1} + \mathbf{G}) = \begin{bmatrix} 1/b_1 + h_{a_1,a_1} & h_{a_1,a_2} \\ h_{a_2,a_1} & 1/b_2 + h_{a_2,a_2} \end{bmatrix} \tag{44}$$

and

$$adj(\mathbf{D}^{-1} + \mathbf{G}) = \begin{bmatrix} 1/b_2 + h_{a_2,a_2} & -h_{a_1,a_2} \\ -h_{a_2,a_1} & 1/b_1 + h_{a_1,a_1} \end{bmatrix} \tag{45}$$

$$\det(\mathbf{D}^{-1} + \mathbf{G}) = (1/b_1 + h_{a_1,a_1})(1/b_2 + h_{a_2,a_2}) - h_{a_1,a_2} h_{a_2,a_1} \tag{46}$$

Then, by re-writing equation (39), we obtain the expression,

$$(h_{pq} - \bar{h}_{pq})[(1/b_1 + h_{a_1,a_1})(1/b_2 + h_{a_2,a_2}) - h_{a_1,a_2} h_{a_2,a_1}]$$

$$= h_{p,a_1} h_{a_1,q} (1/b_2 + h_{a_2,a_2}) - h_{p,a_2} h_{a_1,q} h_{a_2,a_1} - h_{p,a_1} h_{a_2,q} h_{a_1,a_2} + h_{p,a_2} h_{a_2,q} (1/b_1 + h_{a_1,a_1}) \quad (47)$$

and for each absorber,

$$b_1(\omega) = \frac{-\omega^2 m_{a1} k_{a1}}{-\omega^2 m_{a1} + k_{a1}} \quad , \quad b_2(\omega) = \frac{-\omega^2 m_{a2} k_{a2}}{-\omega^2 m_{a2} + k_{a2}} \quad (48)$$

Replacing the subscripts p with k, and q with j, it is very easy to write a modification equation for another receptance $\bar{h}_{kj}$ as,

$$(h_{kj} - \bar{h}_{kj})[(1/b_1 + h_{a_1,a_1})(1/b_2 + h_{a_2,a_2}) - h_{a_1,a_2} h_{a_2,a_1}]$$
$$= h_{k,a_1} h_{a_1,j} (1/b_2 + h_{a_2,a_2}) - h_{k,a_2} h_{a_1,j} h_{a_2,a_1} - h_{k,a_1} h_{a_2,j} h_{a_1,a_2} + h_{k,a_2} h_{a_2,j} (1/b_1 + h_{a_1,a_1}) \quad (49)$$

Hence, combining two equations (47) and (49), and putting $\omega = \omega_1$ into them, we build an equation set including two nonlinear equations with two variables $\{b_1(\omega_1) \quad b_2(\omega_1)\}$. Thus, two absorbers dynamic stiffnesses $b_1(\omega_1)$ and $b_2(\omega_1)$ at frequency ω_1 would be obtained by solving this set of nonlinear equations. Consequently, we can calculate the parameters of the absorbers by following the procedure described in section 4.1 for each absorber in turn.

Example 3: Now we consider the same cantilever beam structure as before, but modified by the addition of two absorbers as shown in Figure 5. The two absorbers are connected to the seventh and seventeenth DOFs respectively and two receptances $h_{(5,13)}$ and $h_{(19,11)}$ are required to be assigned simultaneously.

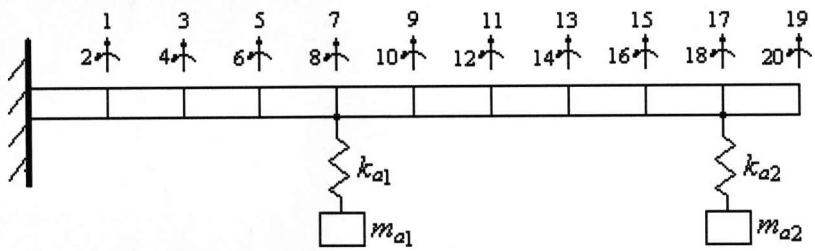

Figure 5. A cantilever beam modified by two absorbers

At the frequency $f_1 = 60Hz$ it is required that the modified value of $h_{(5,13)}$ should be assigned to 0.34 of its original value while the modified value of $h_{(19,11)}$ should be equal to 0.2 of its original value. Analysis of the nonlinear equations leads two possible solutions, so that two absorbers selection options are found to exist,

$$\begin{cases} b_1(\omega_1) = -2.0107 \times 10^4 N/m \\ b_2(\omega_1) = 6.5707 \times 10^3 N/m \end{cases} \quad \text{or} \quad \begin{cases} b_1(\omega_1) = -3.4478 \times 10^3 N/m \\ b_2(\omega_1) = 8.0346 \times 10^2 N/m \end{cases}$$

For each solution, by fixing $m_{a1} = m_{a2} = 2.43 \times 10^{-3} kg$, two absorbers may be found having the following coefficients:

Solution 1 Solution 2

$$\begin{cases} m_{a1} = 2.43\times10^{-3}\,kg \\ k_{a1} = 3.5139\times10^{2}\,N/m \\ m_{a2} = 2.43\times10^{-3}\,kg \\ k_{a2} = 3.2811\times10^{2}\,N/m \end{cases} \quad \text{or} \quad \begin{cases} m_{a1} = 2.43\times10^{-3}\,kg \\ k_{a1} = 3.8380\times10^{2}\,N/m \\ m_{a2} = 2.43\times10^{-3}\,kg \\ k_{a2} = 2.4154\times10^{2}\,N/m \end{cases}$$

Table 3 lists the modification details for all absorber options

Table 3. *Receptance values of $h_{(5,13)}$ and $h_{(19,11)}$ at one frequency*

Solution	Receptance	Original value	Modified value	Modified ratio
1	$h_{(5,13)}$	-2.2113×10^{-4}	-7.5204×10^{-5}	0.3401
	$h_{(19,11)}$	5.1777×10^{-4}	1.0357×10^{-4}	0.2000
2	$h_{(5,13)}$	-2.2113×10^{-4}	-7.5189×10^{-5}	0.3400
	$h_{(19,11)}$	5.1777×10^{-4}	1.0355×10^{-4}	0.2000

It is found that the two solutions are both able to assign the two chosen receptances exactly. Figure 6 and 7 show the original and modified receptance for each of the two-absorber solutions.

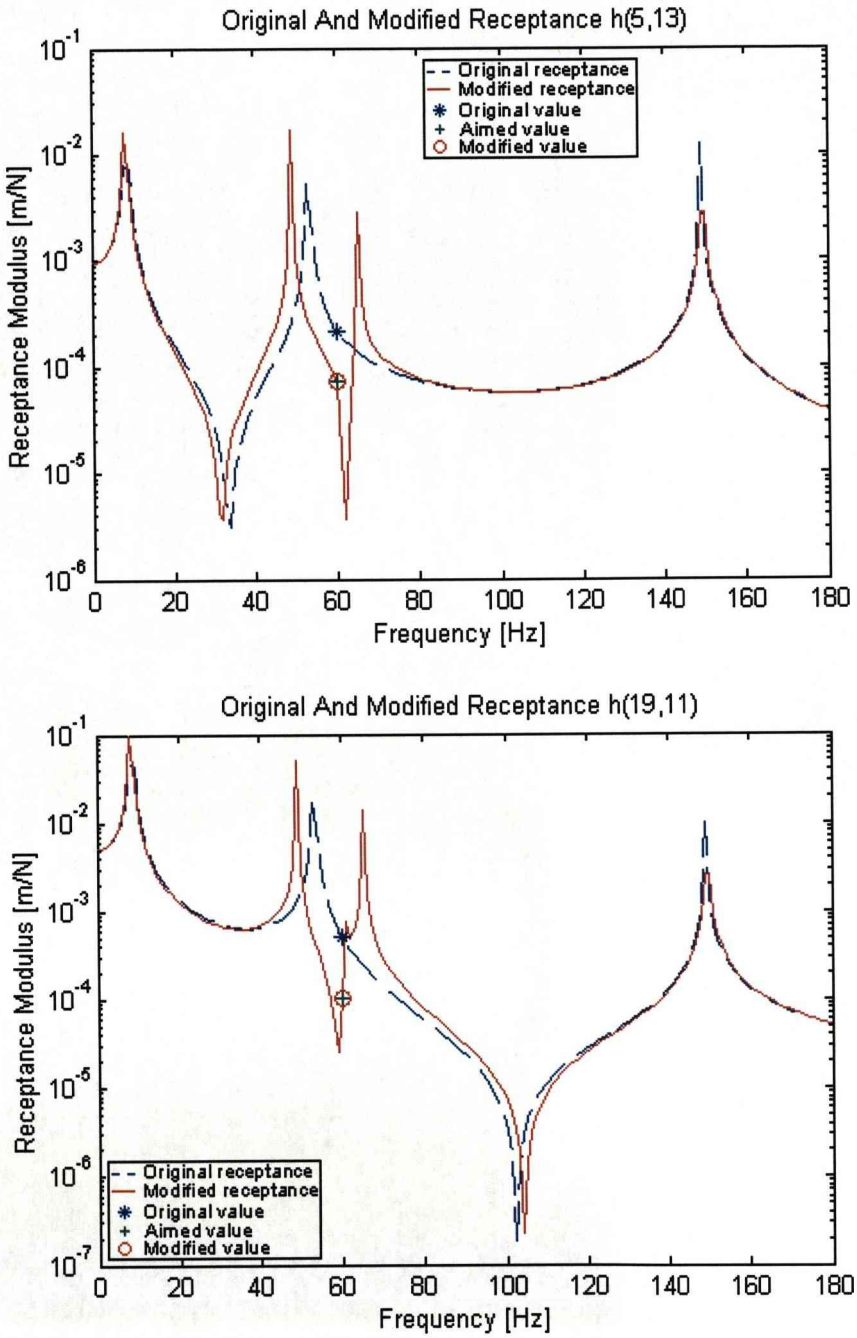

Figure 6. Solution 1 - Assignment of two receptances at one frequency

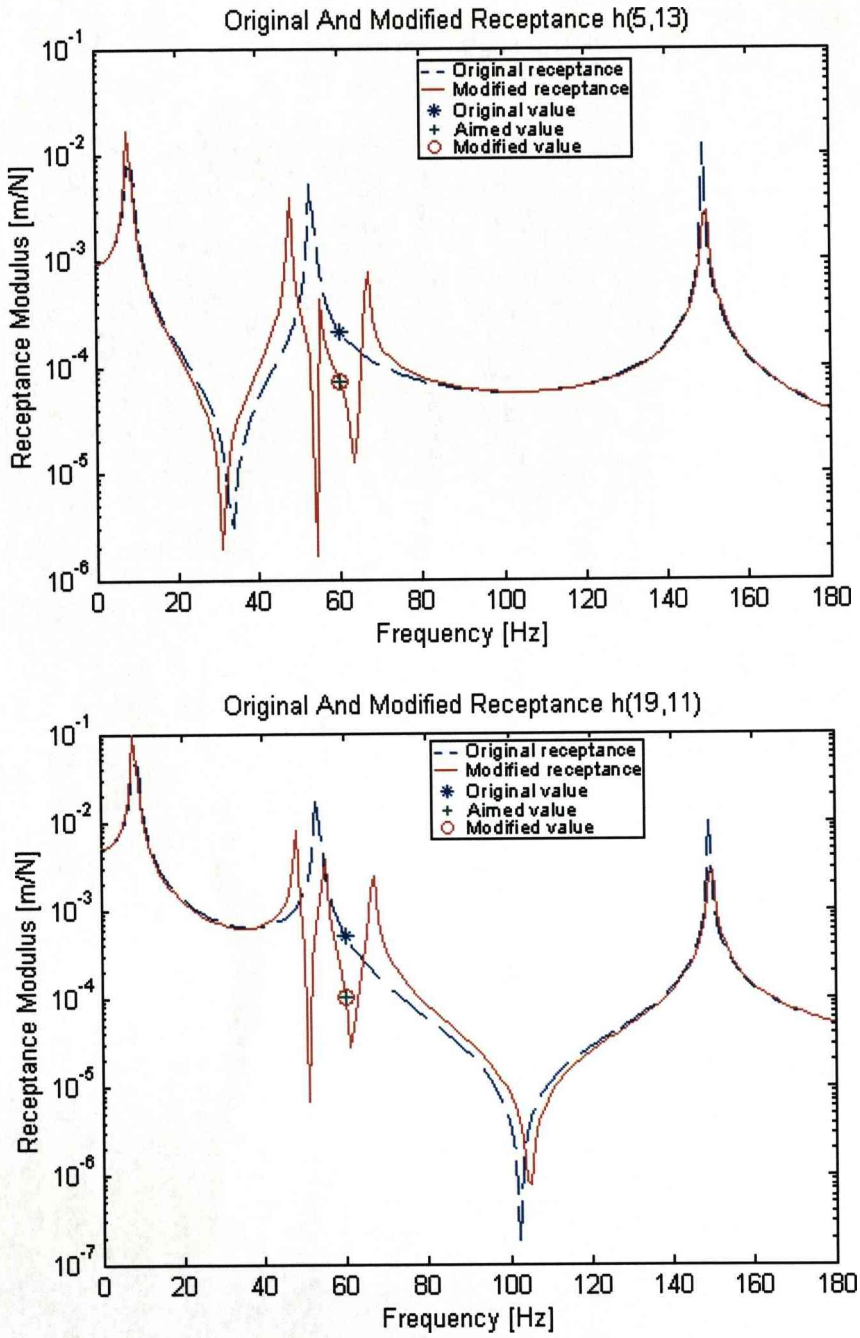

Figure 7. Solution 2 - Assignment of two receptances at one frequency

6.3 Assigning two receptances at two frequencies simultaneously

The calculation for assigning two receptances at one frequency $\omega = \omega_1$ leads to a solution for the absorber coefficients $\{b_1(\omega_1) \quad b_2(\omega_1)\}$ at frequency ω_1. Simply repeating the calculation procedure at another frequency $\omega = \omega_2$ gives us another two absorber dynamic stiffnesses $\{b_1(\omega_2) \quad b_2(\omega_2)\}$ at frequency ω_2. Subsequently, we are be able to determine the absorber mass and stiffness parameters that give the

required coefficients, $\{b_1(\omega_1) \quad b_1(\omega_2)\}$ and $\{b_2(\omega_1) \quad b_2(\omega_2)\}$, at the frequencies ω_1 and ω_2.

Example 4: In this case, it is required that at frequency $f_1 = 60Hz$, the modified value of $h_{(5,13)}$ should be assigned to 0.62 of its original value while the modified value of $h_{(19,11)}$ should be equal to 0.26 of its original value. Simultaneously, at frequency $f_1 = 140Hz$, the modified value of $h_{(5,13)}$ should be 0.34 of its original value while the modified value of $h_{(19,11)}$ should be 0.55 of its original value. Analysis of the nonlinear equations leads to two solutions for the absorber dynamic stiffnesses,

$$\begin{cases} b_1(\omega_1) = -1.5052\times10^3\, N/m \\ b_1(\omega_2) = 2.3843\times10^4\, N/m \\ b_2(\omega_1) = -4.8693\times10^3\, N/m \\ b_2(\omega_2) = 2.3518\times10^4\, N/m \end{cases} \quad \text{or} \quad \begin{cases} b_1(\omega_1) = -9.4544\times10^3\, N/m \\ b_1(\omega_2) = 5.2413\times10^3\, N/m \\ b_2(\omega_1) = 5.0024\times10^3\, N/m \\ b_2(\omega_2) = 1.5318\times10^4\, N/m \end{cases}$$

For each group of dynamic stiffnesses, a set of mass and stiffness parameters is obtained as follows,

Solution 3

$$\begin{cases} m_{a1} = 8.1323\times10^{-3}\, kg \\ k_{a1} = 4.9787\times10^3\, N/m \\ m_{a2} = 2.3171\times10^{-2}\, kg \\ k_{a2} = 1.0173\times10^4\, N/m \end{cases}$$

or

Solution 4

$$\begin{cases} m_{a1} = 1.9368\times10^{-2}\, kg \\ k_{a1} = 3.8832\times10^3\, N/m \\ m_{a2} = -4.2666\times10^{-2}\, kg \\ k_{a2} = 2.8580\times10^4\, N/m \end{cases}$$

(non realistic)

It is clear in the solution 4, m_{a2} is negative and therefore not realistic. This solution is ignored, so that only the solution 3 is now considered. Table 4 lists the modification details. Both receptance assignments are achieved very well. Figure 8 shows the original and modified receptances.

Table 4. *Receptance values of $h_{(5,13)}$ and $h_{(19,11)}$ at two frequencies*

Frequency	Receptance	Original value	Modified value	Modified ratio
60 Hz	$h_{(5,13)}$	-2.2113×10^{-4}	-1.3710×10^{-4}	0.6200
	$h_{(19,11)}$	5.1777×10^{-4}	1.3462×10^{-4}	0.2600
140 Hz	$h_{(5,13)}$	-1.6677×10^{-4}	-5.6712×10^{-5}	0.3401
	$h_{(19,11)}$	-1.3395×10^{-4}	-7.3682×10^{-5}	0.5501

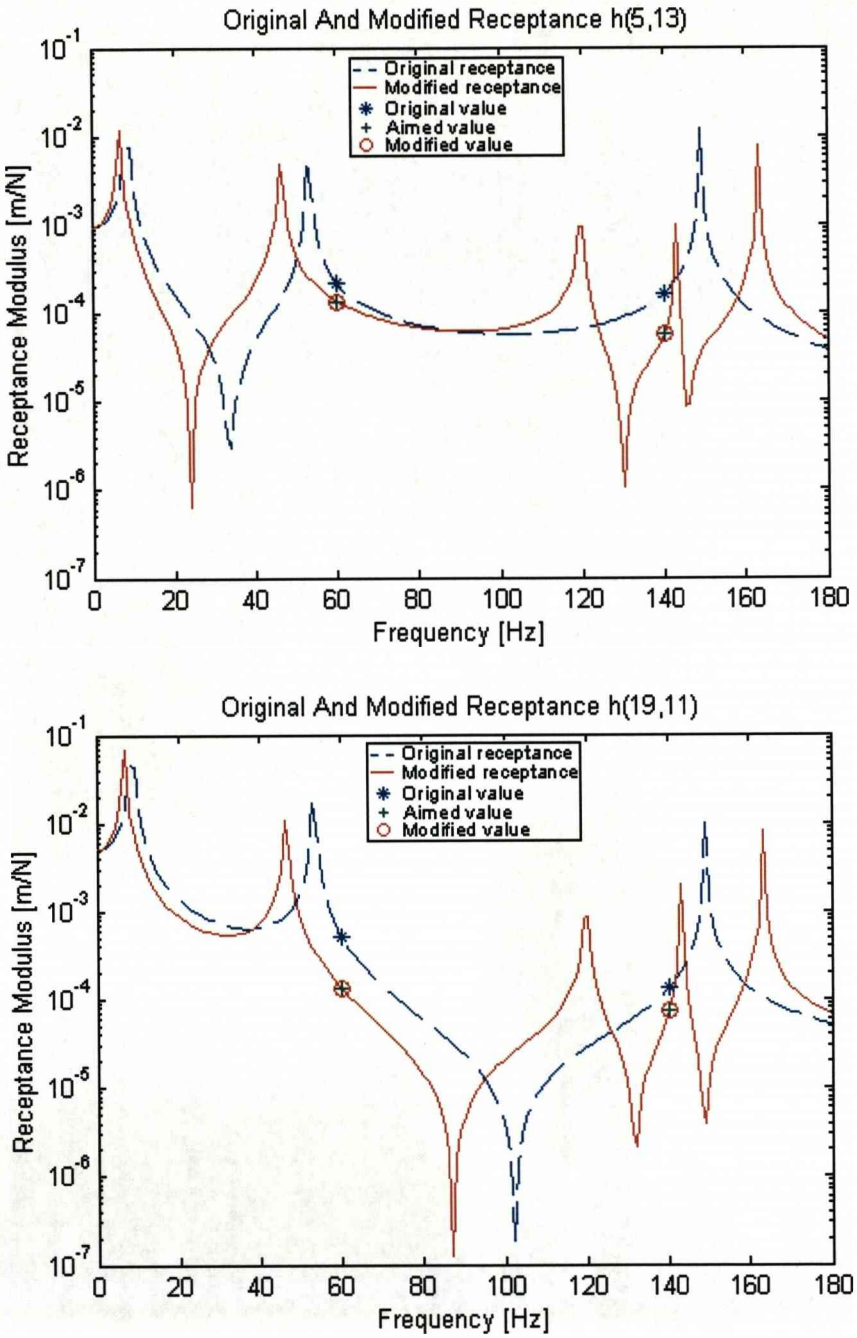

Figure 8. Assignment of two receptances at two frequencies

6.4 Assignment of one receptance at four frequencies

In the analysis presented so far receptances have been assigned at two different frequencies and since an undamped absorber has only two parameters, k_a and m_a, it is clear that three receptances cannot be assigned by using a single absorber. However, with the application of a second absorber, the added mass and stiffness variables

provide the capability to assign one receptance at four frequencies simultaneously.

By combining equations (47) and (48) and entering $\omega = \omega_i, \quad i = 1,\cdots,4$ in turn, we obtain four nonlinear equations in four unknowns $\{m_{a1}, \ k_{a1}, \ m_{a2}, \ k_{a2}\}$. Analysis of these equations generally gives a number of possible absorber solutions.

Example 5: Considering the same structure shown in Figure 5 with two absorbers and making assignments to receptance $h_{(5,13)}$ to take values of 0.4, 0.3, 0.4 and 0.8 of its original values at the frequencies of 10, 55, 100 and 140 Hz respectively, the analysis leads to the six solutions presented in Table 5. Only solutions 5 and 6 give realistic (positive) values for the absorber stiffnesses and masses.

Table 5. *Absorber parameters for the assignment of $h_{(5,13)}$ at four frequencies*

Absorber solution	m_{a1} (kg)	k_{a1} (N/m)	m_{a2} (kg)	k_{a2} (N/m)
1	-1.1430e-001	-4.3148e+002	1.1834e-001	6.8865e+003
2	1.2392e+000	-4.8525e+003	-3.2910e-002	1.8894e+004
3	5.5542e-001	2.2185e+004	-3.2610e-002	1.3088e+005
4	5.7555e-003	2.2333e+003	1.5181e-002	-4.5238e+004
5	3.6362e-003	8.3890e+002	1.4987e-002	3.4563e+003
6	3.0042e-003	1.1877e+003	1.4723e-002	1.6063e+003

Table 6 shows the receptance modification details for the realistic solutions and Figure 9 and 10 show the original and modified receptance $h_{(5,13)}$ using the two absorbers defined by,

Solution 5

$$\begin{cases} m_{a1} = 3.6362\times10^{-3}\,kg \\ k_{a1} = 8.3890\times10^{2}\,N/m \\ m_{a2} = 1.4987\times10^{-2}\,kg \\ k_{a2} = 3.4563\times10^{3}\,N/m \end{cases}$$

and

Solution 6

$$\begin{cases} m_{a1} = 3.0042\times10^{-3}\,kg \\ k_{a1} = 1.1877\times10^{3}\,N/m \\ m_{a2} = 1.4723\times10^{-2}\,kg \\ k_{a2} = 1.6063\times10^{3}\,N/m \end{cases}$$

Table 6. *Receptance values of $h_{(5,13)}$ at four frequencies*

Solution	Frequency	Original value	Modified value	Modified ratio
5	10Hz	-2.3829×10^{-3}	-9.5314×10^{-4}	0.4000
	55Hz	-7.7390×10^{-4}	-2.3214×10^{-4}	0.3000
	100Hz	-5.7930×10^{-5}	-2.3169×10^{-5}	0.4000
	140Hz	-1.6677×10^{-4}	-1.3341×10^{-4}	0.8000
6	10Hz	-2.3829×10^{-3}	-9.5314×10^{-4}	0.4000
	55Hz	-7.7390×10^{-4}	-2.3215×10^{-4}	0.3000
	100Hz	-5.7930×10^{-5}	-2.3179×10^{-5}	0.4001
	140Hz	-1.6677×10^{-4}	-1.3341×10^{-4}	0.8000

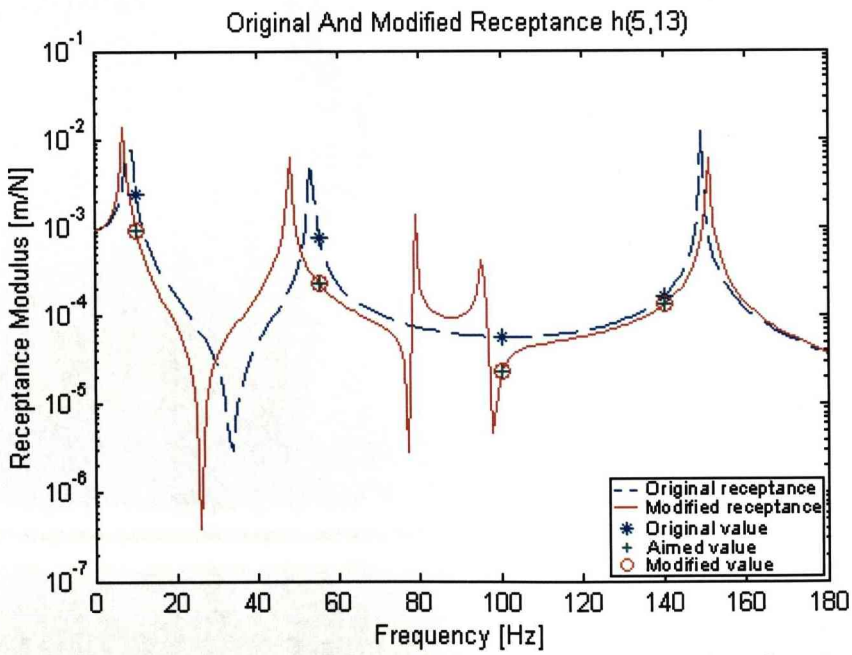

Figure 9. Solution 5 - Assignment of one receptance at four frequencies

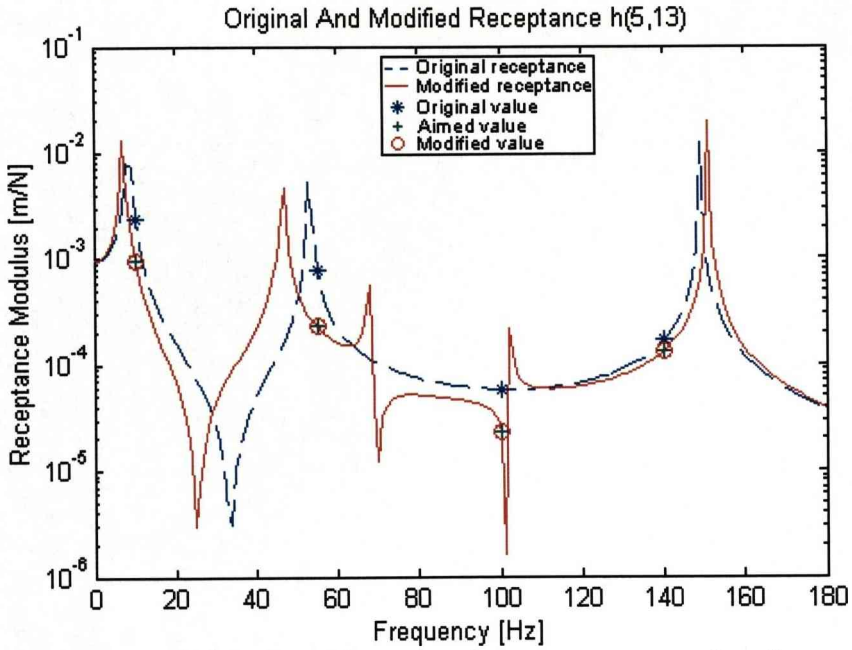

Figure 10. Solution 6 - Assignment of one receptance at four frequencies

7. Modification by three mass-spring absorbers.

The following problems are considered: (a) assigning three receptances simultaneously at a single frequency, (b) assigning three receptances simultaneously at two frequencies, (c) assigning one receptance at six frequencies and (d) assigning two receptances simultaneously at three frequencies. Illustrative examples are given in each case.

7.1 Assigning three receptances simultaneously at a single frequency.

Considering equation (39), but for three mass-spring absorbers case

$$(\mathbf{D}^{-1}+\mathbf{G})=\begin{bmatrix} 1/b_1+h_{a_1,a_1} & h_{a_1,a_2} & h_{a_1,a_3} \\ h_{a_2,a_1} & 1/b_2+h_{a_2,a_2} & h_{a_2,a_3} \\ h_{a_3,a_1} & h_{a_3,a_2} & 1/b_3+h_{a_3,a_3} \end{bmatrix} \tag{50}$$

so that,

$$adj(\mathbf{D}^{-1}+\mathbf{G})=\begin{bmatrix} (1/b_2+h_{a_2,a_2})(1/b_3+h_{a_3,a_3})-h_{a_2,a_3}h_{a_3,a_2} & h_{a_1,a_3}h_{a_3,a_2}-h_{a_1,a_2}(1/b_3+h_{a_3,a_3}) & h_{a_1,a_2}h_{a_2,a_3}-h_{a_1,a_3}(1/b_2+h_{a_2,a_2}) \\ h_{a_2,a_3}h_{a_3,a_1}-h_{a_2,a_1}(1/b_3+h_{a_3,a_3}) & (1/b_1+h_{a_1,a_1})(1/b_3+h_{a_3,a_3})-h_{a_1,a_3}h_{a_3,a_1} & h_{a_2,a_1}h_{a_1,a_3}-h_{a_2,a_3}(1/b_1+h_{a_1,a_1}) \\ h_{a_3,a_1}h_{a_2,a_2}-h_{a_3,a_2}(1/b_2+h_{a_2,a_2}) & h_{a_3,a_1}h_{a_1,a_2}-h_{a_3,a_2}(1/b_1+h_{a_1,a_1}) & (1/b_1+h_{a_1,a_1})(1/b_2+h_{a_2,a_2})-h_{a_1,a_2}h_{a_2,a_1} \end{bmatrix} \tag{51}$$

and

$$\det(\mathbf{D}^{-1}+\mathbf{G}) = (1/b_1 + h_{a_1,a_1})(1/b_2 + h_{a_2,a_2})(1/b_3 + h_{a_3,a_3}) + h_{a_1,a_3}h_{a_3,a_2}h_{a_2,a_1} + h_{a_1,a_2}h_{a_2,a_3}h_{a_3,a_1} - h_{a_1,a_3}h_{a_3,a_1}(1/b_2 + h_{a_2,a_2}) - h_{a_1,a_2}h_{a_2,a_1}(1/b_3 + h_{a_3,a_3}) - h_{a_3,a_2}h_{a_2,a_3}(1/b_1 + h_{a_1,a_1}) \tag{52}$$

Also,

$$\mathbf{p}^T = [h_{p,a_1},\ h_{p,a_2},\ h_{p,a_3}] \tag{53}$$

$$\mathbf{q} = \begin{bmatrix} h_{a_1,q} \\ h_{a_2,q} \\ h_{a_3,q} \end{bmatrix} \tag{54}$$

Thus, by inserting the above into equation (39) we obtain the modification equation for receptance h_{pq} at frequency ω with three absorbers.

Also, we have that,

$$b_i(\omega) = \frac{-\omega^2 m_{ai} k_{ai}}{-\omega^2 m_{ai} + k_{ai}} \quad , \quad i = 1,\ 2,\ 3 \tag{55}$$

Three absorbers modification equations for each receptance h_{pq}, h_{kj}, and h_{mn} at frequency $\omega = \omega_1$ may be written. Combining them results in a set of three nonlinear equations in the three variables $\{b_1(\omega_1)\ \ b_2(\omega_1)\ \ b_3(\omega_1)\}$. Thus, three absorbers' dynamic stiffnesses $b_1(\omega_1)$, $b_2(\omega_1)$ and $b_3(\omega_1)$ at frequency ω_1 may be obtained. Then, we can solve for the parameters of the three aborbers by following the procedure described in section 4.1 for each absorber in turn.

Example 6: If we consider the same cantilever beam structure as before, but modified by the addition of three absorbers attached to the 5th, 13th and 17th DOF as shown in Figure 11. In this case, it is required that three receptances $h_{(17,13)}$, $h_{(19,11)}$ and $h_{(15,9)}$ should be assigned to 0.55, 0.8 and 0.38 of their original values at the frequency $f_1 = 60Hz$ simultaneously.

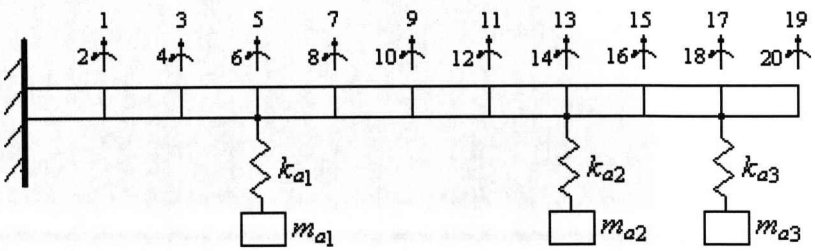

Figure 11. A cantilever beam modified by three absorbers

Analysis of the nonlinear equations set gave us the three absorbers stiffnesses at frequency of 60Hz.

$$\begin{cases} b_1(\omega_1) = -3.1766\times10^2\, N/m \\ b_2(\omega_1) = -8.4774\times10^2\, N/m \\ b_3(\omega_1) = -1.3210\times10^2\, N/m \end{cases}$$

Hence, the solution for the absorber parameters is determined as following.

$$\begin{cases} m_{a1} = 8.9405\times10^{-4}\,kg \\ k_{a1} = 2.1177\times10^{2}\,N/m \end{cases} \quad \begin{cases} m_{a2} = 2.3859\times10^{-3}\,kg \\ k_{a2} = 5.6516\times10^{2}\,N/m \end{cases} \quad \begin{cases} m_{a3} = 3.7178\times10^{-4}\,kg \\ k_{a3} = 8.8064\times10^{1}\,N/m \end{cases}$$

It should be noticed here that for a realistic solution, we choose the absorber's masses to be

$m_{ai} = 0.4\times(-b_i(\omega_1)/\omega_1^2) \qquad i = 1,2,3$

as described in equation (30)

Table 7 lists the modification details. It is found that both receptances were assigned simultaneously to the desired values exactly at frequency $f_1 = 60Hz$. Figure 12 shows the original and modified receptances.

Table 7. *Receptance values of $h_{(17,13)}$, $h_{(19,11)}$ and $h_{(15,9)}$ at one frequency*

Frequency	Receptance	Original value	Modified value	Modified ratio
60Hz	$h_{(17,13)}$	5.3130×10^{-5}	2.9222×10^{-5}	0.5500
	$h_{(19,11)}$	5.1777×10^{-4}	4.1422×10^{-4}	0.8000
	$h_{(15,9)}$	-8.2981×10^{-6}	-3.1533×10^{-6}	0.3800

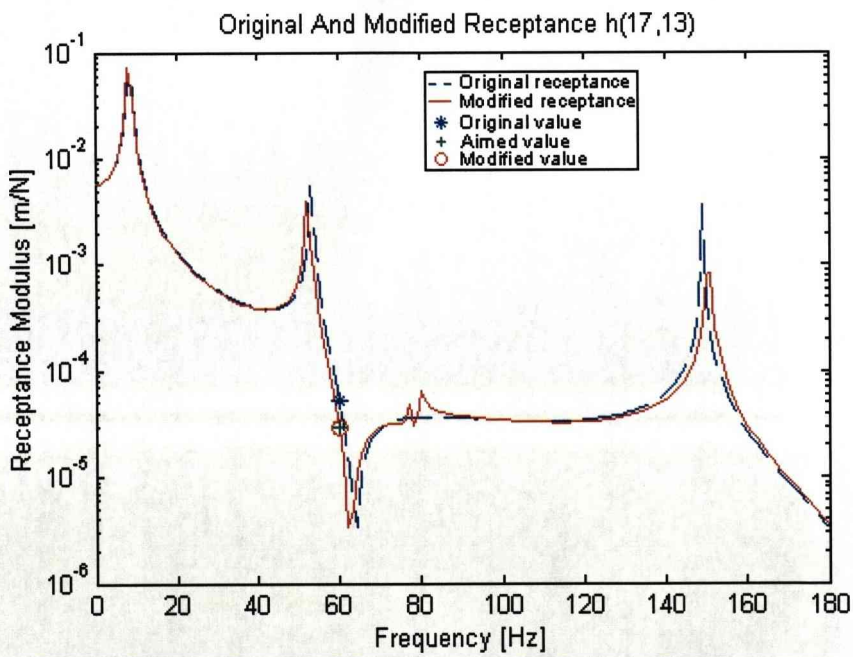

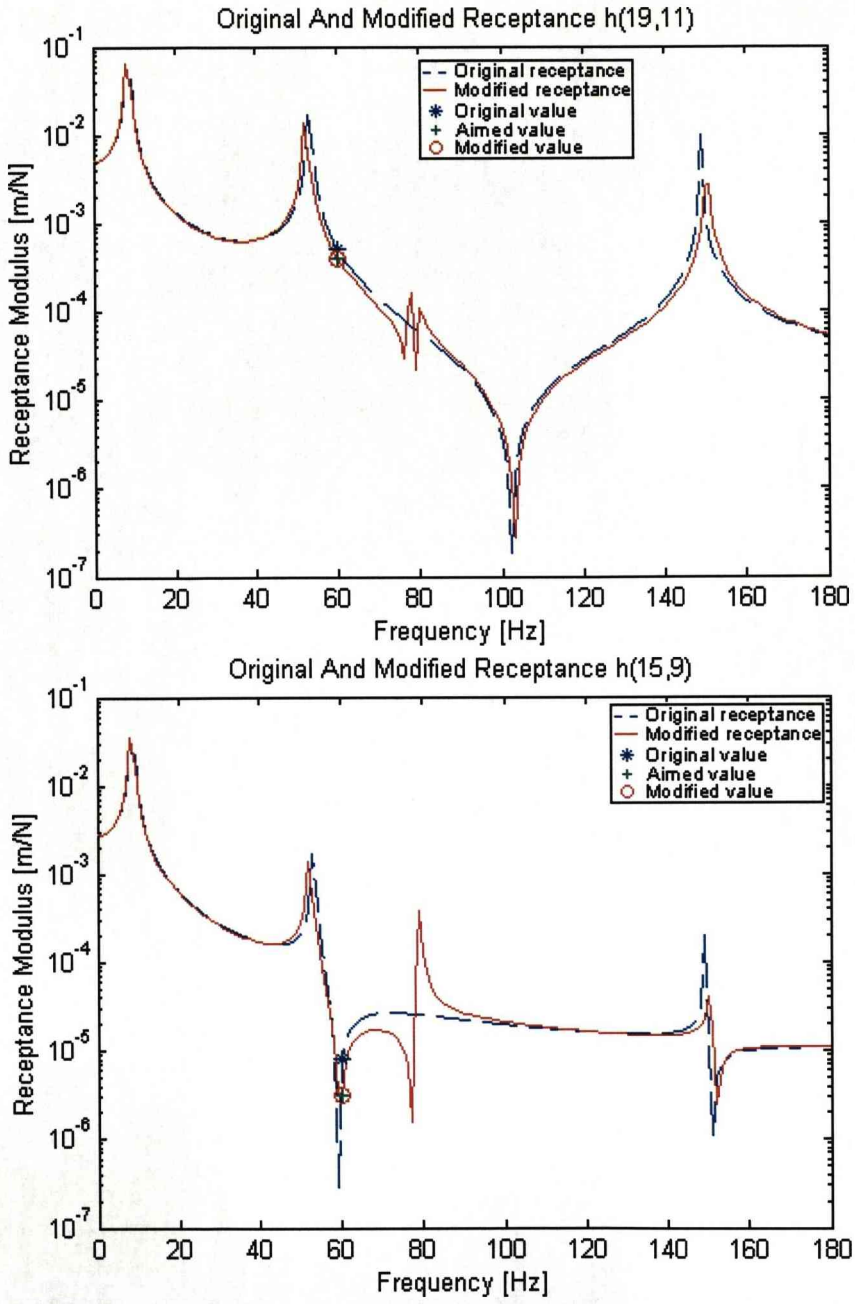

Figure 12. Assignment of three receptances at one frequency

7.2 Assigning three receptances simultaneously at two frequencies.

Repeating the calculation procedure in section 7.1 at both frequencies $\omega = \omega_1$ and $\omega = \omega_2$ we are be able to obtain the absorber stiffnesses at different frequencies, i.e., $\{b_1(\omega_1) \quad b_2(\omega_1) \quad b_3(\omega_1)\}$ and $\{b_1(\omega_2) \quad b_2(\omega_2) \quad b_3(\omega_2)\}$. And then, the mass and stiffness parameters of each absorber can be solved through its absorber stiffness at two frequencies $\{b_i(\omega_1) \quad b_i(\omega_2)\}$, i=1,2,3 .

Example 7: Assume that at the frequency $f_1 = 60Hz$, three receptances $h_{(17,13)}$, $h_{(19,11)}$ and $h_{(15,9)}$ should be assigned to 0.55, 0.8 and 0.38 of their original values, and at the same time, at the frequency $f_2 = 140Hz$, these receptances $h_{(17,13)}$, $h_{(19,11)}$ and $h_{(15,9)}$ should be assigned to 0.6, 0.46 and 0.34 of their original values simultaneously.

Firstly, the absorber dynamic stiffnesses were solved as

$$\begin{cases} b_1(\omega_1) = -3.1766\times10^2\, N/m \\ b_2(\omega_1) = -8.4774\times10^2\, N/m \\ b_3(\omega_1) = -1.3210\times10^2\, N/m \end{cases} \quad \text{and} \quad \begin{cases} b_1(\omega_2) = -7.0265\times10^3\, N/m \\ b_2(\omega_2) = -2.3830\times10^4\, N/m \\ b_3(\omega_2) = 2.2478\times10^4\, N/m \end{cases}$$

Consequently, the absorber parameters were obtained as

$$\begin{cases} m_{a1} = 1.9110\times10^{-3}\, kg \\ k_{a1} = 1.8728\times10^3\, N/m \end{cases} \quad \begin{cases} m_{a2} = 5.0489\times10^{-3}\, kg \\ k_{a2} = 4.6727\times10^3\, N/m \end{cases} \quad \begin{cases} m_{a3} = 7.5431\times10^{-4}\, kg \\ k_{a3} = 5.6889\times10^2\, N/m \end{cases}$$

Table 8 lists the modification details. And Figure 13 shows the original and modified receptance for each receptance. The results demonstrated that three receptances assignment task is achieved exactly at two frequencies simultaneously.

Table 8. *Receptance values of $h_{(17,13)}$, $h_{(19,11)}$ and $h_{(15,9)}$ at two frequencies*

Frequency	Receptance	Original value	Modified value	Modified ratio
60Hz	$h_{(17,13)}$	5.3130×10^{-5}	2.9222×10^{-5}	0.5500
	$h_{(19,11)}$	5.1777×10^{-4}	4.1422×10^{-4}	0.8000
	$h_{(15,9)}$	-8.2981×10^{-6}	-3.1533×10^{-6}	0.3800
140Hz	$h_{(17,13)}$	-6.1756×10^{-5}	-3.7051×10^{-5}	0.6000
	$h_{(19,11)}$	-1.3395×10^{-4}	-6.1606×10^{-5}	0.4599
	$h_{(15,9)}$	-1.5815×10^{-5}	-5.3748×10^{-6}	0.3398

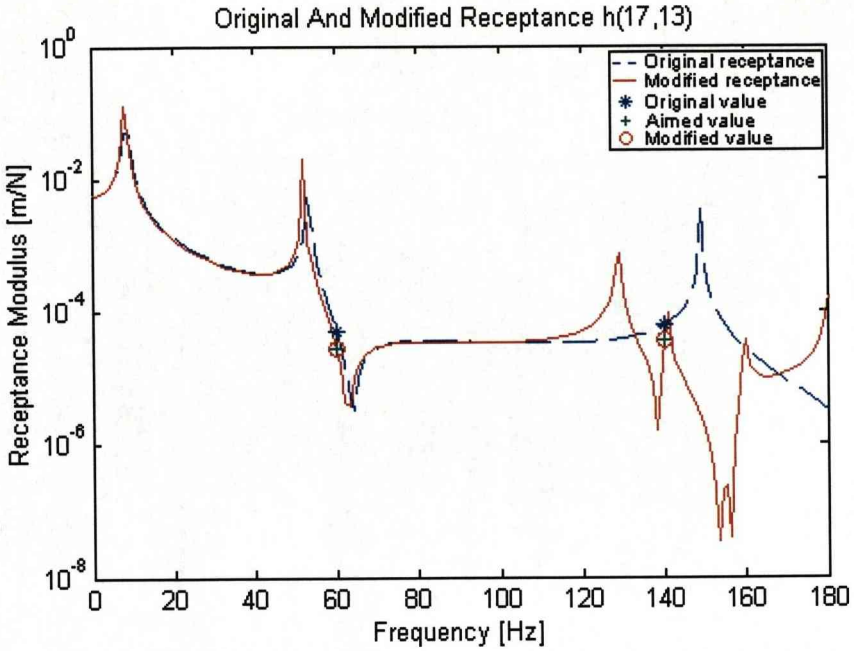
Original And Modified Receptance h(17,13)
Original receptance
Modified receptance
Original value
Aimed value
Modified value
Receptance Modulus [m/N]
Frequency [Hz]

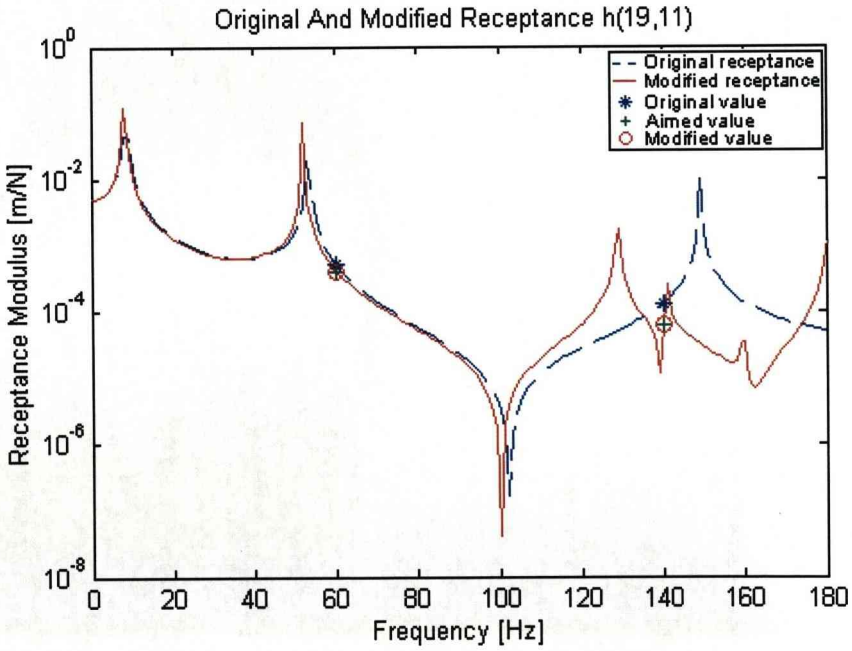
Original And Modified Receptance h(19,11)
Original receptance
Modified receptance
Original value
Aimed value
Modified value
Receptance Modulus [m/N]
Frequency [Hz]

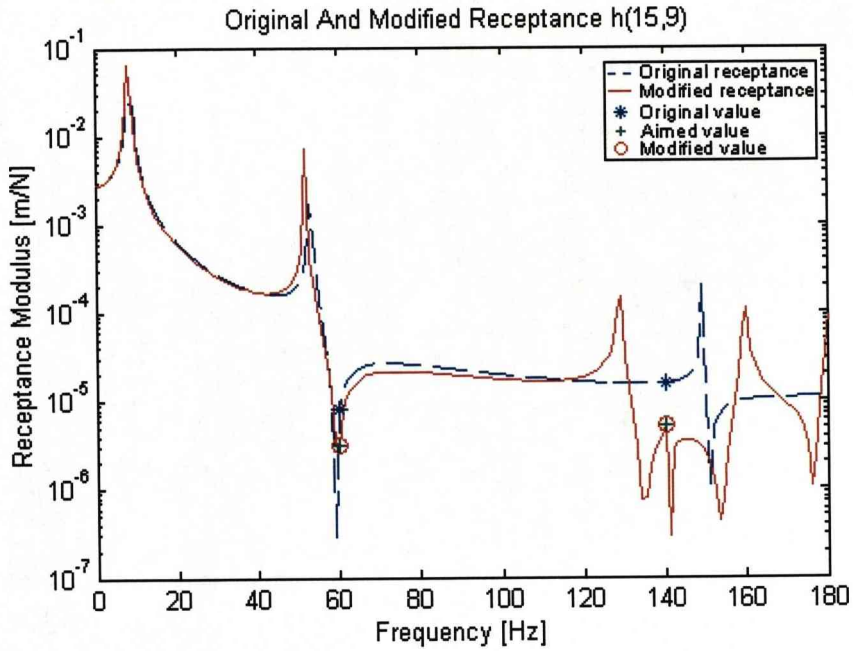

Figure 13. Assignment of three receptances at two frequencies

7.3 Assigning one receptance simultaneously at six frequencies

7.3.1 Case-1: Non-realistic solution

Example 8: Considering the same structure shown in Figure 11 with three absorbers it is required to assign the receptance $h_{(5,13)}$ to be 0.55, 0.8, 0.38, 0.6, 0.46 and 0.34 of its original values at the frequencies of 15, 40, 60, 75, 100 and 140 Hz respectively. Building receptance modification equations will result in a system of six equations in the six absorber parameters $\{m_{a1},\ k_{a1},\ m_{a2},\ k_{a2},\ m_{a3},\ k_{a3}\}$.

An alternative way is to define variables $\omega_{ai}^2 = \dfrac{k_{ai}}{m_{ai}}, (i = 1,2,3)$. This change will make a convenient implementation with Groebner bases. Thus the dynamic stiffness can be expressed as

$$b_i(\omega) = \frac{-\omega^2}{\omega_{ai}^2 - \omega^2} k_{ai} \quad (i = 1,2,3) \tag{56}$$

Then the multivariate polynomials are given with respect to variables $\{\omega_{a1}^2,\ k_{a1},\ \omega_{a2}^2,\ k_{a2},\ \omega_{a3}^2,\ k_{a3}\}$. After the equation system is solved, the absorber masses can be obtained from the equation

$$m_{ai} = \frac{k_{ai}}{\omega_{ai}^2}, (i = 1,2,3) \tag{57}$$

The calculation of this equation system gives the following solution.

$$\begin{cases} m_{a1} = 1.9123 \times 10^{-2}\, kg \\ k_{a1} = 6.6606 \times 10^{3}\, N/m \end{cases} \quad \begin{cases} m_{a2} = 2.3036 \times 10^{-2}\, kg \\ k_{a2} = -5.2745 \times 10^{3}\, N/m \end{cases} \quad \begin{cases} m_{a3} = 5.2976 \times 10^{-3}\, kg \\ k_{a3} = 1.1401 \times 10^{2}\, N/m \end{cases}$$

It is found that there is no realistic absorbers group, shown in Figure 11, for this assignment

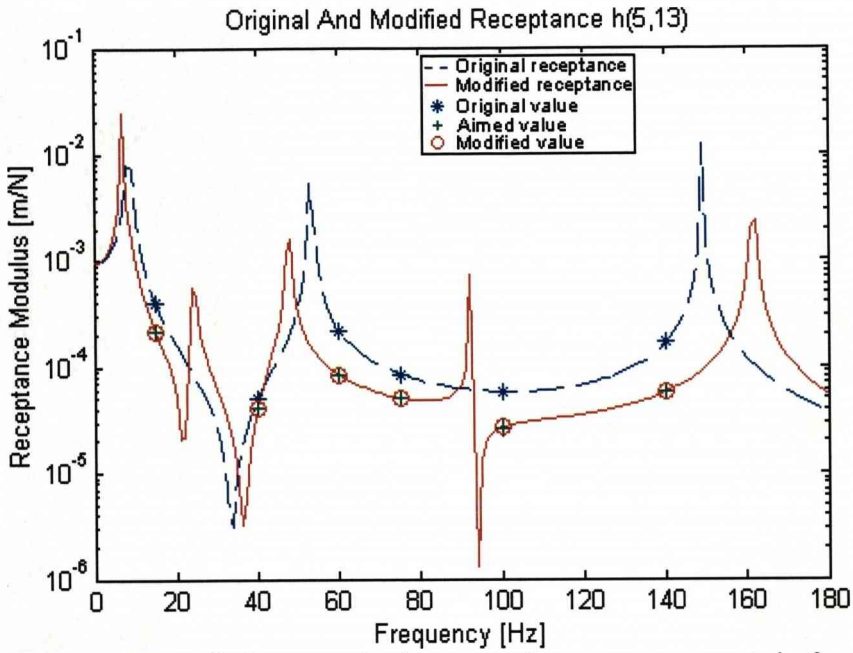

Figure 14. Non-realistic case - Assignment of one receptance at six frequencies

7.3.2 Case-2: Realistic solution

Example 9: In this case, we consider the above example and assign the receptance $h_{(5,13)}$ to be 0.55, 0.8, 0.38, 0.6, 0.8 and 0.34 of its original values at the frequencies of 15, 40, 60, 75, 100 and 140 Hz respectively. The calculation of the receptance modification equation system gives us a realistic solution as following.

$$\begin{cases} m_{a1} = 1.8964 \times 10^{-2}\, kg \\ k_{a1} = 6.3570 \times 10^{3}\, N/m \end{cases} \quad \begin{cases} m_{a2} = 2.4317 \times 10^{-3}\, kg \\ k_{a2} = 4.2646 \times 10^{2}\, N/m \end{cases} \quad \begin{cases} m_{a3} = 7.7549 \times 10^{-3}\, kg \\ k_{a3} = 1.4367 \times 10^{2}\, N/m \end{cases}$$

Table 9 shows the receptance modification details for this realistic solutions and Figures 15 shows the original and modified receptance $h_{(5,13)}$.

Table 9. *Realistic case - Receptance values of $h_{(5,13)}$ at six frequencies*

Frequency	Original value	Modified value	Modified ratio
15Hz	-4.0365×10^{-4}	-2.2179×10^{-4}	0.5495
40Hz	5.0526×10^{-5}	4.0429×10^{-5}	0.8002
60Hz	-2.2113×10^{-4}	-8.3862×10^{-5}	0.3793
75Hz	-8.4885×10^{-5}	-5.0852×10^{-5}	0.5991
100Hz	-5.7930×10^{-5}	-4.6418×10^{-5}	0.8013
140Hz	-1.6677×10^{-4}	-5.6794×10^{-5}	0.3406

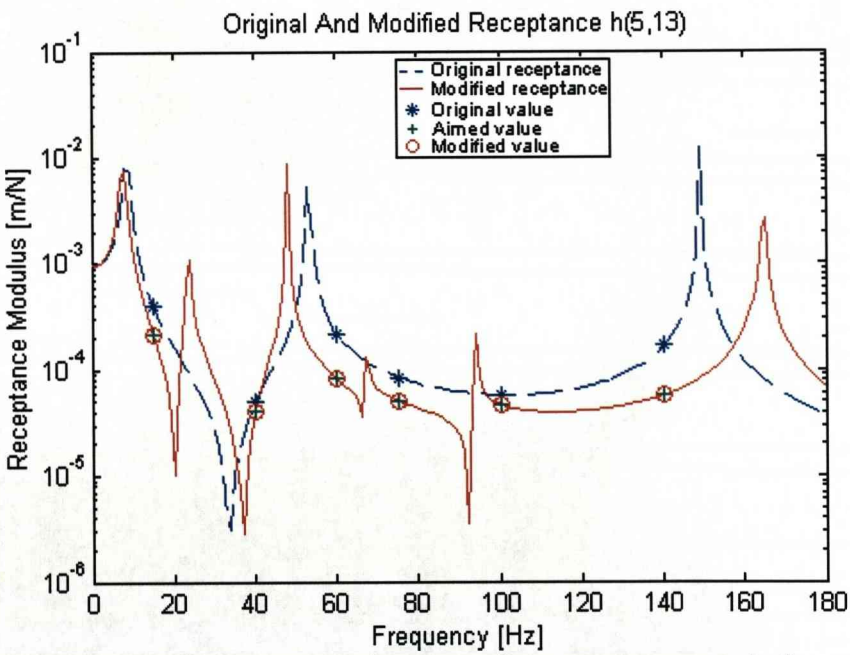

Figure 15. Realistic case - Assignment of one receptance at six frequencies

7.4 Assigning two receptances simultaneously at three frequencies

Example 10: This example considers the structural modification for the assignment of receptance $h_{(5,13)}$ to be 0.55, 0.38 and 0.6 of its original values at the frequencies of 15, 60 and 75 Hz and meanwhile the assignment of receptance $h_{(7,13)}$ to be 0.5, 0.14 and 0.3 of its original values at the frequencies of 20, 45 and 80 Hz. Building the necessary system of equations and solving it gives us the realistic absorber parameters as follows,.

$$\begin{cases} m_{a1} = 6.3735\times10^{-3}\,kg \\ k_{a1} = 1.4845\times10^{3}\,N/m \end{cases} \quad \begin{cases} m_{a2} = 2.0069\times10^{-2}\,kg \\ k_{a2} = 5.8391\times10^{3}\,N/m \end{cases} \quad \begin{cases} m_{a3} = 7.3752\times10^{-3}\,kg \\ k_{a3} = 3.2172\times10^{2}\,N/m \end{cases}$$

Table 10 shows the receptance modification details and Figure 16 shows the original and modified receptance $h_{(5,13)}$ and $h_{(7,13)}$.

Table 10. *Receptance values of $h_{(5,13)}$ and $h_{(7,13)}$ at three frequencies respectively*

Receptance	Frequency	Original value	Modified value	Modified ratio
$h_{(5,13)}$	15Hz	-4.0365×10^{-4}	-2.2187×10^{-4}	0.5497
	60Hz	-2.2113×10^{-4}	-8.3874×10^{-5}	0.3793
	75Hz	-8.4885×10^{-5}	-5.1323×10^{-5}	0.6046
$h_{(7,13)}$	20Hz	-2.8593×10^{-4}	-1.4284×10^{-4}	0.4996
	45Hz	1.4945×10^{-4}	2.1039×10^{-5}	0.1408
	80Hz	-8.8332×10^{-5}	-2.6353×10^{-5}	0.2983

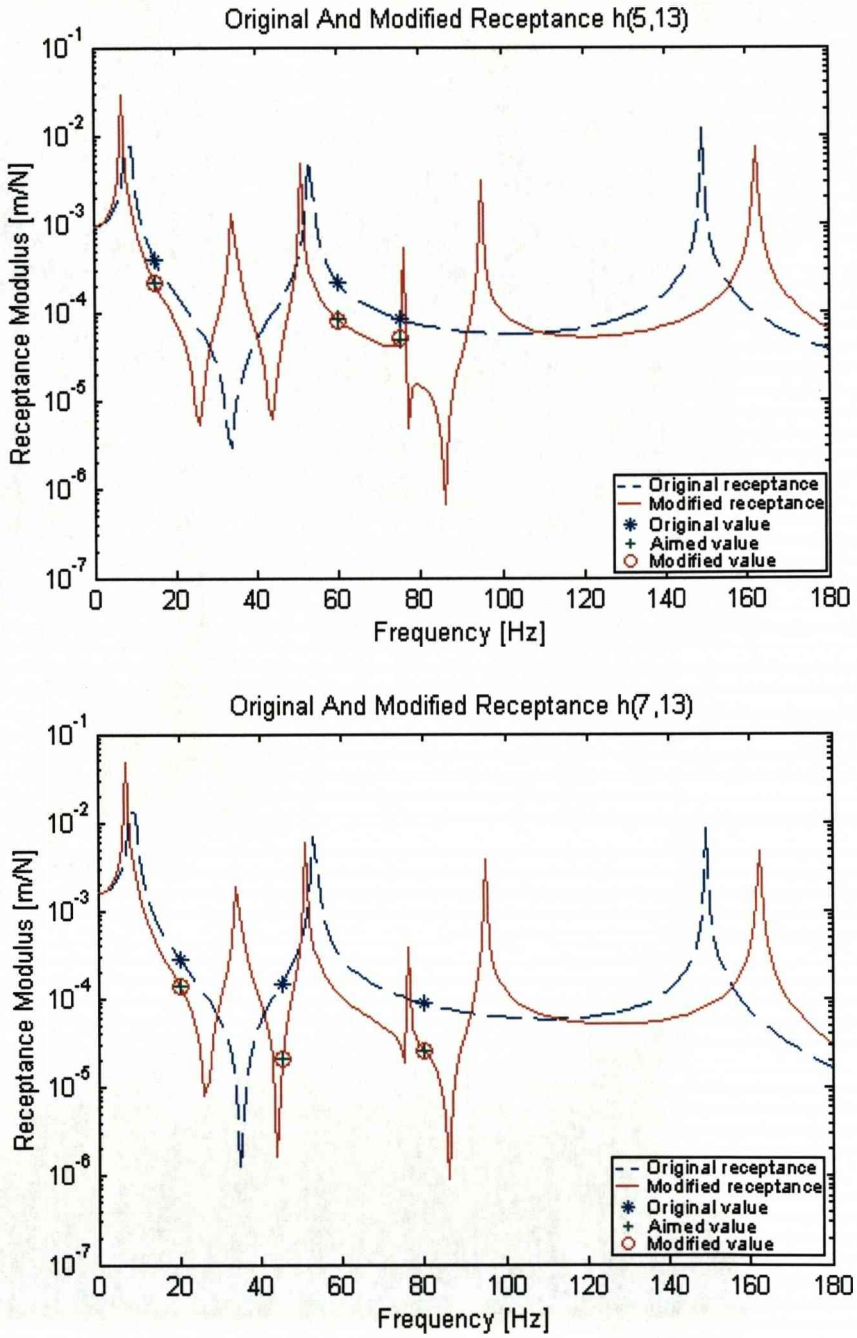

Figure 16. Assignment of two receptances at three frequencies

8. Conclusions

This paper considers the inverse problem of assigning receptances to a vibrating system by connecting multiple classical mass-spring absorbers. When a simple oscillator is attached to a system, one receptance at up to two frequencies can be

assigned simultaneously because one absorber involves two variables, i.e., mass and spring stiffness. The absorber parameters should be restricted to positive values. The calculations are based on the absorber dynamic stiffness $b(\omega)$, so that the absorber parameters may be obtained subsequently.

In order to assign more receptances, more absorbers have to be attached to the original system. The absorber dynamic stiffnesses can be obtained by numerically solving the system of nonlinear modified receptance equations. Many different cases of assigning receptances at chosen frequencies have been considered and numerical examples used to illustrate the analysis. The requirement for positive absorber masses and stiffnesses may result in there being no available solution.

Although one mass-spring absorber introduces two variables, k_a and m_a, the absorber dynamic stiffness $b(\omega)$ must be unique for a single frequency, which means that we can only assign two receptances at one frequency under very restricted conditions. For the same reason, this restriction also appears when multiple absorbers are applied, for example, assignment of three or four receptances at one frequency with two absorbers and assignment of four, five or six receptances at one frequency with three absorbers connected. However, it is demonstrated that there are many other receptance assignment problems that can the assigned arbitrarily, except for the condition of positiveness on k_a and m_a. In many cases multiple solutions are available.

References

1. Frahm, H., 1909, "Devices for Damping Vibration of Bodies", US Patent No. 989958.

2. Ormondroyd, J. and Den Hartog, J. P., 1928, "The theory of the dynamic vibration absorber", *Trans. ASME*, **50**, 9-15.

3. Sun, J. Q., Jolly, M. R. and Norris, M. A., 1995, "Passive, adaptive, and active tuned vibration absorbers – a survey", *Trans. ASME, Journal of Vibration and Acoustics*, **117**, 234-342.

4. Duncan, W. J., 1941, "The admittance method for obtaining natural frequencies of systems", *Philosophical Magazine*, **32**, 401-409.

5. Bishop, R. E. D. and Johnson, D. C., 1960, "The mechanics of vibration", Cambridge University Press.

6. Shahverdi, H., Mares, C. and Mottershead, J. E., 2005, "Model-structure correction and updating of aero engine casings using fictitious mass modifications", *Proceedings of the Institution of Mechanical Engineers, Part C, Journal of Mechanical Engineering Science*, **219(1)**, 19-30.

7. Mottershead, J. E., Tehrani, M. G., Stancioiu, D., James, S. and Shahverdi, H.,

"Structural modification of a helicopter tailcone", *Journal of Sound and Vibration*, submitted.

8. Weissenburger, J. T., 1968, "Effect of local modifications on the vibration characteristics of linear systems", *Trans. ASME, Journal of Applied Mechanics*, **90**, 327-332.

9. Pomazal, R. J. and Snyder, V.W., 1971, "Local modifications of damped linear systems", *AIAA Journal*, **9**, 2216-2221.

10. Bucher, I. and Braun, S., 1993, "The structural modification inverse problem", *Mechanical Systems and Signal Processing*, 7, 217-238.

11. Mottershead, J. E., Mares, C. and Friswell, M. I., 2001, "An inverse method for the assignment of vibration nodes", *Mechanical Systems and Signal Processing*, **15(1)**, 87-100.

12. Mottershead, J. E., 2001, "Structural modification for the assignment of zeros using measured receptances", *Trans. ASME, Journal of Applied Mechanics*, **68(5)**, 791-798.

13. Mottershead, J. E. and Lallement, G., 1999, "Vibration nodes, and the cancellation of poles and zeros by unit rank modifications to structures", *Journal of Sound and Vibration*, **222(5)**, 833-851.

14. Li, T., He, J. and Sek, M., 2001, "Local and global pole-zero cancellation of mass-spring systems", *Mechanical Systems and Signal Processing*, **15(1)**, 121-127.

15. Ram, Y. M., 1998, "Pole assignment for the vibrating rod", *Quarterly Journal of Mechanics and Applied Mathematics*, **51**, 461-476.

16. Singh, A.N. and Ram, Y.M., 2003, "Dynamic absorption in a vibrating beam", *Proceedings of the Institution of Mechanical Engineers, Part C, Journal of Mechanical Engineering Science*, **217**, 187-197.

17. Ram, Y.M. and Elhay, S., 1996, "The theory of a multi degree of freedom dynamic absorber", *Journal of Sound and Vibration*, **195**, 607-615.

18. Mottershead, J. E., 1998, "On the zeros of structural frequency response functions and their sensitivities", *Mechanical Systems and Signal Processing*, **12(5)**, 591-597.

19. Kyprianou, A., Mottershead, J. E. and Ouyang, H., 2004, "Assignment of natural frequencies by an added mass and one or more springs", *Mechanical Systems and Signal Processing*, **18(2)**, 263-289.

20. Lawther, R., "Assessing how changes to a structure can create gaps in the natural frequency spectrum", *International Journal of Solids and Structures*, in press.

21. Mottershead, J. E., Kyprianou, A. and Ouyang, H., 2005, "Structural modification,

part 1: rotational receptances", *Journal of Sound and Vibration*, **284(1-2)**, 249-265.

22. Kyprianou, A., Mottershead, J. E. and Ouyang, H., 2005, "Structural modification, part 2: assignment of natural frequencies and antiresonances by an added beam", *Journal of Sound and Vibration*, **284(1-2)**, 267-281.

23. Mottershead, J. E. and Ram, Y. M., 2006, "Invited Review, Inverse eigenvalue problems in vibration absorption: passive modification and active control", *Mechanical Systems and Signal Processing*, **20(1)**, 5-44.

24. Berman, A., 1984, "System identification of structural dynamic models – theoretical and practical bounds", *AIAA conference paper 84-0929*.

25. Berman, A., 1984, "Limitations on the identification of discrete structural dynamic models", *2nd International Conference on Recent Advances in Structural Dynamics*, Southampton, 427-435.

26. Goldfarb, D., 1972, "Modification methods for inverting matrices and solving systems of linear equations", *Mathematics of Computation*, **26(120)**, 829-852.

27. Buchberger, B., 1965, "An algorithm for finding the basis elements in the residue class ring modulo a zero dimensional polynomial ideal", *PhD Thesis*, Mathematical Institute, University of Innsbruck, Austria.

28. Cox, D., Little, J. and O'Shea Ideals, D., 1995, "Varieties and algorithms", Springer.

29. Press, W. H., Teukolsky, S. A., Vetterling, W. T. and Flannery, B. P., 1992, "Numerical recipes in C, The art of scientific computing", Cambridge University Press.